# The homeostasis and function of plasmatocytes in adult Drosophila

Woodcock, Katie

*Awarding institution:*
King's College London

KING'S College LONDON

# The homeostasis and function of plasmatocytes in adult *Drosophila*

**By Katie Jane Woodcock**

**This thesis is submitted to King's College London**

**for the degree of Doctor of Philosophy**

**March 2013**

# Abstract

Many key immune pathway genes in vertebrates have conserved *Drosophila* counterparts; therefore, the fly has become an influential model for the study of innate immunity. The *Drosophila* immune response consists of a humoral response; characterised by the production of anti-microbial peptides and cytokines and a cellular response; mediated by plasmatocytes, the fly analogue cell to the mammalian macrophage. Plasmatocytes have been studied in detail during the embryonic and larval stages of development however, plasmatocyte homeostasis and function in adult flies remains poorly understood. This thesis firstly characterises plasmatocytes in adult *Drosophila* in terms of their numbers, expression markers and proliferative potential. Secondly the plasmatocyte response to dietary lipids is studied in adult flies, as a model for the mammalian macrophage response to dietary lipids.

Excessive dietary fat consumption in humans is associated with an increased incidence of high fat diet related diseases, including type II diabetes and atherosclerosis. Numerous aspects of high fat diet induced disease pathology in mammals are attributed to lipid induced inflammation, in which macrophage mediated lipid scavenging and/or sensing is believed to be of central importance. We found that as dietary fat content increased; flies exhibited a rise in triglyceride and glucose levels, whilst simultaneously up regulating expression of the *IL-6*-like JAK-STAT cytokine *unpaired3* (*upd3*), in addition, plasmatocytes adopted a lipid laden foam cell-like morphology. These phenotypes are similar to those observed in humans during high fat diet induced diseases. Interestingly plasmatocyte depletion or plasmatocyte specific knock down of the *CD36*-like scavenger receptor *croquemort* (*crq*) or cytokine *upd3* in flies was sufficient to rescue various high fat diet induced phenotypes. Findings in this thesis identify a plasmatocyte specific and therefore macrophage specific role in the progression of high fat diet disease pathophysiology, which could prove significant in allowing for a better understanding of high fat diet disease aetiology in mammals.

## Acknowledgements

I am very grateful to Frédéric Geissmann, Marc Dionne and Leonie Taams for their advice, supervision and encouragement during the 4 years of my PhD.

I would also like to say a special thank you to Natasha, Valérie and Martina for their invaluable help and support on so many levels; it has been really fantastic working with you. Thanks also go to members of the CMCBI past and present for their help at various points over the last 4 years; Céline, Kevin, Claire, Clara, and Christine to name just a few.

To my amazing family; Andrew, Mum, Dad, Ian, Jamie, Grandma Enid, Grandad Claude, Grandma Anne and Grandad Johnny thank you so very much for everything and for always pushing me to believe that anything is possible.

This PhD was funded by the MRC.

## Declaration

I declare that I have personally prepared this thesis and that the work included is my own, unless otherwise stated. All information sources included in this thesis are referenced accordingly.

Katie J Woodcock

March 2013

# Table of Contents

# Table of Figures

# Table of Tables

## Abbreviations

| | |
|---|---|
| 4E-BP | eukaryotic translation initiation factor 4E binding protein 1 |
| Ecdysone | 20-hydroxyecdysone |
| ACC | Acetyl-CoA carboxylase |
| ae | Anterior endoderm |
| AGM | Aorta-gonad-mesonephros |
| AKH | Adipokinetic hormone |
| Akt | Also known as Protein Kinase B (PKB) |
| AMPs | Anti-microbial peptides |
| ApoE | Apolipoprotein E |
| au | Arbitrary units |
| bmm | brummer lipase |
| C3 | Complement component 3 |
| ccp | crystal cell precursors |
| CD | Cluster of differentiation |
| cDNA | Complementary DNA |
| CNS | Central nervous system |
| $CO_2$ | Carbon dioxide |
| crq | croquemort |
| daw | dawdle |
| DCV | Drosophila C Virus |
| Dif | Dorsal-related immune factor |
| DiI-LDL | 3,3'-dioctadecylindocarbocyanine-low density lipoprotein |
| Dilp | Drosophila insulin like peptide |
| DNA | Deoxyribonucleic acid |
| dPIAS | *Drosophila* protein inhibitor of activated STAT |
| dpp | decapentaplegic |
| Dpt | Diptericin |
| Dredd | Death related ced-3/Nedd2-like protein |
| Drs | Drosomcyin |
| DsRed | Discosoma red fluorescent protein |
| Dv | Dorsal vessel |
| E. coli | Escherichia coli |
| EDTA | Ethylenediaminetetraacetic Acid |
| eGFP | Enhanced green fluorescent protein |

| | |
|---|---|
| FACS | Fluorescence-activated cell sorting |
| FAS | Fatty acid synthase |
| FOG | Friend of GATA |
| FOXO | Forkhead box transcription factor |
| Fucci | Fluorescent ubiquitination based cell cycle indicator |
| GABA | γ-Aminobutyric acid neurones |
| gcm | glial cells missing |
| GFP | Green fluorescent protein |
| GNBP | Gram negative binding protein |
| Gp130 | Glycoprotein 130 |
| $H_2O_2$ | Hydrogen peroxide |
| He | Hemese |
| Hml | Hemolectin |
| Hop | Hopscotch (JAK) |
| IFN-γ | Interferon-gamma |
| IL-1R | Interleukin-1 receptor |
| IL-6R | Interleukin-6 receptor |
| Imd | Immune deficiency |
| InR | Insulin receptor |
| IPC | Insulin producing cells |
| IR | Inverted repeats |
| JAK | Janus kinase |
| JNK | c-Jun N-terminal kinase |
| LB | Lysogeny broth |
| Lg | Lymph gland |
| lsd2 | Lipid storage droplet 2 |
| lz | lozenge |
| MAPK | Mitogen-activated protein kinase |
| mdy | midway |
| M. luteus | Micrococcus luteus |
| mRNA | Messenger RNA |
| MyD88 | Myeloid differentiation primary response gene (88) |
| myrRFP | Myristoylated red fluorescent protein |
| NF-κB | Nuclear factor κ light chain enhancer of activated B cells |
| nimC1 | nimrodC1 |

| | |
|---|---|
| nls | Nuclear localisation signal |
| OD | Optical density |
| PBS | Phosphate buffered saline |
| Pepck | Phosphoenolpyruvate carboxykinase |
| PGRP | Peptidoglycan recognition protein |
| PI3K | Phosphoinositide-3-kinase |
| PRR | Pattern recognition receptor |
| Pv | Proventriculus |
| Pvf | PDGF/VEGF factor |
| Pvr | PDGF and VEGF receptor related |
| Pxn | Peroxidasin |
| Rel | Relish |
| RT qPCR | Real time quantitative polymerase chain reaction |
| RNA | Ribonucleic acid |
| RNAi | RNA interference |
| ROS | Reactive oxygen species |
| Rpl-1 | Ribosome protein L4 |
| rpr | reaper |
| RUNX-1 | Runt-related transcription factor-1 |
| S2 | Schneider 2 cells |
| S6K | S6 Kinase |
| S. aureus | Staphylococcus aureus |
| Socs36E | Suppressor of cytokine signalling 36E |
| spz | spätzle |
| srp | serpent |
| STAT | Signal transducer and activator of transcription |
| TAG | Triacylglycerol |
| Tak1 | Transforming growth factor β-activated kinase 1 |
| Tep2 | Thioester-containing protein 2 |
| TGF-β | Transforming growth factor-β |
| TLC | Thin layer chromatography |
| TLR | Toll-like receptor |
| TNF | Tumour necrosis factor |
| TOR | Target of rapamycin |
| TotA | Turandot peptide A |

| | |
|---|---|
| Tub | Tubulin |
| UAS | Upstream activation sequence |
| upd | unpaired |
| upd2 | unpaired 2 |
| upd3 | unpaired 3 |
| VEGF | Vascular endothelial growth factor |
| VWF | Von Willebrand Factor |

# Chapter 1 Introduction

### 1.1 *Drosophila* plasmatocytes

*Drosophila* macrophages, known as plasmatocytes, have been described as the counterpart cell to the mammalian macrophage (Lebestky et al., 2000). They share a variety of characteristics and functions; these include their roles as professional phagocytes and cytokine producers (Charroux and Royet, 2009, Agaisse et al., 2003, Clark et al., 2011). Both macrophages and plasmatocytes are sessile cells and become populations of resident-like cells once terminally differentiated (Elrod-Erickson et al., 2000). Further support for plasmatocyte analogy to mammalian macrophages is the lack of a specific/adaptive immune response in the fly. This makes *Drosophila* plasmatocytes an attractive model to further characterise macrophage functions in response to different cues e.g. infection, waste products, and metabolic products.

### 1.2 Hemocyte development

Embryonic haematopoiesis in *Drosophila* is reminiscent of early haematopoiesis in vertebrates (Figure 1-1). Fly blood cells, known as hemocytes, are derived from the cardiogenic mesoderm. During embryogenesis, vascular progenitors (cardioblasts) and blood precursors migrate dorsally, meet in the midline and form the dorsal vessel, which is flanked by clusters of hematopoietic cells known as the lymph glands (Evans et al., 2007). Hemocytes then undergo differentiation in the lymph glands, the major hematopoietic organ, which persists throughout the larval stages of development (Lebestky et al., 2000), this process is illustrated in Figure 1-2. Similarly, in vertebrates a large proportion of hematopoietic precursor cells are derived from the aorta-gonad-mesonephros (AGM), these cells then migrate to appropriate locations within the embryo to form blood vessels and generate different hematopoietic blood cell lineages (Evans et al., 2003, Evans et al., 2007). The consequent stages of myeloid lineage haematopoiesis exhibit strong similarities to *Drosophila* blood cell development, suggesting a

conservation in blood cell lineage development throughout evolution (Wood and Jacinto, 2007, Crozatier and Meister, 2007).

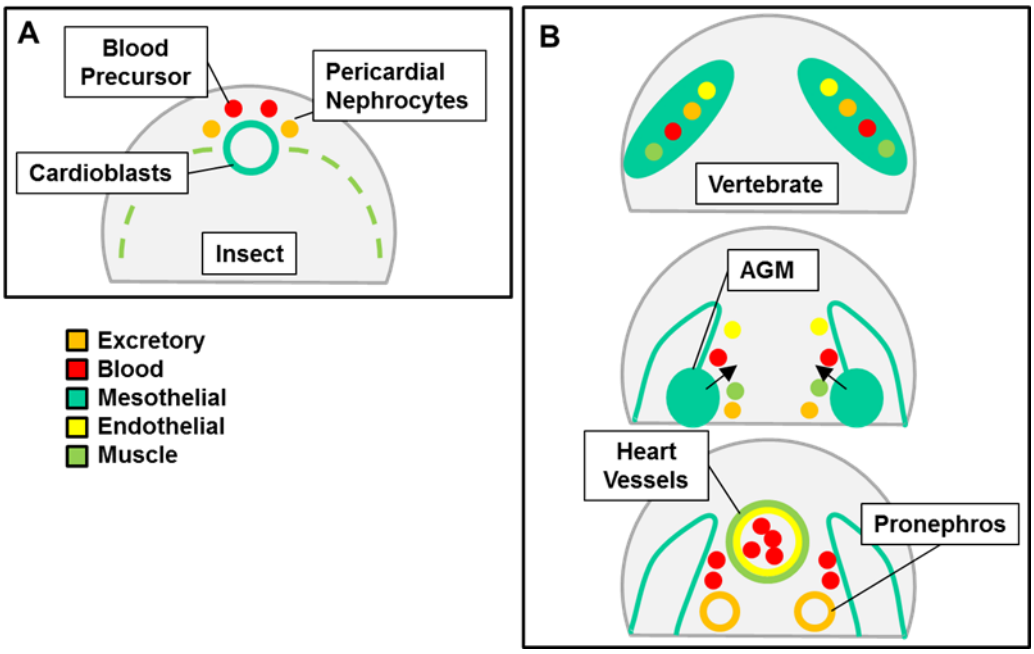


*Figure 1-1 Development of hematopoietic, vascular and mesodermal compartments in insects and vertebrates*
**A.** Insect blood, vascular and excretory cells are derived from a common precursor, the cardiogenic mesoderm. During embryogenesis lymph gland and pericardial nephrocyte cells line up next to the dorsal vessel. **B.** In vertebrates the aorta-gonad-mesonephros (AGM) gives rise to endothelial and blood precursors which migrate to designated sites in the embryo to form vessels. Figure adapted from adapted from Evans et al. (2003).

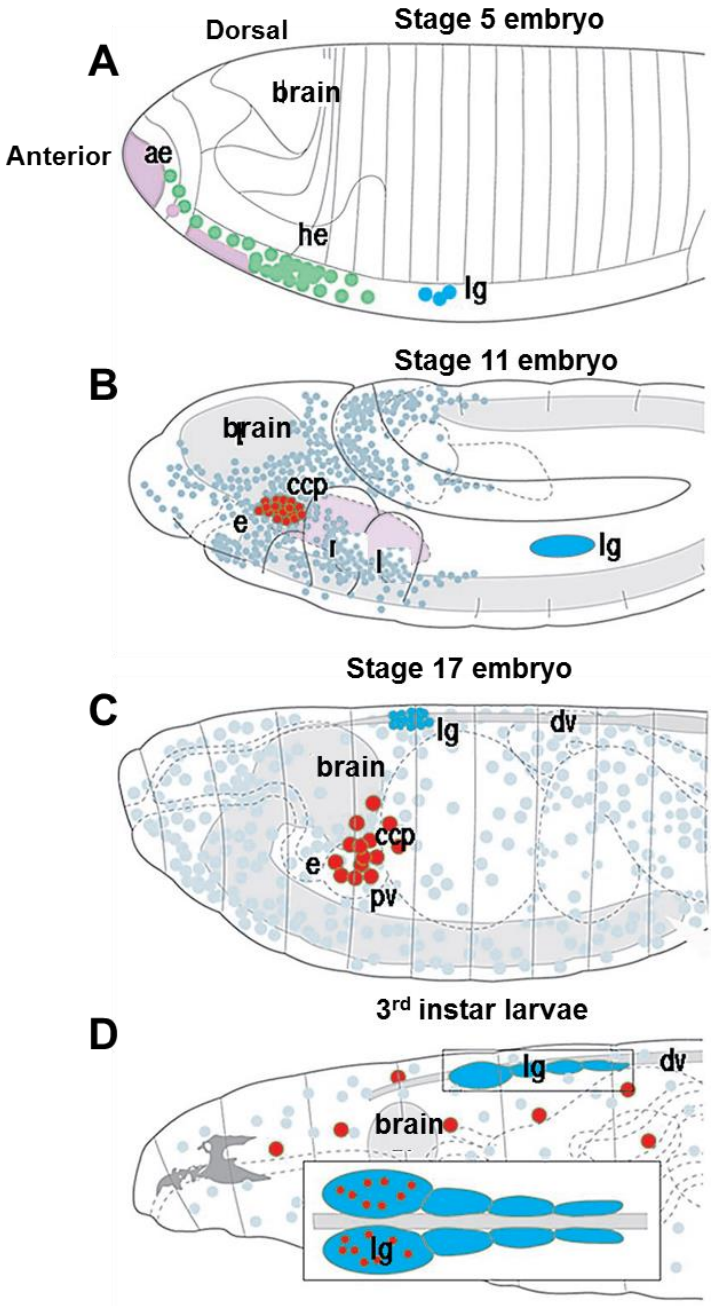


*Figure 1-2 Schematic diagram of embryonic and larval haematopoiesis*
Figure detailing haematopoiesis in stage 5, 11 and 17 embryos (A, B, C) and 3rd instar larvae (D). **A.** In stage 5 embryos the first vital tissues begin to form for the progression of haematopoiesis. The anterior endoderm (ae; light pink), the hemocyte anlagen (he; green) and the lymph gland anlagen cells (lg; blue) are present. **B.** In stage 11 embryos there is an expansion of hemocyte precursors (grey), from which crystal cell precursors (ccp; red) are derived. Lymph gland precursors (blue) are visible in the ventral-lateral trunk mesoderm. **C.** At late stage 17 of embryogenesis CCPs cluster around the proventriculus (pv). The lymph glands (blue) are visible along the dorsal vessel. Plasmatocytes (grey) are dispersed within the endolymph. **D.** In third instar larvae, crystal cells and plasmatocytes (grey) circulate freely throughout the hemolymph. A further population of lymph gland derived hemocytes are released from the lymph glands during metamorphosis (blue). Figure is taken and adapted from Evans et al. (2003).

*1.2.1 Blood cell lineage development from flies to mammals*

Many hematopoietic transcription factors in mammals are also conserved in *Drosophila* (Figure 1-3). The fly transcription factors *serpent* (*srp*) and *lozenge* (*lz*) are homologous to mammalian *GATA-1* and *RUNX-1* (*Runt related transcription factor-1*) transcription factors respectively, and are necessary for the successful continuation of haematopoiesis in *Drosophila* and mammals alike (Lebestky et al., 2000). In addition, both mammals and flies require the JAK-STAT (Janus kinase, signal transducers and activators of transcription) pathway and *Notch* signalling (Luo et al., 1997, Duvic et al., 2002) during haematopoiesis (Figure 1-3). Luo et al. (1997) showed that hyper-activation of the JAK-STAT pathway in larvae resulted in a leukaemia-like phenotype, with a massive over proliferation of hemocytes. Similarly, in humans constitutive activation of the JAK-STAT pathway is associated with the development of leukaemia and lymphomas (Takemoto et al., 1997).

Interestingly, the particular genes which are conserved during fly and mammalian haematopoiesis point towards a conservation between the development of *Drosophila* plasmatocytes and that of mammalian monocytes and macrophages (Figure 1-3). Once again, this suggests fly hemocytes are evolutionarily most closely related to mammalian monocytes and macrophages.

*1.2.2 Existence of a hematopoietic organ or plasmatocyte proliferation in adult flies*

The embryonic mesoderm and the larval lymph gland are the major sites of haematopoiesis in embryos and larvae respectively (Evans et al., 2003). During larval development, all hemocytes which do not reside in the lymph glands are of embryonic origin (Holz et al., 2003), however, the number of circulating and sessile non-lymph gland hemocytes has been shown to increase during larval development (Lanot et al., 2001). Initially gradual hemocyte release from the lymph glands was believed to be the source of this increase in numbers, but interestingly it was shown that proliferation of

embryonic hemocytes during larval development was actually responsible (Holz et al., 2003). An eventual release of lymph gland derived hemocytes takes place late in 3rd instar larval development and finally at the onset of metamorphosis the lymph glands rupture, releasing the remaining larval lymph gland hemocytes into the circulation. Hemocytes which persist in adult flies have been shown to be of both embryonic and larval origin.

To date, there is no evidence for the existence of a hematopoietic organ in adult flies; it is believed that embryonic and larval derived hemocytes serve the fly for the remainder of the adult *Drosophila* lifespan. However, the study or search for a hematopoietic organ in adult *Drosophila* does not appear to have been carried out in detail. Furthermore, the possibility of hemocyte self-renewal and proliferative potential in steady state or in response to immune challenge is yet to be determined in adult flies. These possibilities pose interesting questions which this thesis will address.

### *1.2.3 Hemocyte subsets*

Embryonic and larval hemocytes consist of plasmatocytes, the macrophage-like subset, and crystal cells, required for the melanisation reaction (Rizki and Rizki, 1959). Plasmatocytes and crystal cells account for approximately 95% and 5% of the total hemocyte population respectively (Evans et al., 2003). One further hemocyte subset, known as lamellocytes, has been identified in larvae. Lamellocytes are involved in the encapsulation and killing of large pathogenic invaders, which are too big to be phagocytosed by plasmatocytes. However, studies have indicated that lamellocyte differentiation only occurs in larvae which have been parasitized by wasp eggs and are seldom found in healthy larvae (Rizki and Rizki, 1992, Krzemien et al., 2010).

In adult *Drosophila* it is believed only the macrophage-like plasmatocyte subset exists (Meister and Lagueux, 2003). Expression profiles of hemocyte markers involved in embryonic and larval haematopoiesis have been studied in detail (Figure 1-3); however expression characteristics of adult fly plasmatocytes and their functions are not firmly

established. Nonetheless, there is evidence to suggest that adult fly plasmatocytes are not a homogenous population of cells, for example; they exhibit differential expression of TGF-β signals *decapentaplegic* (*dpp*) and *dawdle* (*daw*) in response to wounding and infection (Clark et al., 2011).

The following section will describe in detail some key plasmatocyte expressed molecules and what is known about their expression profiles and roles to date during *Drosophila* development.

**A**

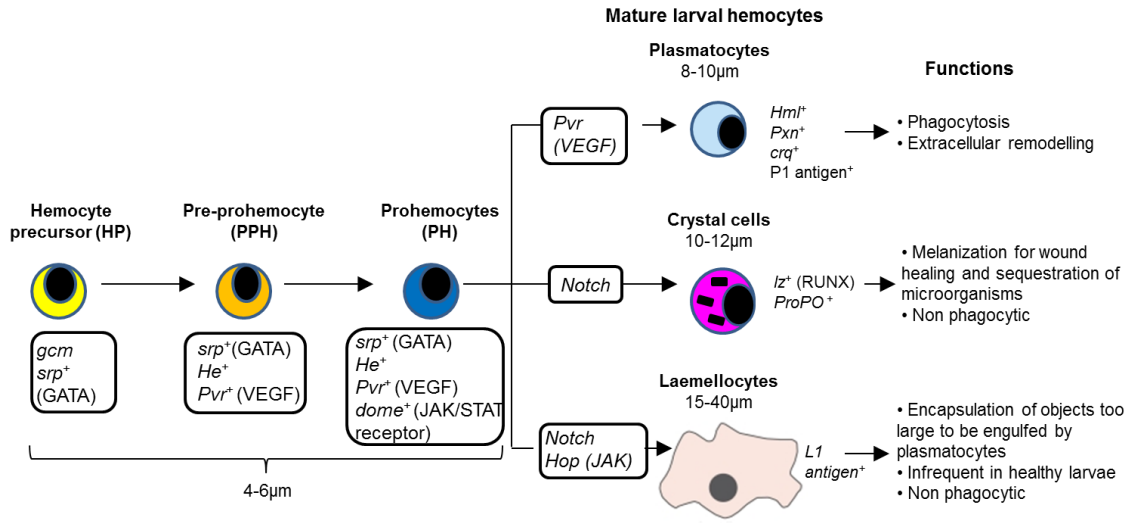


**B**

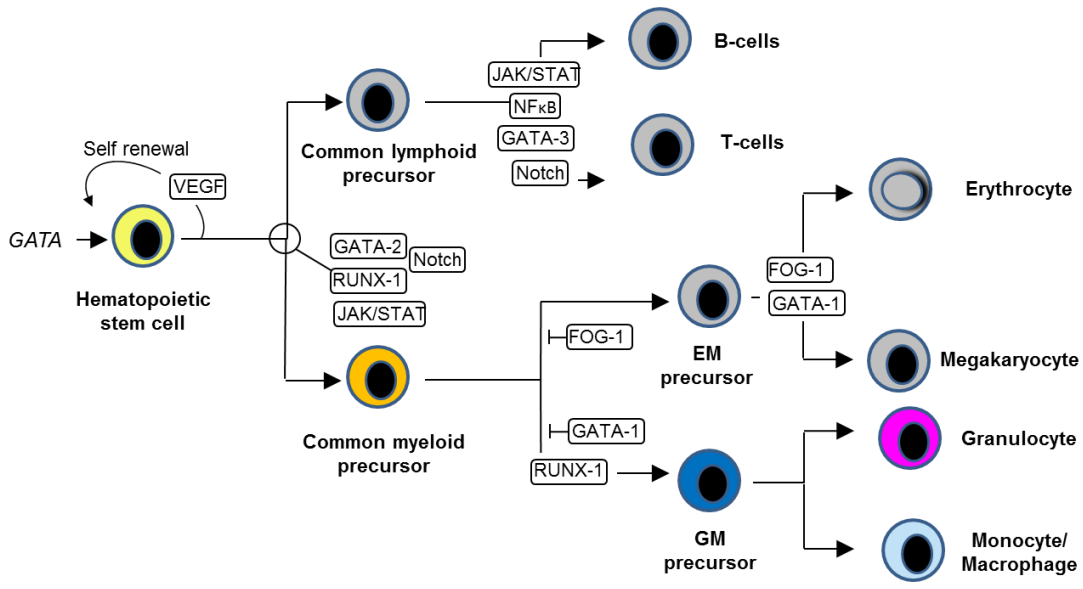


*Figure 1-3 Schematic diagrams of blood cell development in Drosophila and mammals*
**A.** Hemocyte precursors (HP) are the earliest lymph gland cells, expressing the *GATA*-like transcription factor *serpent* (*srp*) and glycophorin-like membrane molecule *Hemese* (*He*). Expression of the *VEGF*-like growth factor *Pvr* is then up regulated and cells become pre-prohemocytes (PPH). Prohemocytes (PH) then initiate expression of *dome*, a gp130-like JAK-STAT pathway receptor. *Dome* expression is then down regulated in PH before the necessary signalling pathways take over for the differential hemocyte subset development (*Notch*, *Pvr* and *Hop* the *Drosophila* JAK), and 'mature' hemocyte markers appear; *Hemolectin* (*Hml*), *Peroxidasin* (*Pxn*), *croquemort* (*crq*), *lozenge* (*lz*), and *prophenoloxidase* (*ProPO*). **B.** Comparative blood cell lineage development in mammals. Grey cells indicate cells which don't appear to have a counterpart in *Drosophila*. Schematic diagrams adapted from Jung et al. (2005) and Evans et al. (2003). GM (granulocyte macrophage precursor) EM (erythrocyte megakaryocyte precursor), *VEGF* (*Vascular endothelial growth factor*), JAK-STAT (Janus kinase, signal transducers and activators of transcription).

## 1.3 Plasmatocyte markers

### *1.3.1 Glial cells missing*

Plasmatocyte lineage differentiation is dependent upon expression of the transcription factor *glial cells missing* (*gcm*). Expression is observed between stages 5 and 11 of embryonic development in hemocyte precursors, however it is not expressed by fully differentiated plasmatocytes (Bernardoni et al., 1997). An antagonism between the expression of *gcm* and the *RUNX-1* related transcription factor *lz* by hemocyte precursors determines cell fate, differentiating as either plasmatocytes when *gcm* is the predominant transcription factor, or crystal cells when *lz* is the predominant transcription factor (Waltzer et al., 2003). In addition, mis-expression of *gcm* in crystal cell precursors is sufficient to change cell fate to from crystal cells to plasmatocytes (Lebestky et al., 2000). Interestingly, *gcm* has also been shown to play a role in hemocyte homeostasis, post haematopoiesis, in the fat body. Inhibition of the *gcm* interaction with *dPIAS* (*Drosophila* protein inhibitor of activated STAT) resulted in the development of melanotic tumours in larvae, furthermore this tumour development was shown to be dependent upon downstream activation of the JAK-STAT pathway (Jacques et al., 2009). These data are indicative of differential roles for *gcm* during *Drosophila* development.

### *1.3.2 Hemese*

*Hemese* (*He*) is a pan hemocyte marker, expressed by all three larval subsets as well as hematopoietic tissue at low levels. *He* expression commences during 2$^{nd}$ instar larval development and is expressed most strongly in the circulating population of larval hemocytes (Jung et al., 2005). HE exhibits similarity at amino acid level to a family of glycophorins expressed by mammalian erythrocytes. There is also evidence to suggest *He* plays a modulatory and suppressive role in the larval immune response, *He* knock down was shown to result in a significant over proliferation of hemocytes after parasitic wasp egg infection (Kurucz et al., 2003). The expression of *He* in adult fly plasmatocytes is

believed to be very low or non-existent (Kurucz et al., 2007b), yet detailed characterisation of expression in adults is yet to be determined.

### *1.3.3 Hemolectin*

*Hemolectin* (*Hml*) is a marker of fully differentiated plasmatocytes; expression is first observed late in embryonic development at stage 17 and persists throughout the remainder of *Drosophila* larval and pupal development. Adult *Drosophila* plasmatocytes have also been shown to express *Hml* (Clark et al., 2011, Agaisse et al., 2003). HML has homology with the human clotting protein, *Von Willebrand factor* (*VWF*) (Goto et al., 2001). Furthermore, bleeding defects have been identified in larvae which lack *Hml* (Goto et al., 2003). To date, *Hml* appears to be the most specific cell marker available for study of plasmatocytes in adult flies.

### *1.3.4 Peroxidasin*

Plasmatocytes also express the extracellular matrix remodelling enzyme *Peroxidasin* (*Pxn*) (Nelson et al., 1994). *Pxn* expression commences at stage 10 of embryogenesis, and is initially restricted to plasmatocytes, but later spreads to the fat body. *Pxn* is reported to be involved in tissue remodelling during *Drosophila* development, however the expression profile of *Pxn* in adult flies has not yet been characterised.

In vertebrates, peroxidase enzymes are heavily involved in the defence against bacterial pathogens. Hydrogen peroxide ($H_2O_2$) is a reactive oxygen species (ROS) secreted by vertebrate leucocytes in response to bacterial infection (Thannickal and Fanburg, 2000). When $H_2O_2$ meets a peroxidase enzyme, a more cytotoxic ROS is generated, which promotes infection clearance. *Drosophila* PXN contains a functional peroxidase domain which shares homology with human myeloperoxidase, with 39% of amino acids being identical and a further 28% being similar. The mechanism of PXN release is unclear, with the peroxidase domain only accounting for 606 of a total 1512

residues, suggesting that *Pxn* could have other unexplored functions. Nelson et al. (1994) alluded to a potential defence, immunological related role for *Pxn*, but this is yet to be confirmed.

### *1.3.5 Croquemort*

A further marker for mature plasmatocytes is the scavenger receptor *croquemort* (*crq*). CRQ has homology at the amino acid level to murine and human CD36 (Franc et al., 1996), and is thought to be required during development for the hemocyte mediated phagocytosis and clearance of apoptotic cells (Sears et al., 2003, Franc et al., 1999). Initially it was believed *crq* expression was restricted to hemocytes alone, as this is where expression is most strongly observed. However it has since become apparent that *crq* is expressed elsewhere in the fly, but the tissue specific expression profile of *crq* is yet to be characterised.

This thesis aims to further investigate plasmatocyte expression markers and the potential existence of plasmatocyte phenotypic subsets in adult flies, in particular by examining adult fly plasmatocyte derived expression of *Hml*, *Pxn* and *crq*.

## 1.4 Hemocyte functions in development

Plasmatocytes are described as the equivalent cell type to mammalian monocytes and macrophages; they share numerous developmental and functional characteristics. This section will discuss hemocyte roles during *Drosophila* development.

### *1.4.1 Apoptotic cell corpse clearance and tissue remodelling*

Hemocytes are involved in a number of processes during embryonic and larval development, much like mammalian macrophages one of their primary roles is phagocytosis. Significant cell death occurs during *Drosophila* development and hemocytes are involved in the disposal of the consequent apoptotic cell bodies, via the

scavenger receptor *crq* (Franc et al., 1999). In *Drosophila* mutants which lack hemocytes, programmed cell death occurs as it does in wild type embryos, suggesting cell death itself arises independently of hemocytes (Tepass et al., 1994). In addition to this, hemocyte depleted *Drosophila* are able to complete embryonic, larval and pupal development and reach adulthood healthily (Charroux and Royet, 2009). These data suggest that hemocytes participate in apoptotic corpse clearance during development; however this activity is not vital for survival.

Plasmatocytes also produce many proteins which are components of the extracellular matrix proteins, including *Pxn* and Collagen IV, which again poses a tissue remodelling role for plasmatocytes during development (Nelson et al., 1994, Fessler et al., 1994).

### *1.4.2 Hemocyte motility and surveillance during development*

*Drosophila* embryonic hemocytes are extremely motile and are able to migrate freely towards sites of inflammation (Stramer et al., 2005). In larvae, two distinct populations of hemocytes have been identified on the basis of their migratory behaviour; a population of sessile, cuticle bound hemocytes and a population of circulating hemocytes. After tissue wounding sessile hemocytes remain tissue bound, however as circulating hemocytes pass the wound site they become attached to it via a process termed ‘adhesive capture’. This process of adhesive capture is different to the migratory behaviour observed in *Drosophila* embryos, as the cells do not actively migrate towards the wound, but become attached to it on passing. These captured hemocytes are eventually released from the wound site once it is healed (Babcock et al., 2008). This suggests a surveillance related role for larval circulating hemocytes. Plasmatocytes in adult *Drosophila* are reported to be sessile and tissue bound (Elrod-Erickson et al., 2000), much like resident mammalian macrophages.

### *1.4.3 Hemocyte roles in central nervous system (CNS) development*

Hemocyte migratory behaviour during embryonic development is a highly regulated process, whereby cells follow very specific migratory routes (Wood and Jacinto, 2007). Hemocytes are responsible for the secretion of various extracellular matrix (ECM) molecules (Nelson et al., 1994), which in turn is vital for many normal embryonic developmental processes. Disruption of the *VEGF*-like factor *Pvr* in *Drosophila* embryos inhibits hemocyte migration along the ventral nerve cord. This results in a lack of ECM deposition by hemocytes and subsequently disrupts CNS development (Olofsson and Page, 2005). In addition to this, blocking of the hemocyte scavenger receptor *crq* has been shown to inhibit normal CNS development, due to a lack of apoptotic cell clearance (Sears et al., 2003).

## 1.5 Hemocytes in *Drosophila* immunity

In mammals macrophages are immune effector cells, they are able to produce a broad range of cytokines in response to infection (Cavaillon, 1994). This is also the case for *Drosophila*, plasmatocytes are able to produce cytokines in response to infection (Agaisse et al., 2003, Clark et al., 2011). Mammalian macrophages and fly plasmatocytes also play scavenging roles in immunity, rapidly phagocytosing potentially toxic products such as bacteria and metabolic products. Furthermore a reduction in phagocytic activity in both mammalian macrophages and fly plasmatocytes results in an increased susceptibility to infection in humans and flies respectively (Suzuki et al., 1997, Charroux and Royet, 2009). See Figure 1-4 for a comparative diagram of mammalian macrophage and fly plasmatocyte responses to challenge.

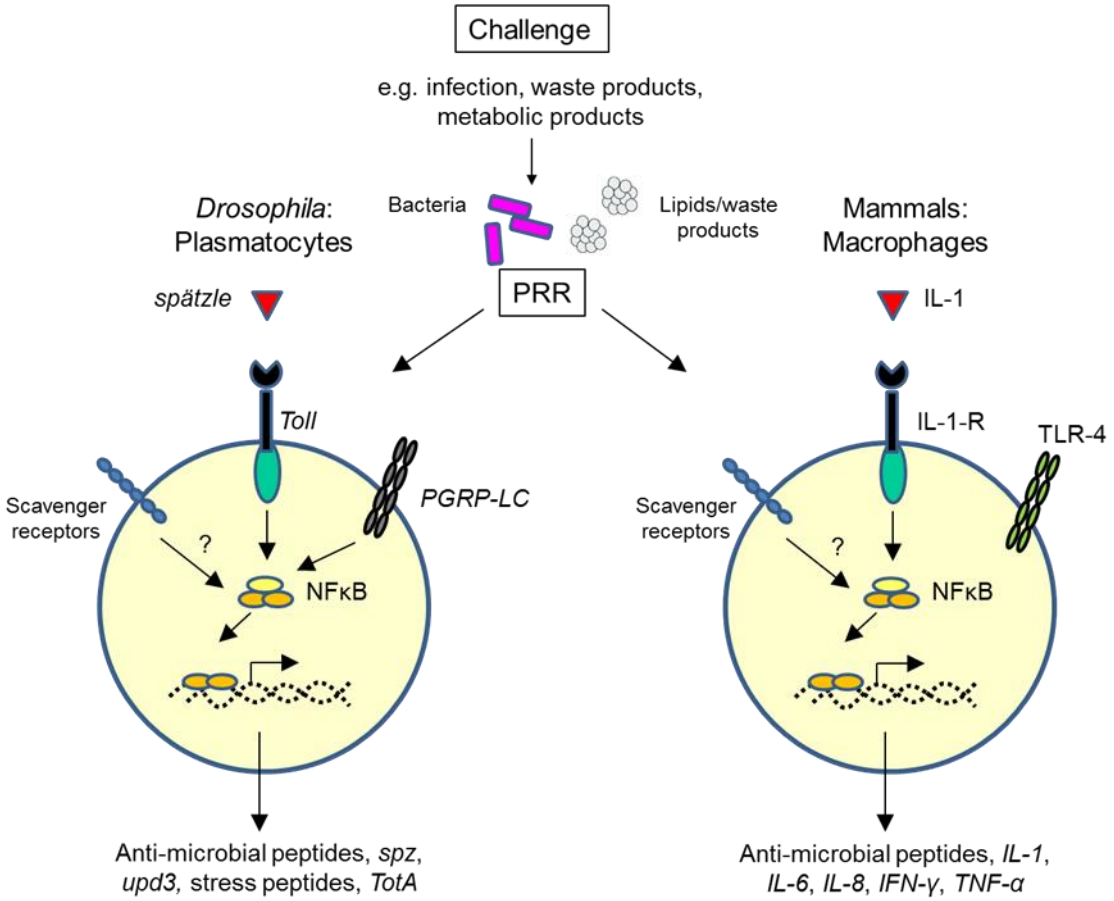


*Figure 1-4 Drosophila plasmatocyte and mammalian macrophage responses to challenge*
**Left**: fly plasmatocyte, expressing scavenger receptors and bacterial recognition receptors including *Toll* and *PGRP-LC* (*peptidoglycan recognition protein-LC*). Binding of external cue (bacteria, metabolic products or waste products) induces signalling cascades which results in the expression of various anti-microbial peptides (AMPs), *spätzle* (*spz*), *unpaired3* (*upd3*) and stress peptides such as *Turandot A* (*TotA*). **Right**: mammalian macrophage, expressing *IL-1R* (*interleukin 1 receptor*), *TLR-4* (*Toll like receptor-4*) and various scavenger receptors. Binding of ligand results in signalling cascade activation to induce expression of various cytokines, including *IL-1*, *IL-6*, *IFN-γ* and *TNF-α*.

*1.5.1 Plasmatocytes as immune effector cells in adult Drosophila*

Fly plasmatocytes have been shown to play a variety of immunological roles, they produce the *VWF*-like clotting factor *Hml* (Goto et al., 2003). Additionally, plasmatocyte depleted flies exhibit an increased susceptibility to bacterial infection, whilst mounting a wild type anti-microbial peptide (AMP) response, this susceptibility was proved to be due to a lack of plasmatocyte phagocytosis (Charroux and Royet, 2009). Similarly, polystyrene bead 'over-loading' induced inactivation of plasmatocyte phagocytosis, was shown to result in a diminished ability of the fly to deal with bacterial infection (Elrod-Erickson et al., 2000). Furthermore, various phagocytic receptors have been identified to be both expressed specifically by plasmatocytes and required for effective phagocytosis of bacteria. These include *eater*, a receptor which has been illustrated to specifically bind bacteria and to be required for plasmatocyte phagocytosis of bacteria (Kocks et al., 2005). In addition, *eater* null flies succumbed to bacterial infection significantly earlier than wild type flies, which was shown to be a direct result of a lack of plasmatocyte phagocytic activity. The receptor *nimrodC1* (*nimC1*), which is structurally similar to *eater*, has also been shown to modulate bacterial phagocytosis (Kurucz et al., 2007a). This suggests plasmatocytes possess bacterial recognition receptors, necessary specifically to limit infection progression and spread. These data imply an immune role for plasmatocytes, in infection clearance.

*1.5.2 Drosophila anti-microbial peptide (AMP) production: Toll and Imd*

The two major immune pathways in the fly are the *Toll* and *Imd* (*Immune deficiency*) pathways (Figure 1-5), their activation is responsible for an up regulation of AMPs and cytokines in response to infection (Lemaitre and Hoffmann, 2007). Aside from hemocytes, the fat body, an organ analogous to the mammalian liver is the most important immune tissue in the fly, being the major producer of AMPs upon immune challenge (Manfruelli et al., 1999). Three *NFκB*-like transcription factors regulate *Toll* and *Imd*

pathway AMP expression, these are *Dif* (*Dorsal-related immunity factor*), *dorsal* and *Rel* (*Relish*) (Ip et al., 1993, Reichhart et al., 1993, Dushay et al., 1996). *Dif* and *dorsal* are primarily involved in *Toll* pathway activation and *Rel* is involved in *Imd* pathway activation. Interestingly, the AMP expression profile mounted in response to infection has been shown to differ significantly dependent on the infectious agent (Lemaitre et al., 1997).

The *Toll* pathway has evolutionarily conserved similarities with the vertebrate *IL-1R* pathway (Gay and Keith, 1991). After infection *spätzle* (*spz*) is cleaved allowing it to bind its cognate receptor *Toll*. *Toll* receptor engagement causes a downstream signalling cascade, ultimately resulting in the transcription of target genes, including the major *Toll* pathway AMP *Drosomycin* (*Drs*) via the *NFκB*-like transcription factors *Dif* and *Dorsal*. *Toll* activation occurs specifically in response to gram positive bacteria and fungi (Lemaitre et al., 1996, Ip et al., 1993). Hemocytes themselves are believed to express the *Toll* receptor and to play a part in the propagation of *Toll* pathway signalling (Rosetto et al., 1995). Irving et al. (2004) observed a hemocyte specific up regulation of *spz* expression in response to infection in larvae, making more *spz* available in the hemolymph for cleavage, thus increasing *Toll* pathway activation in other tissues and consequently increasing AMP expression. This hemocyte mediated rise in *Toll* pathway AMP transcription promotes infection clearance and therefore *Drosophila* survival.

The *Imd* pathway was first described by Lemaitre et al. (1995), flies with a recessive mutation in the *Imd* gene showed an impaired AMP response to infection. It has more recently been shown that the *Imd* pathway is principally responsible for the AMP response mounted to gram negative bacteria (Kaneko et al., 2004, Kaneko and Silverman, 2005). Hemocyte cell lines have been shown to be capable of producing AMPs, via activation of the *Imd* pathway. The predominant *Imd* pathway AMP, *Diptericin* (*Dpt),* is made by hemocyte derived mbn-2 cells in response to gram negative peptidoglycan exposure (Stenbak et al., 2004). In addition, expression of the bactericidal peptide

*Cecropin A1* (*CecA1*) is induced in mbn-2 cells upon infection (Samakovlis et al., 1992). These findings are yet to be replicated in hemocytes *in vivo*, but could indicate hemocytes as potential producers of certain AMP genes alongside the fat body.

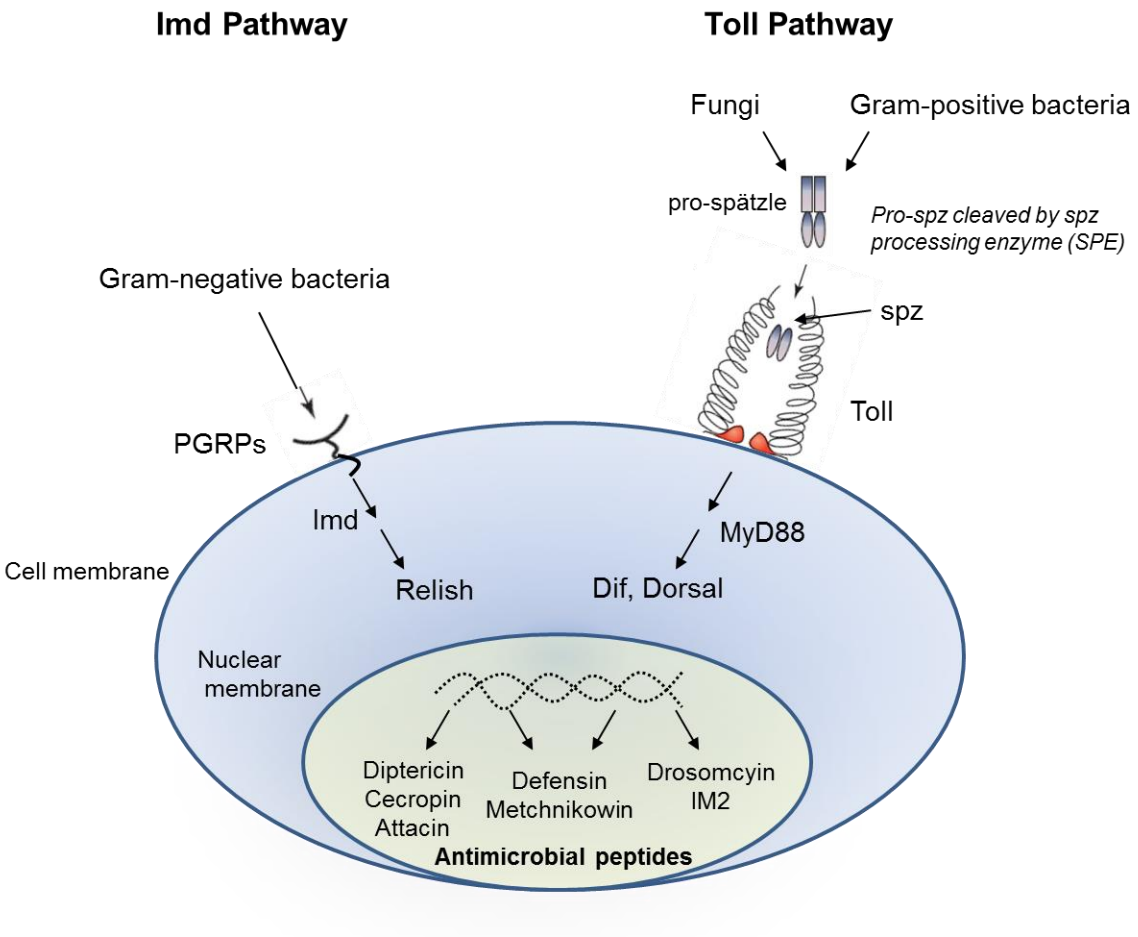


*Figure 1-5 Two pathway model for induction of antimicrobial peptide expression by the fat body* Anti-microbial peptide (AMP) production is induced through two different signalling cascades; the *Toll* and *Immune deficiency* (*Imd*) pathways. **Left:** *Toll* is activated by Gram positive bacterial and fungi, and **right:** *Imd* signalling occurs in response to Gram negative bacterial infections. Both pathways activate *NFκB*-like transcription factors *Dif*, *Dorsal* (*Toll*) and *Relish* (*Imd*) inducing AMP transcription of target AMP genes including; *Diptericin*, *Cecropin*, *Attacin*, *Defensin*, *Metchnikownin*, *Drosomycin* and *IM2*. Figure is adapted from Tanji and Ip (2005).

*1.5.3 Drosophila cytokine production*

Like mammalian macrophages, plasmatocytes have been shown to play an immune signalling role through the production of cytokines. The fly JAK-STAT pathway cytokine *unpaired3* (*upd3*) is produced by plasmatocytes in adult flies in response to bacterial infection (Agaisse et al., 2003). Furthermore subsets of adult fly plasmatocytes have been demonstrated to produce the TGF-β related cytokines *dpp* and *daw* in response to infection (Clark et al., 2011).

*1.5.4 JAK-STAT pathway in fly immunity*

The JAK-STAT pathway is required for multiple processes in embryogenesis including embryonic segmentation, tracheal development, oogenesis and spermatogenesis, as well as playing an immunological role (Hombría and Brown, 2002, Dearolf, 1999). The *Drosophila* genome codes for a single JAK, *Hopscotch* (*hop*), (Binari and Perrimon, 1994) and a single STAT, *Stat92E* (Hou et al., 1996, Yan et al., 1996). The JAK-STAT pathway receptor is DOME, a transmembrane receptor which encompasses a cytokine binding homology module and exhibits similarities to the mammalian IL-3R (Interleukin-3 receptor) and IL-6R (Interleukin-6 receptor) receptor families (Brown et al., 2001). The JAK-STAT family ligands are secreted proteins known as, *unpaired* (*upd*), *unpaired2* (*upd2*) and *upd3* (Harrison et al., 1998, Hombría et al., 2005, Agaisse et al., 2003).

The *upds* have been likened to *IL-6* (*Interleukin-6*) cytokines, on account of the structural similarity of *Drosophila* DOME to the mammalian gp130 subunit of the IL-6R, however, in terms of homology and structure, the *upds* themselves exhibit little similarity to IL-6 (Harrison et al., 1998). Research to date indicates *upd* is crucial for embryonic segmentation, with *upd* mutant flies exhibiting the same developmental segmentation defects as *hop* and *Stat92E* mutants (Harrison et al., 1998). *Upd2* has recently been described to be involved in regulating metabolic homeostasis in the fly, signalling the fed state much like mammalian *leptin* (Rajan and Perrimon, 2012).

Of the *upds*, it appears that *upd3* is the most immunologically relevant. Agaisse et al. (2003) demonstrated that plasmatocytes in adult flies are able to produce *upd3* in response to infection with a mixture of gram positive and negative bacteria. Binding of *upd3* to its cognate receptor *dome* was shown to be required for fat body derived expression of *TotA* (*Turandot A*), a general stress peptide which accumulates in the hemolymph. *TotA* accumulation was most significant in gram negative, *E. coli* infected flies comparatively to gram positive *M. luteus* infected flies. Most interestingly fat body *Imd* pathway activation was shown to be necessary for *TotA* expression via the *NFκB* transcription factor *Rel*. These data indicate an interaction between the JAK-STAT and *NFκB* immune pathways in the fly (Agaisse et al., 2003). Interestingly, *TotA* expression is also up regulated in response to other stress conditions, including ultra violet light exposure, and heat shock (Ekengren and Hultmark, 2001). However, the specific role of *TotA* during infection and stress conditions is yet to be fully understood.

Further immunological roles of the JAK-STAT pathway include the induction of complement C3-like protein *Tep2* (*Thioester-containing protein 2*) in response to infection in adult flies (Lagueux et al., 2000). JAK-STAT signalling has also been shown to play a role specifically in the fly antiviral response. JAK-STAT deficient flies infected with *Drosophila* C Virus (DCV) were incapable of controlling viral load, ultimately resulting in their early death from viral infection comparatively to JAK-STAT competent wild type controls. However, interestingly JAK-STAT deficient flies were still able to mount a wild type AMP response to bacterial infection (Dostert et al., 2005). See Figure 1-6 for a model of plasmatocyte mediated *upd3* expression and JAK-STAT pathway activation, including a potential interaction with the *Imd* pathway.

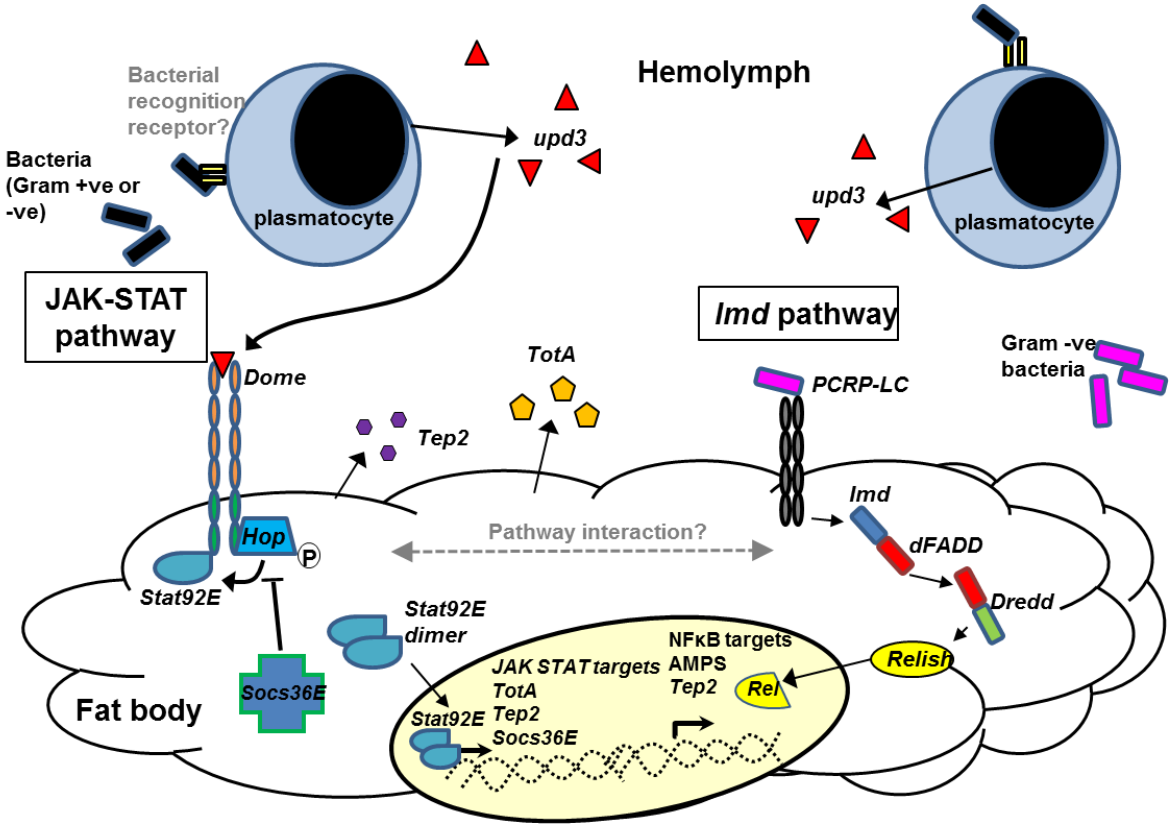


*Figure 1-6 Plasmatocyte derived upd3 activation of JAK-STAT target genes in the fat body and potential Imd pathway interaction*

**Left:** the JAK-STAT pathway; plasmatocytes are stimulated to produce *upd3*, both the plasmatocyte expressed receptor which recognises bacteria and downstream signalling pathways involved in *upd3* transcription are yet to be clarified. Plasmatocyte secreted *upd3* then binds fat body derived *dome*, resulting in *hop* (JAK) activation, which in turn activates *Stat92E*, which dimerises and translocates to the nucleus, initiating transcription of downstream JAK-STAT target genes. **Right:** the *Imd* pathway; upon bacterial binding of *PGRP-LC*, *Imd* is recruited to the *PCRP-LC* (peptidoglycan recognition protein LC) receptor, which interacts with *dFADD*, which itself binds the apical caspase *Dredd* (*Death related ced-3/Nedd2-like protein*). *Dredd* caspase is thought to cleave *Relish*, allowing the *Rel* domain to translocate to the nucleus, resulting in *Imd* pathway target gene transcription. Figure adapted from Hombría and Brown (2002) and Lemaitre and Hoffmann (2007).

## 1.6 The mammalian immune system and metabolism

The prevalence of high fat diet induced diseases including type II diabetes, atherosclerosis and metabolic syndrome have dramatically risen in recent years (Szendroedi and Roden, 2009, Van Herpen and Schrauwen-Hinderling, 2008). Investigation into the mechanisms behind high fat diet diseases has highlighted the immune system as a key mediator of disease pathology (Biswas and Mantovani, 2012, Festa et al., 2002, Xu et al., 2003, Feuerer et al., 2009).

### *1.6.1 Mammalian macrophages in metabolism*

The development and progression of many high fat diet induced diseases has been linked to the macrophage response to chronic dietary lipid exposure. An abundance of lipid laden macrophages known as foam cells, are found in and around atherosclerotic lesions (Rahaman et al., 2006). The macrophage presence in these diseased plaque locations is suggestive of their potential contribution to the ensuing pathology (Glass, 2002). The interaction between blood lipoproteins and macrophage derived scavenger receptors has been proposed as a key component in the atherosclerotic disease mechanism (Suzuki et al., 1997, Rahaman et al., 2006). Macrophages are responsible for both innate immune responses and scavenging, the high fat diet induced accumulation of intracellular lipid and the main effector function of the cell as producers of inflammatory cytokines, could provide a connection between macrophage lipid uptake and the pathology observed in high fat diet induced diseases (Linton and Fazio, 2003).

It largely believed that macrophage recruitment, activation and/or response to fat is pro-inflammatory and results in a disruption of metabolism (Odegaard et al., 2007, Weisberg et al., 2003, Kanda et al., 2006, Kamei et al., 2006), however, the significance of macrophage responses to lipids and the mechanisms and pathways involved in high fat diet induced disease pathology remain unclear. Studies investigating the metabolic effects of macrophage depletion offer conflicting findings, in terms of pro-inflammatory

molecule production and insulin resistance (Feng et al., 2011, Lanthier et al., 2010, Clementi et al., 2009). One study illustrated that a depletion of $CD11c^+$ bone marrow derived cells including activated monocytes and macrophages, improved inflammation and insulin resistance in obese mice (Patsouris et al., 2008). However conversely, fat uptake by murine peritoneal macrophages has been shown to be associated with suppression, rather than activation of pro-inflammatory gene expression (Spann et al., 2012).

Thus, while there is much evidence in mammals to suggest that increased fat consumption promotes both inflammation and the risk of high fat diet related diseases; existing evidence does not strongly support the idea that targeting macrophages alone is sufficient to decrease the overall disease pathology. A better understanding of macrophage functions is required to allow for the development of better preventive and therapeutic strategies.

### *1.6.2 Fly plasmatocyte response to diet*

Mammalian macrophages and *Drosophila* plasmatocytes share multiple developmental and functional similarities. This makes plasmatocytes powerful candidates for further investigation into the *in vivo* roles of macrophages in both dietary lipid scavenging and sensing and how this leads to the induction of a metabolic imbalance and the consequent development of high fat diet induced diseases.

To date, the role of fly plasmatocytes in metabolism, and specifically their response to excess dietary lipid exposure is yet to be studied *in vivo*. However, an *in vitro* study using hemocyte cell lines has illustrated that hemocytes are able to successfully scavenge lipoproteins (Abrams et al., 1992). This thesis will address the role of *Drosophila* plasmatocytes in response to lipid rich diet.

## 1.7 *Drosophila* metabolism

### *1.7.1 High fat diet associated diseases in the fly*

The lifespan of high fat diet fed flies is significantly reduced (Driver and Cosopodiotis, 1979, Heinrichsen and Haddad, 2012), this reduction in lifespan coincides with an increase of both glucose and triglyceride levels and the emergence an insulin-like resistance in flies (Birse et al., 2010, Heinrichsen and Haddad, 2012). These metabolic changes are indicative of the development of a metabolic-like syndrome and insulin pathway dysregulation in high fat diet fed flies. Furthermore, upon a high fat diet, flies have been shown to exhibit a reduction in geotaxic activity, preferentially staying at the bottom of food vials, the opposite of their natural behaviour. Cardiac function was also impaired when flies were exposed to a high fat diet, with a rise in heart derived triglycerides, impaired contractility and a destruction of myofibrillar organisation (Birse et al., 2010).

It appears the fly suffers many of the same metabolic disease symptoms upon exposure to high fat diet as vertebrates do. This makes *Drosophila* an extremely interesting model to try to determine high fat diet disease mechanisms and particularly the role plasmatocytes may play in high fat diet induced pathology.

### *1.7.2 Drosophila fat body: the metabolic hub*

In addition to being a major AMP producing tissue (Manfruelli et al., 1999), the fat body is the primary metabolic tissue in the fly, it is responsible for the metabolism of fly lipids, carbohydrates, nitrogen and amino acids, as well as being a major site of protein synthesis (Arrese and Soulages, 2010). It is described as analogous to the mammalian liver and adipose tissue and also acts as a storage location for glycogen and lipid reserves during development (Canavoso et al., 2001). The fat body is distributed throughout the *Drosophila* body, in lobes bathed by hemolymph, enabling the rapid detection of changes in the levels of circulating hormones and concentrations of energy precursors, allowing

for the subsequent rapid orchestration of appropriate responses to these changes (Arrese and Soulages, 2010).

The larval fat body serves as an energy store during pupal development and in early adulthood, however larval fat body cells are diminished during the first days after eclosion (Aguila et al., 2007). During this time new fat body tissue develops in adult flies to perform the same energy storage function (Hoshizaki et al., 1995).

In addition to the fat body, hepatocyte-like cells known as oenocytes also facilitate lipid metabolism, they act downstream of the fat body and have important roles in regulating growth, development and feeding behaviour. Oenocytes in adult flies are located in the abdominal integument and are arranged in clusters along the inner cuticle surface (Krupp and Levine, 2010). Oenocytes express 22 orthologues of mammalian fat metabolism genes and function to accumulate lipids released from the fat body during periods of starvation, somewhat like mammalian hepatocytes (Gutierrez et al., 2006). See Figure 1-7 for a diagram of metabolic homeostatic mechanisms involving the fat body and oenocytes in larvae.

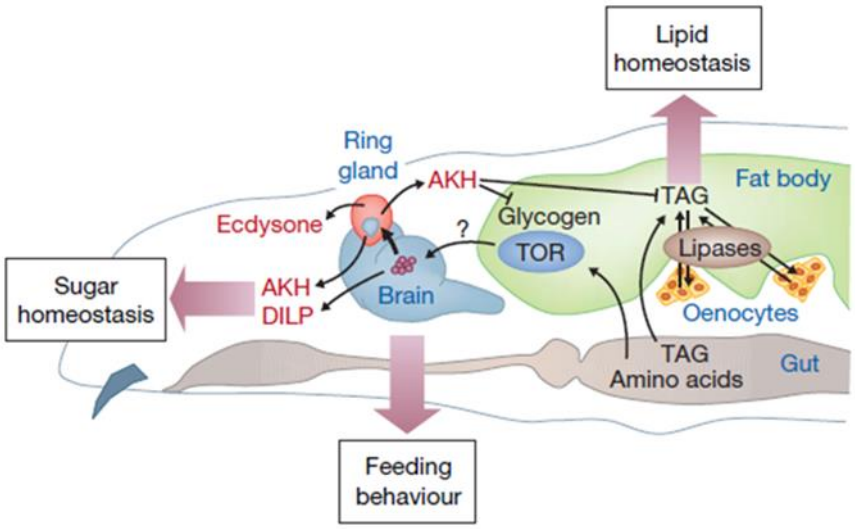


*Figure 1-7 Metabolic homeostasis mechanisms in larvae*
Glucose homeostasis is maintained by IPCs (insulin producing cells) in the brain and the ring gland, which produce both *Dilps* (*Drosophila insulin like peptides*) and *AKH* (*Adiopkinetic hormone*). Upon *AKH* stimulation in the fat body, glycogen phosphorylase is activated and sugar in the form of trehalose is released into the hemolymph. Upon starvation conditions the fat body releases fat which is picked up by oenocytes for energy production. In addition lipases are also activated in starvation conditions. Figure is taken from Leopold and Perrimon (2007). Hormones are in red, tissues/organs in blue. TAG (Triacylglycerol), TOR (Target of Rapamycin).

*1.7.3 TOR– Insulin pathway regulation of lipid metabolism*

TOR (target of rapamycin) is a conserved serine/threonine kinase which is involved in regulating cell growth and metabolism (Wullschleger et al., 2006). Interestingly, detrimental high fat diet induced phenotypes, including cardiac dysfunction and a rise in whole fly triglycerides and glucose could be rescued in TOR mutant flies. (Birse et al., 2010). Furthermore, wild type flies fed a high fat diet were shown to exhibit an increase in *Dilp2* (*Drosophila insulin like peptide 2*) transcript levels and a reduction in phosphorylated Akt, indicative of an insulin pathway dysregulation, however both of these phenotypes were ameliorated in flies lacking TOR (Birse et al., 2010). TOR mutant flies also exhibited a concurrent increase and decrease in the expression levels of *brummer* (*bmm*) lipase and *fatty acid synthase* (*FAS*) respectively, these findings are suggestive of a TOR pathway regulation of the balance between lipid anabolism and catabolism (Birse et al., 2010, Birse and Bodmer, 2011). These data therefore indicate an important role for the TOR-insulin signalling pathways in the development and progression of high fat diet disease pathology. It could be speculated that the 'overloading' of these metabolic pathways with lipid leads to malfunction and consequently renders the fly unable to maintain metabolic homeostasis.

*1.7.4 Drosophila metabolic regulation in fed and starved states*

The steroid hormone *ecdysone* (*20-hydroxyecdysone*), is a negative regulator of *Drosophila* growth via inhibition of insulin pathway signalling, together insulin and *ecdysone* mediate growth and regulate organism size (Colombani et al., 2005). In the fed state, insulin producing cells (IPCs) in the brain release *Drosophila insulin like peptides* (*Dilps*) into the hemolymph. These Dilps bind to the insulin receptor (InR) resulting in activation of the insulin receptor substrate, CHICO, which phosphorylates the downstream pathway antagonist, Akt, which in turn phosphorylates FOXO, rendering it inactive in the cytoplasm and therefore preventing transcription of starvation response

genes, and ultimately promoting nutrient storage in the fat body (Baker and Thummel, 2007). Simultaneous to this, insulin signalling also promotes TOR activation; activated TOR phosphorylates S6 Kinase (S6K) which promotes protein synthesis and cell growth. *Akt* is thought to be an important link between the insulin and TOR pathways, both of which are collectively vital for sufficient growth and nutrient sensing homeostasis (Oldham, 2011).

Conversely, during periods of fasting, TOR activity is lessened and lack of FOXO phosphorylation means it is able to translocate to the nucleus, inducing transcription of target starvation response genes. TOR can also act to act on 4E-BP in conditions of nutrient stress. 4E-BP acts as a metabolic brake to control lipid metabolism, in order to preserve energy stores and promote survival (Teleman et al., 2005). Furthermore, during periods of fasting, adipokinetic hormone (AKH) acts like mammalian glucagon, promoting breakdown of energy stores in the fat body (Schlegel and Stainier, 2007).

In addition to these mechanisms, the fly homolog of mammalian *Perilipin* known as *lipid storage droplet 2* (*lsd2*), found on cellular lipid droplets, acts to promote lipid storage as well as to maintain cellular lipid distribution during fed conditions (Grönke et al., 2003, Welte et al., 2005). Conversely, in starvation periods, *bmm* an *lsd* associated lipase, acts to break down stored TAG to promote energy release (Grönke et al., 2005). These metabolic processes are illustrated during both fed and starved states in the fat body in Figure 1-8.

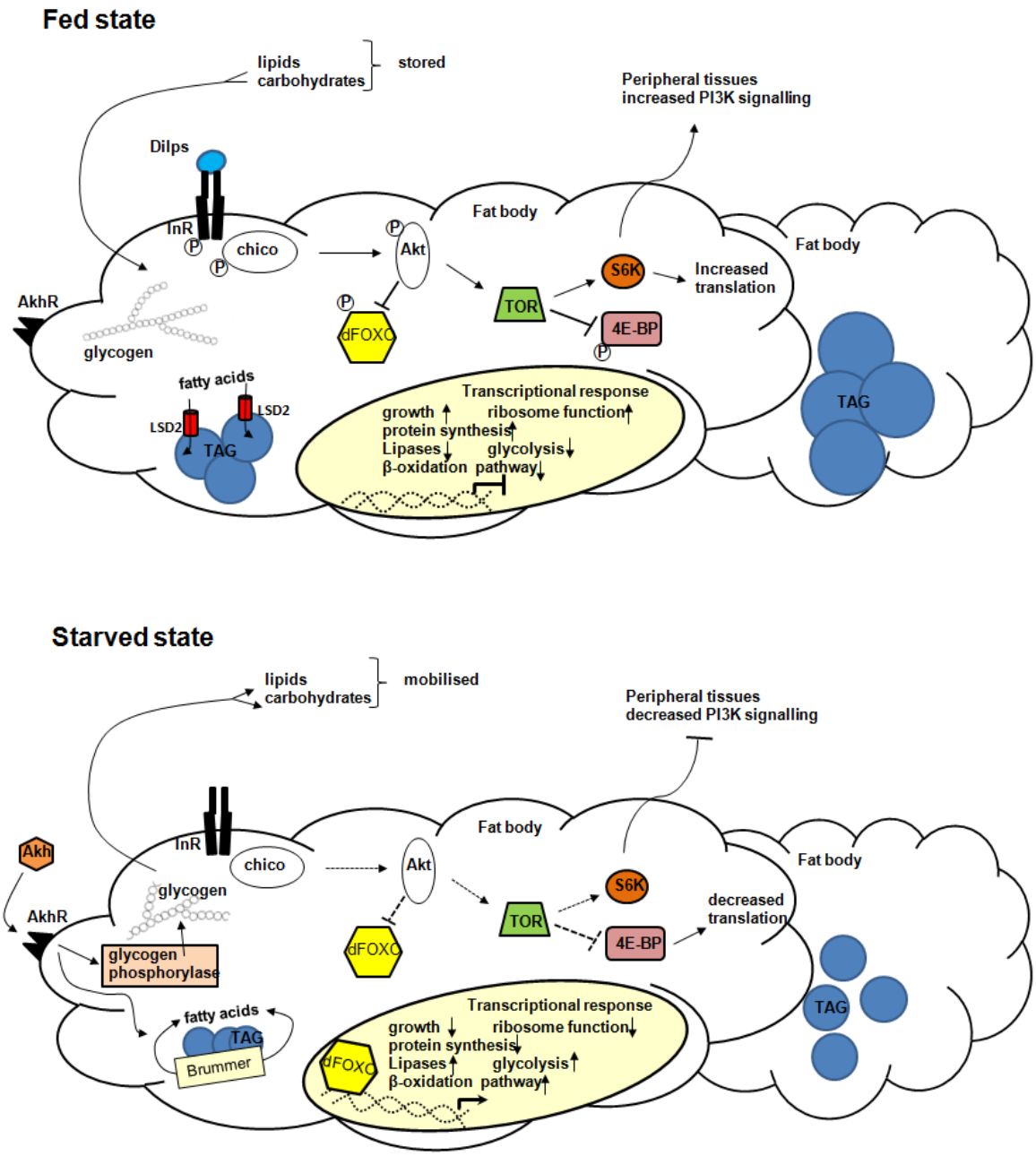


*Figure 1-8 Model of Drosophila fat body metabolism in fed and starved states*
Solid arrows depict active signalling cascades, and dotted lines depict regulatory mechanisms which become active when that signalling pathway is not active. *Dilps* (*Drosophila insulin like peptides*), AkhR (adipokinetic hormone receptor), InR (insulin receptor), TAG (triacylglycerol), TOR (target of rapamycin), S6K (S6 kinase), PI3K (phosphoinositide-3-kinase), LSD2 (lipid storage droplet 2). Figure adapted from (Baker and Thummel, 2007).

### *1.7.5 JAK-STAT pathway and diet*

The JAK-STAT pathway appears to not only be relevant in terms of immunology, but also in metabolism. A recent study identified *upd2* as a metabolic homeostasis regulator, homologous to vertebrate *leptin*, signalling the fed state in *Drosophila* (Rajan and Perrimon, 2012). During periods of starvation *upd2* expression was dramatically reduced, and flies deficient in *upd2* were significantly smaller than controls. Interestingly, *upd2* was shown to activate JAK-STAT signalling in a population of GABAergic neurones in the brain, which project into the IPCs. This JAK-STAT pathway activation resulted in a loss of the GABAergic neurone inhibitory action and the consequential promotion of *Dilp* release by the IPCs, hence promoting growth. These findings are suggestive of a new metabolic role for the *upd* family, and thus the JAK-STAT pathway (Rajan and Perrimon, 2012).

It has already been shown that plasmatocytes express *upd3* during bacterial infection (Agaisse et al., 2003). It would be interesting to explore further roles of the *upd* cytokines and the JAK-STAT pathway in response to conditions of stress, such as chronic high fat diet exposure, this is another question which this thesis will address.

### *1.7.6 The fly as a model system for high fat diet induced diseases*

The fly is a particularly tractable model for examination of the systemic and cell specific metabolic and inflammatory responses to lipids. There are a multitude of reasons for this, including the existence of a wide range of mutant fly lines and the ease at which new mutations can be induced. RNA interference (RNAi) lines are also readily available for a huge majority of the *Drosophila* genome. In addition a library of fluorescent reporter fly lines exist, meaning expression of given genes can be followed visually, *in vivo* during development or in response to different cues. These sophisticated genetic and molecular tools allow for screening of mutant and knock down fly lines for phenotypes of interest (Beckingham et al., 2007).

In addition, the Gal4-UAS expression system (Brand and Perrimon, 1993) enables not only cell and tissue specific driven expression of a given target, be it a fluorophore, or an RNAi, but fundamentally it provides a tool for studying the effect of a given gene, on a specific cell type, thus taking into account the importance that gene may have elsewhere in the fly. The cell and tissue specific limitations encountered in human and rodent models are particularly abundant when studying the macrophage specific response to lipids. Thus the fly is an extremely useful model to study the role of different tissues in high fat diet induced diseases *in vivo*.

## 1.8 Thesis outline

### *1.8.1 Fly plasmatocytes as models for the mammalian macrophage response to dietary lipids*

This thesis focuses on the plasmatocyte response to chronic dietary lipid exposure and the systemic effects that plasmatocytes may mediate during the course of high fat diet induced disease progression. Previous studies have highlighted the close relationship between mammalian macrophages and the induction and progression of high fat diet induced diseases (Linton and Fazio, 2003). This thesis aims to further clarify the mechanisms involved in the development of high fat diet induced diseases using the fly as a model.

*Drosophila* are an attractive model, as the vast array of genetic tools available mean that tissue specific knock down of candidate genes of interest can be carried out with ease. Furthermore, studies have already indicated the induction of a metabolic-like syndrome in flies upon high fat diet (Birse et al., 2010), which again supports the fly as a high fat diet induced disease model. In addition, the relatively short lifespan of the fly means lifelong survival experiments are possible, which is rarely the case in other animal models.

### *1.8.2 General hypothesis*

Plasmatocytes, like mammalian macrophages, influence the development and pathological consequences of high fat diet induced diseases in flies.

### *1.8.3 Thesis structure*

Materials and methods used during the course of this study are described in Chapter 2. Chapter 3 describes the generation and development of various tools and techniques, which allowed for the in depth study of adult *Drosophila* plasmatocytes. This includes the cloning of plasmatocyte reporter flies and plasmatocyte proliferation marker 'Fucci flies' (fluorescent ubiquitination based cell cycle indicator). Chapter 3 also characterises plasmatocytes in adult *Drosophila*, in terms of numbers, motility, proliferative potential and expression markers. A protocol for plasmatocyte FACS (fluorescence-activated cell sorting) was additionally established allowing for the purification of plasmatocytes from adult flies, the development of this technique, which is published in Clark et al. (2011), is also described in Chapter 3.

Chapter 4 describes the effect of different dietary lipids upon *Drosophila* lifespan. The metabolic and immunological effects of chronic high fat diet exposure are also examined over time. Additionally experiments using FACS sorted plasmatocytes from control diet and high fat diet flies illustrated that plasmatocytes from high fat diet fed flies accumulated intracellular lipids, much akin to mammalian macrophage foam cell formation (Rahaman et al., 2006). Furthermore, flies fed a high fat diet up regulated expression of the cytokine *upd3*. This was extremely interesting, as the *upd3* analogue, *IL-6*, has been shown to be up regulated in many high fat diet related diseases in vertebrates (Bastard et al., 1999, Mohamed-Ali et al., 1997).

To examine the plasmatocyte specific role of high fat diet induced diseases and the up regulation of *upd3*, plasmatocyte depleted flies were generated. Interestingly, survival of flies lacking plasmatocytes upon lipid rich diets was actually enhanced

comparatively to wild type plasmatocyte competent flies. The metabolic and immunological profiles of these flies were also examined at various time points. Interestingly, plasmatocyte-less flies did not display an increase of *upd3* expression after chronic high fat diet exposure. This finding suggested that plasmatocytes may be responsible for the increase in *upd3* levels or for the regulation of *upd3* production by other tissues in high fat diet fed flies.

Chapter 5 describes a screen for detection of plasmatocyte expressed scavenger receptors which may be involved in lipid uptake. Of the scavenger receptors screened, *nimC1* and *crq* were confirmed to be expressed by adult *Drosophila* plasmatocytes and their knock down in plasmatocytes resulted in a significant reduction of lipid uptake. This led to the pursuit of these two candidate genes for the effect that their plasmatocyte specific knock down may have upon the survival of high fat diet fed flies. Intriguingly, a loss of *crq* expression specifically in plasmatocytes rescued survival of flies upon high fat diet to the survival phenotype observed in control genotype, *crq* competent, flies upon control diet. Metabolic and inflammatory profiles were subsequently examined in these flies, findings illustrated that a lack of plasmatocyte specific *crq* expression also resulted in a reduction of *upd3* expression.

Due to the elevation of *upd3* expression observed in wild type flies after chronic high fat diet exposure and the lack of this up regulation observed in plasmatocyte-less and plasmatocyte specific *crq* knock down flies, the effect of plasmatocyte specific *upd3* knock down upon survival and metabolism in high fat diet fed flies was investigated in Chapter 6.

Chapter 7 is a discussion of the data presented in the results chapters in relation to what is already known in the literature, and comparatively to the appropriate mammalian counterpart genes.

# Chapter 2 Materials and Methods

## 2.1 *Drosophila melanogaster* maintenance

### *2.1.1 General fly stock maintenance*

*Drosophila* were kept in incubators at 60% humidity, at either 18°C, 25°C or 29°C running with 12hr light: 12hr dark cycles in order to maintain fly circadian rhythm (Konopka and Benzer, 1971). Individual non-experimental stocks were kept in duplicate, in plastic vials (90mm height, 25mm diameter) containing approximately 8ml of control diet food in 18°C incubators until required, at which point the required stock would be expanded and moved to 25°C incubators. Fly stocks were transferred without $CO_2$ anaesthesia to fresh food vials every 4-5 weeks. Stocks were also checked at regular intervals for the correct phenotypic characteristics and mite contamination.

### *2.1.2 Experimental flies*

Flies involved in any experiment included in this thesis were kept at 25°C until they were required for either sample collection or imaging. The only exception to this was when temperature sensitive $Gal80^{ts}$ stocks were used (see section 2.2.3 in this chapter for further details on $Gal80^{ts}$ stocks), in which case these stocks were kept at 18°C until inhibition of $Gal80^{ts}$ was required, at which point flies were switched to 29°C. Male flies were used for all experiments unless otherwise stated, due to the differences induced in female flies after mating (McGraw et al., 2004).

### *2.1.3 Discrimination of males and females*

Flies were anaesthetised under a light microscope on porous gas pads with $CO_2$; physical separation of flies was carried using a soft bristled paint brush. Males and females can be easily distinguished through genital differences; in addition males are smaller and have darker melanin pigmentation, and different patterning (Ashburner, 1989). A further sex marker is the presence of sex combs, structures on the first pair of legs of male flies.

These structures are used by males during mating for attachment to females (Ashburner, 1989).

*2.1.4 Virgin collection and crosses*

Virgin females were separated from males within the first five hours following eclosion, during which period they do not mate (Ashburner, 1989). Vials containing hatching pupae were cleared of all adults and left for five hours for further virgin collection. All adults present after this were presumed to have eclosed during that five hour window and to be virgins. Virgin females were also distinguished visibly, through their lighter pigmentation and a dark patch on their abdomens (Greenspan, 2004). Collected virgin females were then kept in separate vials, on control diet at 25°C for 3 days before carrying out crosses, to ensure they were in fact virgins and that no eggs or larvae were present, any vials containing eggs or larvae and therefore, non-virgins were discarded.

Fly crosses were carried out in standard plastic vials containing approximately 6-7 virgin female flies and approximately 5 males. For each cross carried out, all virgin females used were of the same genotype and were crossed to males of the same genotype. This was done to ensure that all the male progeny inherited the same X chromosome from their mothers and Y chromosome from their fathers, therefore reducing the genetic variation between experimental flies. Crosses were kept at 25°C, allowing for collection of progeny approximately 10 days after performing the cross. Male flies were collected from crosses in an age matched manner for use in various experiments described later in this chapter. Crosses involving temperature sensitive $Gal80^{ts}$ fly lines were an exception to this rule and were carried out at 18°C in order for successful $Gal80^{ts}$ repression of Gal4 activity during development.

## 2.2 *Drosophila* stocks

During the course of this thesis various *Drosophila melanogaster* stocks were used, which are described and listed below.

### *2.2.1 Wild type stocks*

The $w^{1118}$, white eyed wild type line, with isogenic X, 2 and 3 chromosomes, was predominantly used as a wild type control stock. Furthermore, $w^{1118}$ flies were also used in crosses to generate heterozygote experimental control flies. Oregon-R flies were used as a second wild type stock for some survival experiments.

### *2.2.2 Gal4, UAS transgenic stocks*

The Gal4, UAS (upstream activation sequence) expression system allows for both visualisation and manipulation of cells and tissues of interest dependent on what is linked to the UAS (Figure 2-1). This could be a fluorophore to enable imaging of a tissue of interest, or an RNAi to knock down expression of a given gene. The UAS can also be linked to a gene in order to induce over expression of that gene, or it can be linked to a pro-apoptotic protein to induce cell death in a given population of cells. Furthermore, flies are able to express more than one UAS at the same time e.g. simultaneous fluorophore expression by a tissue of interest, as well as the knock down of a given gene in that tissue (Brand and Perrimon, 1993).

The Gal4, UAS system was frequently utilised during this thesis. One such example is crossing of *Hml* reporter flies (w;*Hml*Δ-Gal4,UAS-2xeGFP) to a knock down line (e.g. w;;UAS-crq-IR). This allows for both visualisation and imaging of *Hml* positive plasmatocytes as well them simultaneously lacking the scavenger receptor *crq*. Table 2-1 details the genotypes of transgenic fly stocks utilised during the course of this thesis, including a brief description of their specific uses in experiments.

### *2.2.3 Gal80$^{ts}$ temperature sensitive stocks*

Temperature sensitive Gal80 (Gal80$^{ts}$) is a repressor of Gal4 activity at certain temperatures. At temperatures below 29°C Gal80$^{ts}$ binds and represses Gal4 transcription initiation at UAS sites. At 29°C Gal80$^{ts}$ repressor activity is inhibited and Gal4 activity and therefore transcription of target genes can commence. This expression system allows for temporal and spatial control of the expression of Gal4 linked genes (McGuire et al., 2004).

The Gal80$^{ts}$ expression system is used in this thesis in order to delete plasmatocytes in a time and tissue dependent manner. For generation of plasmatocyte depleted flies Gal80$^{ts}$ expression is under control of the ubiquitous driver *Tubulin*, meaning the Gal4, UAS expression system is blocked in all cells, at temperatures below 29°C. These flies additionally code for expression of pro-apoptotic protein, *reaper* (*rpr*) and 2xeGFP under control of the plasmatocyte specific driver, *Hml*-Gal4. At 29°C repression of Gal4 is lost, and expression of genes linked to the Gal4, UAS are transcribed in target cells. Therefore, *Drosophila* are able to reach adulthood before plasmatocytes are deleted, controlling for developmental effects which may arise as a result of plasmatocyte deficiency. Furthermore, the presence of UAS-2xeGFP allows for visualisation of plasmatocytes before switching the flies to 29°C as a control for efficient plasmatocyte cell death.

### *2.2.4 RNA interference (RNAi) stocks*

In order to investigate certain genes in more detail, RNAi lines were obtained for various genes of interest (all UAS-RNAi stocks are listed in Table 2-2). These RNAi lines were linked to a UAS and so were used in combination with Gal4 drivers in order to knock down expression of the target gene in a given tissue, see Figure 2-2 for an example of RNA interference.

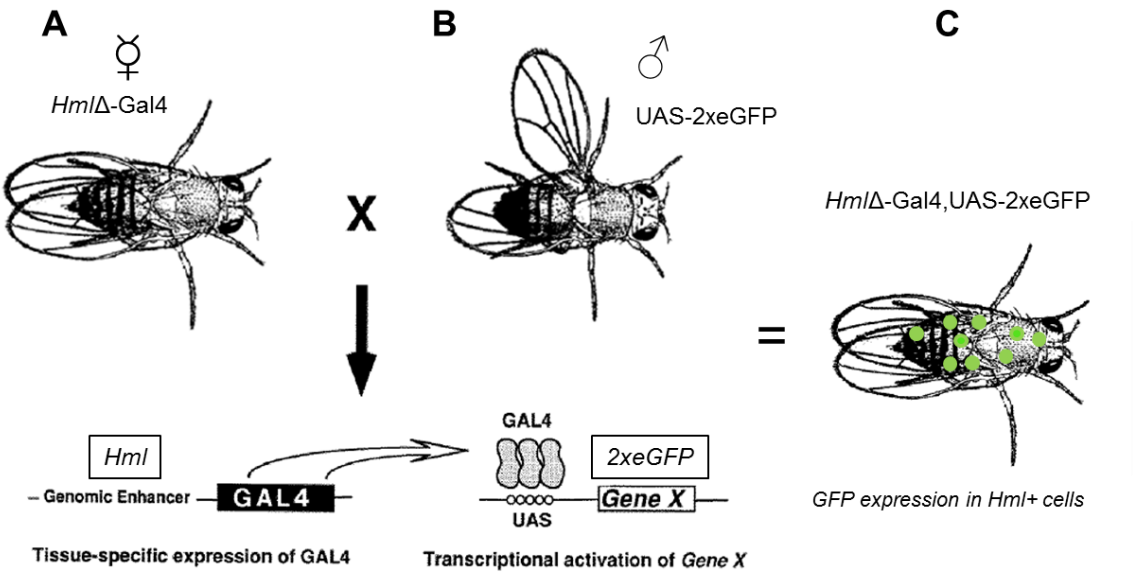


*Figure 2-1 Diagrammatic representation of the Gal4-UAS expression system*
Crossing virgin female fly **A**, (*Hml*Δ-Gal4) to male fly **B**, (UAS-2xeGFP), will result in progeny which express both the *Hml*Δ-Gal4 transgene and the UAS-2xeGFP transgene (fly **C**, green dots represent GFP expressing $Hml^{+}$ plasmatocytes). Therefore, Gal4 expression which is restricted to cells expressing *Hml*, a plasmatocyte specific lectin (Goto et al., 2001), will result in transcriptional activation of genes downstream of the UAS, resulting in GFP expression which is restricted to *Hml* positive cells, figure adapted from Brand and Perrimon (1993).

*Table 2-1 Transgenic fly stocks used in the course of this thesis*

| **Fly stock & chromosomal location of insertions** | **Purpose/Description of line expression & use(s)** |
|---|---|
| $w^{1118}$;*Hml*Δ Gal4,UAS-2xeGFP (on 2nd) | *Hml* Gal4 driven hemocyte/plasmatocyte specific reporter line. Allowing for hemocyte visualisation. Described and donated by Sinenko and Mathey-Prevot (2004). |
| $w^{1118}$;*Hml*Δ-DsRed/SM6a (on 2nd)<br>$w^{1118}$;;*Hml*Δ-DsRed (on 3rd) | *Hml* driven hemocyte/plasmatocyte specific Gal4, UAS independent reporter line. Cloning of these lines described in this thesis (Chapter 3). Published in Clark et al. (2011). |
| $w^{1118}$;UAS-2xeGFP;*crq*-Gal4/TM6C.Sb[1] (on 2nd & 3rd) | Hemocyte/plasmatocyte expressed, *crq* Gal4 driven reporter line. |
| $w^{1118}$;;*Tubulin*-Gal4/TM6c.Sb[1] (on 3rd) | Drives expression ubiquitously in the fly tissues using *Tubulin* Gal4. |
| $w^{1118}$;*Tubulin*-Gal80$^{ts}$;*crq*-Gal4,UAS-CD8Cherry/TM6C.Sb[1] (on 2nd & 3rd) | Temperature sensitive Gal80 hemocyte/ plasmatocyte expressed *crq* driven reporter line. |
| $w^{1118}$;;UAS-*reaper*/TM3 (on 3rd) | Over expression line for pro-apoptotic protein *reaper* (*rpr*). |
| $w^{1118}$;;*Pxn*-Gal4,UAS-GFP (on 3rd) | Hemocyte/plasmatocyte expressed *Pxn* Gal4 driven reporter line. |
| $w^{1118}$;;*crq*-Gal4/TM6c.Sb[1] (on 3rd) | Hemocyte/plasmatocyte expressed *crq* Gal 4 driver. |
| $w^{1118}$*Hml*Δ-Fucci-Green$G_2$S,M (on X)<br>$w^{1118}$;*Hml*Δ-FucciGreen$G_2$S,M (on 2nd)<br>$w^{1118}$;;*Hml*Δ-FucciGreen$G_2$S,M (on 3rd) | *Hml* driven, Gal4, UAS independent Fucci (fluorescent ubiquitination based cell cycle indicator) lines; indicating cells are in the $G_2$, S or M phases of mitosis for investigation of plasmatocyte proliferative potential (Sakaue-Sawano et al., 2008). Cloning of these lines is described in this thesis (Chapter 3). |
| $w^{1118}$;*Hml*Δ-Fucci-Orange$G_1$ (on 2nd) | *Hml* driven Fucci line indicating cells are in the $G_1$ phase of mitosis, as above. Cloning of this line is also described in this thesis (Chapter 3). |
| $w^{1118}$;*Hml*Δ Gal4,UAS-2xeGFP;*Tubulin*-Gal80$^{ts}$/TM6C.Sb[1] (on 2nd and 3rd) | Temperature sensitive Gal80 hemocyte/ plasmatocyte specific *Hml* driven reporter line. |
| $w^{1118}$;;TM2/TM6c,Sb[1] (on 3rd) | Third chromosome balancer fly line, used to determine chromosomal locations of the cloned HmlΔ-DsRed and *Hml*Δ-Fucci flies. |
| $w^{1118}$;noc$^{sco}$/SM6a (on 2nd) | Second chromosome balancer fly line, used to determine chromosomal locations of the cloned *Hml*Δ-DsRed and *Hml*Δ-Fucci flies. |

Table 2-1 lists the transgenic fly stocks used during the course of this thesis, with a brief description of their uses.

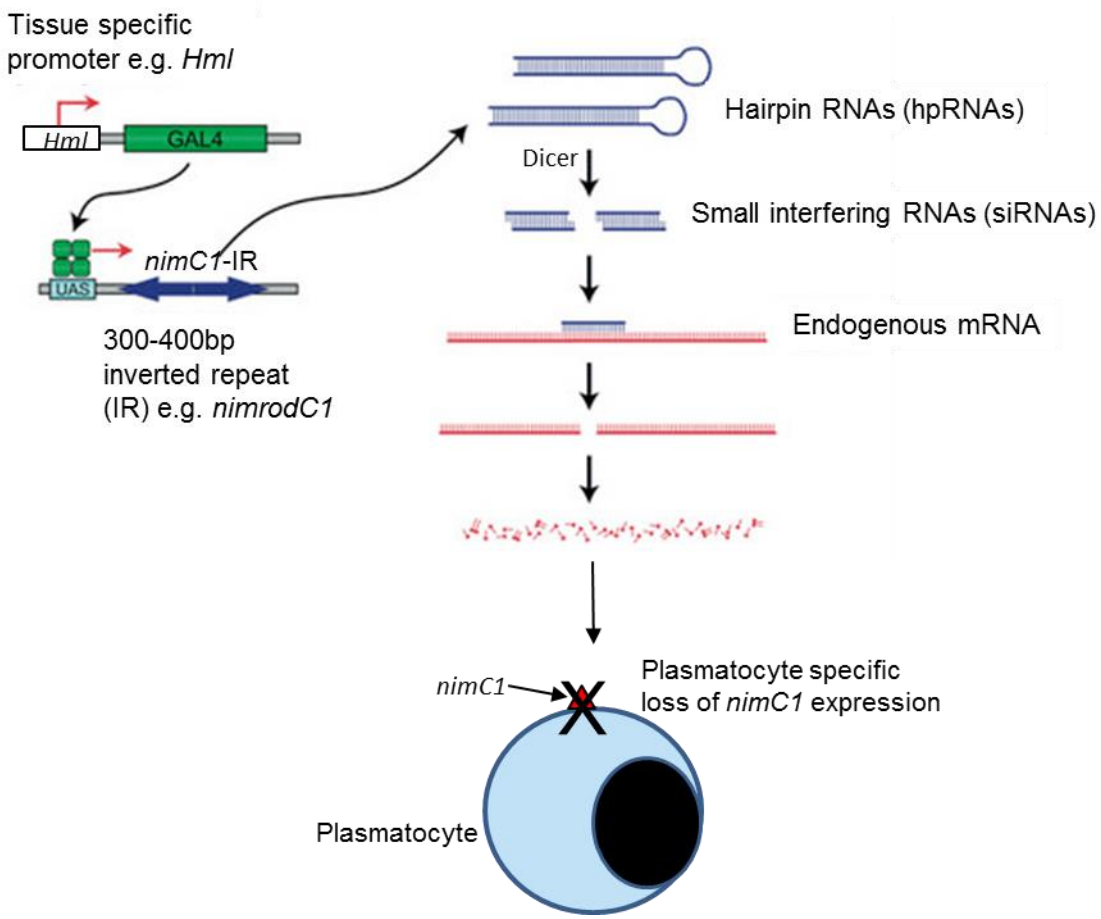


*Figure 2-2 RNA interference in Drosophila using the Gal4, UAS expression system*
The Gal4, UAS system is used to drive the expression of a hairpin RNA (hpRNAs). In this instance the Gal4 promoter is the plasmatocyte expressed gene *nimC1*. These double-stranded RNAs are processed by the enzyme *Dicer* into small interfering RNAs (siRNAs) which direct sequence-specific degradation of the target *nimC1* mRNA, resulting in a loss of translation of the *nimC1* gene specifically in *Hml* expressing cells, figure adapted from (VDRC, 2013).

*Table 2-2 RNA interference knock down lines used in this thesis*

| **Knock down line (CG number)** | **Gene name** | **Chromosomal location** | **Stock centre** | **Transformant ID / stock number** |
|---|---|---|---|---|
| UAS-CG7228-IR | *peste (pes)* | II | VDRC | 100391 |
| UAS-CG7422-IR | n/a | II | VDRC | 101136 |
| UAS-CG8942-IR | *nimrodC1 (nimC1)* | II | Bloomington stock centre | 25787 |
| UAS-CG3829-IR | n/a | II | VDRC | 103492 |
| UAS-CG1887-IR | n/a | II | VDRC | 100219 |
| UAS-CG31770-IR | *Hemese (He)* | II | VDRC | 107469 |
| UAS-CG3212-IR | Sr-CIV | II | VDRC | 100487 |
| UAS-CG7227-IR | n/a | II | VDRC | 108059 |
| UAS-CG2736-IR | n/a | II | VDRC | 102672 |
| UAS-CG10345-IR | n/a | II | VDRC | 100252 |
| UAS-CG4280-IR | *croquemort (crq)* | III | VDRC | 45884 |
| UAS-CG4280-IR | *croquemort (crq)* | II | VDRC | 45883 |
| UAS-CG33542-IR | *unpaired3 (upd3)* | II | VDRC | 106869 |

Table 2-2 lists the knock down fly stocks used during the course of this thesis, including their chromosomal locations, and their stock centre reference numbers. The UAS-knock down lines can be crossed to a Gal4 line to drive knock down in a tissue of interest. VDRC (Vienna *Drosophila* RNAi center).

## 2.3 Fly food preparation

During the course of this thesis, the fly response to lipid rich diet exposure was investigated comparatively to flies fed control diets. Details below describe the preparation and ingredients in both the control and lipid rich diets.

### *2.3.1 Control diet*

Flies were maintained on food containing 8.2% weight for volume Brewer's yeast, 1.6% polenta and 0.7% agar, (MP Biomedicals) 6.6% fructose (Sainsbury's supermarkets Ltd), 0.4% nipagin (Methyl 4-hydroxybenzoate, Sigma-Aldrich) in 15% in ethanol, and 0.6% propionic acid (Sigma-Aldrich).

Agar and polenta was added to half of the total water and brought to the boil, and then simmered for two minutes whilst being stirred constantly. The heat was then reduced before adding fructose and yeast, along with the remaining water, in order to cool the food down. Once the food temperature had cooled to 60°C, 15% nipagin in ethanol and propionic acid were added as antimicrobial agents. Approximately 8ml of food was pumped into each vial (see Table 2-3 for further details on dietary composition), and the vials were sealed immediately after cooking with a bung to prevent any possible contamination. As fly food was cooked in bulk, it was stored in the cold room at 4°C until required, at which point it was left to warm to room temperature before placing new flies on it.

### *2.3.2 Fructose-low, lipid rich diet*

The fructose low diet was prepared in the same way as the control diet, but either 95% or 50% of the fructose content was substituted with lard. The lard was added to the food at the same time as the fructose and yeast. Resulting in a 3.3% and a 6.3% weight for volume lipid rich, fructose low diets (see Table 2-3 for further details on dietary composition).

### *2.3.3 Lard, Coconut oil and Olive oil supplemented lipid rich diets*

Lipid supplemented diets were prepared in the same way as the control diet and the given fat was added at the same time as the yeast and fructose. Lard (Sainsbury's supermarkets Ltd), coconut oil (Holland and Barrett Retail Ltd) or olive oil (Sainsbury's supermarkets Ltd) was added to the control diet recipe in a weight for volume manner, substituting water for fat at 3.3%, 6.3% or 15%, as described by Birse et al. (2010). See Table 2-3 for further details regarding dietary ingredients and composition.

### *2.3.4 Generation of blue fly food diets*

Blue food diets for the feeding assay experiments (described in this chapter, in section 2.10.3) were prepared exactly as described above. Control or 15% lard diets were cooked and bromophenol blue (Sigma-Aldrich) and xylene cyanol (Invitrogen) were added for the blue colouring, just before the fly food was pumped. Bromophenol blue and xylene cyanol were added at 0.1% and 0.5% per litre of food respectively.

*Table 2-3 Dietary components: control, lipid rich fructose low, and supplemented lipid rich diets*

| **Ingredients/litre of food** | **Control diet (0.12% fat)** | **Fructose low, lipid rich diets (lard)** | | **Supplemented, weight for volume lipid rich diets (lard, coconut oil or olive oil)** | | |
|---|---|---|---|---|---|---|
| | | **3.3% fat** | **6.3% fat** | **3.3% fat** | **6.3% fat** | **15% fat** |
| Added fat (g) | 0g | 4g | 76g | 40g | 76g | 182g |
| Fructose (g) | 80g | 40g | 4g | 80g | 80g | 80g |
| Polenta/corn (g) | 20g | 20g | 20g | 20g | 20g | 20g |
| Yeast (g) | 100g | 100g | 100g | 100g | 100g | 100g |
| Agar (g) | 8g | 8g | 8g | 8g | 8g | 8g |
| 15% Nipagin in ethanol (ml) | 5ml | 5ml | 5ml | 5ml | 5ml | 5ml |
| Propionic acid (ml) | 7.5ml | 7.5ml | 7.5ml | 7.5ml | 7.5ml | 7.5ml |
| Water (ml) | 1000ml | 960ml | 924ml | 960ml | 924ml | 818ml |

Table 2-3 lists the quantities of the ingredients in each of the fly diets used in this thesis.

## 2.4 Cloning of new plasmatocyte reporter flies

### *2.4.1 Generation of plasmatocyte, Gal4 independent reporter fly Hml⊿-DsRed*

Cloning was carried out in order to generate a plasmatocyte specific, Gal4 independent reporter fly line, which is described in detail in Chapter 3 section 3.3. The plasmid pCaSpeR-4-*Hml*ΔGal4, a gift from Sergey Sinenko (Sinenko and Mathey-Prevot, 2004), was used to obtain the *Hml* promoter and the p-Red H-Stinger plasmid, a gift from Joe Bateman, described in (Barolo, 2004) was used to obtain the DsRed fluorophore (see Appendix 1 for *Hml*Δ-DsRed cloned plasmid map).

### *2.4.2 Generation of plasmatocyte driven Fucci flies*

The Fucci (fluorescent ubiquitination based cell cycle indicator) constructs p-Fucci-$G_1$ Orange and p-Fucci-S/$G_2$/M Green were obtained from MBL International. Fucci allows the visualisation of mitotic phases through fluorescence and flies were generated in order to investigate plasmatocyte proliferative potential (Sakaue-Sawano et al., 2008). The Fucci fluorescent fusion proteins from these constructs were inserted into the previously generated *Hml*Δ-DsRed in place of the DsRed, therefore generating plasmatocyte specific *Hml* driven Fucci flies (see Appendices 2 and 3 for the cloned *Hml*Δ-Fucci-Orange$G_1$ and *Hml*Δ-Fucci-Green$G_2$SM plasmid maps respectively).

### *2.4.3 Gel electrophoresis and gel extraction*

Plasmids were digested with specific restriction enzymes (New England Biolabs) to obtain the correct vector and insert fragments. The fragments generated by the restriction digest were separated on the basis of size (base pairs) via gel electrophoresis. Gel electrophoresis was carried out in 50ml or 100 ml gel tanks (Thermoscientific OWL Fasycast B2, or Peqlab Biotechnologie GmbH tanks). Gels were made with 1% Agarose (Invitrogen) in 0.5% TAE and 0.5% TAE was used as the running buffer. Gels were

labelled with Ethidium Bromide at 5µl/50ml (Invitrogen) to allow for DNA band visualisation. Electrophoresis was run between 100-120V at 300 milliamps using a Sigma-Aldrich Consort EV243 power supply. Gels were imaged for DNA bands using a Bio-Rad Gel Doc EZ Imager. A 10kb molecular weight marker ladder (Eurogentec SmartLadder) was used to determine the correct size bands, which were excised with a scalpel and gel extraction was carried out using the QIAquick Gel Extraction kit according to manufacturer's instructions.

*2.4.4 Ligation, Transformation and Miniprep*

Ligation was performed using the TaKaRa DNA Ligation Kit LONG (Takara Bio Inc.) according to the manufacturer's instructions. Invitrogen One Shot TOP10 Competent *E. coli* cells (Invitrogen) were used for transfection and the recommended Invitrogen protocol was followed. The cells were then plated on LB (Invitrogen) agar ampicillin (Invitrogen) plates and incubated overnight at 37°C. Only successfully transfected cells should be ampicillin resistant, as the ampicillin resistance gene was only present in the newly generated constructs. Colonies were then isolated and grown overnight in a 37°C shaking incubator in LB Broth supplemented with ampicillin at 100µg/ml (Invitrogen). The plasmids were extracted using the QIAprep Spin Miniprep Kit (Qiagen). Finally diagnostic restriction digests were completed to confirm the correct plasmid, containing the insert was present.

*2.4.5 Transgenic insertions*

Embryonic injections of the *Hml*Δ-DsRed, *Hml*Δ-Fucci$G_1$, *Hml*Δ-Fucci$G_2$,S,M constructs was performed by BestGene Inc. Plasmids were shipped to Bestgene Inc. in dd$H_2O$ containing 1mM EDTA and upon arrival plasmids were transformed and purified by miniprep. Microinjection of the plasmids was performed into 200 $w^{1118}$ embryos, per generated construct. The surviving $G_0$ adults were back crossed individually to $w^{1118}$ flies,

and then expanded by crossing $G_1$ flies again to $w^{1118}$ flies. Finally $G_2$ transgenic flies were received in the lab, and the chromosomal location of insertions was mapped using balancer fly lines, allowing for stable stocks to be established.

## 2.5 Fluorescence-activated cell sorting (FACS)

### *2.5.1 FACS of Drosophila plasmatocytes*

Approximately 90 adult male *Drosophila* (w;*Hml*Δ-Gal4,UAS-2xeGFP) were homogenised through a 70µm cell strainer (BD Biosciences) with ice cold 1x PBS-EDTA (2mM) into a 50ml falcon. The filtered sample was then centrifuged at 4°C for 15 minutes at 150g, the supernatant was discarded and the pellet was re-suspended in a 5ml of PBS-EDTA (2mM), and passed once again through a 70µm cell strainer, this wash step was repeated. GFP positive *Hml* positive plasmatocytes were sorted through a 100µM nozzle at 20psi pressure using a FACS Aria II. For every sort, a GFP negative sample was first analysed in order to calibrate the sorter for detection of GFP positive cells. Cells were sorted into either RLT buffer from the RNeasy Plus Micro kit (Qiagen) in order to extract RNA for cDNA generation and perform RT qPCR, or cells were sorted into PBS in order to fix and stain them for imaging. See Chapter 3 section 3.5.2 for the GFP positive plasmatocyte gating strategy.

### *2.5.2 Oil Red O staining of FACS sorted plasmatocytes*

FACS sorted plasmatocytes were stained for neutral triglyceride and lipid presence using Oil Red O (Sigma-Aldrich). Cells were sorted into 1x PBS-EDTA (2mM), after the sort cells were spun down at 4°C for 7 minutes at 150g. The cells were re-suspended in 50µl *Drosophila* Schneider's medium (Invitrogen), and were transferred onto a poly-L-lysine (Sigma-Aldrich) coated coverslip, which was placed inside a well of a 24 well non-tissue culture plate. After a 30 minute incubation at 37°C a further 500µl Schneider's medium was added and the incubation was repeated. All media was then removed and the cells

were fixed with 4% PFA (paraformaldehyde) (Sigma-Aldrich) for 30 minutes at room temperature. After this the PFA was removed, and the cells were washed quickly with 60% isopropanol (Sigma-Aldrich). Oil Red O was then added to the cells for 30 minutes at room temperature. The Oil Red O was then removed and the coverslip was washed with distilled water. The coverslip was then inverted and mounted onto a superfrost slide (VWR International), in 10µl of vectashield mounting media (Vector Laboratories) containing 1/1000 DAPI (4',6-diamidino-2-phenylindole) for nuclei staining. Mounting media was left to set for approximately 24 hours before cells were imaged with a confocal microscope (Leica SP5).

## 2.6 RT qPCR (Real time quantitative polymerase chain reaction)

### *2.6.1 Whole fly cDNA sample generation*

RNA extractions were carried out using TRIzol (Invitrogen), following the recommended Invitrogen directions. Each sample contained three flies homogenised in 100µl of TRIzol, using small pestles which were compatible with the bottom of eppendorf tubes. Chloroform (Sigma-Aldrich) was added to each sample for washing and the eppendorfs were inverted several times before being left for 3 minutes and then spun at 4°C for 15 minutes at 12000g. The upper aqueous phase was decanted into a new tube, and mixed with 50µl of isopropanol and vortexed well in order to precipitate the RNA. Samples were left for 10 minutes at room temperature and then spun at 4°C for 10 minutes at 12000g. Supernatant was discarded and RNA pellets were washed with 250µl of 75% ethanol and spun at room temperature for 5 minutes at 13000 rpm. Once again the supernatant was discarded, and the RNA pellet was re-suspended in RNAse free water. RNA was then treated for 30 minutes at 37°C with DNase I (Fermentas) to rid samples of any residual genomic DNA. Reverse transcription and cDNA synthesis was carried out using the First Strand cDNA Synthesis Kit (Fermentas). Samples were first primed with

random hexamers for 5 minutes at 70°C and were then treated with M-MuLV Reverse Transcriptase (Fermentas) alongside RNasin (Fermentas) RNase inhibitors and 10mM dNTPs (deoxyribonucleotides) for 1 hour at 37°C. Finally the enzymes were inactivated by heating the samples to 70°C for 10 minutes, ultimately resulting in a 20µl sample of generated cDNA. Generated cDNA was stored at -20°C before use in RT qPCR experiments.

*2.6.2 FACS sorted plasmatocyte sample cDNA preparation*

Plasmatocytes sorted from whole flies (as described in this chapter, in section 2.5) were sorted directly into RLT buffer (Qiagen) for lysis of cells prior to RNA extraction. RNA extraction was completed using Qiagen RNeasy microkit, following the manufacturer's instructions. Finally reverse transcription was carried out upon the extracted RNA, first priming it with random hexamers, and secondly performing cDNA synthesis with M-MuLV Reverse Transcriptase (Fermentas) as described above.

*2.6.3 RT qPCR*

The resulting cDNA from the above described protocols was used to generate a 1:5 serial dilution (for whole fly samples) or a 1:3 serial dilution (for sorted plasmatocyte cDNA) resulting in a set of 7 standards. Samples were diluted to 1:20 (for whole fly cDNA samples) and 1:5 (for FACS sorted plasmatocyte cDNA). A no template control was also run alongside the standards to check for any contamination of reagents and surfaces. RT qPCR was performed with Sensimix SYBR Green no-ROX (Bioline) on a Corbett Rotor-Gene 6000. The cycling settings used were: Hold 95°C for 10 minutes, then between 40 and 55 cycles of 95°C for 15 seconds, 63.4°C for 30 seconds, 72°C for 30 seconds. The total reaction volume was 10µl, including 5µl Sensimix, 0.2µl primer, 2.3µl dd$H_2O$ (only

added to whole fly cDNA reactions) and 2.5µl or 4.8µl of template cDNA and standard cDNA if the cDNA was whole fly derived, or sorted plasmatocyte derived respectively.

Table 2-4 Primer sequences used during the course of this thesis

| **Primer (qPCR)** | **Left** | **Right** |
|---|---|---|
| *Rpl1* | TCCACCTTGAAGAAGGGCTA | TTGCGGATCTCCTCAGACTT |
| *upd2* | CGGAACATCACGATGAGCGAAT | TCGGCAGGAACTTGTACTCG |
| *CG10345* | AACAAAAACCAGCGCAATG | CCGAGATTATCACCAGGGAACC |
| *CG3829* | TGCCTCTTTTCTGCAACTGA | GATAGTCTGTCGCTGCACGTT |
| *nimC1* | CGCACCGAGTATTATACAGACG | TCCATGTTGAGGACACTGTTG |
| *CG2736* | CGTCGCTGTTCTCTACAACG | TTAGGGCCGATGTTGACTGT |
| *CG3212* | AGCACAATGACAGCCAACAG | GTCAGATGGGATTGGTCCAG |
| *peste* | CGCAACTGGATCGATATGTTT | CTCGAATGATCGTGAATTGG |
| *CG7422* | TTTGACCACCTGTTTGGATG | ATTTTGCGGTACTCATTCGAG |
| *CG1887* | GAGACTTTGTCTTTCCGGTCA | ATGGCAGGTGTCAGCTCAG |
| *upd3* | ACTGGGAGAACACCTGCAAT | GCCCGTTTGGTTCTGTAGAT |
| *CG7227* | GTGGAGCCCAAAACTCATTT | TGTAATCCGCCCAGATCAA |
| *Hemese* | GTCGTTTTCCTGGCACTGTT | TGGAGATGGACGGTTGCTA |
| *Hml* | CGATGATGACGACGAGGATA | GGCTTTGAGGATGTTGAAGC |
| *crq* | GCAGATAACCTTGTAGAGGATGG | CTCAGGTAAATGGGGATAGGTG |
| *ACC* | AGGTCCTGATTGCCAACAAC | ACATTTCGTACGCCCATCTC |
| *Pepck* | ATGCCCTCCCAGAACACAC | GAACACCATCTTCACGAACG |
| *midway* | CTCTTTAGTGCATATCTCGCTCTG | AACAAGCCCAAGCCCTCT |
| *Dilp2* | ATCCCGTGATTCCACCACAAG | GCGGTTCCGATATCGAGTTA |
| *Dilp3* | CAACGCAATGACCAAGAGAA | TGAGCATCTGAACCGAACT |
| *Dilp5* | GCCTTGATGGACATGCTGA | AGCTATCCAAATCCGCCA |
| *Diptericin* | ACCGCAGTACCCACTCAATC | CCCAAGTGCTGTCCATATCC |
| *Drosomycin* | GTACTTGTTCGCCCTCTTCG | CTTGCACACACGACGACAG |
| *Socs36E* | AAAAAGCCAGCAAACCAAAA | AGGTGATGACCCATTGGAAG |
| *Pxn* | CTGCCCCAGGATACACAAAC | TGGGCGAGACCACTGAAC |

## 2.7 Confocal microscopy

A Leica SP5 microscope was used for all images included in this thesis. Images were acquired using the Leica LAS-AF software using either the 10x, NA (numerical aperture) 0.4 objective, the 20x Dry NA 0.5 objective, or the 40x Oil NA 1.25 objective. Images were all acquired with a resolution of either 1024x1024 or 512x512 pixels, at a scan speed of 400Hz. Between 3 and 6 line averages were carried out during imaging in order to obtain the highest quality images possible. Tile scanning was used in order to image whole flies, as even with the lowest objective (10x) it was not possible to image the whole fly in a single tile. At the end of image acquisition Leica LAS software automatically merges the two images (tiles), resulting in an image of the whole fly.

Flies were anaesthetised for imaging using a $CO_2$ chamber for which was part of the confocal microscope. Flies were left for 15 minutes inside the $CO_2$ chamber to ensure they had stopped moving prior to imaging. In some instances when specifically imaging the dorsal side of the fly, flies were anaesthetised with $CO_2$ before being stuck to glass coverslips using a drop of superglue (Loctite). This permitted imaging of the fly's dorsal side, a position which would not have been possible without immobilising them in this way. Furthermore, it also enabled the fly's wings to be fixed to the coverslip in such a way that they were not obstructing the imaging of this area. FACS sorted, fixed and stained plasmatocytes were imaged through glass coverslips using the 40x Oil NA 1.25 objective.

## 2.8 Life span assays

Male flies were collected soon after eclosion for 2-3 days and groups of 20-30 age matched flies per genotype were placed on the given control and lipid rich diets. All survival experiments were conducted at 25°C, unless temperature sensitive lines were used.

For the temperature sensitive plasmatocyte depleted survival assays, fly crosses were carried out at 18°C to prevent Gal4 activity during development. Again flies were collected soon after eclosion, over 2-3 days and were then placed at 29°C for 48 hours to initiate the inhibition of Gal80, and therefore the transcription of *reaper*, a pro-apoptotic protein to induce plasmatocyte cell death in adult flies. Once the plasmatocytes had been eliminated in these flies they were put in groups of 20-30 males, per genotype, and placed on the given diets and the survival assay was carried out at 25°C.

Finally for the Gal80 temperature sensitive plasmatocyte specific knock down of *upd3* survival assays; again crosses were carried out at 18°C to prevent Gal4 activity during development. Flies were collected soon after eclosion over 2-3 days, but were placed at 29°C for the entire survival assay, in order to ensure the expression of *upd3* remained abrogated in plasmatocytes throughout the fly lifespan.

Flies involved in survival assays were of a $w^{1118}$ genetic background in order to control for the survival differences which may exist between different wild type strains. In all survival assays carried out, vials were checked each day for any fly deaths, which were recorded. Food vials were kept on their sides to minimise the possibility of fly death from becoming stuck to the food and vials were changed for fresh food every other day, flies were transferred onto the new vials without using $CO_2$.

## 2.9 Infection and injection assays

### *2.9.1 Injection calibration*

Microinjection needles for fly injection were produced in the lab using glass capillaries and a needle puller (Narishige, Model PC-10). Injection was performed using a PicospritzerR III, and injection volume was calibrated by injecting a drop into a plot of oil (mineral oil and halo carbon oil 700). Expelled drops were measured to obtain a final injection volume of 50 nanolitres (nl). Flies were anesthetised with $CO_2$ under a light microscope on porous gas pads prior to abdominal injection.

*2.9.2 Bacterial infection*

Stocks of *Micrococcus luteus* (*M. luteus*) and *Escherichia coli* (*E. coli*) were stored at -80°C, cultures were grown from these stocks by selecting a small quantity of bacteria using a pipette tip and dipping the tip in LB broth. A Bunsen flame was used during this process to ensure culture of only the bacteria of interest. These individual *E. coli* and *M. luteus* cultures were grown in a 37°C shaking incubator overnight. The following morning the cultures were centrifuged at 4°C at 1600rpm for 10 minutes. Bacterial pellets were re-suspended in PBS (Invitrogen) and the optical density (OD) was measured at the wavelength of 600nm (OD600). Mixed septic infections were carried out with an equal mix of OD-adjusted *E. coli* and *M. luteus* cultures (retaining a final OD of 1). Injection, and drop calibration was performed as described above on adult male flies aged between 7 and 10 days. Experiments also included 'wounded' control flies, in which flies were simply pricked with the needles rather than being infected with bacteria. These flies were included as controls for the immune response that the needle wound itself may have initiated in the fly.

After infection or wounding, flies were homogenised in TRIzol and stored at -20°C ready for cDNA synthesis and RT qPCR, in this case flies were homogenised 6 hours post infection in order to observe maximal AMP induction. For confocal imaging infection experiments, flies were imaged 24 hours post infection or wounding for induction of GFP expression in *Pxn* reporter flies (w;;*Pxn*-Gal4,UAS-GFP).

*2.9.3 DiI-LDL (red fluorescent lipid) injection*

Adult male plasmatocyte reporter flies (w;*Hml*Δ-Gal4,UAS-2xeGFP) aged between 7 and 10 days were injected abdominally, as described above, with 50nl of DiI-LDL (3,3'-dioctadecylindocarbocyanine-low density lipoprotein, Sigma-Aldrich). Flies were imaged with a confocal microscope 1 hour post injection for plasmatocyte uptake of the DiI-LDL.

## 2.10 Metabolic assays

### *2.10.1 Thin Layer Chromatography (TLC) for triglyceride measurement*

TLC experiments were adapted from Al-Anzi and Zinn (2010). Groups of 10 flies, in quadruplicate per genotype, per diet were anesthetised using $CO_2$ and then placed in 100µl of 3:1 ratio of chloroform: methanol. Samples were centrifuged for 3 minutes at 13,000rpm at 4°C, flies were then homogenised with pestles. A set of standards were prepared using lard dissolved in 3:1 chloroform: methanol (Sigma-Aldrich) for standard curve generation and quantification of whole fly triglycerides. Samples and standards were loaded onto a silica gel and a 4:1 mix of hexane: ethyl ether (Sigma-Aldrich) was prepared as the mobile phase. Gels were then stained using a general oxidising stain, ceric ammonium heptamolybdate and baked at 80°C for 20 minutes. Baked gels were imaged with a BioRad Molecular Imager and gels were analysed for triglyceride bands using BioRad Image Lab software. All TLC experiments included in this thesis were repeated 2-3 times per genotype per diet with similar findings (See Figure 2-3 for an example of a TLC gel).

### *2.10.2 Glucose and trehalose quantification: colorimetric assay*

Flies were starved for 1 hour, and then homogenised in 75µl TE + 0.1% Triton X-100 in groups of 3 flies, per genotype, per diet, samples were immediately frozen at -80°C until required, five samples were prepared per genotype per diet. For the assay samples were thawed and then heated at 90°C for 20 minutes to inactivate fly enzymes. Glucose standards were prepared (10 series, 1:2 dilution) for quantification. Samples were loaded, 5µl for each condition, into flat bottom 96 well tissue culture plates. Each fly sample was run twice, first alongside water for calculation of fly background absorbance, second with glucose reagent (Alere) plus trehalase (Sigma-Aldrich), allowing for measurement of both glucose and the glucose released from trehalose. The major fly sugar is trehalose (Leopold and Perrimon, 2007), which is why samples were treated with trehalase, in order

to take into account any trehalose present along with glucose in whole flies. Furthermore, each lane was run with $H_2O$ alone in order to control for inherent spectrophotometer detection differences. Plates were then incubated at 37°C for 1 hour before reading with a Wallac spectrophotometer at 490nm.

*2.10.3 Feeding assay*

Feeding assay experiments were performed as described in Rajan and Perrimon (2012). Groups of 5 adult males (in triplicate or quadruplicate) were placed on blue food, and control non-blue food for background subtraction for 4 hours at 25°C, flies were then decapitated to avoid the potential effects the eye pigmentation may have on absorbance values. The resulting fly torsos were then homogenised in PBS and centrifuged for 20 minutes. Supernatant was collected, and absorbance measured at 625nm. See section 2.3 for further detail regarding blue fly food preparation.

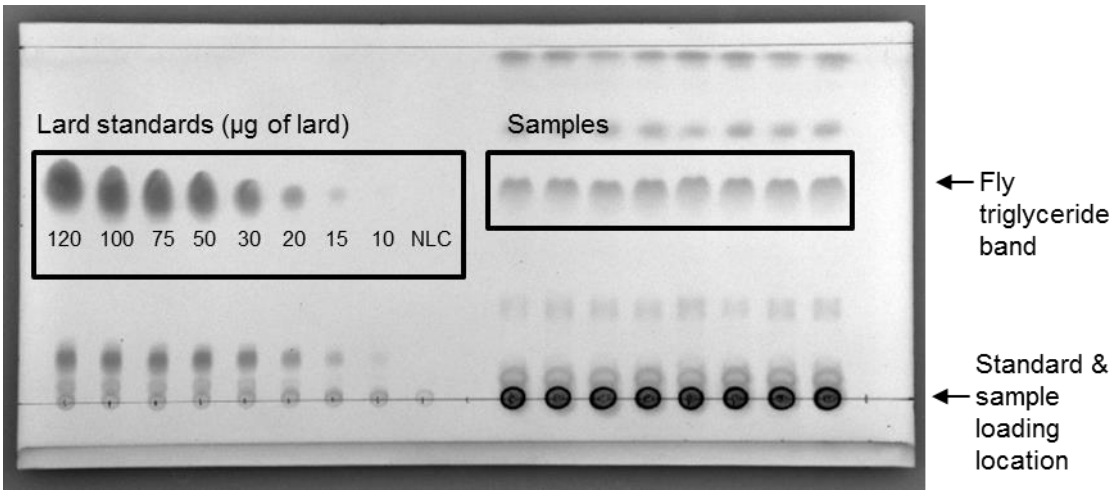


*Figure 2-3 Thin layer chromatography silica gel*
This figure displays an example TLC silica gel. The lard standards are displayed in the box on the left hand side, indicated in µg of lard. All samples and standards are loaded on the bottom line, indicated with an arrow. The box on the right hand side indicates triglycerides present in the fly samples. The standard bands are quantified for band intensity using BioRad Image lab software, and a standard curve is generated. The sample band intensities (also indicated by an arrow) are calculated from the standard curve. (NLC = No lard control).

## 2.11 Statistical analysis

### *2.11.1 Statistical significance and error bars*

In all experimental figures included in this thesis, the statistical significance stars are indicative of p values being less than, or less than or equal to the following; $p<0.05$/*, $p\leq0.01$/**, $p\leq0.001$/***. Non-statistically significant data p values were equal to or greater than $p\geq0.05$ / ns (not significant). All error bars included in figures in this thesis represent the standard error of the mean.

### *2.11.2 RT qPCR analysis*

The calculated concentrations of gene expression levels were obtained using a standard curve which was generated for every primer set tested. Expression levels of each individual sample was normalised to the housekeeping gene *Rpl1* (*Ribosomal Protein L4*) expression level for that given sample in all cases. RT qPCR data was only analysed when the $R^2$ value for standard set linearity was 0.99 or above and if efficiency of the primers was 0.7 or above (See Figure 2-4 for an example). A melting curve was also obtained for each RT qPCR experiment carried out, in order to ensure the presence of cDNA in each of the samples and the lack of contamination of the no template control sample, in which water was added. For each of the experimental conditions investigated between 3 and 7 samples were included (3 flies per sample) and individual experiments were repeated 2-3 times. Statistical significance of RT qPCR data was performed with an unpaired t test using Microsoft Excel 2007 or 2010.

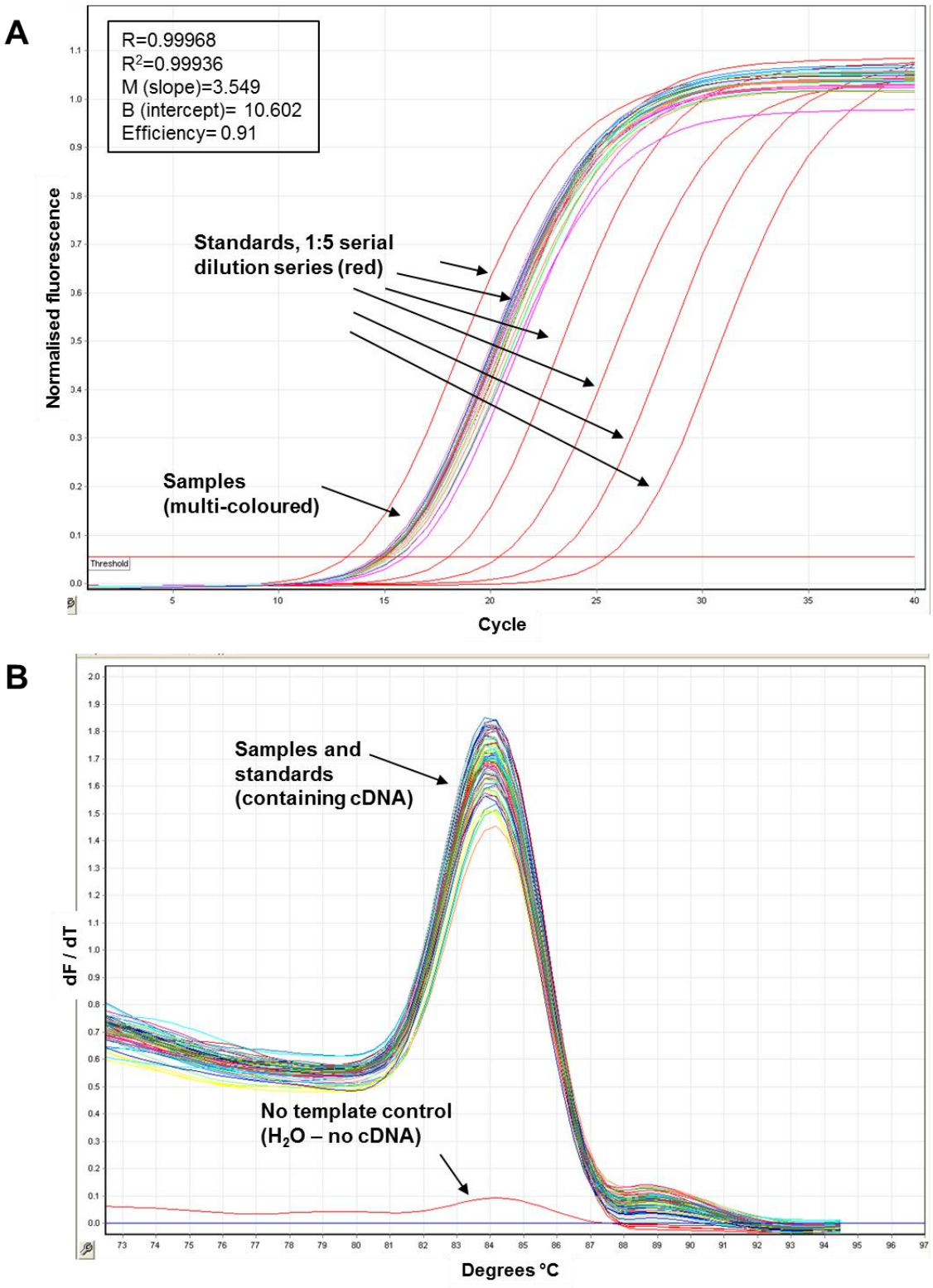


*Figure 2-4 RT qPCR standard curve and melt curve*
Examples of a whole fly cDNA standard curve and melt curve. **A.** Standards are indicated by red lines, and samples by multi-coloured lines, the $R^2$ value (0.99936) and efficiency (0.92) meet requirements for analysis of expression levels detected in each sample. **B.** Melt curve, indicating the presence of cDNA in samples (multi-coloured lines) and the lack of cDNA in the no template control, in which water is added instead of cDNA (red line) dF/dT = derivative of fluorescence versus derivative temperature, which represents the significant change in fluorescence caused by the temperature induced melting of double stranded DNA to single stranded DNA.

*2.11.3 Image processing and analysis*

Images were processed and analysed using either Imaris 7.3.0, Fiji, or Metapmorph imaging software packages. Cell counts and co-localisation analysis of double positive plasmatocytes were performed using Imaris MATLAB spot detection and co-localisation respectively. Cell counts were performed on between 3-6 individual flies per genotype, per experiment. Statistical significance of cell count data was performed using an unpaired t test in all instances using Microsoft Excel 2007 or 2010.

Fiji was used in order to quantify saturation of Oil Red O staining in FACS sorted plasmatocytes, as well as to calculate the cell area ($\mu m^2$). FACS sorting experiments for Oil Red O staining in this thesis is representative of 3 independent experiments. Statistical significance of Oil Red O staining, and plasmatocyte size was performed using an unpaired t test using Microsoft Excel 2007 or 2010.

*2.11.4 Survival analysis*

Lifespan experiments included 20-30 flies per genotype per diet. Experiments were repeated between 3 and 6 times for each experiment included in this thesis. Survival curve statistical significance was analysed using GraphPad Prism. Comparison of survival distributions between different genotypes and diets was performed using both Log Rank and Wilcoxon survival significance tests provided by Prism software package.

*2.11.5 TLC gel analysis*

TLC gel images were taken and analysed using Bio-Rad Image lab software. A standard curve was created from the band intensities of known concentrations of lard in order to calculate the approximate quantity of lard in µg in each fly sample. A total of 10 flies were included per sample, in quadruplicate per genotype for each TLC experiment. All TLC experiments included in this thesis were repeated 2-3 times per genotype per diet

with similar findings. Statistical significance of TLC data was performed with an unpaired t test using Microsoft Excel 2007 or 2010.

*2.11.6 Glucose and trehalose colorimetric assay analysis*

Glucose and trehalose data was exported from the Wallac spectrophotometer in excel files displaying absorbance and the data was analysed in Microsoft Excel 2007 or 2010. A standard curve was produced from levels of standard absorbance minus the background absorbance of reagent alone. The dataset was only analysed when the $R^2$ value was 0.99 or above. Levels of absorbance from water alone and from fly and water were subtracted from one another to leave the level of fly background alone for each individual sample, this value was then subtracted as 'background' from each individual sample. Finally the value for the absorbance of the glucose reagent alone (without a fly sample added) was then subtracted from each sample reading, leaving just the value for levels of glucose and glucose released from trehalose per sample. The addition of trehalase allowed for the measurement of glucose released from trehalose, the major fly sugar (Leopold and Perrimon, 2007). The quantity of glucose and glucose released from trehalose in μg was then calculated from the standard curve equation, allowing for the calculation of the quantity of glucose and glucose released from trehalose per fly. Each assay included 5 samples (each sample containing 3 flies) per genotype, per diet. Glucose and trehalose assay experiments included in this thesis were repeated 2-3 times. Statistical significance of the colorimetric assay data was performed with an unpaired t test using Microsoft Excel 2007 or 2010.

*2.11.7 Feeding assay analysis*

The level of absorbance from samples in which flies were fed blue control and 15% lard diets (bromophenol blue and xylene cyanol supplemented), and non-blue control and 15% lard diets were read at 625nm. Absorbance values from flies fed non-blue control and

non-blue lard diets were subtracted from the absorbance values of blue control and blue lard diets respectively. This was in order to remove any fly background absorbance which may have been detected. The mean level of absorbance of samples at 625nm was then determined for control and 15% lard diets. Finally statistical analysis was performed on these absorbance values via an unpaired t test using Microsoft Excel 2007 or 2010.

# Chapter 3 Characterisation of plasmatocytes in adult *Drosophila*

### 3.1 Introduction, aims and objectives

Three subsets of hemocyte exist in larvae, plasmatocytes, lamellocytes and crystal cells, each with distinct functions. In adult *Drosophila* it is thought that only the plasmatocyte subset exists (Evans et al., 2003). For the remainder of this thesis, adult fly hemocytes will be referred to as plasmatocytes and any discussion of hemocytes in non-adult flies, such as in the embryonic or larval stages will simply be referred to as hemocytes.

Plasmatocytes in *Drosophila* are described as the counterpart cell to the mammalian macrophage, they share many developmental and functional similarities (Martinez-Agosto et al., 2007). Both macrophages and plasmatocytes are professional phagocytes and produce cytokines in response to infection (Cavaillon, 1994, Agaisse et al., 2003). This thesis aims to investigate *Drosophila* plasmatocytes as model cells to study the conserved functions of macrophages throughout species and in particular the macrophage response to excess dietary lipids.

This chapter describes the development of the tools necessary for investigation and characterisation of plasmatocytes. Plasmatocytes were visualised using readily available Gal4, UAS reporter flies (Brand and Perrimon, 1993), in which a plasmatocyte specific promoter drives fluorophore expression. In addition, a 'Gal4 independent' fly line was also generated, allowing for visualisation of plasmatocytes, whilst concurrently using the Gal4, UAS expression system for another experimental aspect. This is particularly advantageous for imaging purposes, enabling visualisation of two fluorescent plasmatocyte reporters simultaneously, thus permitting characterisation of adult fly plasmatocyte markers. Visualisation of plasmatocytes also allowed for quantification of their numbers in adult flies.

Furthermore, plasmatocyte proliferative potential was investigated using Fucci (Fluorescent ubiquitination based cell cycle indicator). Flies were cloned in which the plasmatocyte specific marker, *Hemolectin*, drove expression of Fucci fluorescence,

allowing for visual distinction of the different phases of the cell cycle dependent on the fluorophore expressed.

In order to better characterise plasmatocytes, in terms of their gene expression profiles, a strategy for plasmatocyte purification from whole flies was devised. This allowed for experiments in which gene expression of plasmatocytes alone could be investigated.

Together the tools described in this chapter allowed for the investigation of multiple aspects in plasmatocyte physiology in adult flies. In turn this enabled comparison of plasmatocyte characteristics to those of macrophages, providing further validation for the comparison of *Drosophila* plasmatocytes to mammalian macrophages.

### *3.1.1 Objective and aims*

Chapter 3 objective: To better understand the characteristics of adult *Drosophila* plasmatocytes.

The aims of this chapter are:

1. Characterisation of plasmatocyte numbers during the fly lifespan.
2. Investigation into plasmatocyte self-renewal, and the existence of a hematopoietic organ in adult flies.
3. Characterisation of plasmatocyte expression profile in adult flies (in particular examination of *Hemolectin, croquemort* and *Peroxidasin* expression profiles).
4. Establishment of a protocol for purification of plasmatocytes.

## 3.2 Plasmatocyte number and proliferative potential

### *3.2.1 Hemolectin driven GFP expression in plasmatocytes*

*Hemolectin* (*Hml*) is a plasmatocyte specific protein, involved in hemostasis, hemolymph coagulation and wound healing (Lesch et al., 2007). *Hml* shares homology with the mammalian clotting factor, *VWF*. Plasmatocyte expression of *Hml* commences at stage 17 of embryogenesis and persists throughout larval development through to adult flies (Goto et al., 2003, Clark et al., 2011, Agaisse et al., 2003).

The *Hml* reporter fly; w;*Hml*ΔGal4,UAS-2xeGFP (Sinenko and Mathey-Prevot, 2004) displayed the greatest plasmatocyte specificity and consistency of expression, thus experiments most frequently utilised *Hml* as a plasmatocyte specific driver (Figure 3-1). Most importantly, *Hml* is one of the few plasmatocyte specific markers known to be expressed in adult fly plasmatocytes.

### *3.2.2 Plasmatocyte numbers*

Previous studies have hypothesised that adult *Drosophila* contain an estimated 1-2000 plasmatocytes, but this has not been quantified (Lanot et al., 2001). The number of *Hml* expressing plasmatocytes in w;*Hml*ΔGal4,UAS-2xeGFP flies was assessed using confocal microscopy in order to examine plasmatocyte number and stability over time. Flies were imaged after eclosion from the pupal case (day of hatching) and then at 1, 2, 3 and 4 weeks into the adult fly life. GFP positive *Hml* expressing cells were quantified in both male and female flies, at each of the designated time points. Imaging data indicated that the number of *Hml* positive cells gradually declined over time (Figure 3-2 A, B), this observation was quantified by counting GFP positive cells in aged male and female flies (Figure 3-3 A). The observed decline in *Hml* positive cells was not statistically significant from one time point for the next; however, it was statistically significant when comparing cell numbers from the day of hatching, to week 4 of adult fly life.

Female flies appeared to contain more visible plasmatocytes comparatively to males at all time points examined, this may reflect the fact that adult female flies are larger than males (Cowley and Atchley, 1988). However, the increase in *Hml* positive plasmatocyte numbers observed in female flies was only statistically significant from the numbers of cells in male flies on the day of hatching. Male flies were used in all future experiments included in this thesis due to the changes which are induced by mating in females (McGraw et al., 2004).

To re-confirm the observed slow reduction of *Hml* expressing cells over time, RT qPCR was performed to examine *Hml* transcript levels in wild type ($w^{1118}$) flies. In line with the results obtained from the quantification of the imaging data, *Hml* transcript levels appeared to gradually decline with age (Figure 3-3 B), however, this decline was not statistically significant. These data suggest that plasmatocytes only slowly decline with increasing fly age. The total reduction of plasmatocytes represents a significant change when comparing cell numbers from flies at day of hatching, to 4 week old flies, yet the general decline as assessed at weekly intervals over 4 weeks is not drastic, and occurs at a gradual non-statistically significant pace. All experiments carried out in this thesis involved the use of age matched flies, to ensure similar plasmatocyte numbers between experimental cohorts of flies.

This slow reduction of *Hml* positive cells could be due to two possibilities. Firstly, *Hml* expressing cells may slowly die during the lifespan of the fly, or secondly plasmatocytes may switch off the expression of *Hml*. It was not possible to ascertain which of the two possibilities were correct, however it is clear that the number of *Hml* positive cells decline slowly during the flies lifespan.

### *3.2.3 Plasmatocyte morphology in adult Drosophila*

In addition to *Hml* positive plasmatocytes slowly declining with time, the morphology of the cells also appeared to be different on the day of hatching compared to imaging at later

stages in the adult fly life (Figure 3-4). This could be due to the changes which arise in plasmatocyte migration capabilities during *Drosophila* development. In embryos and larvae hemocytes are highly motile and are able to migrate to sites of inflammation (Stramer et al., 2005), embryonic and larval hemocytes possess lamellae, which are responsible for this motility. Conversely in adult flies plasmatocytes are believed to be tissue bound sessile cells (Elrod-Erickson et al., 2000). Plasmatocytes on the day of hatching appear reside in a network, in which many of the cells appear to be interlinked with one other. The cells also exhibit a more 'mottled' appearance (Figure 3-4 A, B) and the remnants of the lamellae appear to be present. Plasmatocytes rapidly lose this interlinked lamellar-like network appearance, and become spherical during the first 24 hours after hatching (Figure 3-4 C, D). In line with this observation, during imaging there was no observation of plasmatocyte migration in adult flies, during both steady state and inflammatory infection conditions (data not shown). This suggests that the change observed in plasmatocyte lamellipodia morphology could be due to the transformation of these cells from highly motile, to sessile tissue bound cells.

*Figure 3-1 Confocal microscopy of a Hml driven Gal4, UAS plasmatocyte reporter fly*
Confocal microscopy of a male *Hml* reporter fly, aged 2 weeks. GFP positive plasmatocytes have been false coloured white. Genotype: w;*HmlΔ*-Gal4,UAS-2xeGFP. Scale bar = 250μm, imaging was carried out with a 10x objective, Z stack volume= 400μm, Z step size= 10μm.

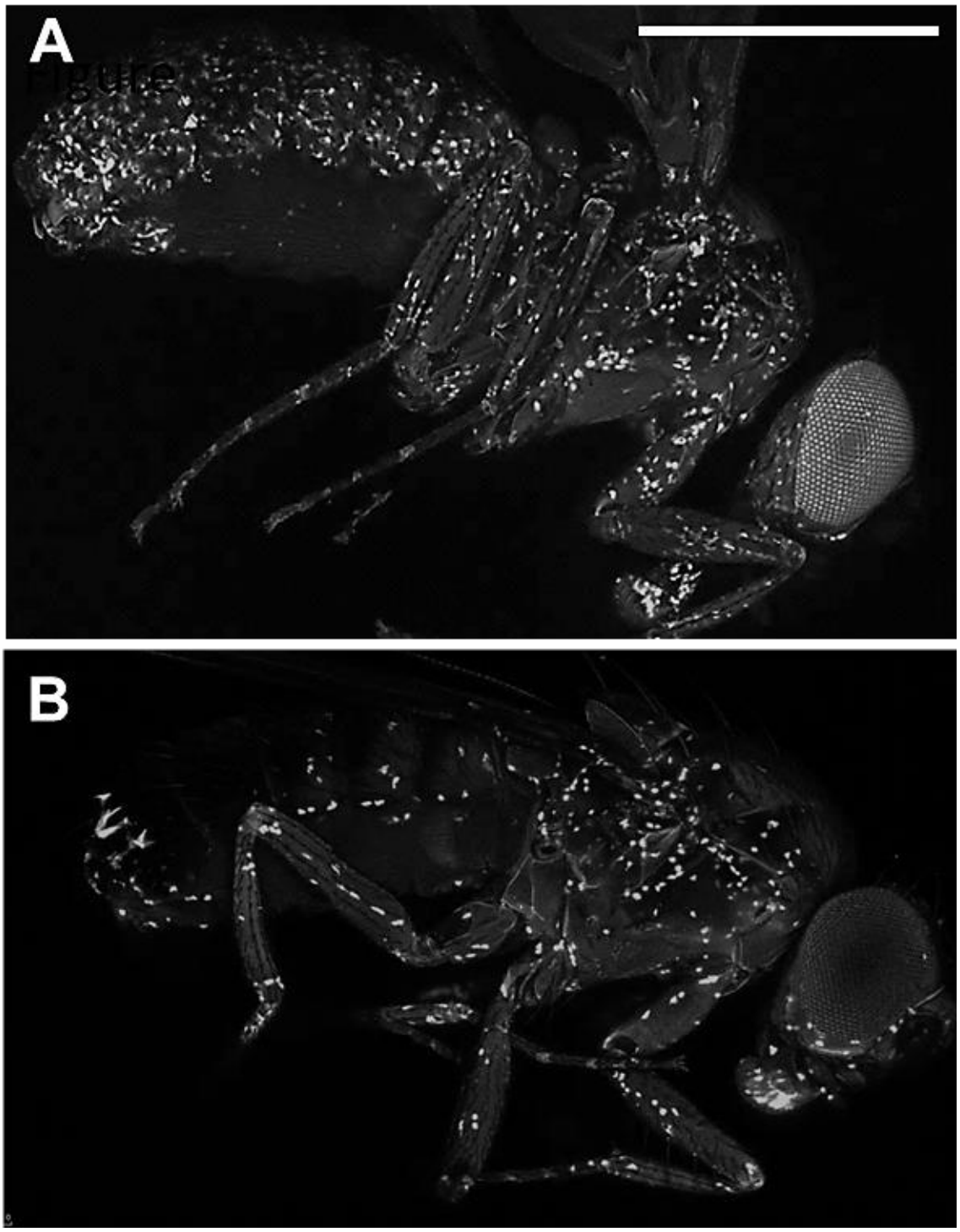


*Figure 3-2 Imaging of Hml$^{+}$ plasmatocytes during adult Drosophila lifespan*
Confocal microscopy of w;*HmlΔ*-Gal4,UAS-2xeGFP plasmatocyte reporter flies on **A.** day of hatching and **B**. 4 weeks post hatching. GFP positive plasmatocytes are false coloured white. Scale bar= 750µm, imaging was carried out with a 10x objective, Z-Stack size = 400µm, Z-Step size = 10µm.

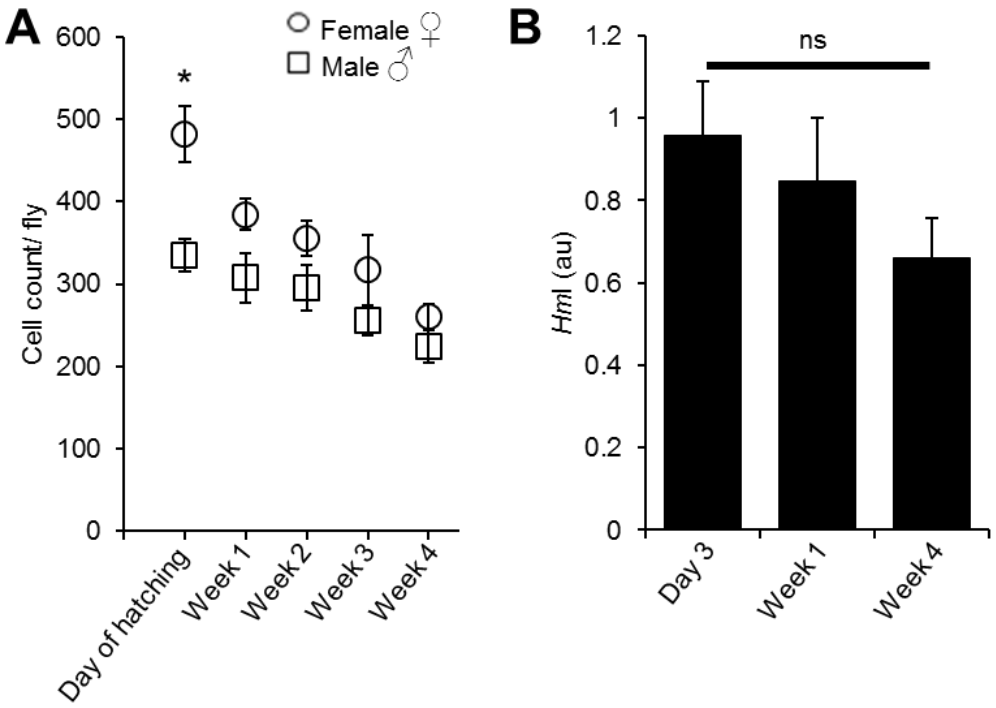


*Figure 3-3 Quantification of Hml$^{+}$ plasmatocytes during adult Drosophila lifespan*
**A.** GFP positive cell count (Imaris) in male (squares) and female (circles) w;*HmlΔ*-Gal4,UAS-2xeGFP plasmatocyte reporter flies. Data represents the mean of n= 4 flies imaged per time point per sex. Error bars represent the standard error of the mean. Female flies have significantly more plasmatocytes than males at day of hatching (p=0.02009/*), no significant difference in plasmatocytes between male and female flies was observed at any of the later time points. In addition, the decline of plasmatocyte numbers from one time point to the next was not statistically significant in either sex, however, the decline from day of hatching compared directly to week 4 was significant in both females and males, p=0.00403/** and p=0.01654/* respectively (unpaired t tests). **B.** RT qPCR analysis of *Hml* expression over time in wild type ($w^{1118}$) flies. *Hml* expression is normalised to housekeeping gene *Rpl1*, (au = arbitrary units) data represents the mean of n=5 samples per time point. Error bars represent standard error of the mean, no significant reduction of *Hml* expression was observed from one time point to the next (unpaired t tests).

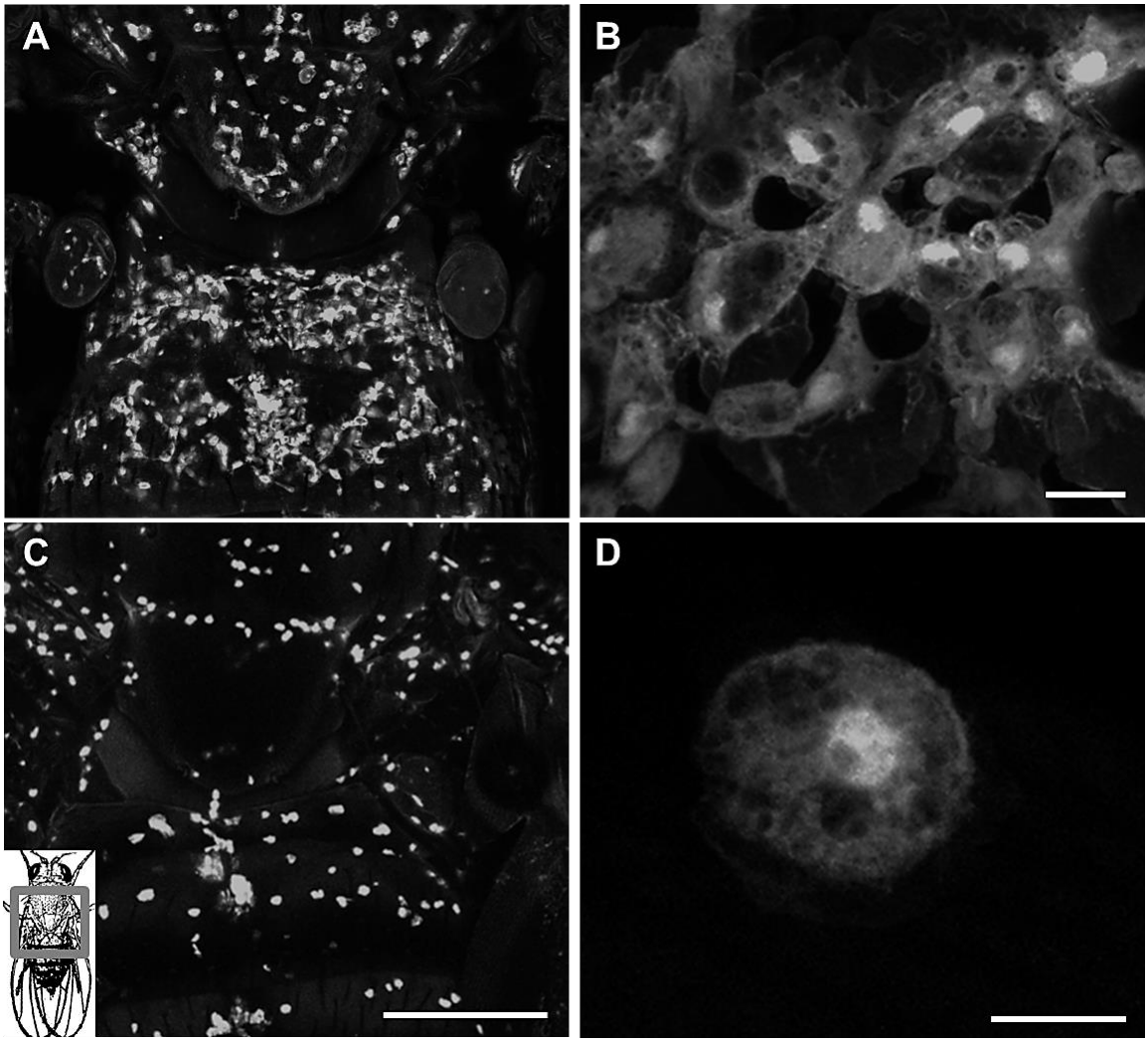


*Figure 3-4 Plasmatocyte morphological changes during the first days after fly eclosion*
Confocal microscopy of *Drosophila Hml* positive plasmatocytes (w;*Hml*Δ-Gal4,UAS-2xeGFP), GFP positive plasmatocytes are false coloured white. Imaging was carried out on **A, B** the day of eclosion from the pupal case and **C, D** at 5 days after eclosion. Flies are affixed to coverslips on the dorsal side for imaging at higher magnification imaging of plasmatocytes shown in **B** (scale bar= 10µm) and **D** (scale bar= 5µm). In lower magnification images in **A** & **C** Scale bar=250 µm. Inset diagram in C represents the fly orientation during imaging, and the grey box represents the approximate location of imaging for the images in A & C. Imaging settings for: A & C; 10x objective, Z stack volume= 400µm, Z step size= 10µm and B & D; 40x objective, Z stack volume= 30µm, Z step size= 2µm.

*3.2.4 Plasmatocyte proliferation*

To further investigate plasmatocyte number, and proliferative potential in adults, Fucci (fluorescent ubiquitination based cell cycle indicator) flies were generated. Fucci is a technique described by Sakaue-Sawano et al. (2008) which allows for the visual identification of mitotic phases via nuclear localised fluorescence. This is achieved using two proteins involved in mitosis, Cdt1 and Geminin. Cdt1 is required for cellular chromosome DNA synthesis; it is ubiquitinated and destabilised by $SCF^{Skp2}$ during S and $G_2$ phases. Cdt1 is fused to the fluorescent protein monomeric kusabira-orange 2 (mKO2) and its presence in the nuclei indicates the cell is in $G_1$. Geminin inhibits Cdt1, interfering with the binding of factors to the origin of replication during S phase. During M and $G_1$ phases of mitosis Geminin is targeted for degradation by the ubiquitin ligase $APC^{cdh1}$. Geminin is fused with monomeric azami-green1 (mAG1) and allows for the visualisation of S, $G_2$ and M phase (Figure 3-5 E).

*Hml* driven Gal4 independent Fucci constructs were generated using the cloned *Hml*Δ-DsRed construct (the cloning of this construct is described in this chapter, in section 3.3). The *Hml*Δ-DsRed construct codes for ampicillin resistance and the *white* gene, for selection of successfully transformed colonies, and selection of new Fucci transgenic flies via eye colour respectively. The Fucci fluorescent fusion proteins were inserted where the DsRed fluorophore gene was previously located. Therefore, two plasmatocyte (*Hml*) specific and Gal4 independent Fucci fly lines were generated (*Hml*Δ-Fucci-$G_1$ Orange and *Hml*Δ-Fucci-S/$G_2$/M Green).

*3.2.5 Cloning of two Hml driven Fucci constructs*

Firstly, the Fucci constructs were digested with HindIII and BamHI in order to excise both of the Fucci fluorescence genes; Fucci-$G_1$ Orange and Fucci-S/$G_2$/M Green (see Figure 3-5 A for the Fucci constructs and the restriction sites). The p-Red H-Stinger-*Hml*Δ-DsRed plasmid was digested with BamHI and SpeI in order to cut out and remove

DsRed from the plasmid, whilst leaving the *Hml* promoter in place. T4 DNA polymerase was used for blunting on all three of the individually digested plasmids, and all three plasmids were digested once again with BamHI, in preparation for a sticky-blunt ligation. Ligations were transformed into chemically competent *E. coli* cells and colonies containing the plasmid were selected via ampicillin resistance. Finally miniprep was carried out with the ampicillin resistant colonies. Diagnostic digestions were performed on the Fucci orange and Fucci green miniprep DNA (Figure 3-5 C & D). The *Hml*Δ-Fucci-$G_1$ Orange and *Hml*Δ-Fucci-S/$G_2$/M Green constructs were both cut using XbaI and XhoI, these sites were located upstream of the *Hml*Δ promoter and within both Fucci fusion protein genes respectively. As predicted, in successfully cloned constructs this digestion yielded a 1.6kb band. A further digestion was carried out on both constructs using XbaI and HpaI. The HpaI restriction site is specific to Fucci orange fusion protein gene. As predicted, this restriction digest resulted in a 1.3kb band from the *Hml*Δ-Fucci-$G_1$ Orange plasmid, and no band from *Hml*Δ-Fucci-S/$G_2$/M Green digest. These digestions indicated the presence of the fluorescent Fucci fusion proteins within the p-Red H-Stinger-*Hml*Δ vector (See Figure 3-5 B for linear plasmid maps of the two new Fucci constructs).

Finally the separate Fucci constructs were then injected into $w^{1118}$, white eyed *Drosophila* embryos by BestGene Inc. Successful integration of the cloned Fucci plasmids resulted in the presence of the eye pigment gene, *white*. Therefore newly generated plasmatocyte specific Fucci reporter flies will have orange/red eyes. These individual transgenic Fucci flies were crossed to $w^{1118}$ flies by BestGene Inc. and the first generation was received in the lab. Flies from this cross were then used to ascertain the chromosomal location of the various Fucci insertions in the fly genome. We obtained a single *Hml*Δ-Fucci-$G_1$ Orange fly stock, located on the 2$^{nd}$ chromosome and three *Hml*Δ-Fucci-S/$G_2$/M Green fly lines were established, on the X, 2$^{nd}$ and 3$^{rd}$ chromosomes (See

Appendices 2 and 3 for detailed plasmid maps of the cloned *Hml*Δ-Fucci$G_1$-Orange and *Hml*Δ-Fucci$S/G_2$/M Green constructs).

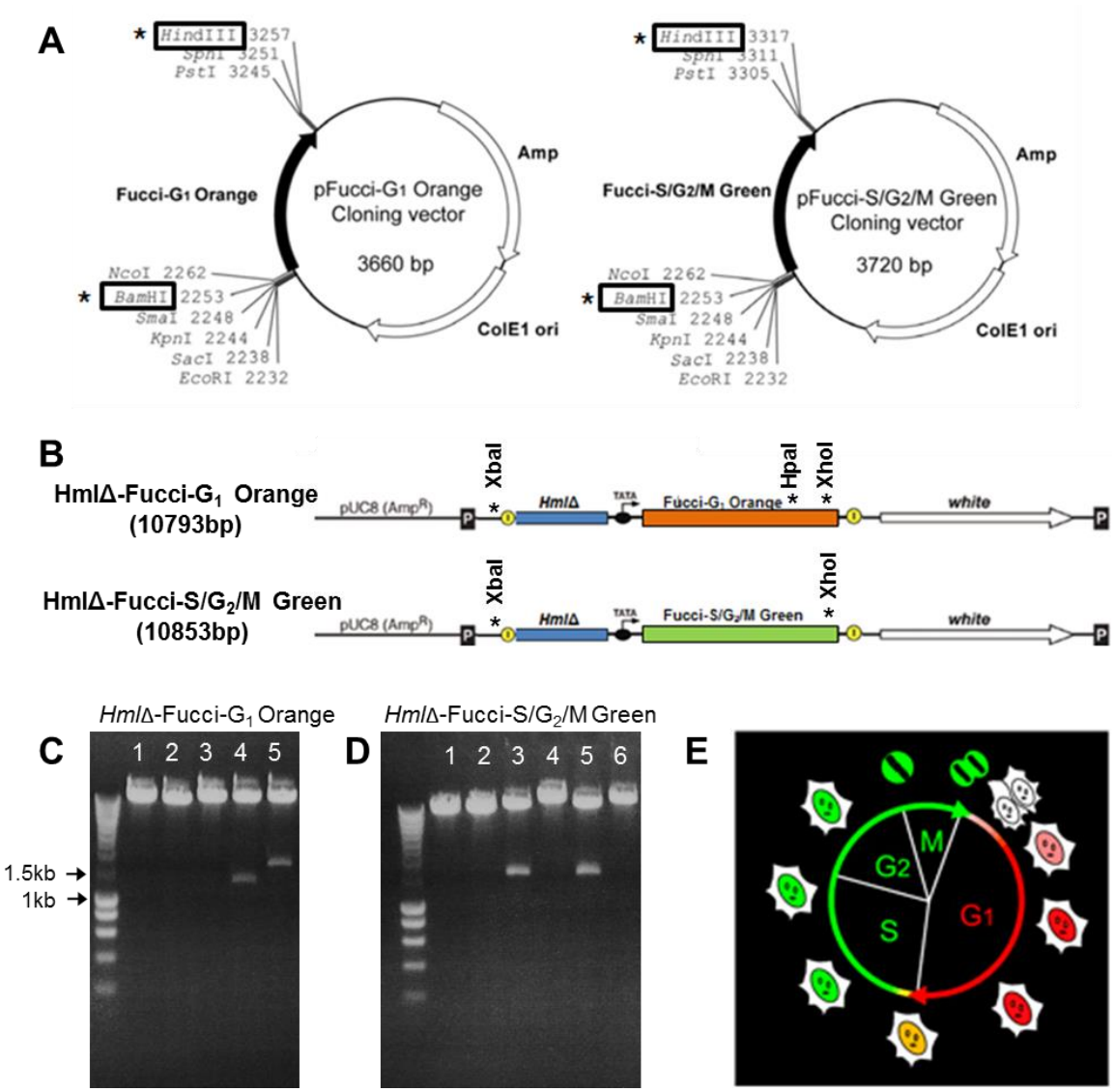


*Figure 3-5 Cloning of Hml driven, plasmatocyte specific Fucci constructs*
*Hml* driven Fucci S/$G_2$/M Green and Fucci $G_1$ Orange constructs were cloned. Fucci fluorescent fusion proteins were inserted downstream of the *Hml*Δ promoter using a previously generated plasmid; p-Red H-Stinger-*Hml*Δ-DsRed (generation of which is described in this chapter, in section 3.3) **A.** pFucci-$G_1$ Orange (left) and pFucci-S/$G_2$/M Green (right) cloning vector plasmid maps, stars * indicate restriction sites utilised during the cloning process. **B.** Linear plasmid maps of cloned *Hml*Δ-Fucci-$G_1$ Orange and *Hml*Δ-Fucci-S/$G_2$/M Green, stars * indicate restriction sites used during diagnostic digestions. **C.** Diagnostic digestion of *Hml*Δ-Fucci-$G_1$ Orange construct. Lanes 1-3, no insert present. Lanes 4 & 5 are the same mini prep DNA; lane 4 was digested with XbaI and HpaI (HpaI is specific to Fucci-Orange) resulting in a predicted 1.3kb band. Lane 5 was digested with XbaI and XhoI for a 1.6kb band, as predicted. **D.** Diagnostic digestion of *Hml*Δ-Fucci-S/$G_2$/M Green constructs. Lanes 1-2, no insert present. Lanes 3-4 represent the same miniprep DNA, and likewise for lanes 5-6. Lanes 3 and 5 were digested with XbaI and XhoI resulting in predicted 1.6kb band. Lanes 4 and 6 were digested with XbaI and HpaI, resulting in no band, as the Hpa1 restriction site is not present in Fucci Green. **E.** Schematic representation of Fucci cell-cycle labelling. Fucci-$G_1$ Orange labels $G_1$ phase nuclei in orange and Fucci-S/$G_2$/M Green labels nuclei in phases S/$G_2$/M green.

*3.2.6 Adult fly plasmatocyte self-renewal*

The plasmatocyte specific *Hml*Δ-Fucci-$G_1$-Orange and *Hml*Δ-Fucci-S/$G_2$/M-Green flies were crossed to each other, resulting in flies expressing both of the Fucci fluorescent fusion proteins, thus allowing for confocal microscopy of plasmatocytes in different mitotic stages. These *Hml⊿*-Fucci flies were imaged for both red (kusabira-orange 2- $G_1$) and green (azami-green1 – S/$G_2$/M) Fucci fluorescence. This was initially carried out in 1$^{st}$ instar larvae as a positive control for hemocyte proliferation. Results indicated that the *Hml* positive cells in the double transgenic *Hml⊿*-Fucci flies were capable of expressing both Fucci $G_1$ Orange and Fucci-S/$G_2$/M-Green and so that hemocytes were cycling. Some cells were positive for both Fucci Orange and Fucci green, indicating that *Hml* positive cells were cycling and moving from $G_1$ to S phase in these larvae (Figure 3-6 A). Proliferation of larval embryonic derived hemocytes has been previously described by Holz et al. (2003).

Experiments were then performed to investigate the proliferative potential of plasmatocytes in adult flies, under steady state conditions (Figure 3-6 B). In all flies imaged *Hml* positive plasmatocytes appeared to be arrested in the $G_1$ phase of mitosis, as would be expected in terminally differentiated cells (Buttitta et al., 2007). We found no evidence to suggest that *Hml* positive plasmatocytes proliferate or self-renew under steady state, non-immune challenged conditions, as has been previously advocated (Lanot et al., 2001).

*3.2.7 Hematopoietic organ existence in adult Drosophila*

Flies were additionally imaged for areas of plasmatocyte proliferation (e.g. areas of cells expressing both Fucci Green and Fucci Orange) for the existence of a hematopoietic organ, although it has been previously reported that no such organ exists in adult *Drosophila* (Lanot et al., 2001). Late in pupal development metamorphosis occurs and the lymph gland, the major larval hematopoietic organ, ruptures releasing the larval derived

hemocytes into the circulation. After this point it is believed that *Drosophila* no longer possesses a hematopoietic organ. Imaging was carried out paying particular interest to the area close to the fly heart and dorsal vessel, which is where the lymph gland would once have been located prior to rupture. Once again no areas of *Hml* positive cell proliferation were observed in adult flies.

### *3.2.8 Adult fly plasmatocyte proliferative potential after infection*

Experiments were also carried out to investigate whether *Hml* positive plasmatocytes were able to divide upon immune challenge. Flies expressing both of the *HmlΔ*-Fucci proteins were injected abdominally with a mixture of gram positive *M. luteus* and gram negative *E. coli* in order to activate both *Toll* and *Imd* pathways, and imaged at various time points post infection, including 6, 12 and 24 hours. In multiple infection experiments no evidence of plasmatocyte proliferation was observed, cells did not leave the $G_1$ phase of mitosis (data not shown), much like what was observed in adult flies in steady state non-infected conditions (Figure 3-6 B).

Once again, at the same time these infected flies were also imaged for any areas of proliferation, which could represent a hematopoietic organ stimulated upon infection. However, nothing was detected to suggest this was the case. These data suggest that *Hml* positive plasmatocytes, once entering the adult stage of the *Drosophila* life cycle remain as 'resident' terminally differentiated cells, and their numbers, although they do diminish slowly with time, remain relatively stable, regardless of immune challenge.

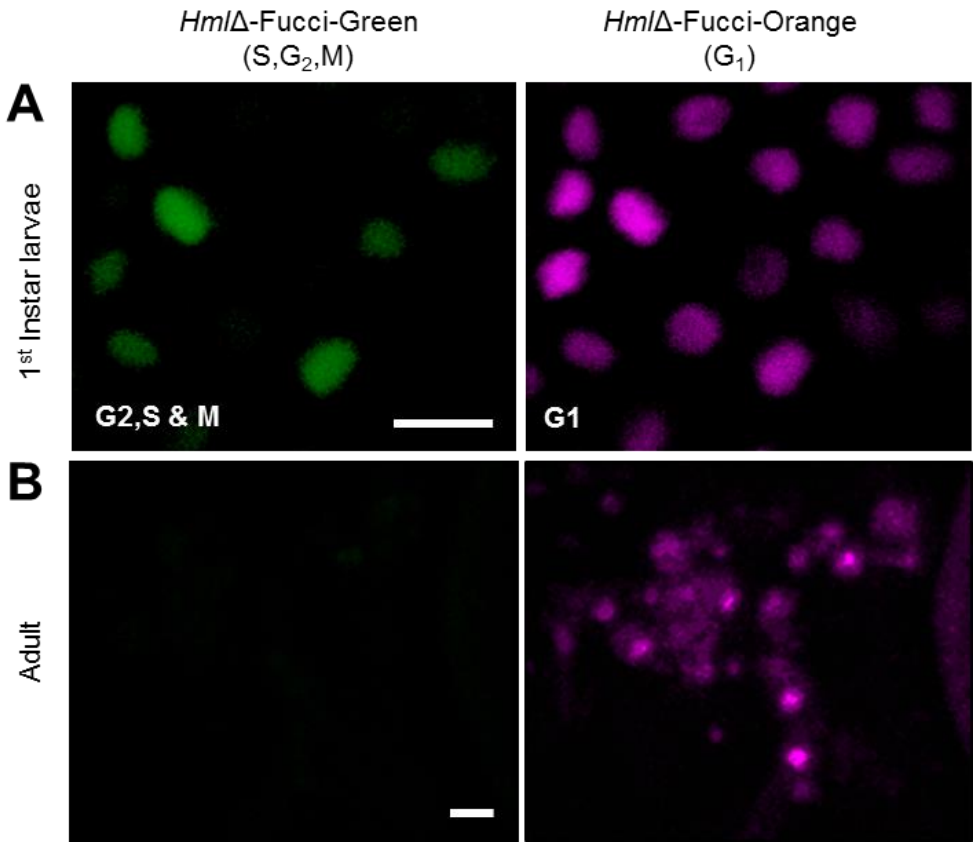


*Figure 3-6 Cycling hemocytes in 1st instar larvae and arrested non-cycling plasmatocytes in adult flies*

Confocal microscopy of w;*Hml*Δ-Fucci-$G_1$ Orange/+;*Hml*Δ-Fucci-S/$G_2$/M Green/+ *Drosophila*, at the 1st instar larval stage of development and in adult flies for the presence of cycling cells. Labelled nuclei of cycling *Hml* positive hemocytes in **A.**1st instar larvae (scale bar= 10µm) and **B.** 10 day old adult male fly (scale bar= 250µm). Green represents cells in S/ $G_2$/M phases of mitosis, and magenta represents cells in the $G_1$ phase of mitosis. These images are representative of n=5 1st instar larvae and n=5 adult flies. Imaging in panel A was carried out with a 40x objective Z stack volume= 20µm, Z step size= 2µm. Imaging in panel B was carried out with a 10x objective, Z stack volume=200µm, Z step size= 7µm. This experiment was repeated 5 times with reproducible findings.

### 3.3 Generation of a Gal4 independent reporter fly

The generation of a Gal4 independent plasmatocyte transgenic reporter fly allowed for deeper characterisation of plasmatocyte pan markers in adult flies. The plasmatocyte transgenic lines available to date operate under the Gal4, UAS expression system e.g. w;*Hml*Δ-Gal4,UAS-2xeGFP and w;;*crq*-Gal4;UAS-myrRFP. In this instance, crossing the two plasmatocyte Gal4, UAS reporter flies together fails to give true expression characteristics of the two genes. This is because as soon as Gal4 is transcribed, transcription will be initiated at all of the UAS sites present. For imaging purposes, this would mean all cells which had initiated transcription of either of the Gal4 linked genes would be double positive for both GFP and myrRFP, regardless of whether *Hml*, *crq* or both were being produced by the given cell.

On the contrary, use of a Gal4 independent transgenic fly allows for imaging of two independent plasmatocyte markers simultaneously, via crossing a Gal4, UAS plasmatocyte reporter fly, to a Gal4 independent reporter fly. Therefore, cloning of a Gal4 independent plasmatocyte reporter fly facilitated investigation into the existence of phenotypic plasmatocyte subsets in adult *Drosophila*.

#### *3.3.1 Cloning of HmlΔ-DsRed*

*Hml* was chosen as a plasmatocyte specific driver for cloning of the Gal4 independent reporter fly. This is because *Hml* displayed the greatest plasmatocyte specificity and consistency of expression. Furthermore *Hml* is one of the few plasmatocyte specific markers to be expressed in adult flies.

The p-Red H-Stinger plasmid (Barolo, 2004) was used as a vector, because of the presence of a DsRed.nls (nuclear localisation signal) fluorescent protein (Figure 3-7 A). Nuclear localisation was preferred for imaging purposes, given that all other reporter stocks had cytoplasmic, or both cytoplasmic and nuclear localisation. Furthermore, it was anticipated that fluorophore expression without the Gal4-UAS expression system would

be weaker. Therefore, confining DsRed expression to the nuclei restricts the fluorescence to a smaller subcellular area, potentially resulting in a brighter fluorescence in the nuclei. In turn, this increases the possibility of successfully visualising the fluorescence.

The p-Red H-Stinger construct also codes for ampicillin resistance and the *white* gene, necessary respectively for the selection of successfully transformed colonies and identification of flies which have successfully integrated the plasmid into their genomic DNA. The *Hml*Δ promoter insert required to drive the expression of DsRed was obtained from the pCaSpeR-4-*Hml*ΔGal4 plasmid (Sinenko and Mathey-Prevot, 2004).

A sequential restriction digest was performed on both plasmids using KpnI and BamHI, in order to open the p-red H-Stinger vector, and to obtain the *Hml*Δ promoter from the pCaSpeR-4-*Hml*Δ-Gal4 construct, leaving both the vector and the insert with sticky ends. The digestions were then separated on the basis of size via gel electrophoresis. The correct size bands were extracted, ~10.5kb for p-Red H-Stinger, and 844bp for the *Hml*Δ promoter. The *Hml*Δ promoter was then ligated into the multiple cloning site (MCS) of p-Red H-Stinger upstream of the DsRed. Ligations were transformed into chemically competent *E. coli* cells and colonies containing the insert were selected via ampicillin resistance. Finally miniprep was performed with the ampicillin resistant colonies. Two diagnostic digestions were completed on the miniprep DNA to confirm presence of the *Hml*Δ insert. First using KpnI and BamHI to cut out the *Hml*Δ promoter insert (Figure 3-7 B). Secondly the plasmids were digested with PshAI, a site present only in the *Hml*Δ promoter, and BamHI. Both digestions confirmed the presence of the *Hml*Δ promoter within the p-Red H-Stinger-*Hml*Δ construct (see Appendix 1 for a plasmid map of the *Hml*Δ-DsRed construct). The p-Red H-Stinger-*Hml*Δ plasmid (Figure 3-7 C) was then injected into $w^{1118}$, white eyed embryos by BestGene Inc. Successful integration of the cloned plasmid resulted in the presence of the *white* gene, which codes for eye pigment. Therefore newly generated plasmatocyte specific nuclear DsRed reporter flies would have orange/red eyes. The new transgenic fly

lines were crossed to $w^{1118}$ flies by BestGene Inc. before being received in the lab. The flies from this cross were then used to ascertain the chromosomal location of the *Hml*Δ-DsRed plasmid in the fly genome. Fortunately we obtained one stock on the 2nd chromosome, and another on the 3rd chromosome, which was optimal for use of both stocks in various crosses.

### *3.3.2 Imaging of HmlΔ-DsRed flies*

These new *Hml*Δ-DsRed fly lines were imaged and plasmatocytes were visible using confocal microscopy in both lines, with no difference in expression profiles between the two (Figure 3-7 D). It was noted however that expression of the DsRed appeared to be brightest when flies were maintained at 25°C, and expression was weak at room temperature or at 18°C. Interestingly similar findings are shown by Baird et al. (2000), it was observed that DsRed took several days at room temperature to reach maximal fluorescence, which may suggest temperature is a confounding issue in DsRed generation time, and stability. However, as experiments with these flies were routinely carried out at 25°C this did not pose issues for the continued study of these flies.

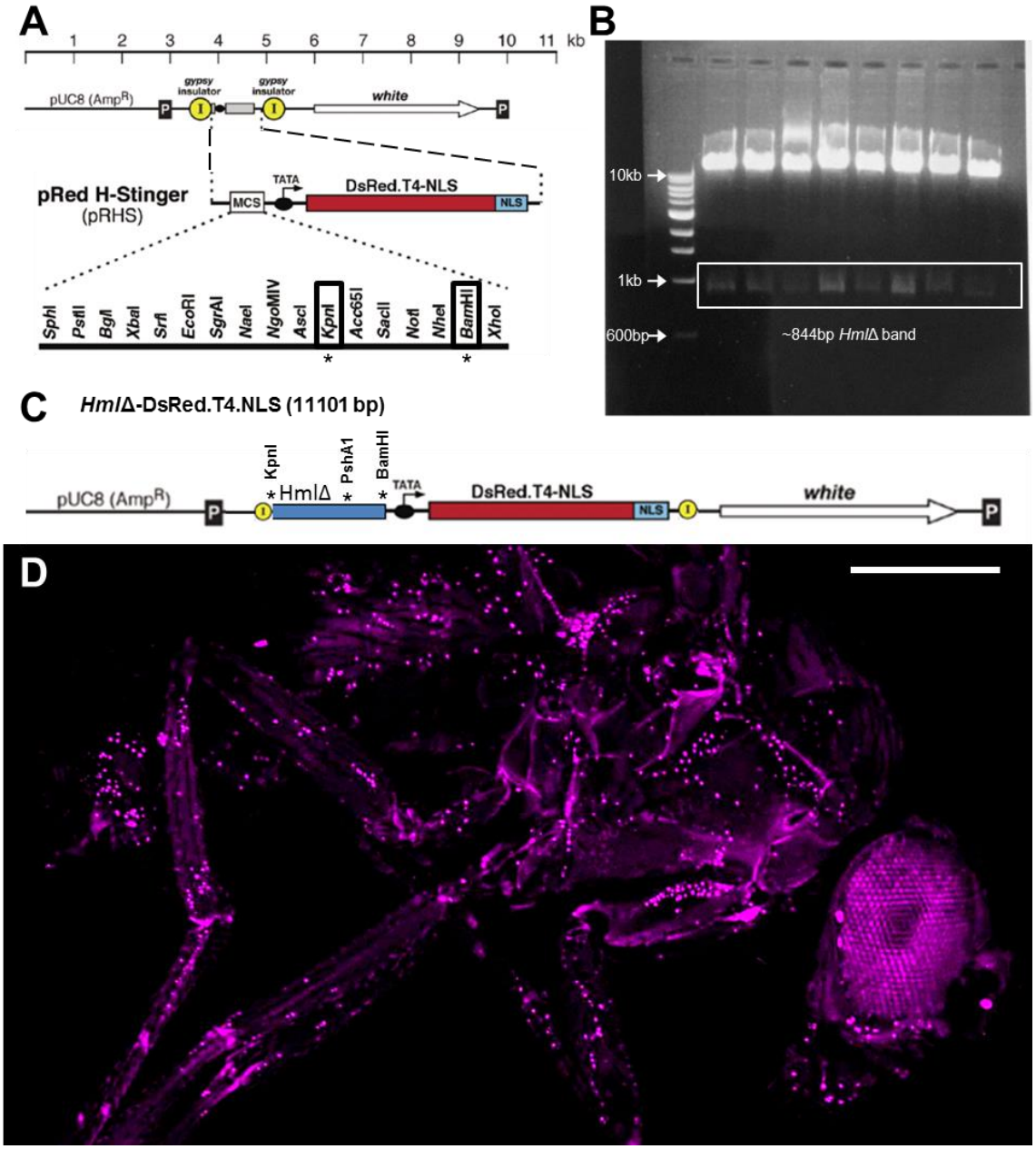


*Figure 3-7 Cloning and confocal microscopy of HmlΔ-DsRed reporter flies*
This figure details the cloning of the *Hml*Δ-DsRed, Gal4 independent plasmatocyte reporter fly line, including confocal microscopy of a *Hml*Δ-DsRed fly. **A.** p-Red H-Stinger construct, including multiple cloning site (MCS) restriction sites, stars * indicate restricted sites used during the cloning process. **B.** Diagnostic digestion of miniprep DNA with KpnI & BamHI, ~10.5kb p-Red H-Stinger and 844bp *Hml*Δ bands present in all colonies selected, suggestive of successfully cloned *Hml*Δ-DsRed constructs. **C.** Linear plasmid map of cloned *Hml*Δ-DsRed.nls construct, stars * indicate KpnI, BamHI, PshAI restriction sites used for ligation and diagnostic digestions). **D.** Confocal microscopy of a cloned w;;*Hml*Δ-DsRed fly (on the 3rd chromosome), scale bar= 750µm. Imaging was carried out with a 10x objective, Z-Stack size= 400µm, Z-Step size= 10µm. *Hml*Δ-DsRed positive plasmatocytes are false coloured magenta.

### 3.4 Characterisation of adult fly plasmatocyte pan markers

Adult *Drosophila* plasmatocytes are derived from both the embryonic and larval waves of haematopoiesis (Holz et al., 2003). Imaging experiments were performed using the newly generated *Hml*Δ-DsRed, Gal4 independent fly line crossed to *crq* and *Pxn* gal4, UAS plasmatocyte reporter flies in order to characterise expression of *Hml*, *crq* and *Pxn* as markers of adult fly plasmatocytes.

#### *3.4.1 Crq expression by plasmatocytes*

*Crq* is a *CD36*-like scavenger receptor responsible for engulfment of apoptotic cell corpses, and is expressed by hemocytes and in the gut during larval and pupal development (Franc et al., 1996, Lee et al., 2002). *Crq* has also been shown to be a marker of plasmatocytes in adult flies (Clark et al., 2011). Expression of *crq* in adult fly plasmatocytes was monitored visually using *crq* Gal4, UAS reporter flies (w;UAS-2xeGFP;*crq*-Gal4) over time. Plasmatocyte expression of *crq* in adult flies persisted throughout the fly lifespan, much like the expression profile seen in *Hml* Gal4, UAS flies (Figure 3-8).

Crossing the Gal4 independent *Hml*Δ-DsRed fly to a Gal4, UAS *crq* reporter fly (w;UAS-2xeGFP;*crq*-Gal4) allowed for visualisation of cells expressing both *Hml*, *crq* or both markers (Figure 3-9 A-C). Expression of both *Hml* and *crq* was quantified, and results suggested that the vast majority of *Hml* positive cells were additionally positive for *crq* expression (Figure 3-9 D), there was however a population of *Hml* and *crq* single positive cells, accounting for approximately 10% of the total plasmatocyte population each. It was difficult to ascertain if these single positive cells were separate populations of plasmatocytes, or if imaging restrictions resulted in some cells being missed. For example, confocal microscopy is only able to penetrate to a depth of approximately 8-10μm into the fly, meaning populations of cells deeper within the fly tissue would be missed. Furthermore, the longer wavelength of the 561 laser, used for imaging of DsRed

fluorescence enables deeper penetration into fly tissue than the 488 laser used to image GFP, which has a shorter wavelength. Therefore, potentially more DsRed signal could be detected than GFP signal purely due to inherent differences in laser penetration (Helmchen and Denk, 2005).

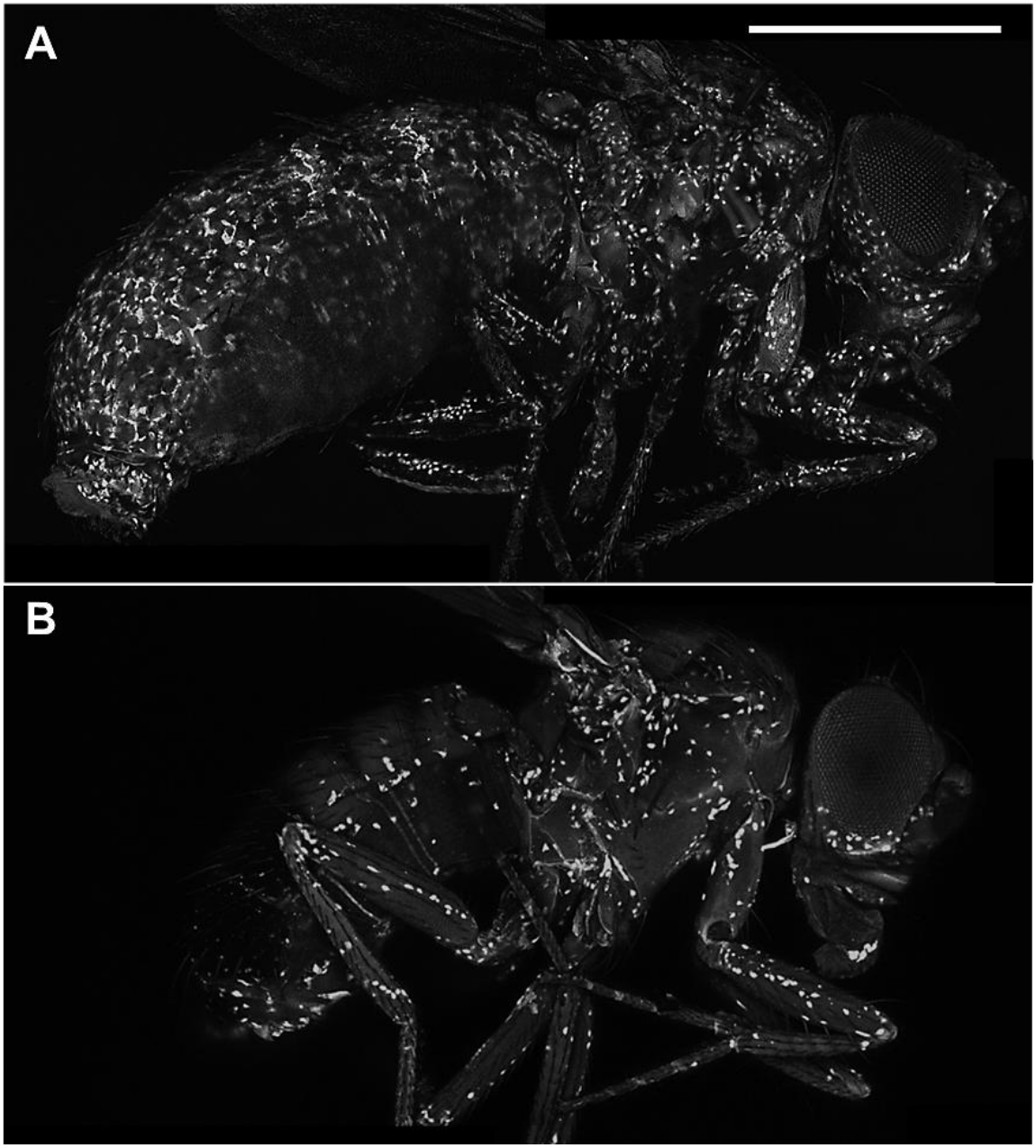


*Figure 3-8 Confocal microscopy of crq driven Gal4, UAS plasmatocyte reporter flies over time*
*Crq* reporter flies (w;UAS-2xeGFP;*crq*-Gal4) were imaged for plasmatocyte derived expression of *crq* and therefore GFP expression over time on **A.** the day of hatching fly and **B.** at 6 weeks after hatching, in adult male *Drosophila* (Scale bar= 750µm) GFP positive plasmatocytes are false coloured white. Imaging was carried out with a 10x objective Z-Stack size = 400µm, Z-Step size = 10µm. Imaging is representative of n=5 flies per time point.

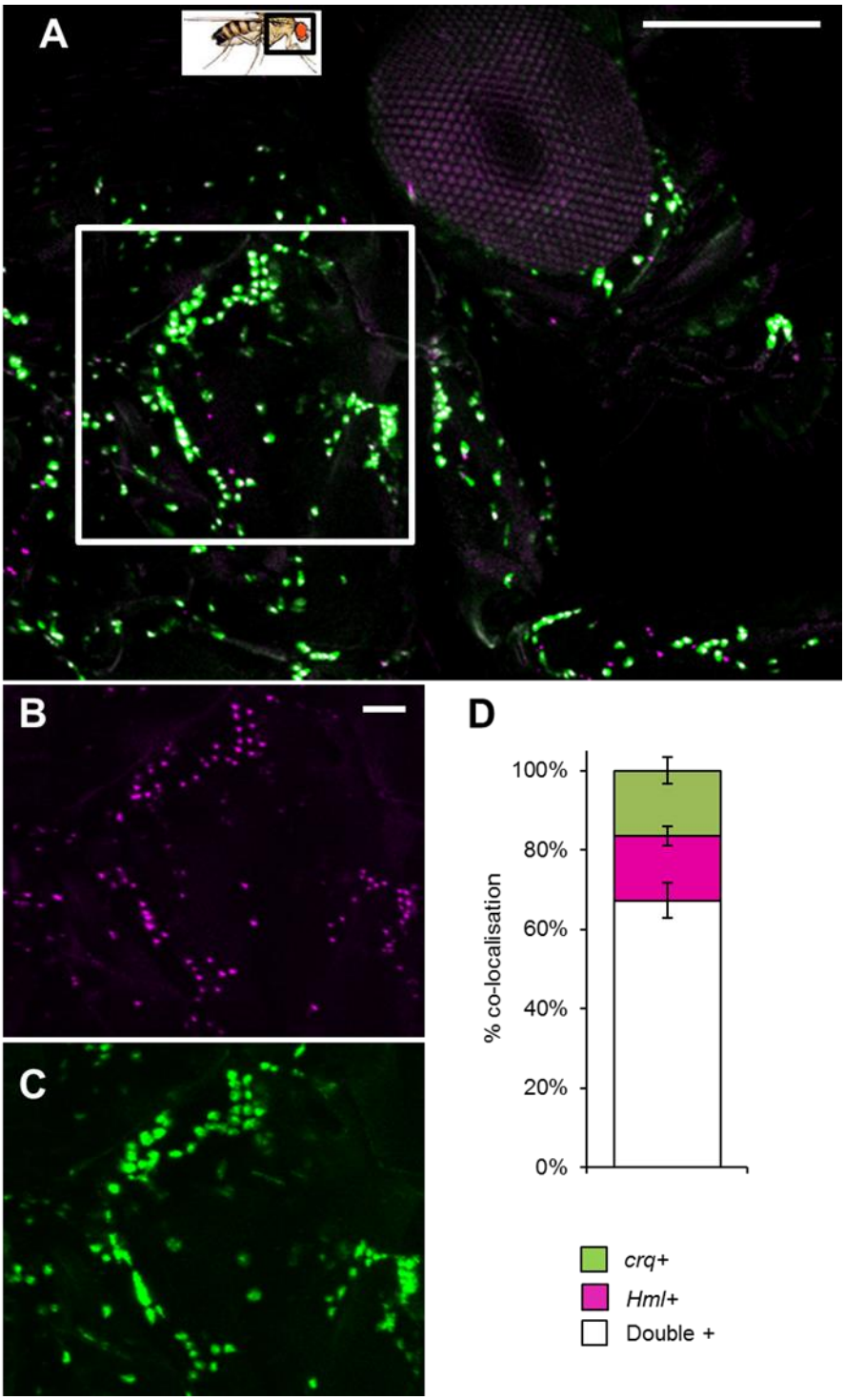


*Figure 3-9 Co-localisation of Hml and crq expression by adult fly plasmatocytes*
Confocal microscopy and quantification of w;UAS-2xeGFP;*crq*-Gal4/*Hml*Δ-DsRed flies for expression of *Hml* and *crq* by plasmatocytes. **A.** 1 week old male, fly inset picture indicates fly orientation during imaging and the black square illustrates the imaged area of fly (scale bar 250µm). The white square illustrates zoomed area from A shown in panels B and C. **B.** DsRed labelled *Hml* positive cells, false coloured magenta **C.** GFP labelled *crq* positive cells, scale bars in C and D= 50µm, imaging was carried out with a 10x objective. **D.** Percentage co-localisation of *Hml* and *crq* positive cells, calculated from the average total number of plasmatocytes per fly, $crq^{+}$ = single *crq* positive cells (green), $Hml^{+}$ = single *Hml* positive cells (magenta), $double^{+}$ = *Hml* and *crq* double positive cells (white). Data represents the mean of n=5 flies, error bars represent standard error of the mean.

*3.4.2 Peroxidasin expression in adult Drosophila plasmatocytes*

*Peroxidasin* (*Pxn*) is expressed by hemocytes and the fat body during embryonic and larval development. *Pxn* is believed to be involved in extra cellular matrix remodelling, and the phagocytosis of cells undergoing apoptosis (Nelson et al., 1994). Imaging of the *Pxn* reporter fly (w;;*Pxn*-Gal4,UAS-GFP) indicated that numbers of GFP expressing plasmatocytes, as well as the intensity of the GFP expression in these positive cells decreased rapidly during the first 2 weeks of adult fly life (Figure 3-10). This could be due to the death of *Pxn* expressing plasmatocytes. To test this hypothesis *Pxn* reporter flies were crossed to *Hml*Δ-DsRed flies to determine whether *Pxn* was expressed by *Hml* positive cells, as previous data in this thesis suggests that *Hml* positive plasmatocytes decline only slowly during adult *Drosophila* lifespan. As indicated in Figure 3-11 A, A', *Hml* and *Pxn* were co-expressed by plasmatocytes in newly eclosed adult flies, but it was only *Hml* expressing cells that remained in older flies (Figure 3-11 B, B'), suggesting that *Pxn* and *Hml* double positive plasmatocytes were not dying. This imaging observation was quantified by counting numbers of *Hml* and *Pxn* double positive cells in adult flies on the day of hatching and at 2 and 4 weeks of age. Findings replicated what was observed though imaging, *Hml* positive plasmatocytes appeared to lose expression of *Pxn* over time (Figure 3-11 C).

To re-confirm this decline of *Pxn* expression in adult flies, RT qPCR for *Pxn* expression over time was carried out using wild type $w^{1118}$ flies Figure 3-11 D). Indeed expression of *Pxn* was also diminished when observing transcript levels, therefore replicating what was observed via microscopy. These data consequently suggest that *Pxn* is down regulated in *Hml* positive plasmatocytes during the first few weeks of adult *Drosophila* life.

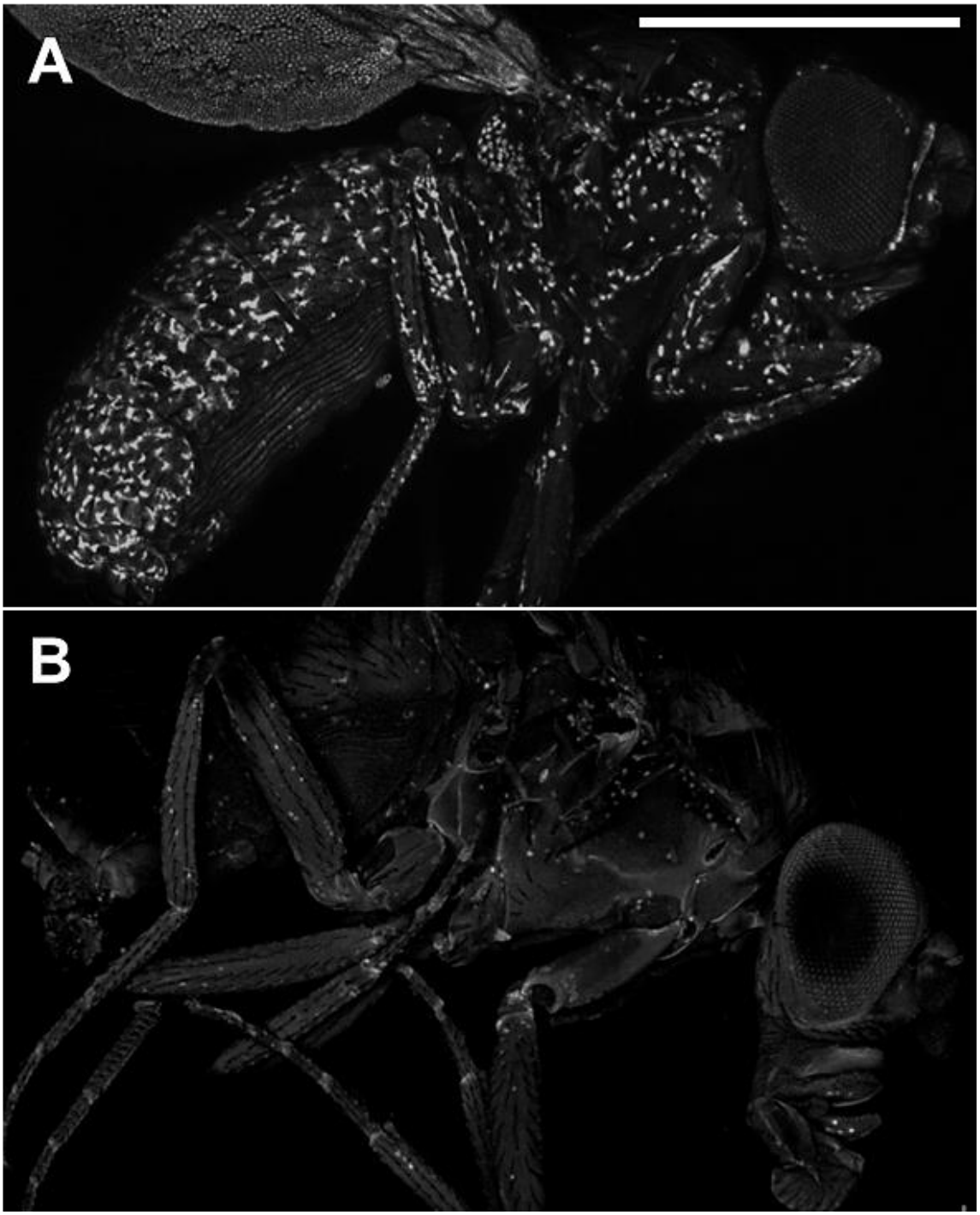


*Figure 3-10 Confocal microscopy of Pxn driven Gal4, UAS plasmatocyte reporter flies over time*
*Pxn* reporter flies (w;;*Pxn*-Gal4,UAS-GFP) were imaged for plasmatocyte derived expression of *Pxn* and therefore GFP expression over time, on **A.** the day of hatching fly and **B.** at 2 weeks after hatching, in adult male *Drosophila*. Scale bar= 750µm, imaging was carried out with a 10x objective, Z-Stack size = 400µm, Z-Step size = 10µm. GFP positive plasmatocytes are false coloured white. Imaging is representative of n=5 flies per time point.

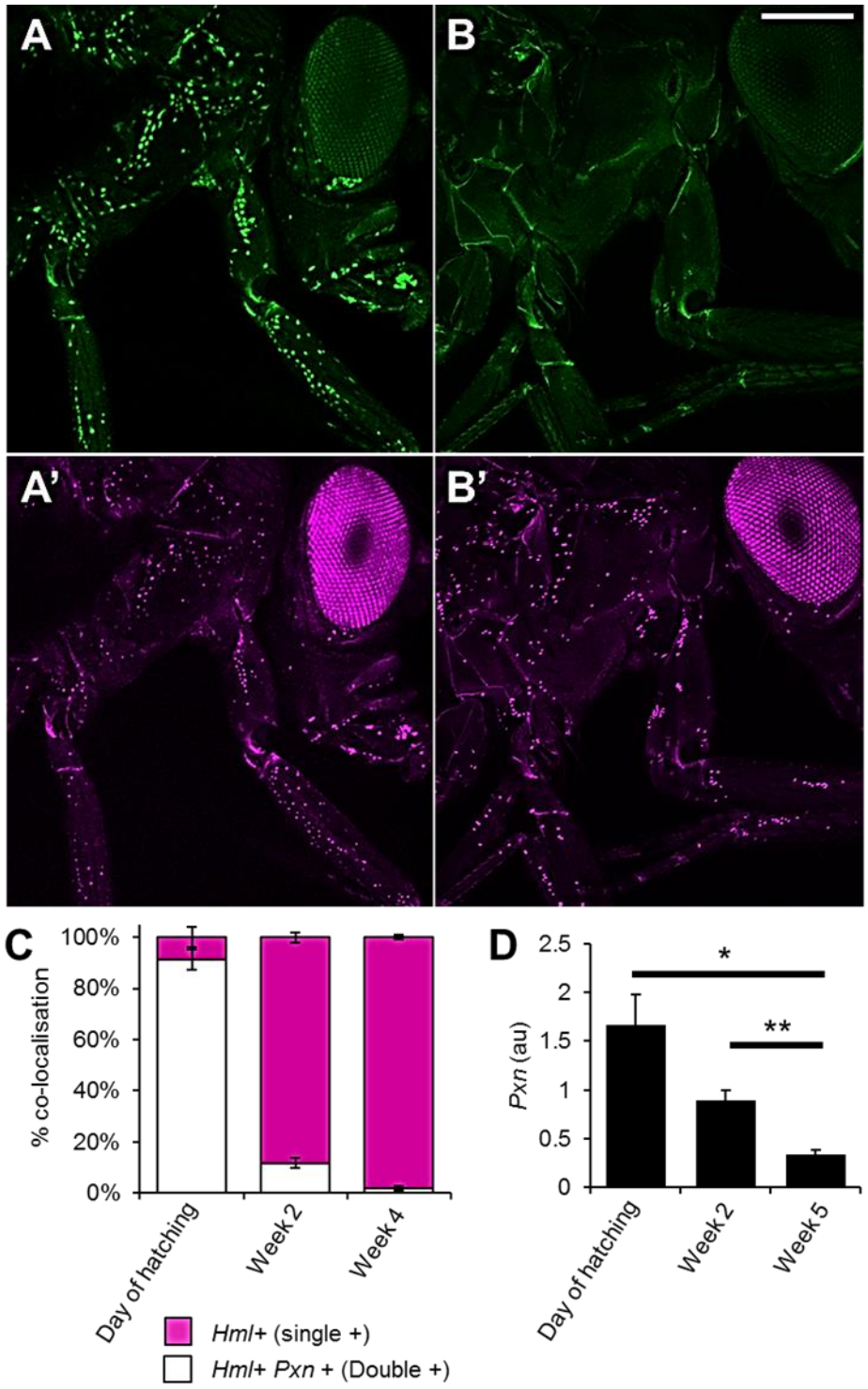


*Figure 3-11 Co-localisation of Pxn and Hml expression in plasmatocytes*
Confocal microscopy for *Hml* and *Pxn* co-expression in plasmatocytes using w;;*Pxn*-Gal4,UAS-GFP/*Hml*Δ-DsRed double reporter flies at 2 days post eclosion A, A' and at 4 weeks B, B'. **A, B.** *Pxn* GFP positive plasmatocytes. **A', B'**. *Hml*Δ-DsRed positive plasmatocytes (Scale bar=250µm, imaging was carried out with a 10x objective, Z-Stack size = 400µm, Z-Step size = 10µm). **C.** The mean percentage of *Hml*Δ-DsRed positive cells (magenta) co-expressing *Pxn* (white) over time on day of hatching, week 2 and week 4, data represents the mean of n=4 flies per time point, error bars represent standard error of the mean. **D.** RT qPCR analysis of *Pxn* in wild type $w^{1118}$ *Drosophila*, *Pxn* transcript levels normalised to that of housekeeping gene *Rpl1*, (au = arbitrary units). Data represents the mean of n= 4-6 flies per time point, error bars represent standard error of the mean. Statistical significances between day of hatching and week 2 p=0.07926 (ns), week 2 and week 5 p=0.00662, and day of hatching and week 5 p=0.01379 (unpaired t tests,* $p<0.05$, ** $p\leq0.01$).

*3.4.3 Plasmatocyte expression of Pxn is not inducible after infection*

In vertebrates peroxidase enzymes are heavily involved in defence against bacterial pathogens. Hydrogen peroxide ($H_2O_2$) is a reactive oxygen species secreted by vertebrate leucocytes in response to bacterial infection (Thannickal and Fanburg, 2000). *Drosophila Pxn* has a functional peroxidase domain which shares homology with human myeloperoxidase (Nelson et al., 1994). Expression of *Pxn* is gradually lost by *Hml* positive plasmatocytes early in the adult fly life in steady state, non-inflammatory conditions (Figure 3-10). Given the peroxidase domain encompassed within the PXN protein (Nelson et al., 1994), and the role of leucocytes producing peroxidases in mammalian infection, experiments were performed to investigate whether *Pxn* expression is inducible in plasmatocytes in response to infection.

*Pxn* and *Hml* double reporter flies (w;*Hml*Δ-DsRed;Pxn-Gal4,UAS-GFP) were used for the infection experiment to allow for visualisation of plasmatocytes regardless of *Pxn* expression. Flies were infected on day 10 of adult fly life; this time point was chosen due to the majority of plasmatocyte derived *Pxn* expression being lost by this point. Infection was carried out via abdominal injection, with a mixture of both gram negative *E. coli* and gram positive *M. luteus*, in order to activate both *Toll* and *Imd* pathways. Flies were imaged 24 hours post infection for induction of *Pxn* expression, alongside wounded (data not shown) and non-injected controls. A 24 hour time point was chosen in order to allow the maximum time for *Pxn* and therefore, GFP generation in the *Pxn* reporter flies. Results illustrated that *Pxn* driven induction of GFP expression was not induced by infection; this was re-confirmed by RT qPCR for *Pxn* expression in wild type $w^{1118}$ flies. Flies were homogenised for sampling 6 hours post infection, due to this being reported to be the optimal time point for AMP induction of AMP expression after infection (Lemaitre et al., 1997). Expression of *Drosomycin* (*Drs*) was examined as a positive control, *Drs* expression is known to be up regulated post infection (Lemaitre et al., 1997). No increase in *Pxn* expression was observed, both when imaging *Pxn* reporter flies (Figure 3-12 A,

B), and when examining *Pxn* transcript levels post infection (Figure 3-12 C). Conversely a strong induction of *Drs* was observed, which acted as a positive control for infection (Figure 3-12 D). These data suggest that *Pxn* is not induced upon infection, and that it is primarily involved in development and particularly pupal development where considerable tissue remodelling takes place.

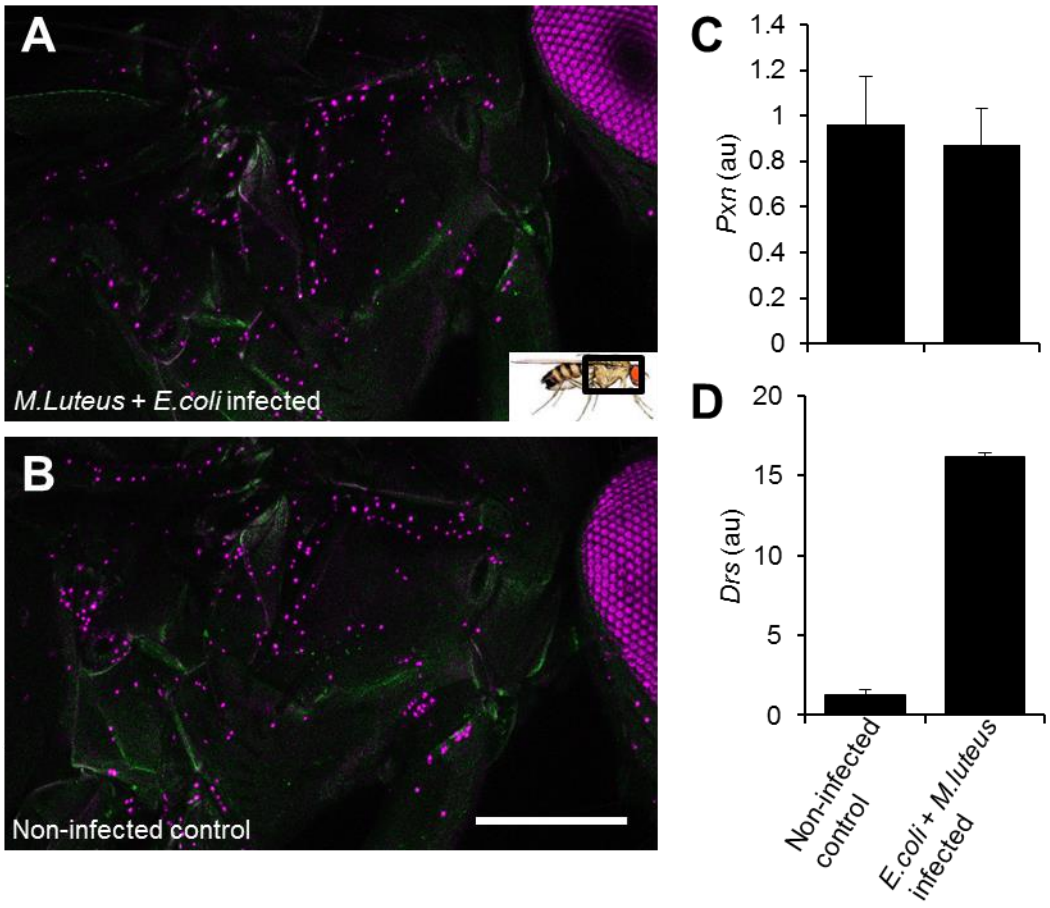


*Figure 3-12 Pxn expression by plasmatocytes upon immune challenge*
Confocal microscopy was carried out using 10 day old male w;;*Pxn*-Gal4,UAS-GFP/*Hml*Δ-DsRed double reporter flies, 24 hours post infection to determine whether *Pxn* was up regulated by plasmatocytes post infection. Images are representative of 3 independent experiments, n=3-4 flies per condition. **A.** *M. luteus* and *E. coli* co-infected fly, inset fly picture indicates fly orientation during imaging and the black square illustrates the imaged area of fly **B.** Non-infected control fly n= 4 flies per condition, scale bar= 250µm, imaging was carried out with a 10x objective, Z-Stack size = 400µm, Z-Step size = 10µm. RT qPCR of wild type $w^{1118}$ *M. luteus* and *E. coli* co-infected flies versus control non-infected flies 6 hours post infection for transcript levels of **C.** *Pxn* (unpaired t test p=0.735, ns) and **D.** *Drs* ($p \leq 0.001$/ ***). Expression levels of *Pxn* and *Drs* normalised to housekeeping gene *Rpl1*, (au = arbitrary units). The mean of n=5-6 samples is shown per condition, (3 flies per sample). Error bars represent standard error of the mean. These data are representative of 4 independent experiments.

## *3.5* Purification of plasmatocytes from adult *Drosophila*

In order to better characterise plasmatocytes in adult flies, a FACS (fluorescence-activated cell sorting) protocol was developed and optimised. This technique has previously only been published for larval hemocytes (Tirouvanziam et al., 2004). A standardised protocol was established, which is published in Clark et al. (2011), and cells were successfully sorted from whole flies. Availability of this technique made new experiments possible, including the sorting of plasmatocytes from whole flies, to carry out RT qPCR specifically with plasmatocyte derived cDNA. In addition, the technique was useful for sorting plasmatocytes in order to carry out fixing and staining protocols for imaging.

### *3.5.1 Optimisation of a protocol for FACS of adult fly plasmatocytes*

Sorting of plasmatocytes appeared to be most efficient using reporter flies in which the cells cytoplasm, or both cytoplasm and nuclei is labelled with fluorophore expression rather than nuclei alone. This is because of the increase in the visible area of fluorescence when the cell cytoplasm is labelled. For this reason, FACS experiments were optimised using w;*Hml*Δ-Gal4,UAS-2xeGFP plasmatocyte reporter flies, in which GFP is expressed in both the nuclei and cytoplasm of plasmatocytes.

Flies aged approximately 7-10 days old were used for FACS experiments, and they were maintained at 25°C prior to the sorting. The optimal number of flies for a sort was approximately 80-90 adult males, using fewer flies than this resulted in very small numbers of plasmatocytes, making them difficult to work with. Conversely using more flies than this resulted in the FACS sorter becoming clogged frequently with debris from the flies. The number of cells obtained from 80-90 w;*Hml*Δ-Gal4,UAS-2xeGFP reporter flies was usually between 10,000 – 20,000, with the sort taking from 2-4 hours (See Chapter 2, section 2.5 for a more detailed description of the FACS sorting protocol).

*3.5.2 Gating strategy for plasmatocyte purification*

The established gating strategy utilised wild type $w^{1118}$ flies as GFP negative controls for each individual sort, in order to apply the best gate to obtain GFP positive cells (Figure 3-13 A & B). During the sort, debris and doublets (more than one cell stuck together) were excluded in the first and second gates respectively, using the gating strategy illustrated in Figure 3-13. In the third gate GFP positive cells, and therefore *Hemolectin* expressing plasmatocytes, are selected and sorted. These sorted Plasmatocytes could be stained and imaged (Figure 3-13 C). The cells appeared to be morphologically stable and exhibited a plasmatocyte-like morphology, being spherical and approximately 8-10µm in diameter after sorting. The plasmatocytes also maintained the *Hml* driven GFP expression, and were positive for the nuclear stain Hoechst.

*3.5.3 Purity of the plasmatocyte sorted population*

Purity of the sorted plasmatocyte population was ascertained by re-analysing once sorted populations of GFP positive cells (Figure 3-14), which confirmed the presence of GFP positive plasmatocytes. The approach does have its limitations, as debris can still be found during the purity analysis; however it is difficult to determine the reason for this. It could be due to non-plasmatocyte cells being sorted, but it is more likely that the procedure of sorting itself may be responsible for cell death.

In addition to this, sorting of plasmatocytes is slower than that of many human blood cell sorts, this is due to the fact that flies contain significantly fewer plasmatocytes comparatively to the huge numbers of cells that can be obtained from human blood cell samples. In addition to this, the extra presence of debris in fly samples reduces the flow rate at which sorting can be carried out. Thus the duration of the sorts is another limiting factor.

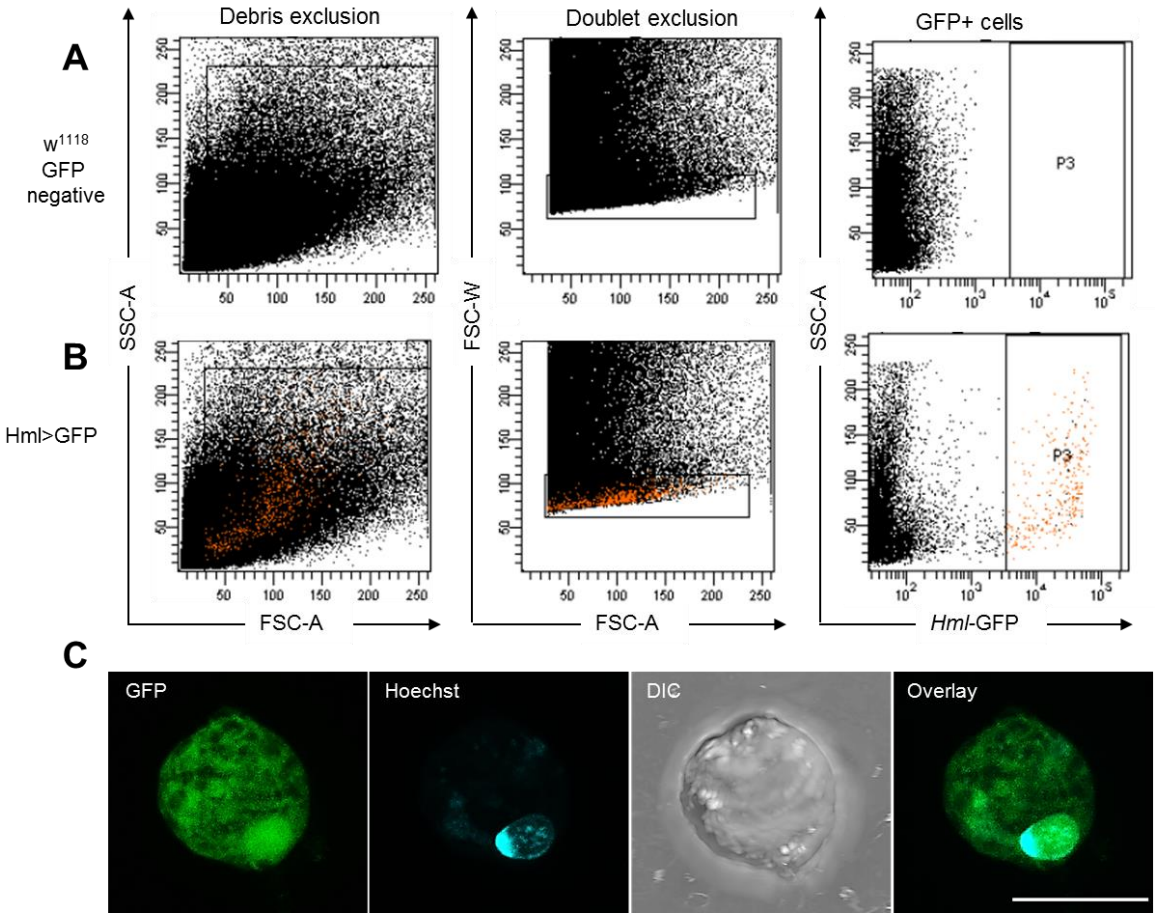


*Figure 3-13 FACS of $Hml^{+}$ $GFP^{+}$ plasmatocytes from adult Drosophila*
Plasmatocytes can be successfully sorted from adult *Drosophila*, on the basis of *Hml*, plasmatocyte specific, GFP expression. Gating strategies for **A.** Control non-GFP expressing $w^{1118}$ flies and **B.** w;*Hml*Δ-Gal4,UAS-2xeGFP flies. The first gate excludes debris, events too large or small to be cells. The second gate excludes doublets (clumps of cells), and the final gate shows GFP positive cells (indicated by orange dots), of which none are present in the $w^{1118}$ GFP negative control sample. **C.** Confocal microscopy of a FACS sorted live *Hml* GFP plasmatocyte. GFP channel: *Hml* positive cell, cyan channel: Hoechst staining for nuclei, DIC (Differential interference contrast) imaging for further visualisation of cellular morphological features. Overlay represents an overlay of the GFP and Hoechst channels. Scale bar = 10µm, imaging was carried out with a 40x objective, Z-Stack size = 20µm, Z-Step size = 1µm.

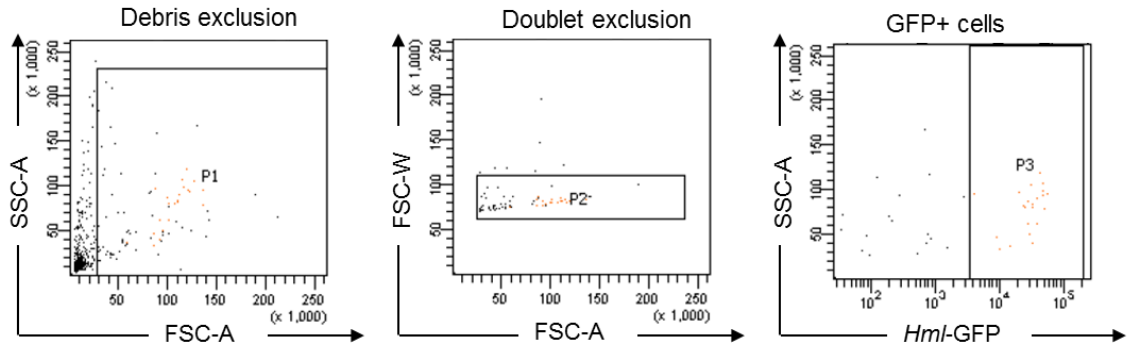


*Figure 3-14 Re-analysis of FACS sorted plasmatocytes for determination of population purity*
The populations of GFP positive plasmatocytes which were sorted from w;*Hml*Δ-Gal4,UAS-2xeGFP flies were re-analysed post sorting to determine the sort purity. The first gate excludes debris, events too large or small to be cells. The second gate excludes doublets (clumps of cells), and the final gate shows GFP positive cells (indicated by orange dots), thus indicating that it is possible to detect GFP positive plasmatocytes in populations of once sorted cells.

## 3.6 Chapter 3 overview and discussion

### *3.6.1 Imaging as a means to quantify absolute plasmatocyte numbers*

Adult *Drosophila* are estimated to contain several thousand plasmatocytes (Lemaitre and Hoffmann, 2007), however cell numbers have not been quantified to date. It was also previously unknown if plasmatocytes persist throughout the adult *Drosophila* lifespan.

Quantification of GFP, *Hml* positive plasmatocytes in imaging experiments indicated that plasmatocyte numbers steadily fall throughout the adult *Drosophila* lifespan. This said, imaging does have limitations, firstly each fly was imaged laterally (on their sides) in order to obtain the best representation of plasmatocytes in as many anatomical locations simultaneously. Therefore plasmatocytes on the other side of the fly were not included in the estimate of plasmatocyte numbers. Secondly, confocal microscopy laser penetration reaches an imaging depth of approximately 10µm. This means many plasmatocytes localised deeper in the fly tissue would be missed. Despite this, confocal microscopy of plasmatocyte reporter flies allowed for an accurate quantification of changes in plasmatocyte numbers over time, but not their absolute numbers.

Initially study of plasmatocyte numbers in adult flies was planned to be determined using FACS sorting. However, due to the significant differences in cell yield from one sort to the next results were not reproducible enough to allow for the calculation of plasmatocyte numbers per fly.

### *3.6.2 Generation of UAS-Fucci flies*

It is widely believed that plasmatocytes do not have the capacity to proliferate in adult flies, at steady state, or after immune challenge (Lemaitre and Hoffmann, 2007). Experiments carried out in this thesis found no evidence to disprove this theory. Hemocyte proliferation was observed in 1$^{st}$ instar larvae using *Hml* driven, Fucci flies. However, in adult *Drosophila* all visible *Hml* positive plasmatocytes adopted a terminally

differentiated state, during both steady state and after infection. However it is important to note that due to the nature of the imaging experiments carried out, if the hematopoietic organ and, or proliferating/self-renewing plasmatocytes were located deeper in fly tissue, in the gut or brain for example they could have been overlooked. This is because *in vivo* imaging was carried out using live plasmatocyte reporter flies, meaning the depth of imaging was limited to approximately 10µm.

In order to study plasmatocyte proliferation in more detail it would also be interesting to clone UAS-Fucci constructs, allowing visualisation of Fucci using different plasmatocyte specific drivers. Additionally, use of UAS-Fucci flies would allow for testing of a proliferation positive control in adult *Drosophila*.

Self-renewal of murine macrophages after pathogen exposure has recently been reported (Jenkins et al., 2011). Although no evidence was observed for plasmatocyte self-renewal, this was in response to two, non-fatal bacterial infectious agents *E. coli* and *M. luteus*. It would be interesting to investigate plasmatocyte proliferative potential in response to different bacterial and viral pathogens.

### *3.6.3 Existence of phenotypic of plasmatocyte subsets*

The vast majority of plasmatocytes (80%) appear to co-express both *Hml* and *crq* however; the remaining cells were single positive for either *crq* (10%) or *Hml* (10%) expression alone. It is difficult to prove whether this is due to existence of true phenotypic subsets, or if it is a result of imaging restrictions. One example of this is an issue of laser penetration. The laser for detection of DsRed expression (561 laser) is actually able to penetrate deeper into the fly cuticle than the laser that detects GFP expression (488 laser) (Helmchen and Denk, 2005). This could potentially mean *Hml*Δ-DsRed positive cells are able to be imaged at a deeper level within tissue than *crq* positive GFP cells.

*3.6.4 Peroxidasin is not a marker of adult Drosophila plasmatocytes*

The embryonic and larval hemocyte marker *Pxn* appears to be expressed only in young adult *Drosophila*, and expression quickly diminishes during the first two weeks of the adult fly lifespan, this was confirmed both by confocal microscopy of *Pxn* reporter flies, and in wild type flies via RT qPCR. Furthermore, expression of *Pxn* was not re-inducible upon bacterial infection, suggesting that peroxidase activity is employed by plasmatocytes principally during development for tissue remodelling purposes, as discussed by Nelson et al. (1994).

*3.6.5 Plasmatocyte purity*

A protocol for plasmatocyte purification from whole adult *Drosophila* was established. However, re-analysis of once FACS sorted plasmatocytes indicated debris was still present within the sorted population of cells. In view of this, it is important to be cautious when using FACS sorted plasmatocytes in experiments. The effect of purity upon imaging experiments is minimal, as GFP positive *Hml* positive plasmatocytes can be identified visually. Additionally, apoptotic cells have a characteristic appearance which would be visible during imaging, allowing for exclusion of these cells (Ziegler and Groscurth, 2004). In addition to this, plasmatocytes utilised for cDNA generation were sorted directly into to a lysis buffer, thus minimising any cell death which occurred during the time period between cell sorting and use of the cells.

Regardless of these limitations, the fact that plasmatocytes could be successfully sorted from whole adult *Drosophila* was a great advantage to the study of plasmatocytes specifically, and allowed for in depth analysis of these cells later in this thesis.

*3.6.6 Fly plasmatocytes as models for mammalian macrophages*

In this chapter, adult *Drosophila* plasmatocytes are characterised as *Hml* and *crq* expressing, sessile, non-proliferative cells. Plasmatocyte numbers remain relatively

stable, with them declining slowly during the adult fly lifespan. The similarities observed during development (Evans et al., 2003), and characteristics of plasmatocytes as tissue bound sessile cells, once again likens them to mammalian macrophages. This chapter also describes the development of tools and protocols in order to study plasmatocyte functions in more detail in adult flies. The remainder of this thesis studies plasmatocyte functions in adult flies and in particular, the response of plasmatocytes to chronic dietary lipid exposure.

# Chapter 4 *Drosophila* response to high fat diet

## 4.1 Introduction, aims and objectives

### *4.1.1 High fat diet induced diseases*

In humans high fat diet and the subsequent induction of high fat diet induced diseases results in premature death (Taubes, 2001). The prevalence of high fat diet induced diseases, including type II diabetes, atherosclerosis and metabolic syndrome, are rapidly rising (Ford et al., 2004), however the precise mechanisms behind high fat diet disease induction are not fully understood.

Interestingly, increasing the quantity of dietary lipids results in a significant reduction in *Drosophila* lifespan, which appears to be dose dependent (Driver and Cosopodiotis, 1979). In line with this finding, high fat diet has also been shown to cause a metabolic-like syndrome in the fly. Much like the phenotypes observed in humans, flies with a metabolic-like syndrome exhibit an increase in glucose and triglyceride levels, and develop insulin resistance (Birse et al., 2010, Eckel et al., 2005). Therefore the fly is a valuable model to try to further understand the development and progression of high fat diet induced disease pathology.

### *4.1.2 Macrophage role in high fat diet disease development and progression*

In vertebrates lipids are known to be scavenged by macrophages, the counterpart cell in the fly is the plasmatocyte (Meister and Lagueux, 2003). The act of scavenging itself is believed to result in the downstream induction of pro-inflammatory cytokine expression, resulting in inflammation (Yudkin et al., 2000). In humans this is directly associated with the development of atherosclerotic plaques in blood vessels, which upon rupture can result in thrombus formation and subsequent pathological effects, including myocardial infarction and strokes (Berliner et al., 1995). The relationship between lipid scavenging and the function of, or protection against inflammation remains unclear and difficult to study *in vivo*. The fly is an attractive model to try to further understand the interaction

between macrophages and lipids, and in turn to uncover primitive functions of macrophages which are conserved throughout the species.

### *4.1.3 Hypothesis and aims*

Fly plasmatocytes, like mammalian macrophages, contribute to high fat diet related pathophysiology.

The aims are this chapter are as follows;

1. Study of the fly response, in terms of survival, metabolic and immunological phenotypes, to high fat diet exposure.
2. Study of the plasmatocyte specific role in high fat diet related pathophysiology in plasmatocyte depleted flies.

### 4.2 Effects of different dietary fats upon adult *Drosophila* survival

In order to characterise the effect of lipid rich diet exposure on *Drosophila*, survival experiments with different lipid enriched diets were carried out, to determine whether chronic dietary lipid exposure was detrimental to the survival of *Drosophila*. Findings reproduced what had been previously observed by Driver and Cosopodiotis (1979), fly lifespan was significantly reduced upon lipid rich diets compared to control diet (Figure 4-1). Wild type $w^{1118}$ flies were placed on three different lipid rich diets, lard (animal fat), coconut oil, and olive oil (vegetable fats); alongside the control diet (See Table 4-1 for detailed information on fat composition and saturation). Lard and coconut oil diets were chosen due to them being previously tested in studies by Driver and Cosopodiotis (1979) and Birse et al. (2010) respectively, and olive oil was chosen due to its low saturation level and hence the belief that it is one of the healthier types of fat. The fat saturation levels in coconut oil, lard and olive oil are all somewhat different, and therefore allowed for a comparison of the effects of differential fat saturation levels upon fly lifespan.

Fly lifespan was significantly reduced in all lipid rich diets tested, in a dose dependent manner (Figure 4-1). The lard, fructose low diet was not used in future experiments from this point on; this was because survival phenotypes could be influenced by the lack of glucose, as well as the presence of extra lipid. In addition to this, the olive oil diet was not utilised in the rest of the experiments discussed in this thesis. Although survival phenotypes upon this diet were interesting, particularly because olive oil is classed as one of the more healthy fats, survival results were less reproducible than in the lard and coconut oil enriched diets. One potential reason for this was that in some instances the sides of the olive oil enriched food vials became coated with the oil, in this case, fly death due to becoming caught in the oil, rather than from the consumption of it cannot be ruled out. Of the three fats tested, olive oil is liquid at room temperature whereas the coconut oil and lard are both solid, making food consistency more stable. However, before a conclusion can be drawn with regard to the true cause of fly death on

olive oil enriched diets, further experiments to control for the flies becoming stuck in the olive oil should be carried out.

On the basis of the described survival experiments (Figure 4-1), future experiments included in this thesis were carried out using the lard and coconut oil diets (Figure 4-1 A, C) at either 6.3%, or 15%, this was because these diets gave the most reproducible findings in terms of survival and food consistency.

In order to reconfirm the effect of dietary lipids upon survival of wild type flies, replication of the observed reduction of lifespan using another wild type strain was important as a control for effects caused by the genetic background of the fly. Indeed, survival data indicated that upon a lard enriched diet the Oregon R wild type strain exhibit similar survival phenotypes to that of the $w^{1118}$ wild type flies, and succumb earlier than flies upon a control diet (Figure 4-2).

*Table 4-1 Fat compositions*

| Fat | Saturated (g/100g) | Monounsaturated (g/100g) | Polyunsaturated (g/100g) | Cholesterol (mg/100g) |
|---|---|---|---|---|
| Lard | 40.8 | 43.8 | 9.6 | 93 |
| Coconut oil | 85.2 | 6.6 | 1.7 | 0 |
| Olive oil | 14.0 | 69.7 | 11.2 | 0 |

Table indicating levels of saturated, monounsatuated and polyunsaturated fat, as well as cholesterol in the 3 fats (lard, coconut oil and olive oil) which were studied for their effect on wild type $w^{1118}$ fly survival. Numbers represent grams per 100 grams (g/100g: saturated, monounsaturated and polyunsaturated), and milligrams per 100 grams (mg/100g:cholesterol).

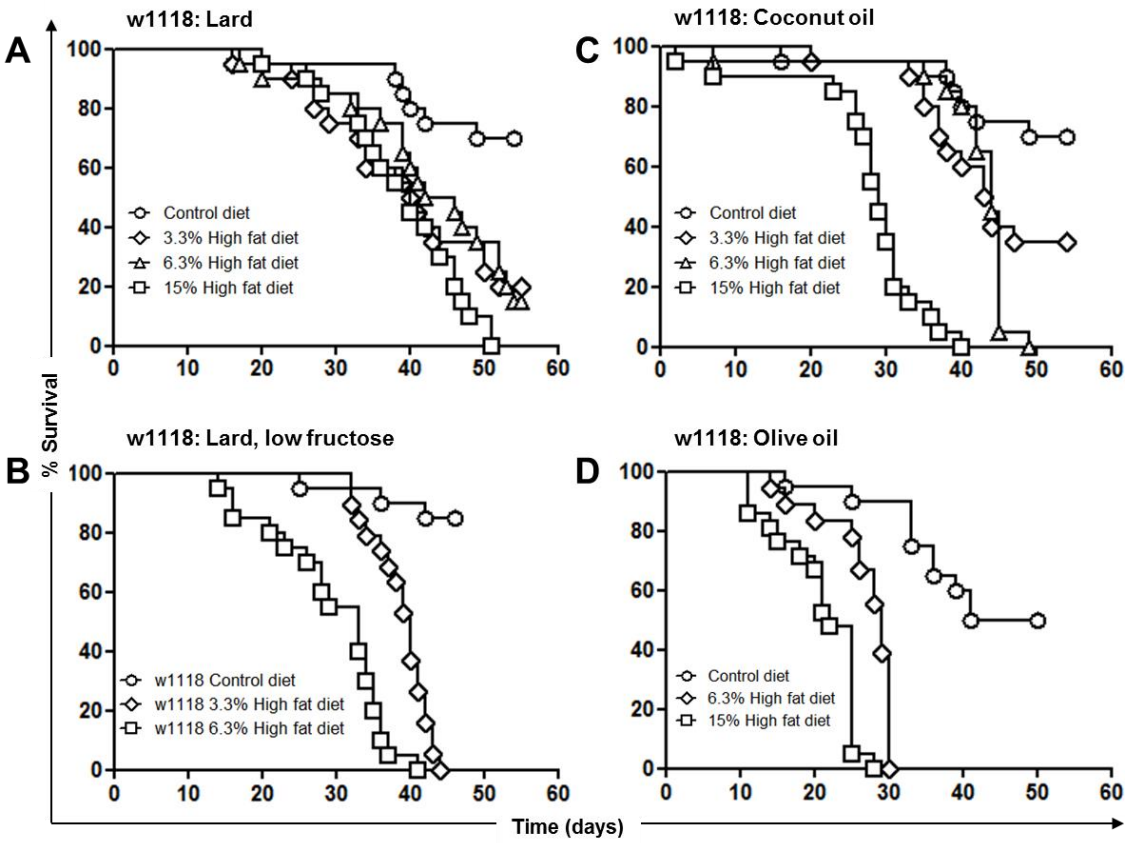


*Figure 4-1 $w^{1118}$ wild type fly survival upon high fat diet*

Wild type ($w^{1118}$) flies, in groups of 20 per experiment per diet, were placed on the diet of interest. Flies were observed daily for deaths and percentage survival was calculated over time (days). **A**. Fly survival upon control diet compared to 3.3% lard diet (log rank $X^2$ = 9.925, p=0.0016, Wilcoxon $X^2$ = 8.782, p=0.0030, 95% CI of ratio 0.1038 to 0.5900), 6.3% lard diet (log rank $X^2$ = 10.67, p=0.0011, Wilcoxon $X^2$ = 8.020, p=0.0046, 95% CI of ratio 0.1038 to 0.5677), and 15% lard diet (log rank $X^2$ = 21.10, p=<0.0001, Wilcoxon $X^2$ = 15.23, p=<0.0001, 95% CI of ratio 0.06036 to 0.3237). Lard was added to the control diet recipe weight for volume at 3.3%, 6.3% and 15%. **B.** Fly survival upon control diet compared to 3.3% lard diet low fructose diet (log rank $X^2$ = 29.25, p=<0.0001, Wilcoxon $X^2$ = 21.81, p=<0.0001, 95% CI of ratio 0.03038 to 0.1949), 6.3% lard diet (log rank $X^2$ = 36.78, p=<0.0001, Wilcoxon $X^2$ = 29.55, p=<0.0001, 95% CI of ratio 0.02147 to 0.1402). Lard was substituted for fructose in the control diet recipe, in a weight for volume manner at 3.3% and 6.3%. **C.** Fly survival upon control diet compared to 3.3% coconut oil diet (log rank $X^2$ = 4.837, p=0.0229, Wilcoxon $X^2$ = 4.611, p=0.0318, 95% CI of ratio, 0.1417 to 0.8937), 6.3% coconut oil diet (log rank $X^2$ = 15.91, p=<0.0001, Wilcoxon $X^2$ = 10.43, p=0.0012, 95% CI of ratio 0.07309 to 0.4097) and 15% coconut oil diet (log rank $X^2$ = 36.26, p=<0.0001, Wilcoxon $X^2$ = 28.75, p=<0.0001, 95% CI of ratio 0.02199 to 0.1433). Coconut oil was added to the control diet recipe weight for volume at 3.3%, 6.3% & 15%. **D.** Fly survival upon control diet compared to 6.3% olive oil diet (log rank $X^2$ =27.24, p=<0.0001, Wilcoxon $X^2$=22.52, p=<0.0001, 95% CI of ratio, 0.02878 to 0.1997), and compared to 15% olive oil diet (log rank $X^2$ =32.59, p=<0.0001, Wilcoxon $X^2$=28.03, p=<0.0001, 95% CI of ratio, 0.02641 to 0.1693). All survival experiments were repeated at least 3 times with reproducible findings.

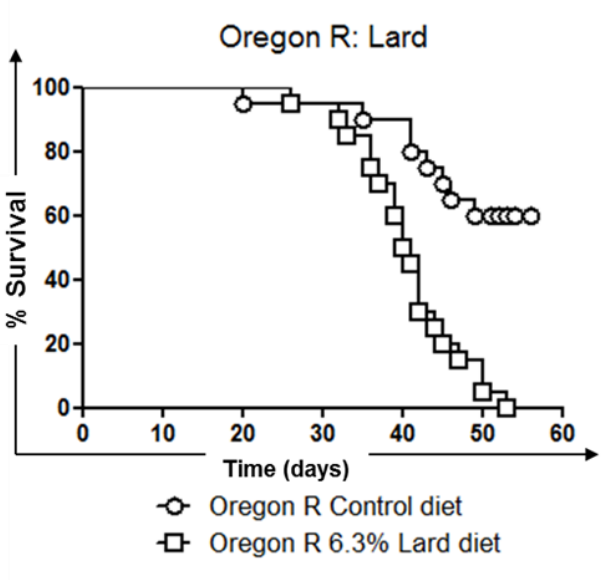


*Figure 4-2 Oregon R wild type fly survival upon a lard enriched diet*
Oregon R, wild type flies were placed on a 6.3% weight for volume lard enriched diet, in groups of 20 flies per diet. Flies were observed daily for deaths and percentage survival was calculated over time (days). Fly survival upon control diet compared to 6.3% lard diet (log rank $X^2$ = 16.82, p=<0.0001, Wilcoxon $X^2$ = 11.96, p=0.0005, 95% CI of ratio 0.08269 to 0.4145). This survival experiment was repeated more than 3 times with reproducible findings.

## 4.3 Metabolic and immune effects of high fat diet in wild type flies

To investigate the metabolic profiles of flies under a lipid rich diet, wild type $w^{1118}$ flies were examined over time for various metabolic read outs. Flies were collected after eclosion and sampled at approximately day 3 of life; this time point was described as time 0, and indicates the metabolic status of the fly before being placed on a high fat diet. Flies were then sampled after a given amount of days (e.g. 10, 20 or 30 days) upon high fat diet, and control diet for comparison. Fly glucose and triglyceride levels were ascertained, alongside examination of the transcript levels of various genes of interest.

### *4.3.1 Triglyceride and glucose regulation upon high fat diet*

After 10 days upon 15% lard enriched diets, wild type ($w^{1118}$) flies exhibited a significant increase in triglyceride levels, as determined by thin layer chromatography (TLC), (Figure 4-3 A). This firstly suggests an accumulation of lipids in flies fed a lipid rich diet and secondly is a confirmation that the flies are eating this lipid enriched diet.

A loss in the control of glucose homeostasis was induced in flies upon a lard enriched diet. A progressive rise in glucose levels was observed in high fat diet flies comparatively to control diet flies over time, which may also indicate dysregulation of insulin pathway signalling (Figure 4-3 B). The rise in triglycerides and glucose observed in flies is similar to the phenotypes observed in human metabolic syndrome (Eckel et al., 2005), furthermore these metabolic effects have also been previously reported in high fat diet fed flies (Birse et al., 2010). These data are suggestive of the development of a metabolic-like syndrome in flies fed a lipid rich diet.

### *4.3.2 Quantification of fly food intake*

Fly food intake was also examined in upon both control and 15% lard diets. This was carried out in order to confirm that flies were eating similar quantities of the lipid enriched food as they did the control diet food, and therefore to ensure the phenotypes

observed are due to lipid consumption, rather than being due to the flies simply not eating, or eating more. Age matched wild type $w^{1118}$ flies were placed on control or 15% lard diet food which had been supplemented with blue dyes (bromophenol blue and xylene cyanol). Simultaneous to this, age matched flies were also placed on normal, non-blue control or non-blue 15% lard diets. This allowed for measurement of fly food intake on the basis of the absorbance of the blue dyes present in fly carcases. Flies were left on the diets for equal periods of time, before being decapitated in order to eliminate any issues eye pigment could cause when measuring absorbance, finally fly torsos were then homogenised in PBS. The fly homogenate was then spun down, and absorbance of the supernatant was measured. Absorbance of flies fed the non-blue diets was measured as 'fly background' absorbance and this value was subtracted from the absorbance measured in blue diet fed flies. Results indicated that no significant difference in food intake between 15% lard diet and control diet flies existed (Figure 4-3 C). See Chapter 2 section 2.10.3 for further details on the feeding assay which was adapted from Rajan and Perrimon (2012).

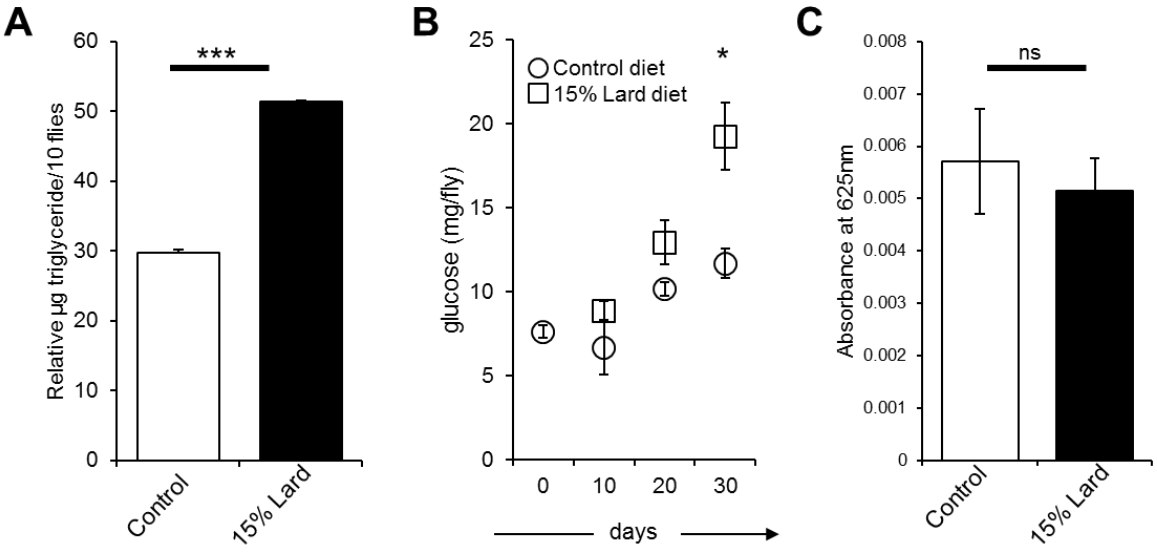


*Figure 4-3 Triglyceride and glucose levels in wild type Drosophila upon high fat diet*
Wild type $w^{1118}$ flies were placed on the given diet before being sampled at a designated time points for **A.** Thin layer chromatography (TLC) analysis of whole fly triglyceride content after 10 days on the given experimental diet. Data represents the mean of four groups of 10 flies per diet (40 flies per diet) which were placed control (white bars) or 15% lard (black bars). Error bars represent standard error of the mean, unpaired t test p≤0.0001/***. **B.** Glucose and trehalose content of wild type male flies fed a 15% lard high fat diet (squares) or a control diet (circles) at day 0 (time point prior to being placed on given diet) and at days 10, 20, and 30 upon given diet. Trehalose present was converted to glucose (see experimental methods). Data represents the mean of n=5 samples per time point, per diet (3 flies per sample), error bars represent standard error of the mean, unpaired t test day 30 p=0.010903/*, experiment was repeated 3 times with reproducible findings **C.** Fly food intake per 10 flies, absorbance of supernatant from blue control diet, and blue 15% lard diet fed, age matched $w^{1118}$ flies as a measure of fly food intake. Data represents the mean of n=4 samples (10 flies per sample), experiment was repeated 3 times with reproducible findings. Error bars represent standard error of the mean, p=0.65231, ns (unpaired t test).

*4.3.3 Glucose regulation in high fat diet fed flies: Pepck and Dilps*

Wild type flies were also examined at days 0, 10 and 30 after lipid rich diet exposure for expression levels of metabolic genes of interest via RT qPCR. Interestingly the rise in whole fly glucose levels (Figure 4-3 B) coincided with a reduction in transcript levels of *Pepck* (phosphoenolpyruvate carboxykinase), the rate limiting enzyme of gluconeogenesis (Yang et al., 2009) in high fat diet fed flies (Figure 4-4 A). However, as a rise in glucose levels was still observed in high fat diet fed flies, this suggests that the reduction in gluconeogenesis was not sufficient to control or prevent the onset of a hyperglycaemia-like phenotype in high fat diet fed flies.

Expression levels of *Dilp2*, *Dilp3* and *Dilp5* were also investigated via RT qPCR. These particular *Dilps* were studied due to their expression having been previously described in adult flies (Broughton et al., 2005). No statistically significant change in *Dilp* expression levels was observed at any of the time points post high fat diet exposure (Figure 4-4 B-D). However, the glucose level data from these flies would suggest that high fat diet fed flies have a difficultly maintaining glucose homeostasis, but this does not seem to result in a significant effect upon *Dilp* expression.

Interestingly, a diabetic-like hyperglycaemia phenotype is induced when adult *Drosophila* IPCs in the brain are ablated (Broughton et al., 2005), which is a consequence of a lack of *Dilps*. A similar hyperglycaemic phenotype is observed in flies in response to chronic high fat diet exposure (Figure 4-3 B), however; this hyperglycaemic phenotype appears to occur independently of any significant up or down regulation of *Dilp* expression (Figure 4-4 B-D). This apparent lack of *Dilp* regulation could be suggestive of the development of an insulin-like resistance in these flies, or of glucose homeostasis being modulated by some other metabolic pathway in high fat diet fed flies.

Additionally, development of cardiac dysfunction, insulin resistance and metabolic syndrome in the fly has been linked to a TOR-insulin pathway interaction (Birse et al., 2010). Once more, the development of these high fat diet induced

pathologies in the fly is strikingly similar to what is observed in mammals when there is excessive consumption of dietary lipids. These findings suggest the fly is a relevant model to try to further understand the mechanisms behind high fat diet induced diseases.

### *4.3.4 Lipid metabolism gene regulation in high fat diet fed flies*

Lipid metabolism gene expression was also measured via RT qPCR from fly samples collected at 10 and 30 days upon control or high fat diet. Firstly expression of *midway* (*mdy*) was investigated. The *mdy* gene encodes a protein similar to mammalian *acyl coenzyme A* and functions as a diacylglycerol acyltransferase (DGAT) therefore; *mdy* facilitates the conversion of diacylglycerol (DAG) into triacylglycerol (TAG). Expression of *mdy* is required by nurse cells, which are responsible for providing the oocyte with various proteins required for the continuation of oogenesis. Mutation of *mdy* results in a severe reduction of TAG storage within nurse cells, which leads to premature nurse cell death during oogenesis (Buszczak et al., 2002) however, *mdy* expression characteristics in other tissues in adult *Drosophila* has not yet been studied. Observation of *mdy* expression in RT qPCR experiments indicated no significant change in the regulation of expression after chronic high fat diet exposure (Figure 4-4 E).

Expression levels of Acetyl-CoA carboxylase (*ACC*) were also examined in flies fed high fat diet comparatively to control diet flies. *ACC* is an enzyme which catalyses early steps of fatty acid synthesis (Hardie and Pan, 2002). No statistically significant change in expression of *ACC* levels was observed at any of the time points examined (Figure 4-4 F), however, in future experiments it would be interesting to examine differing lipid metabolism genes, in order to further investigate effects high fat diet may have on fly lipid metabolism.

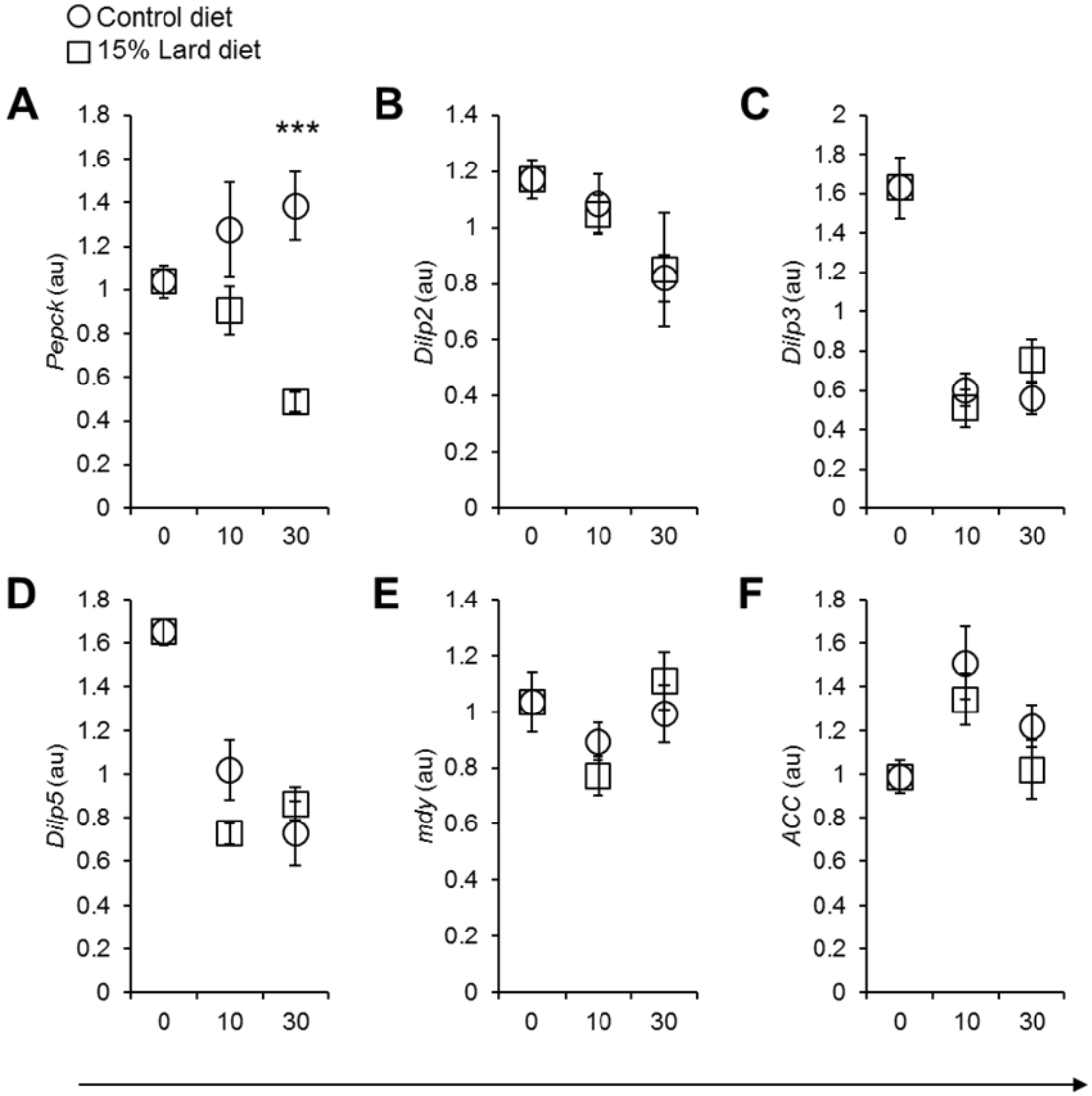


*Figure 4-4 Transcript levels of metabolic genes in wild type flies after high fat diet exposure*
Wild type $w^{1118}$ flies were samples were collected for RT qPCR sample preparation at day 0 (as a time point for the metabolic status of the fly before being placed on given diets), and days 10 and 30 on either control (circles) or 15% lard (squares) diets. All RT qPCR data is normalised to the housekeeping gene *Rpl1*, (au = arbitrary units). **A.** Normalised *Pepck* transcript levels in wild type flies fed a control or 15% lard diet for 10 days (unpaired t test p=0.16583, ns) and 30 days (unpaired t test p=0.000527/***) days. Normalised transcript levels of **B.** *Dilp2*, **C.** *Dilp3* and **D.** *Dilp5* at days 0, 10 and 30 on the designated diets. No significant change in *Dilp* transcript levels was observed at any of the time points tested (unpaired t test). **E & F.** Normalised transcript levels of *midway* (*mdy*) and *ACC* (*Acetyl-CoA carboxylase*) respectively, unpaired t tests were not significant at each of time points. Error bars represent the standard error of the mean, data represents the mean of n=5 samples per time point per diet (each sample contains 3 flies). When no stars are present, this indicates data was not statistically significant (unpaired t tests).

*4.3.5 Fly JAK-STAT pathway response to high fat diet*

JAK-STAT pathway family members were also investigated for expression levels after chronic high fat diet exposure. This was primarily due to the inflammatory phenotypes reported in mammals upon chronic high fat diet exposure, which often involve an increase in the JAK-STAT activating cytokine *IL-6* (Wellen and Hotamisligil, 2005). The fly JAK-STAT pathway ligands *upd2* and *upd3* are *IL-6*-related, cytokines which bind the gp130 and *IL-6-R*-like receptor *dome* (Brown et al., 2001). Expression levels of *upd2* and *upd3* were investigated, along with a downstream JAK-STAT pathway target gene *Socs36E* (*Suppressor of cytokine signalling 36E*).

Interestingly, *Drosophila* presented with an early and sustained increase of the cytokine *upd3* under a 15% lard high fat diet (Figure 4-5 B). Expression levels of *upd2* were initially higher upon control diet although this was not statistically significant however, by day 30 *upd2* expression levels were significantly up regulated in lipid rich diet fed flies comparatively to control diet flies (Figure 4-5 A). Previous studies have shown that plasmatocytes are able to produce the *IL-6*-like cytokine *upd3* in response to infection (Agaisse et al., 2003). This could provide a link between the rise in *upd3* expression observed upon high fat diet and the plasmatocyte specific role in high fat diet induced diseases. Likewise, mammalian macrophages have been shown to be responsible for *IL-6* production in diet induced obesity (Lumeng et al., 2007).

*Upd2* is produced by the fat body, the functional equivalent to the vertebrate liver and adipocytes, and stimulates *Dilp2* secretion by insulin-producing cells (Rajan and Perrimon, 2012). The rise in *upd2* transcript levels is particularly interesting with regard to the hyperglycaemia observed in high fat diet fed flies, although as previously shown, no change in *Dilp2* expression was observed in high fat diet fed flies. The hyperglycaemia and rise in *upd2* expression levels observed are suggestive of a high fat diet induced dysregulation of glucose metabolism.

Consistent with this increase in *upd2* and *upd3* cytokine expression, we observed an increase in expression of JAK-STAT pathway target gene *Socs36E* (Karsten et al., 2002) in high fat diet fed flies (Figure 4-5 C). The involvement of the JAK-STAT pathway in response to chronic high fat diet exposure is extremely interesting, particularly with regard to the seemingly conserved up regulation of *upd3* and *IL-6* observed in both *Drosophila* and vertebrates respectively. These findings may highlight an *IL-6* and JAK-STAT related role in the progression of various high fat diet induced diseases (Yudkin et al., 2000).

*4.3.6 Does lipid rich diet affect activation of the NFκB-like Toll and Imd pathways?*

The major immune pathways in the fly, *Toll* and *Imd* result primarily in the expression of AMPs. Due to the inflammatory responses which have been documented in response to excess dietary lipids in mammals (Badimon et al., 2011, Linton and Fazio, 2003), experiments were carried out in order to examine the potential effects of a lipid rich diet on fly AMP production, at steady state and after infection. RT qPCR experiments were carried out using wild type $w^{1118}$ flies to investigate the expression of *Drosomycin* (*Drs*) and *Diptericin* (*Dpt*), the major *Toll* and *Imd* pathway AMPs respectively after infection, in both high fat diet fed, and control diet fed flies. Flies were aged for 10 days upon the given diet before being infected with a mixture of *M. luteus* and *E. coli*, in order to activate both the *Toll* and *Imd* pathways. A separate cohort of flies were pricked with empty injection needles as controls for any AMP induction induced by the injection wound itself, a further set of non-infected flies were also included in this experiment as controls. Flies were homogenised for sampling 6 hours post infection or wounding, a time point previously described to be optimal for AMP induction (Lemaitre et al., 1997). Experiments indicated that while a statistically significant increase in *Drs* and *Dpt* was observed after infection, between infected and non-infected flies, no significant difference in the level of *Drs* and *Dpt* induction was observed between the sets of infected flies,

wounded flies or non-infected flies on either 6.3% lard or control diets (Figure 4-6 A, B). This experiment suggests that the fly *Drs* and *Dpt* AMP production in response to infection, wounding, or in non-immune challenged flies is not affected by lipid enriched diet. These data would therefore suggest that expression of the major *Toll* and *Imd* pathway AMPs; *Drs* and *Dpt* is not regulated by high fat diet, after 10 days exposure.

### *4.3.7 Induction of AMPs in response to lipid rich diet in aged flies*

Unfortunately AMP expression levels were inconsistent and not reproducible at later time points on high fat diet e.g. days 20 and 30. For this reason AMP data in relation to diet is not included in the remainder of this thesis, therefore it was not possible to determine whether chronic high fat diet affected AMP transcription in non-infected flies at later time points upon a high fat diet.

### *4.3.8 Summary: effect of chronic high fat diet upon wild type flies*

High fat diet induces hyperglycaemia, excessive levels of triglycerides, and promotes early death in flies. These data support what has already been published (Birse et al., 2010), advocating that flies fed high fat diet begin to suffer with an obesity-like phenotype and develop a metabolic syndrome, similar to what is observed in vertebrates. Flies also display an increase in expression of the JAK-STAT pathway family members; *upd2*, *upd3* and *Socs36E*, yet no significant difference in AMP expression levels was observed regardless of diet.

Most significantly the rise in expression of the JAK-STAT pathway *IL-6*-like cytokines *upd2* and *upd3* and the similar increase in *IL-6* seen in human high fat diet induced diseases (Yudkin et al., 2000), further highlights the fly as a relevant model for the study of high fat diet diseases. The next part of this chapter will address the potential metabolic and immunological roles plasmatocytes may mediate in high fat diet induced pathophysiology.

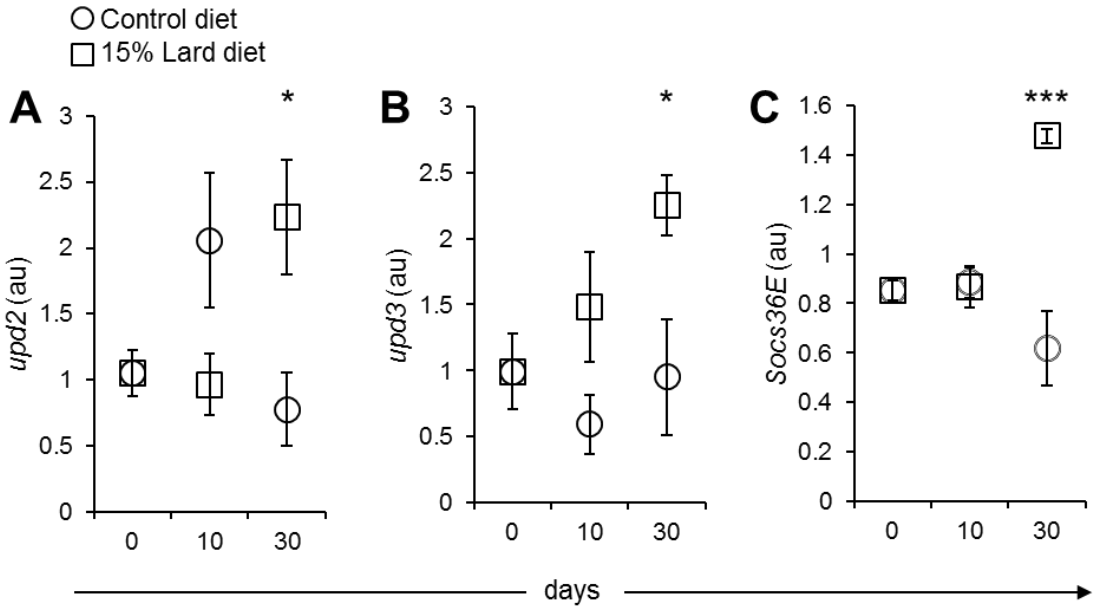


*Figure 4-5 Transcript levels of JAK-STAT pathway genes in wild type flies after high fat diet exposure*

Wild type $w^{1118}$ flies were collected for RT qPCR sample preparation at day 0 (as a time point for the metabolic status of the fly before being placed on given diets), and days 10 and 30 on either control (circles) or 15% lard (squares) diets. All RT qPCR data is normalised to the housekeeping gene *Rpl1*, (au = arbitrary units). Normalised transcript levels of **A.** *upd2*, **B.** *upd3*, **C.** and *Socs36E* in wild type $w^{1118}$ flies fed a control or 15% lard diet for 10 and 30 days. Statistical significance was calculated using unpaired t tests (*upd3* day 30 p=0.029852, *upd2* day 30 p=0.022972, *Socs36E* day 30 p=0.000467, all other time points were not significant). Error bars represent the standard error of the mean, data represents the mean of n=5 samples per time point per diet and each sample contained 3 flies, (unpaired t tests, * $p<0.05$, *** $p\leq0.001$).

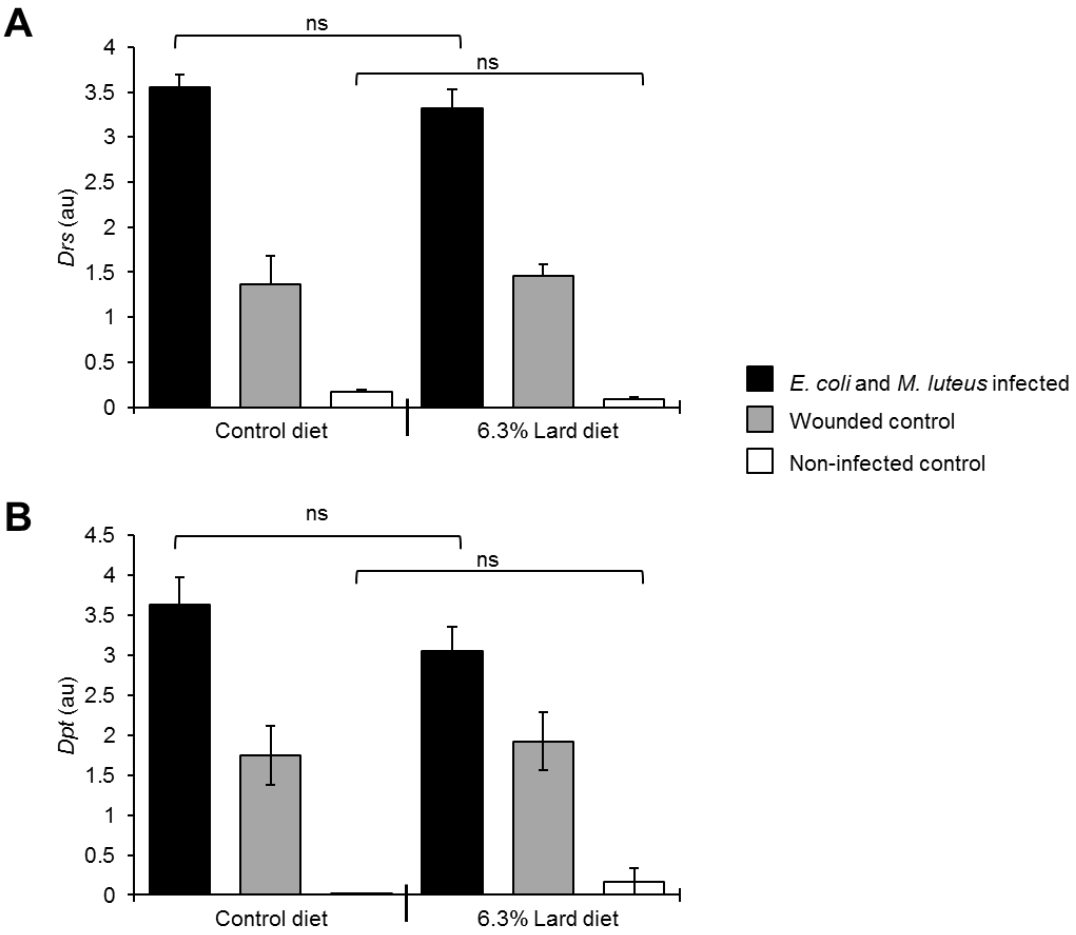


*Figure 4-6 AMP induction in infected $w^{1118}$ flies upon control or 6.3% lard diets*
Wild type $w^{1118}$ flies were aged for 10 days on either control or 6.3% lard diets, before being infected with a mixture of *E. coli* and *M. luteus*, or being wounded with a glass needle, in order to control for any AMP induction by to the injection injury itself. Samples were prepared from the infected (grey bars) and wounded (black bars) 6 hours post infection, alongside a non-infected control population of flies (white bars). RT qPCR was carried out with these flies for expression levels of **A.** *Drs* and **B.** *Dpt*. The up regulation of *Drs* and *Dpt* expression was significant in infected flies compared to wounded controls ($p \leq 0.01$ in all cases, unpaired t tests) and non-infected controls ($p \leq 0.001$ in all cases, unpaired t tests). However no significant difference in *Drs* or *Dpt* induction was observed between infected or wounded flies upon control and 6.3% lard diets (unpaired t test, $p \geq 0.05$ in all cases). In addition, no significant difference in *Drs* or *Dpt* expression was observed between non-infected flies upon control diets ($p \geq 0.05$ in all cases, unpaired t tests). Data represents the mean of n=5 samples (3 flies per sample), error bars represent standard error of the mean. Data is representative of findings from 3 independent experiments.

## 4.4 Plasmatocytes and high fat diet

The observed reduction in fly lifespan under a variety of high lipid diets and the implicated involvement of macrophages in the development of high fat diet induced diseases in humans, including atherosclerosis, makes *Drosophila* plasmatocytes an interesting candidate model for study of the macrophage response to lipid. In addition, the rise in *upd3* expression observed in wild type flies upon high fat diet implicates a potential plasmatocyte role, as plasmatocytes have been shown to be a major producer of *upd3* in response to infection in adult *Drosophila* (Agaisse et al., 2003).

### *4.4.1 Plasmatocyte number and morphology upon high fat diet*

Plasmatocyte numbers in high fat diet fed flies were studied using *Hml* reporter flies (w;*Hml*Δ-Gal4,UAS-2xeGFP). Flies were placed on either control or 15% lard enriched diet for 10 days before confocal microscopy was performed with them to determine if high fat diet exposure resulted in any changes, in both in plasmatocyte number or morphology. Plasmatocyte numbers appeared to remain stable regardless of diet (Figure 4-7 A). Conversely high fat diet appeared to alter plasmatocyte morphology, in some but not all flies upon high fat diet, an example of these morphological alterations are shown in (Figure 4-7 B, C). In particular plasmatocytes in high fat diet fed flies appeared to be larger, however visually the flies themselves did not appear to increase in size or become noticeably ‘fatter’ than control diet fed flies.

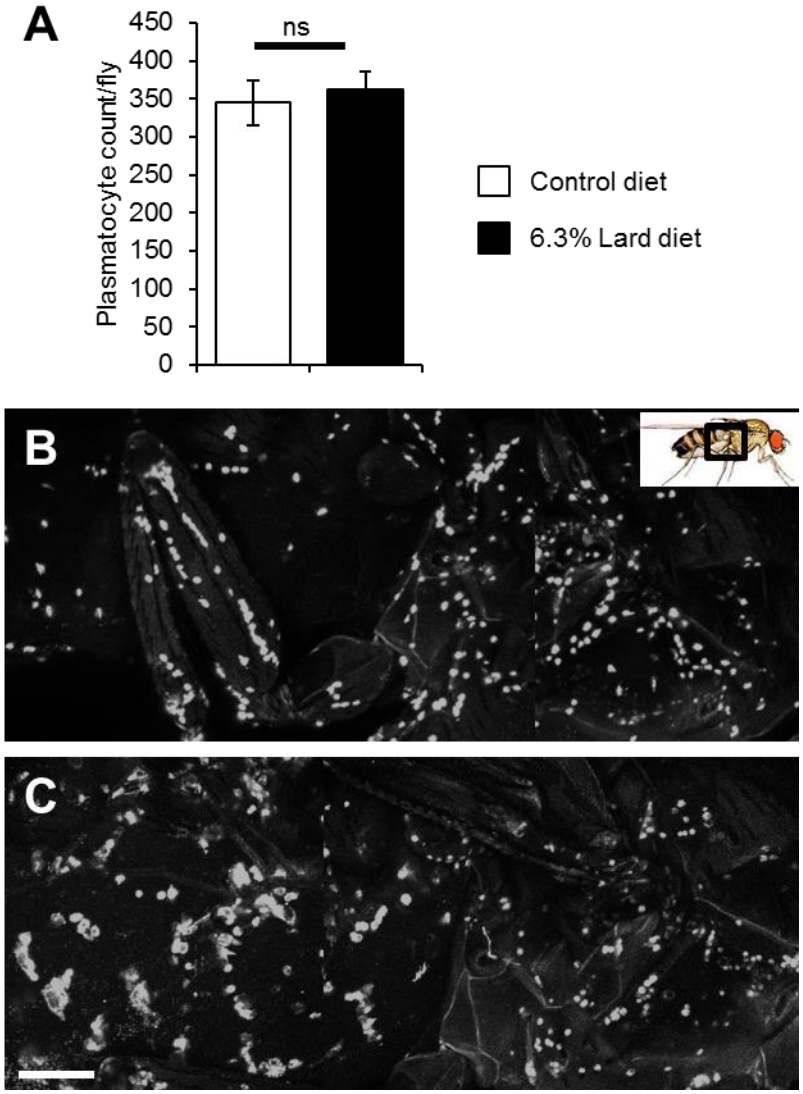


*Figure 4-7 Plasmatocyte numbers and morphology upon high fat diet*
**A.** w;*HmlΔ*-Gal4,UAS-2xeGFP male flies were placed on control (white bar), or 6.3% lard high fat diets (black bars) post hatching. Flies were imaged after 7 days exposure to high fat diet, no significant difference was observed in plasmatocyte number. Quantification represents the mean cell counts of n=5-6 flies per diet, error bars represent standard error of the mean (unpaired t test p=0.310, ns). **B.** Confocal microscopy of w;*HmlΔ*-Gal4,UAS-2xeGFP flies upon control, and **C.** 6.3% lard high fat diet (Scale bar=150µm). Inset diagram in panel B. represents fly orientation, and black box represents approximate imaging location represented in both B and C. Images were acquired using a 10x objective, Z-stack volume 400µm, Z-step size 10µm.

*4.4.2 High fat diet fly plasmatocytes contain elevated lipid quantities*

Confocal microscopy of plasmatocyte reporter flies (w;*HmlΔ*-Gal4,UAS-2xeGFP) indicated that plasmatocytes in high fat diet fed flies appeared to be larger, in some, but not all flies imaged (Figure 4-7). In order to better examine plasmatocytes for lipid content, FACS sorting experiments were performed using high fat diet fed and control diet fed flies. Sorted plasmatocytes were fixed and stained for neutral triglycerides and lipids with Oil Red O. The cells were then imaged firstly; to determine whether plasmatocytes contained scavenged dietary lipids and secondly, whether the quantity of intracellular lipid was increased in high fat diet fed flies. The cells were also examined for any morphological changes, such as in cell size, which may have been induced by a lipid rich diet.

Age matched male plasmatocyte reporter flies (w;*HmlΔ*-Gal4,UAS-2xeGFP) were placed on a lard enriched diet, or control diet for 7-10 days. Flies were then homogenised through 70µm filters with PBS-EDTA buffer (Phosphate Buffered Saline-Ethylenediaminetetraacetic Acid) in order to exclude as much debris as possible, EDTA was used to prevent clumping of cells together. The resulting whole fly extract was FACS sorted for *Hml* GFP positive plasmatocytes. Further details regarding the protocol for FACS sorting of fly plasmatocytes can be found in Chapter 2, section 2.5. The sorted population of plasmatocytes were then stained for neutral triglycerides and lipids using Oil Red O (Koopman et al., 2001). Plasmatocytes were identified through their inherent expression of *Hml* driven GFP, and subsequently these GFP positive cells were imaged for Oil Red O positive lipid staining and nuclei (DAPI).

Plasmatocytes sorted from flies fed a high fat diet contained lipid vacuoles, which were more frequent and larger than those observed in plasmatocytes from control diet flies (Figure 4-8 A, B). This observation was quantified by calculating the normalised sum fluorescent intensity (SFI) per cell (Figure 4-8 C). Furthermore, quantification of cell size illustrated that plasmatocytes from high fat diet fed flies also appeared to be larger

than those sorted from control diet fed flies (Figure 4-8 D). This increase in size could be explained by the increased presence of lipid droplets within plasmatocytes. Similarly, this increase in cell size coincided with previous observations made when imaging plasmatocytes in whole flies, in which the cells from high fat diet fed flies also appeared to be larger (Figure 4-7 B, C).

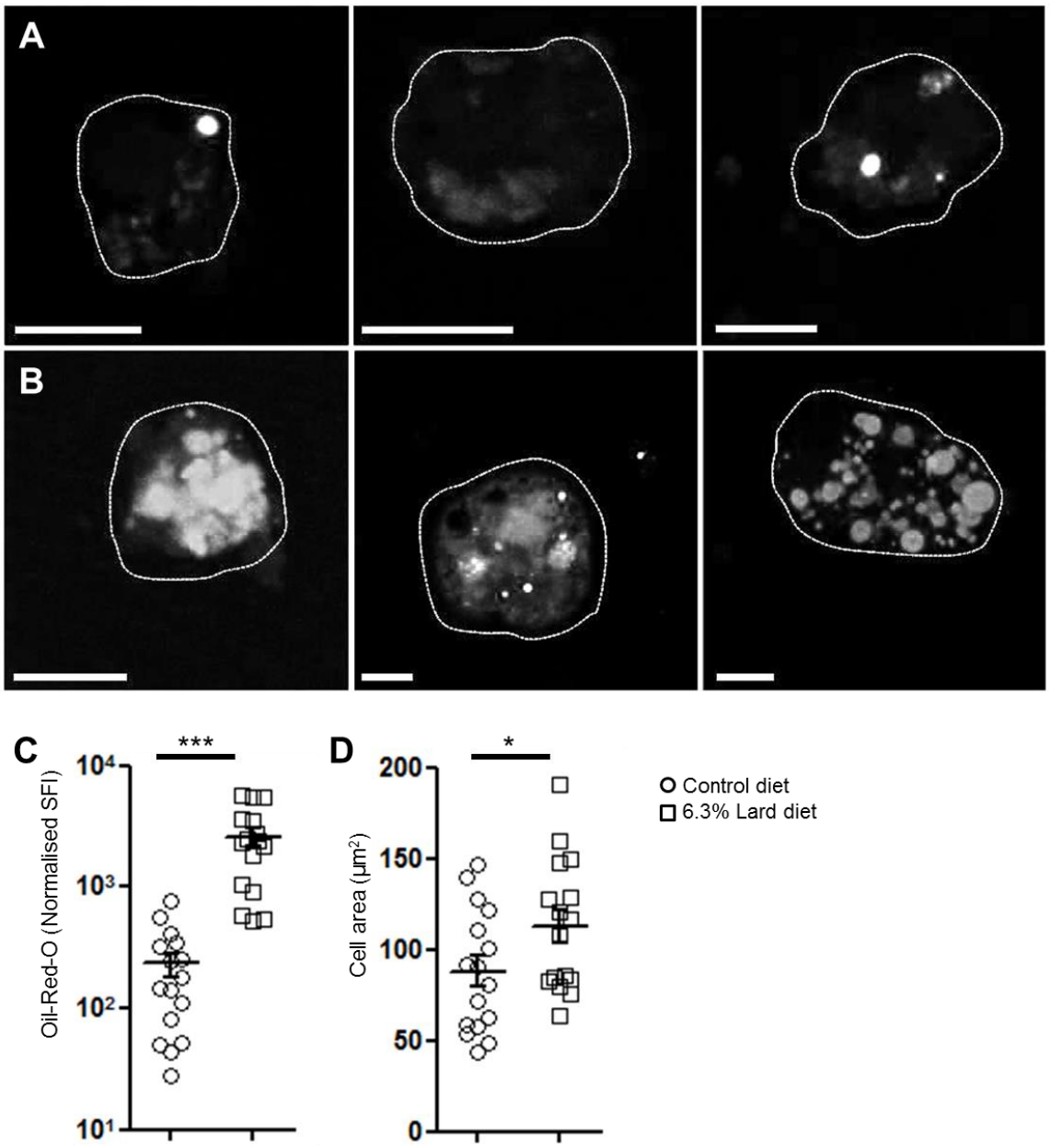


*Figure 4-8 Lipid stained FACS sorted plasmatocytes from control and high fat diet fed flies*
Age matched plasmatocyte GFP reporter flies (*Hml*ΔGal4,UAS-2xeGFP) were placed on either 6.3% lard or control diets for 7-10 days after eclosion, before being homogenised through filters for FACS sorting. After sorting, cells were stained with Oil Red O for presence of neutral triglycerides and lipids (Oil Red O stain is false coloured white) **A.** Control diet plasmatocytes, **B.** 6.3% lard diet plasmatocytes. Dotted lines around cells indicates the cell membrane, scale bars= 5µm **C.** Sum normalised fluorescent intensity (SFI) of plasmatocyte Oil Red O stain in control diet (circles) and 6.3% lard diet (squares) plasmatocytes, unpaired t test $p \leq 0.001$/***. **D.** plasmatocyte size on control diet (circles) or 6.3% lard diet (squares), based on 2D area ($\mu m^2$) per cell, unpaired t test $p < 0.05$/*. Data in C and D represent the mean of n=16 cells per diet and error bars represent the standard error of the mean. This experiment was repeated 3 times with reproducible findings.

*4.4.3 Plasmatocytes scavenge injected lipids*

High fat diet exposure resulted in a significant reduction in lifespan in wild type flies under a variety of high fat diets (Figure 4-1). In addition to this, under lipid rich diets, FACS sorted *Hml* positive plasmatocytes were larger and accumulated lipids within large Oil red O positive lipid vacuoles (Figure 4-8). This process is reminiscent of *foam cell* formation, a typical feature of the macrophage response to a lipid-rich diet in rodents and humans (Li and Glass, 2002). Macrophages have been implicated in the development of atherosclerosis, amongst other high fat diet related diseases and are found in high numbers within atherosclerotic plaques (Silverstein and Febbraio, 2000).

In addition to the plasmatocyte ability to scavenge dietary lipids, they are also able to scavenge injected lipids (Figure 4-9 A, B, C). Plasmatocyte reporter flies (w;*Hml*Δ-Gal4,UAS-2xeGFP) were injected with DiI-LDL (3,3'-dioctadecylindocarbocyanine-low density lipoprotein), a fluorescently labelled low density lipoprotein (LDL) and flies were imaged via confocal microscopy for examination of their lipid scavenging capacity. Within 1 hour of injection into the hemolymph, more than 80% of the total plasmatocytes imaged were also positive for DiI-LDL (Figure 4-9 D). These findings suggest that *Drosophila* plasmatocytes share their mammalian counterpart's ability to scavenge lipids (Figure 4-9).

Together these data highlight *Drosophila* plasmatocytes as a relevant model for the study of macrophages in high fat diet related disease development and progression.

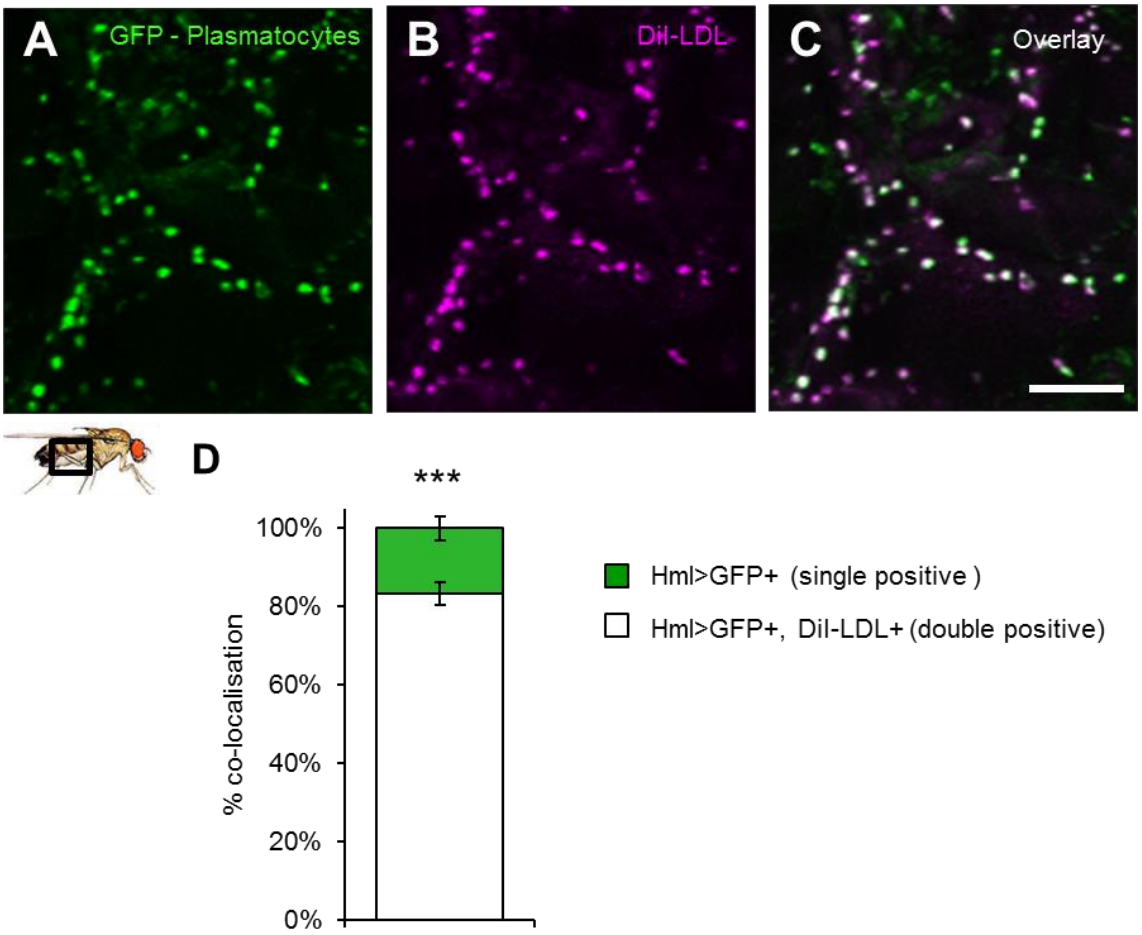


*Figure 4-9 Plasmatocytes scavenge injected fluorescent LDL*
Age matched 7 day old male plasmatocyte reporter flies (w;*Hml⊿*-Gal4,UAS-2xeGFP) were injected abdominally with DiI-LDL (3,3'-dioctadecylindocarbocyanine-low density lipoprotein). Flies were imaged 60 minutes post injection, scale bar=100µm. Fly picture below panel A represents fly orientation, and black box represents approximate imaging location represented in images A, B and C**.** GFP positive plasmatocytes (*Hml*>GFP), **B.** red fluorescent lipid, (DiI-LDL), false coloured magenta. **C.** Overlay of GFP positive plasmatocytes and DiI-LDL, white indicates a co-localisation between GFP and DiI-LDL. **D.** Percentage $Hml^{+}$ plasmatocytes which were either single positive GFP only (green) or double positive, GFP and DiI-LDL co-localised cells (white). Data represents the mean of n=5 flies, and error bars represent standard error of the mean, unpaired t test $p \leq 0.0001$/***.

### 4.5 Inducible plasmatocyte deletion in adult *Drosophila*

To test whether plasmatocytes were involved in the pathology resulting in early death of flies upon high fat diet, plasmatocyte-less flies were generated. Plasmatocytes were deleted in adult flies using the temperature sensitive Gal80 expression system, allowing for temporally controlled deletion of plasmatocytes specifically in adult flies. An advantage of this system is that plasmatocytes can be deleted once fly embryonic and larval development is over, in adult flies. This allows for the exclusion of possible developmental effects which could be induced in plasmatocyte-less embryos and larvae.

Plasmatocyte cell death was triggered in adult flies by inducible expression of the pro-apoptotic protein *reaper* (*rpr*) (White et al., 1994). *Rpr* expression was controlled by both the temperature sensitive driver, *Tubulin*-Gal80$^{ts}$ and either the plasmatocyte specific driver *Hml*Δ-Gal4 or the plasmatocyte expressed driver *crq*-Gal4 (McGuire et al., 2004). In these flies the ubiquitous *Tub*-Gal80$^{ts}$ promoter represses Gal4 activity in all tissues at temperatures lower than 29°C. Upon fly transfer to 29°C, Gal80$^{ts}$ repression is lost, and expression of the pro-apoptotic protein *rpr* can commence in either *crq* or *Hml* positive plasmatocytes, resulting in cell death. After 2 days at 29°C, w;*Tubulin*-Gal80$^{ts}$/+;*crq*-Gal4,UAS-myRFP/UAS-*rpr* flies are rendered plasmatocyte-less (Figure 4-10 A), while the control genotype flies w;*Tubulin*-Gal80$^{ts}$/+;*crq*-Gal4,UAS-myRFP/+ express plasmatocyte derived RFP (Figure 4-10 B).

The loss of plasmatocytes was quantified, and the loss of visible plasmatocytes was extremely significant, with more than 99% of plasmatocytes having been successfully deleted (Figure 4-10 C). Subsequent experiments investigated the effect of plasmatocyte deletion upon both fly survival and upon the expression levels of previously studied metabolic and JAK-STAT pathway genes.

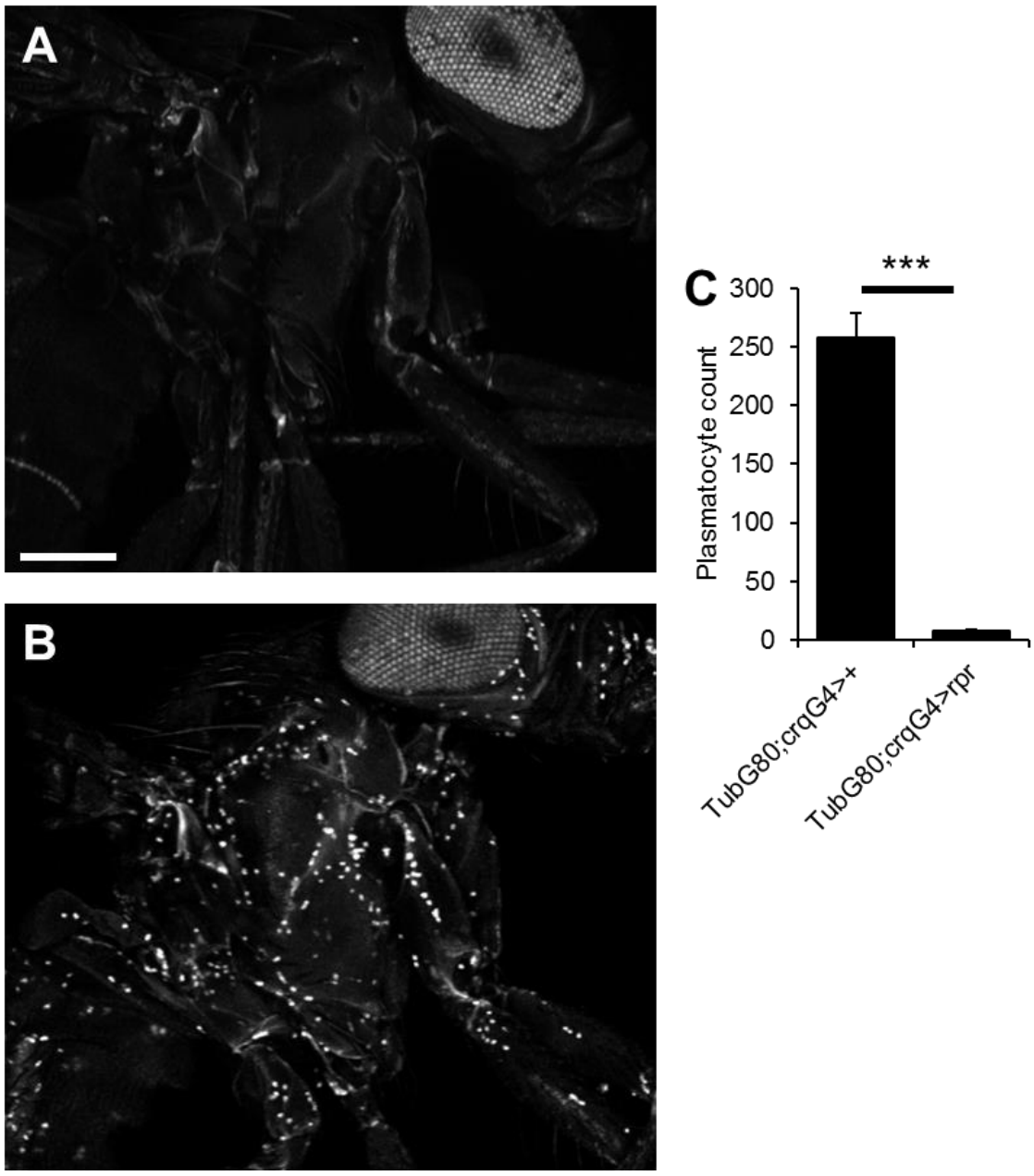


*Figure 4-10 Temperature sensitive Gal80 controlled deletion of plasmatocytes in adult flies*
Flies were developed at 18°C to prevent Gal4 activity. Age matched plasmatocyte-less flies (w;*Tubulin*-Gal80ts/+;*crq*-Gal4,UAS-myrRFP/UAS-*rpr*) and control genotype flies (w;*Tubulin*-Gal80ts/+;*crq*-Gal4,UAS-myrRFP/+) were collected, and placed at 29°C for 48 hours to induce Gal4 expression prior to imaging. Confocal microscopy of **A.** plasmatocyte-less fly and **B.** plasmatocyte competent fly. **C.** Quantification (Imaris spot detection) of plasmatocyte numbers from imaging experiments of plasmatocyte-less flies versus controls, results represent the mean of n=3 flies per genotype. Unpaired t test, p=0.00028/***, error bars represent standard error of the mean.

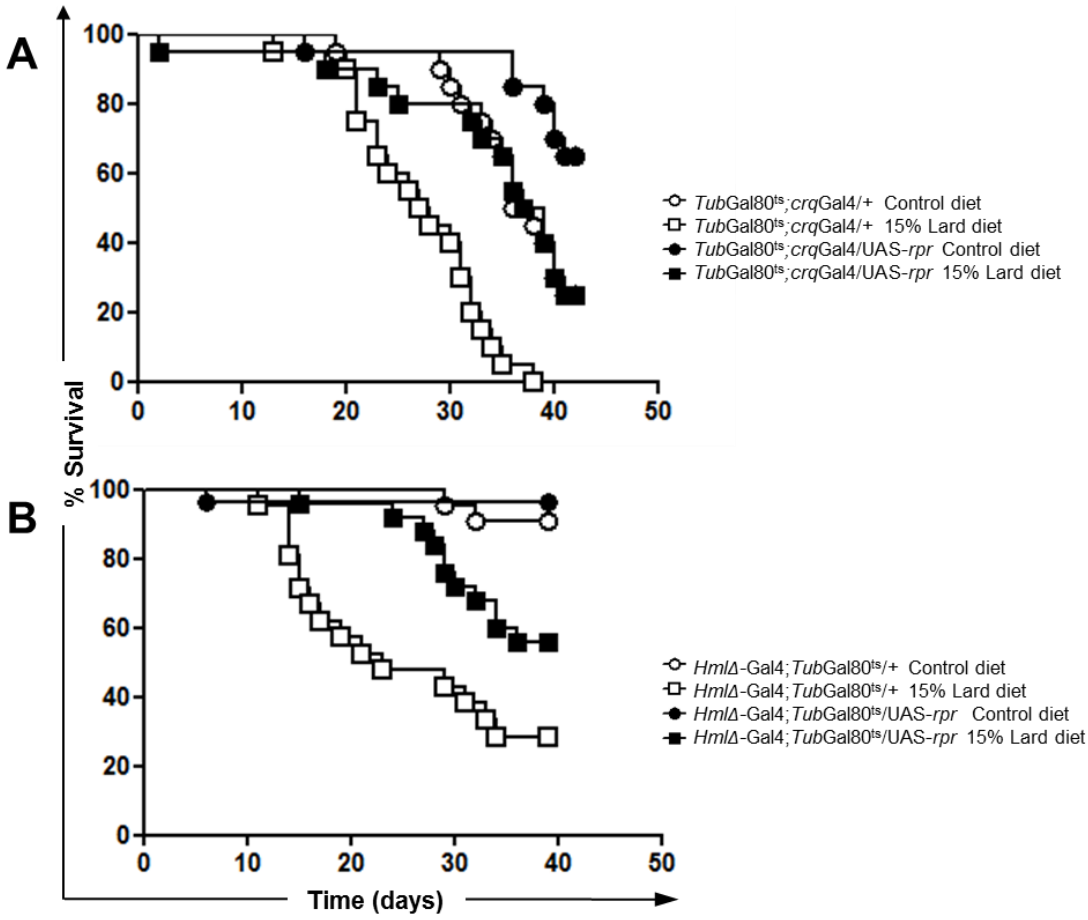


*Figure 4-11 Survival of plasmatocyte depleted, and control flies upon control and high fat diets*
Inducible temperature sensitive plasmatocyte depletion using: **A.** *crq* and **B.** *Hml* and as drivers for expression of the pro-apoptotic protein *reaper* (*rpr*). Flies were developed at 18°C to prevent Gal4 activity. Age matched plasmatocyte-less flies (**A.** w;*Tubulin*-Gal80$^{ts}$/+;*crq*-Gal4,UAS-myrRFP/UAS-*rpr* or **B.** w;*HmlΔ*-Gal4;*Tubulin*-Gal80$^{ts}$/UAS-*rpr*) and control flies (**A.** w;*Tubulin*-Gal80$^{ts}$/+;*crq*-Gal4,UAS-myrRFP/+ or **B.** w;*HmlΔ*-Gal4;*Tubulin*-Gal80$^{ts}$/+) were collected, and placed at 29°C for 48 hours to induce Gal4 expression and hence plasmatocyte depletion. Flies were then placed on the given diets (control; circles or 15% lard; squares) and checked daily for deaths. The percentage survival over time was calculated, (n=20 flies per genotype per diet). **A.** Survival of plasmatocyte depleted (black symbols) and plasmatocyte competent controls (white symbols) fed on control (circles $X^2$=7.828, p=0.0051, Wilcoxon $X^2$=7.752, p=0.0054, 95% CI of ratio 1.461 to 8.623) or 15% lard (squares, log rank $X^2$ = 17.49, p=<0.0001, Wilcoxon $X^2$=11.87, p=0.0006, CI of ratio 0.2117 to 1.236). **B.** Survival of plasmatocyte depleted (black symbols) and plasmatocyte competent controls (white symbols) fed on control (circles, log rank $X^2$=0.5616, p=0.4536, Wilcoxon $X^2$=0.5257, p=0.4684, 95% CI of ratio 0.2455 to 23.19) or 15% coconut oil diet (squares, log rank $X^2$=6.194, p=0.0128, Wilcoxon $X^2$=8.118, p=0.0044, 95% CI of ratio 1.249 to 6.484). Survival experiments were repeated at least 5 times with reproducible findings, these curves are representative of findings.

*4.5.1 Plasmatocyte-less fly survival and metabolic profile upon high fat diet*

Lifespan was significantly increased in plasmatocyte-less flies on lipid enriched lard diets, using both *crq* (Figure 4-11 A) and *Hml* (Figure 4-11 B) as drivers for *rpr* induced plasmatocyte depletion. Furthermore, in some cases plasmatocyte-less flies survived better, even when compared to flies that were plasmatocyte competent upon control diet (Figure 4-11 A). This effect on survival would suggest that plasmatocytes themselves are in some way detrimental to the survival of the fly, particularly in conditions of chronic high fat diet exposure, this finding is the opposite to the protective role plasmatocytes play during infection (Charroux and Royet, 2009).

*4.5.2 Glucose and triglyceride regulation in plasmatocyte-less flies*

Remarkably as well as rescuing fly survival, plasmatocyte deletion also prevented the onset of hyperglycaemia after 30 days upon a lipid rich diet (Figure 4-12 B). However, no difference in triglyceride accumulation was observed between plasmatocyte-less and control plasmatocyte competent flies fed a 15% lard diet for 20 days (Figure 4-12 A). This suggests that flies fed a lipid rich diet develop a dysregulated glucose metabolism, which can be rescued when plasmatocytes are deleted. In addition, the lack of whole fly lipid accumulation suggests that it is not the lipid itself that contributes to the death of the fly, but the plasmatocyte mediated response to lipids.

*4.5.3 Metabolic gene regulation in high fat diet fed plasmatocyte-less flies*

Metabolic gene expression was also investigated in plasmatocyte-less flies via RT qPCR. Plasmatocyte depletion was responsible for preventing the increase in *Pepck* transcript levels observed in control plasmatocyte competent flies upon 15% lard diet (Figure 4-13 A). Alterations in *Dilp* expression levels remained unclear (Figure 4-13 B), with no statistical difference between their expression levels between plasmatocyte-less and plasmatocyte competent flies after 20 days upon control or 15% lard diets.

The lipid metabolism gene *mdy* appeared to be elevated in plasmatocyte depleted flies compared to controls, however this was only statistically significant at 10 days upon a 15% lard diet (Figure 4-13 C). Levels of *ACC* expression remained unchanged regardless of plasmatocyte presence (Figure 4-13 D). An increase in *mdy* could suggest an increase in lipid storage in plasmatocyte-less flies, which is a phenotype indicative of metabolic syndrome, yet plasmatocyte-less flies actually survived better than flies that had plasmatocytes. This may again suggest that it is the plasmatocyte response to the lipid which is detrimental to fly survival rather than the presence of the lipid itself.

### *4.5.4 JAK-STAT pathway response to high fat diet in plasmatocyte depleted flies*

Chronic high fat diet exposure in wild type flies induced an increase of JAK-STAT pathway cytokines *upd2 and upd3*, as well as an increase in the downstream pathway target *Socs36E*. Most interestingly, plasmatocyte depletion abolished the increase in *upd3* observed in control flies (Figure 4-14 A), levels of Socs36E were also reduced in plasmatocyte-less flies; however this did not reach statistical significance (Figure 4-14 B). These findings suggest a plasmatocyte specific role in regulating the metabolic and JAK-STAT pathway responses to dietary lipids.

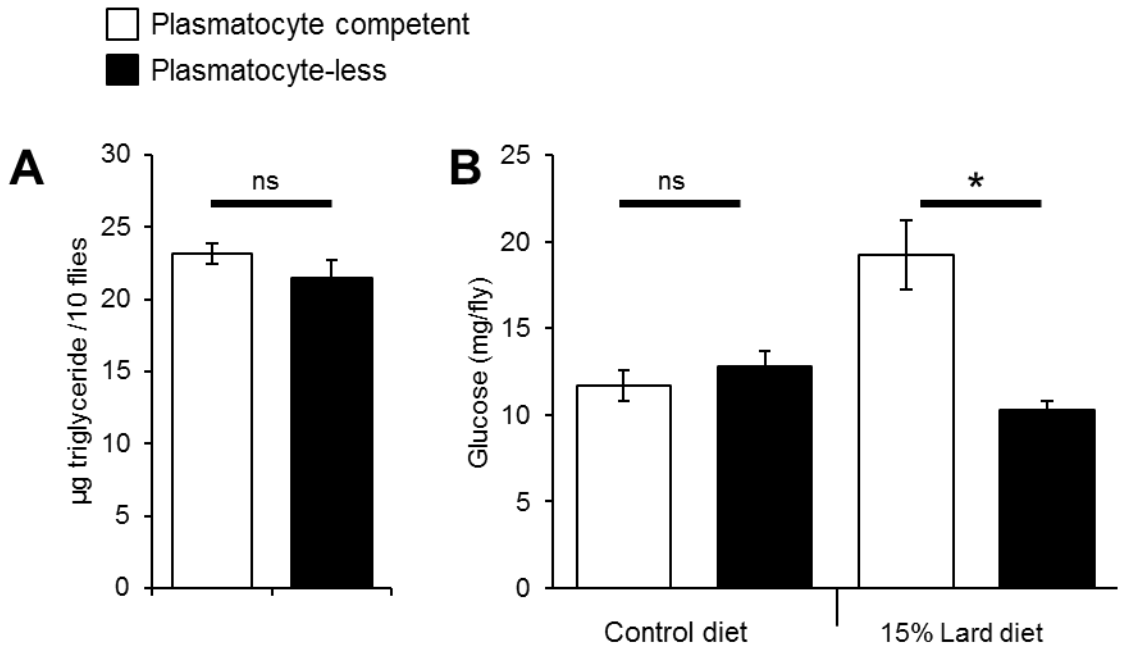


*Figure 4-12 Triglyceride and glucose levels in plasmatocyte-less flies compared to control flies*
Plasmatocyte-less flies (w;*Tubulin*-Gal80$^{ts}$/+;*crq*-Gal4,UAS-myrRFP/UAS-*rpr*, black bars) and control flies (w;*Tubulin*-Gal80$^{ts}$/+;*crq*-Gal4,UAS-myrRFP/+, white bars) were placed on a 15% lard diet for examination of **A.** Triglyceride content via thin layer chromatography (TLC) after 20 days on a 15% lard diet. Data represents the mean of four groups of 10 flies per diet (n=40 flies per diet). Error bars represent standard error of the mean, unpaired t test p=0.7938, ns. **B.** Glucose and trehalose content of plasmatocyte-less, and control genotype flies on both control and 15% lard diets for 30 days. Trehalose present was converted to glucose with trehalase (see experimental methods). Error bars represent standard error of the mean. Glucose and trehalose levels in plasmatocyte ablated compared to control plasmatocyte competent flies after 30 days upon 15% lard diet, unpaired t test p= 0.016447/*, lack of stars indicates the data was not statistically significant, $p \geq 0.05$. The data in **A** and **B** are representative of 3 independent experiments.

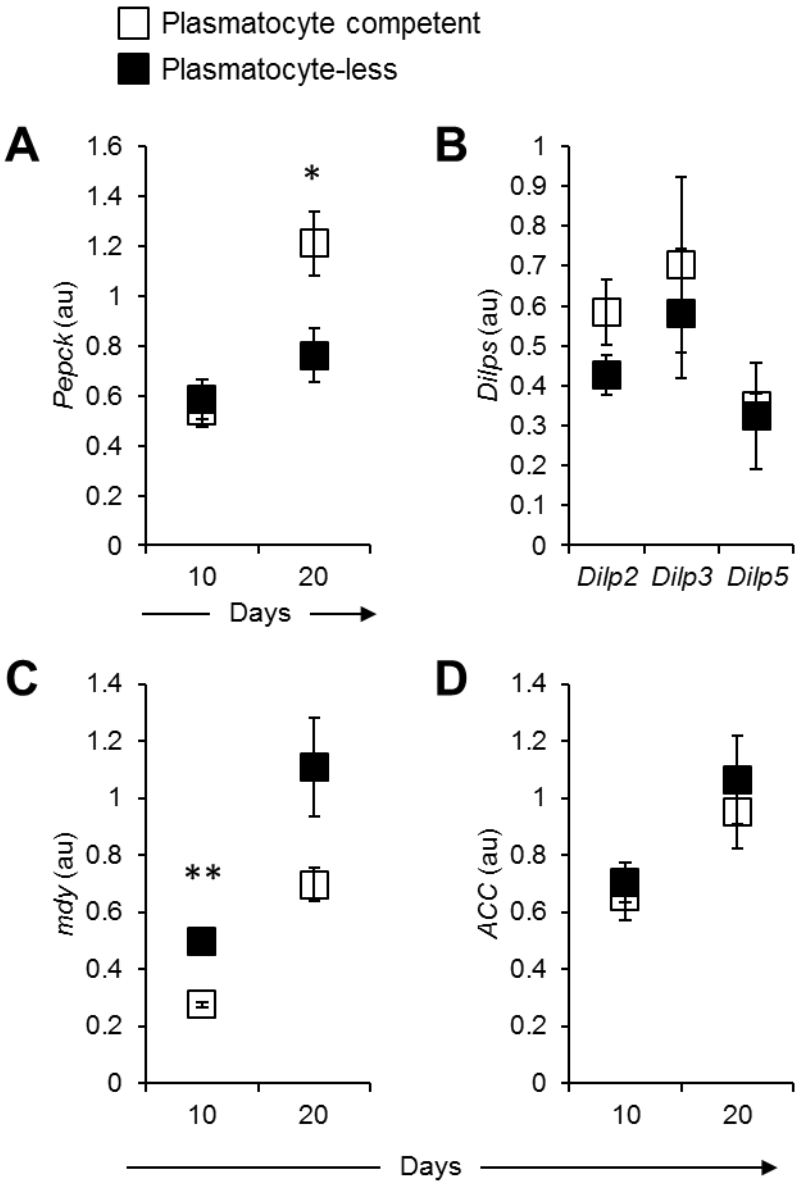


*Figure 4-13 Transcript levels of metabolic genes in plasmatocyte-less flies compared to control flies upon high fat diet*

Plasmatocyte depleted (w;*Tubulin*-Gal80$^{ts}$/+;*crq*-Gal4,UAS-myrRFP/UAS-*rpr*, white shapes/bars) and control plasmatocyte competent flies (w;*Tubulin*-Gal80$^{ts}$/+;*crq*-Gal4,UAS-myrRFP/+, black shapes/bars) were collected for RT qPCR sample preparation at days 20 and 30 after high fat diet exposure (15% lard diet). All RT qPCR data is normalised to the housekeeping gene *Rpl1*, (au = arbitrary units). Data represents the mean of n=5 samples per genotype, per time point, each sample contained 3 flies. **A.** Normalised *Pepck* in plasmatocyte depleted and plasmatocyte competent flies (day 10 p≥0.05/ns, day 20, unpaired t test, p=0.029478/*). **B.** Normalised *Dilp2, Dilp3 and Dilp5* transcript levels in plasmatocyte depleted, and plasmatocyte competent flies at day 20 upon 15% lard diet (*Dilp* p values were not significant at any of the time points examined). Normalised transcript levels at day 10 and 20 of **C.** *midway* (*mdy*) and **D.** *ACC* (*Acetyl-CoA carboxylase*) in plasmatocyte depleted and plasmatocyte competent flies. (Unpaired t test, *mdy* 10 days p=0.00127/**). Where no stars are present, this indicates data was not statistically significant.

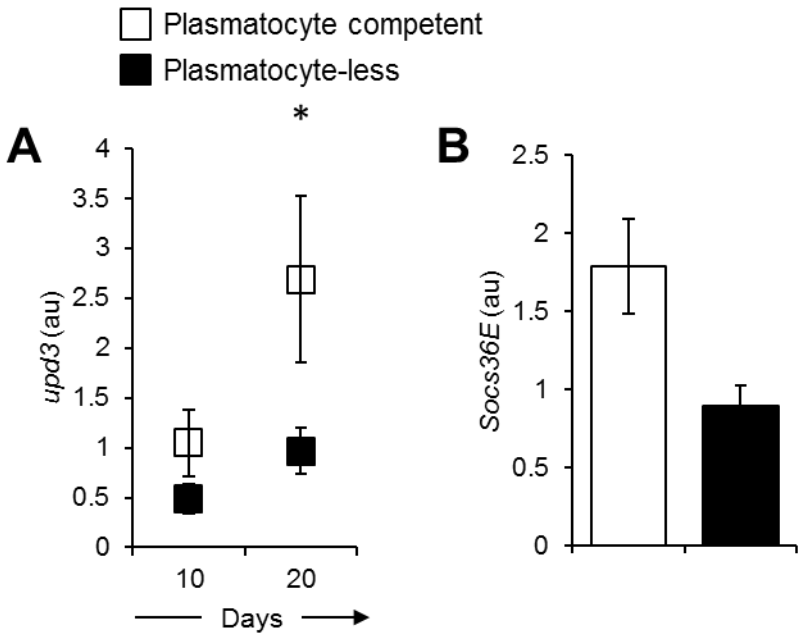


*Figure 4-14 Transcript levels of JAK-STAT pathway genes in plasmatocyte-less flies and control flies upon high fat diet*

Plasmatocyte depleted (w;*Tubulin*-Gal80$^{ts}$/+;*crq*-Gal4,UAS-myrRFP/UAS-*rpr*, black bars/shapes) and control plasmatocyte competent flies (w;*Tubulin*-Gal80$^{ts}$/+;*crq*-Gal4,UAS-myrRFP/+, white bars/shapes) were collected for RT qPCR sample preparation at days 20 and 30 after high fat diet exposure (15% lard diet). All RT qPCR data is normalised to the housekeeping gene *Rpl1*, (au = arbitrary units). Data represents the mean of n=5 samples, per genotype, per time point, each sample contained 3 flies. Normalised transcript level of **A.** *upd3* (day 20 unpaired t test p=0.03141/*) and **B.** *Socs36E* (day 20 p=0.05027, ns) in plasmatocyte depleted and plasmatocyte competent flies. Where no stars are present, this indicates data was not statistically significant.

### 4.6 *Peroxidasin* (*Pxn*) and lipid rich diet

Peroxidase enzymes are pro-inflammatory, and given the reduction of lifespan observed in flies upon lipid rich diet, experiments were carried out to determine if plasmatocytes up regulate *Pxn* expression in response to lipid scavenging, which in turn could contribute to the premature death observed in these flies.

Flies were examined for induction of *Pxn* expression after both acute lipid rich diet exposure for 24 hours, and after chronic exposure to a high lipid diet, for 2 weeks. *Pxn* reporter flies (w;;*Pxn*-Gal4,UAS-2xeGFP) were selected and aged for 10 days, in order to ensure the majority of plasmatocytes no longer expressed *Pxn* (see Figure 3-10 for microscopy illustrating the loss of *Pxn* expression by plasmatocytes). Flies were placed on 6.3% lard diets for either 24 hours or 2 weeks and imaged for induction of *Pxn* expression in plasmatocytes. In both cases, no significant increase in *Pxn* expressing cells was observed upon lipid rich diets (Figure 4-15 A, B). A further experiment was carried out, involving the injection of DiI-LDL, a red fluorescent lipid in order to further investigate a potential *Pxn* induction in response to lipid scavenging. There was no significant difference in the number of *Pxn* positive plasmatocytes after lipid injection (Figure 4-15 C). However, plasmatocytes were nicely labelled on the basis that they had successfully phagocytosed the fluorescent injected DiI-LDL (Figure 4-15 D, E), providing a control for the presence of plasmatocytes.

Together these data suggest that *Pxn* expression is not induced in response to an increase in dietary lipids or by the act of lipid scavenging itself. Thus *Pxn* induction does not appear to be involved in the pathophysiology resulting in early death of high fat diet fed flies, via either plasmatocyte mediated lipid sensing or scavenging.

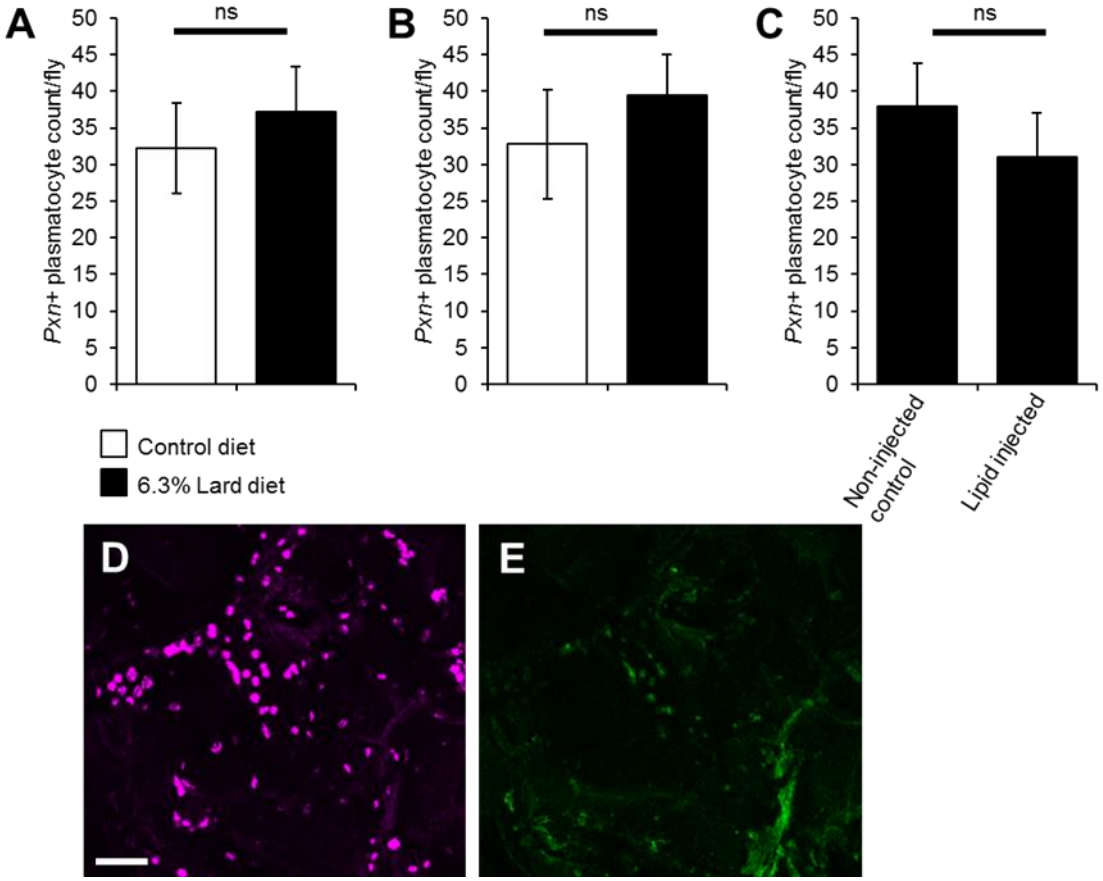


*Figure 4-15 Plasmatocytes do not up regulate Pxn after dietary or injected lipid exposure*
Confocal microscopy of w;;*Pxn*-Gal4,UAS-GFP flies for quantification of *Pxn* expression by plasmatocytes in response to dietary lipids and injected lipids. All error bars represent standard error of the mean **A.** *Pxn* positive (GFP+) plasmatocyte count in flies 24 hours post 6.3% lard diet exposure, data represents the mean of n=4 flies per diet (unpaired t test p=0.4968/ns). **B.** *Pxn* positive (GFP+) plasmatocyte count in flies fed 6.3% lard diet for 2 weeks, data represents the mean of n=4 flies per diet, (unpaired t test p=0.5858/ns). **C.** *Pxn* positive (GFP+) plasmatocyte count in flies injected with red fluorescent low density lipoprotein (DiI-LDL), flies imaged 24 hours post injection, data represents the mean of n=3 flies per condition, (unpaired t test p=0.4518/ns). **D, E.** Confocal microscopy of DiI-LDL injected w;;*Pxn*-Gal4,UAS-2xeGFP fly (Scale bar=100µm). **D.** DiI-LDL channel, indicating plasmatocytes which have scavenged the injected lipid. **E.** GFP channel, *Pxn*-GFP positive plasmatocytes.

## 4.7 Chapter 4 Overview and discussion

High fat diet exposure resulted in a reduction of lifespan in wild type flies (Driver and Cosopodiotis, 1979). This coincided with a hyperglycaemia phenotype and an up regulation of JAK-STAT cytokines *upd2* and *upd3* in the whole fly. In accordance with this, high fat diet fed flies developed lipid laden, foam cell-like, plasmatocytes. Interestingly, this phenomenon is observed in mammalian macrophages upon high fat diet exposure and presence of these foamy macrophages is implicated in development and progression of high fat diet induced diseases, and including atherosclerosis (Glass, 2002).

Plasmatocyte depletion appeared to be protective in flies fed a lipid rich diet. A loss of fly plasmatocytes extended lifespan and prevented both the onset of hyperglycaemia and activation of the JAK-STAT pathway which was observed in plasmatocyte competent flies. Conversely, plasmatocyte deletion has been shown to be detrimental to fly survival after infection (Charroux and Royet, 2009). These data are suggestive of very differing protective and detrimental roles for plasmatocytes dependent on the environmental cue. These observations indicate that the plasmatocyte response to dietary lipids shortens fly life expectancy, potentially through their effect on the JAK-STAT pathway and ultimately glucose metabolism.

### *4.7.1 Further investigation into effects of olive oil upon fly survival and metabolism*

The current dogma regarding the healthiness of different dietary lipids is suggestive of lower levels of saturation being the healthier option. In humans an increased consumption of saturated fats is associated with an increased prevalence of heart disease (Ascherio et al., 1996), however, consumption of unsaturated fats has been shown to reduce the risk of heart disease more significantly than by simply reducing the level of saturated fat intake (Hu et al., 2001). This would point towards olive oil as being a healthier fat than coconut oil or lard, both of which have higher levels of saturation. Interestingly findings in this thesis would suggest that olive oil supplemented diets were actually equally, if not more

detrimental to fly survival than the coconut oil or lard supplemented diets. As previously alluded to, this could be due to the fact that olive oil is liquid at room temperature (the opposite is true of coconut oil and lard), therefore, during the survival experiments there were instances in which the food vials became coated in oil and fly death could be simply have been due to them becoming stuck, rather than due to the consumption of dietary lipids.

Experiments could be carried out to control for this, for example a more oily control diet food could be generated. More interestingly, the metabolic and immune phenotypes of olive oil fed flies could be studied, in comparison to the phenotypes observed in 15% lard diet fed flies. If similar findings were observed at earlier time points post olive oil diet exposure, for example, a rise in whole fly glucose and triglyceride levels and a simultaneous increase and decrease in *upd3* and *Pepck* expression levels respectively, this could be suggestive of the consumption of the olive oil diet itself being the cause of death, rather than flies becoming stuck in it.

### *4.7.2 Plasmatocyte-less fly survival upon olive oil enriched diet*

A further experiment to investigate the effects of olive oil upon fly survival could be to examine plasmatocyte-less fly survival phenotypes upon an olive oil enriched diet. Survival of plasmatocyte-less flies surpasses that of plasmatocyte competent flies on coconut oil and lard diets. Therefore, if similar findings were observed in flies fed an olive oil enriched diet, it would be suggestive of an oil related effect on survival, whereas if plasmatocyte-less and plasmatocyte competent flies die at the same time, this would be suggestive of flies becoming stuck in the food.

### *4.7.3 Examination of upd expression under a lipid rich diet*

Experiments were carried out in which transcript levels of *upd2* and *upd3* were monitored in wild type flies via RT qPCR after a differing number of days upon a lipid rich diet.

However, expression of the other JAK-STAT ligand *upd* was not investigated, considering the apparent dietary regulation of *upd2* and *upd3* it would be interesting to examine *upd* expression levels in high fat diet fed flies to determine if it is regulated in the same way. In addition to this, considering the apparent abrogation of *upd3* up regulation in plasmatocyte depleted flies, experiments could be carried out to investigate whether the loss of plasmatocytes in adult flies would also affect expression of *upd*.

### *4.7.4 RT qPCR for upd2 expression in plasmatocyte-less flies*

It was not possible to carry out RT qPCR for *upd2* expression in the plasmatocyte-less cohort of aged flies in time for inclusion in this thesis. It would be interesting to see if *upd2* expression is altered when flies lack plasmatocytes, particularly because of the increase in *upd2* observed in wild type flies chronically fed a lipid rich diet. This experiment may shed further light on whether *upd2* expression is in some way regulated by plasmatocytes in adult flies.

### *4.7.5 Does high fat diet induce other, non-AMP related differences during infection*

In humans, obesity is associated with an increased susceptibility to infection (Falagas and Kompoti, 2006). In this chapter we show that high fat diet fed flies accumulate triglycerides, which could be likened to the development of an obesity-like phenotype in flies, simultaneous to this, plasmatocytes adopted a lipid filled, foam cell-like morphology. Levels of *Drs* and *Dpt* AMPs remained similar after before and after infection, regardless of diet, however the infection was carried out after flies were fed high fat diets for 10 days. Given the apparent up regulation of the JAK-STAT pathway family member's *upd2*, *upd3* and *Socs36E* at later time points upon a lipid rich diet (e.g. 20-30 days), it would be interesting to monitor the AMP response to infection in flies which have been fed a high fat diet for 20 or 30 days. This may give a better indication as to whether chronic dietary lipid exposure could affect the fly AMP responses to infection.

Furthermore, it would also be interesting to carry out experiments to determine whether flies are rendered more susceptible or respond differently to infection after chronic high fat diet exposure in other ways. For example, fly plasmatocytes accumulate lipids after high fat diet exposure and plasmatocytes are known to play an important phagocytic role in adult flies during infection. In addition, flies lacking plasmatocytes have been shown to exhibit an increased susceptibility to bacterial infection (Charroux and Royet, 2009). Experiments in which survival of flies infected with an ultimately fatal infectious agent could be monitored, comparing survival traits of control diet infected flies to high fat diet infected flies. Experiments such as this may allow for a deeper insight into both the effects of a lipid rich diet and of the presence of excess lipids within plasmatocytes, upon plasmatocyte functions and therefore upon the fly response and susceptibility to infection.

*4.7.6 Upd3 and IL-6 (interleukin 6)*

The *upds* have been likened to *IL-6* cytokines, due to the structural similarity of the JAK-STAT pathway receptor, DOME to the mammalian IL-6R (Harrison et al., 1998). Plasmatocytes in adult flies have been previously shown to produce *upd3* in response to bacterial infection (Agaisse et al., 2003). Interestingly, numerous studies have indicated that *IL-6* is produced by macrophages and adipose tissue in humans, and importantly that *IL-6* concentrations are significantly increased among obese individuals compared to non-obese controls (Mohamed-Ali et al., 1997, Bastard et al., 1999, Gray and Kim, 2011).

These data, coupled with findings in this chapter would suggest that plasmatocytes are able to produce *upd3*, or that plasmatocytes in some way regulate the expression of *upd3* by other tissues. Experiments in this chapter have demonstrated that the increase of *upd3* expression induced by chronic high fat diet was significantly reduced in plasmatocyte-less flies. This may suggest that expression of *upd3* by plasmatocytes after lipid rich diet exposure is a conserved function, as production of the *upd3* counterpart in

mammals; *IL-6* has been frequently reported in patients suffering from type II diabetes, metabolic syndrome and atherosclerosis (Vozarova et al., 2001, Scheller and Rose-John, 2012).

# Chapter 5 Plasmatocyte scavenger receptor screen

## 5.1 Identification of plasmatocyte expressed genes involved in lipid uptake

The observations documented in Chapter 4 indicate that the *Drosophila* plasmatocyte response to a lipid rich diet shortens fly life expectancy. This reduction in fly lifespan coincides with both a dysregulation of glucose homeostasis, and the production of the *IL-6*-like cytokine *upd3* in response to chronic lipid rich diet exposure. Additionally plasmatocytes in high fat diet fed flies become lipid laden and adopt a foam cell-like morphology.

To better elucidate the mechanisms involved in lipid uptake and sensing by plasmatocytes and the potential downstream mechanisms involved, the fly genome was screened for putative scavenger receptors and a list of candidate genes was compiled. These genes were then investigated in detail with the use of UAS, scavenger receptor RNAi (RNA interference) lines, allowing plasmatocyte specific knock down of scavenger receptors of interest using the Gal4, UAS expression system.

### *5.1.1 Screen aims*

Ultimately, this screen aimed to firstly identify candidate scavenger receptors which were expressed by plasmatocytes. Secondly, to clarify the knock down efficiency of the RNAi lines of interest, allowing for further study of the function of the given scavenger receptors in plasmatocytes. Thirdly, the effect of scavenger receptor knock down specifically in plasmatocytes upon their lipid scavenging ability was examined. Finally, if plasmatocyte derived expression of the gene was detected and knock down was effective, and a significant effect on plasmatocyte lipid uptake was observed upon knock down, these genes of interest would be investigated further.

Further experiments with the interesting candidates identified in this screen were carried out, with a view to attempt to further characterise some of the plasmatocyte related phenotypes observed after high fat diet exposure, using flies in which

plasmatocyte lipid scavenging is impaired. This allowed for deeper characterisation of the plasmatocyte response to dietary lipids.

### *5.1.2 Chapter 5 hypothesis*

Plasmatocyte expressed scavenger receptor(s) play a role in lipid scavenging, which in turn affects fly metabolic and immunological responses to chronic high fat diet exposure.

### *5.1.3 Chapter 5 aims; Part 1*

Screening of candidate scavenger receptor genes;

1. Characterisation of the expression of candidate scavenger receptors in adult fly plasmatocytes.
2. Characterisation of knock down efficiency and reliability of candidate scavenger receptor UAS-RNAi lines.
3. Investigation into the effects of plasmatocyte specific knock down of differing scavenger receptor genes upon plasmatocyte lipid scavenging capabilities.

### *5.1.4 Chapter 5 aims post screen; Part 2*

Deeper examination of genes highlighted in the screen;

1. Study of the effects of plasmatocyte specific knock down upon survival.
2. Investigation of the effect of plasmatocyte specific knock down upon whole fly glucose and triglyceride levels.
3. Study of the effect of plasmatocyte specific knock down on metabolic and inflammatory gene transcript levels in the whole fly.

### 5.2 Candidate plasmatocyte scavenger receptors

The fly genome was investigated for candidate scavenger receptor genes. Receptors were selected on the basis of previous evidence of scavenger receptor activity in the literature, or bioinformatical prediction of scavenger receptor activity. The selected genes are described in Table 5-1. *Hemese* was included in the cohort as a non-scavenger receptor (Kurucz et al., 2003).

*Drosophila* UAS-knock down gene lines were obtained (see Chapter 2, Table 2-2 for further details on knock down lines), allowing for plasmatocyte specific knock down of the candidate gene of interest. Knock down flies were crossed to plasmatocyte Gal4, UAS reporter flies (w;*Hml*Δ-Gal4,UAS-2xeGFP). The end result was fluorescently labelled plasmatocytes in adult *Drosophila*, which simultaneously had expression of a gene of interest knocked down (e.g. knock down genotype: w;*Hml*Δ-Gal4,UAS-2xeGFP;UAS-*crq*-IR, meaning *crq* is knocked down specifically in plasmatocytes).

Of the 11 candidate genes investigated, 8 of them, (*CG10345, CG1887, CG2736, CG3829, CG7227, CG7422/Snmp2, crq, pes*) were members of the scavenger receptor Class B type I (SR-BI) family. The SR-BI family is a transmembrane class of CD36 related membrane proteins, that are involved in uptake of cholesterol (Herboso et al., 2011). Interestingly *CD36* has been strongly implicated in development of high fat diet induced diseases, and is proposed to have a lipid scavenging and sensing function (Martin et al., 2011).

*Table 5-1 Putative scavenger receptor and control genes*

| **Knock down line (CG number)** | **Gene name** | **Reported / predicted functions, and tissue specific expression data, where available** |
|---|---|---|
| UAS-*CG7228*-IR | *peste (pes)* | Reported to be required for mycobacterial phagocytosis in hemocyte cell lines, *CD36* family member. (Philips et al., 2005, Nichols and Vogt, 2007). Strong expression has been observed throughout 3rd instar larval development in a variety of larval tissues including the fat body, salivary glands, ovaries, testes, midgut and hindgut (Herboso et al., 2011). |
| UAS-*CG7422*-IR | *Snmp2* | Sensory neurone membrane protein (*Snmp*) family member, which belongs to the *CD36* family (Nichols and Vogt, 2007). Expression is observed in testes of 3rd instar larvae (Herboso et al., 2011). |
| UAS-*CG8942*-IR | *nimrodC1 (nimC1)* | Phagocytic receptor, involved in bacterial phagocytosis, but not involved in bacterial adhesion to immune cells (Kurucz et al., 2007a). |
| UAS-*CG3829*-IR | n/a | Autophagic cell death, cell adhesion, scavenger receptor activity (Gorski et al., 2003, Nichols and Vogt, 2007). Expression detected in the fat body and testes of 3rd instar larvae (Herboso et al., 2011). |
| UAS-*CG1887*-IR | n/a | Scavenger receptor activity, defence, integral to plasma membrane (Nichols and Vogt, 2007). Expression also detected in fat body and testes in 3rd instar larvae (Herboso et al., 2011). |
| UAS-*CG31770*-IR | *Hemese (He)* | Glycophorin-like membrane molecule expressed by hemocytes and hematopoietic organs, modulatory role in immune activation (Kurucz et al., 2003). |
| UAS-*CG3212*-IR | *Sr-CIV* (Scavenger receptor class C type IV) | Transmembrane receptor, transcript levels found to be enriched in larval lymph gland / hemocyte samples (Irving et al., 2004). Conversely it is reported by Lazzaro (2005) to be a potential pseudogene. |
| UAS-*CG7227*-IR | n/a | Scavenger receptor activity, cell adhesion, defence (Nichols and Vogt, 2007). Expression detected only in 3rd instar larval testes (Herboso et al., 2011). |
| UAS-*CG2736*-IR | n/a | *CD36* family member (Nichols and Vogt, 2007). Strong expression has been described by Herboso et al. (2011) specifically in the fat body, during 3rd instar larval development. |

| **Knock down line (CG number)** | **Gene name** | **Reported / predicted functions, and tissue specific expression data, where available** |
|---|---|---|
| UAS-*CG10345*-IR | n/a | Scavenger receptor activity, defence, integral to plasma membrane (Nichols and Vogt, 2007). Expression detected in 3rd instar larval testes (Herboso et al., 2011). |
| UAS-*CG4280*-IR (two independent knock down lines obtained) | *croquemort (crq)* | Phagocytosis of apoptotic cells, 23% homology at amino acid level to human and murine CD36. Expression observed in adult fly hemocytes (Franc et al., 1996). Expression detected during development of 3rd instar larvae in testes, gastric caeca and the midgut, suggesting *crq* is not hemocyte specific (Herboso et al., 2011). |

This table indicates the given UAS-IR (inverted repeat) knock down lines investigated, with both either CG (computed gene) numbers and where possible gene names. Details of each genes predicted function, and expression locations are included in the final column.

### *5.2.1 FACS for characterisation of plasmatocyte expression and knock down of candidate genes*

The UAS knock down lines above were each crossed to *Hml* driven reporter flies (w;*Hml*Δ-Gal4,UAS-2xeGFP), in order to specifically knock down expression in plasmatocytes. Groups of approximately 80-90 male flies were collected, and plasmatocytes were FACS cell sorted on the basis of their inherent GFP expression. RNA extraction was performed and cDNA generated from these cells, as well as from a control, driver only (w;*Hml*Δ-Gal4,UAS-2xeGFP/+) population of plasmatocytes. Plasmatocyte specific knock down and plasmatocyte derived expression of the candidate genes was confirmed via RT qPCR in 5 of the lines in this way (Figure 5-1). The remaining 6 lines were successfully sorted, but no expression could be detected by RT qPCR, thus a confirmation of expression and knock down of expression specifically in plasmatocytes could not be confirmed.

Plasmatocyte derived expression and knock down (knock down efficiency displayed as a percentage, calculated from comparison to control cells) of *nimC1* (82%), *crq* (91%), *Hemese* (99%), *CG3829* (37%) and *CG2736* (59%) was detected via RT qPCR of plasmatocyte cDNA.

### *5.2.2 Hml (plasmatocyte) driven, and Tubulin (ubiquitous) driven knock down*

Experiments were carried out alongside the FACS sorting experiments to further determine knock down efficiency. This was to both re-clarify the results obtained in the FACS sorting experiments and to also determine expression and knock down of those genes which could not be characterised by FACS.

As in the FACS sorting fly sample generation, the UAS scavenger receptor lines above were each crossed to *Hml* driven reporter flies (w;*Hml*Δ-Gal4,UAS-2xeGFP). This gave a repertoire of flies in which knock down of the candidate gene was knocked down only in plasmatocytes. Age matched flies were collected for whole fly cDNA sample

preparation after 1 week of adult life. RT qPCR was performed with cDNA generated from both the knock down gene of interest and in control genotype whole fly cDNA. In addition to this, various different knock down whole fly cDNA samples were also used as controls for off-target effects of the RNAi lines (Figure 5-2).

Similarly, the same whole fly sample preparation was carried out using a ubiquitous driver, *Tubulin* (w;;*Tub*-Gal4), to drive knock down of the gene of interest in all fly tissues, rather than just plasmatocytes. The reason *Tub* and *Hml* were both used to drive knock down, was that to see an effect of knock down in whole fly cDNA using *Hml* as a driver would mean that the gene of interest's expression would need to be either; restricted to specifically to plasmatocytes, or plasmatocytes would need to be a predominant cell type expressing that gene. If for example every cell expressed the candidate gene, including plasmatocytes, expression specificity to plasmatocytes, and effective knock down could not be determined using only *Hml* to drive knock down. Therefore *Tub* driven knock down was carried out in order to further determine the knock down efficiency of genes which may not be specific to plasmatocytes.

*He* and *nimC1* are examples of plasmatocyte specific genes, this is because expression is similarly abrogated when driving knock down using *Hml* (Figure 5-2 A and C), as well as *Tubulin* (Figure 5-3 A and C). However, *crq* is an example of a gene that is expressed by plasmatocytes, but that appears to also be expressed by other cell types. This is because knock down with *Hml* induces only a partial a reduction of *crq* expression, which is suggestive of other, non-plasmatocyte tissue types expressing *crq* (Figure 5-2 B). In support of this theory, knock down using the ubiquitous driver *Tubulin* is sufficient to induce a strong reduction of *crq* expression in the whole fly (Figure 5-3 B). Finally *CD10345* was a gene in which knock down was effective, yet expression appeared to be plasmatocyte non-specific. This is because a strong reduction of expression of *CG10345* could be observed when driving knock down with *Tubulin* (Figure 5-3 D), yet no knock down could be observed when using *Hml* as a driver (Figure 5-2 D).

See Table 5-2 for a summary of the investigated candidate genes, detailing their expression by plasmatocytes, and the efficiency of knock down using either *Hml* or *Tub* as a driver.

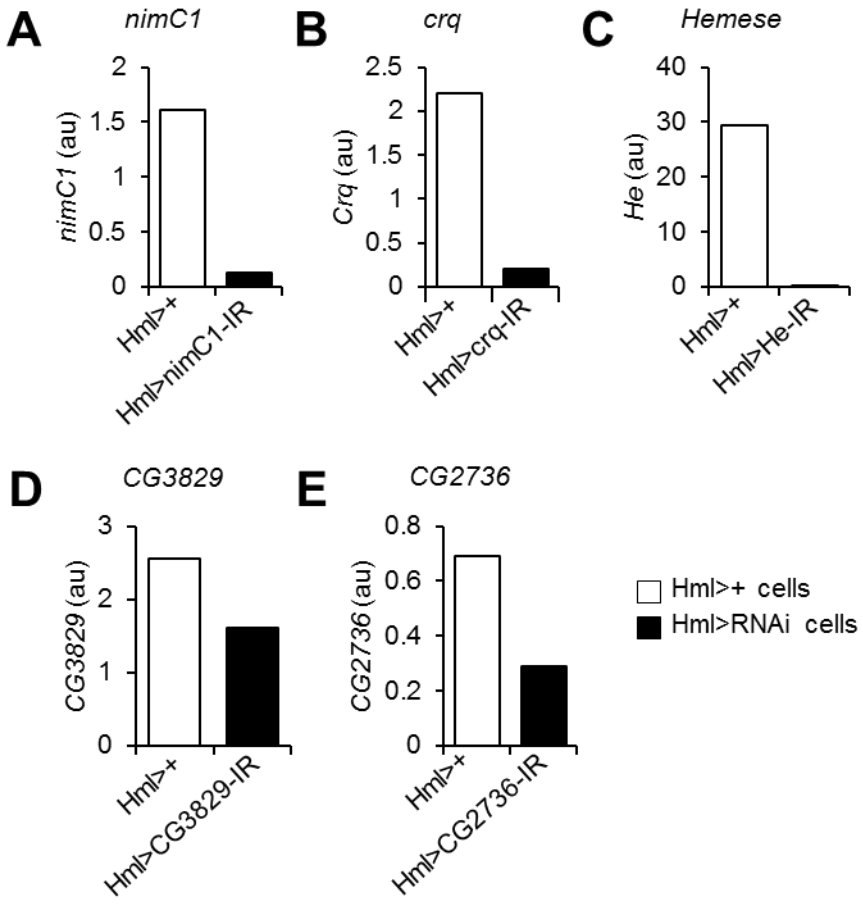


*Figure 5-1 Expression and knock down of candidate genes in FACS sorted plasmatocytes*
RT qPCR analysis of FACS sorted *Hml* positive plasmatocytes from plasmatocyte specific knock down line flies (w;*Hml*Δ-Gal4,UAS-2xeGFP;UAS-knock down, black bars) compared to control driver only flies (w; *Hml*Δ-Gal4,UAS-2xeGFP/+, white bars). Transcript level of all genes is normalised to housekeeping gene *Rpl1* and displayed as arbitrary units (au). RT qPCR transcript levels of **A.** *nimC1,* **B.** *crq,* **C.** *He,* **D.** *CG3829,* and **E.** *CG2736* in FACS sorted plasmatocytes. Cell sort numbers: driver only control cell populations; 5,700, 3,000, or 5,972 cells. *Hml* driven knock down cell numbers; *nimC1*= 10,000, *crq*= 1,892, *He*= 1,850, *CG3829*= 5,850 and *CG2736*= 4,000. Due to the slow cell sort rate in FACS experiments, it was not possible to re-sort further populations of knock down cells, which is why no error bars are present and statistical analysis could not be performed.

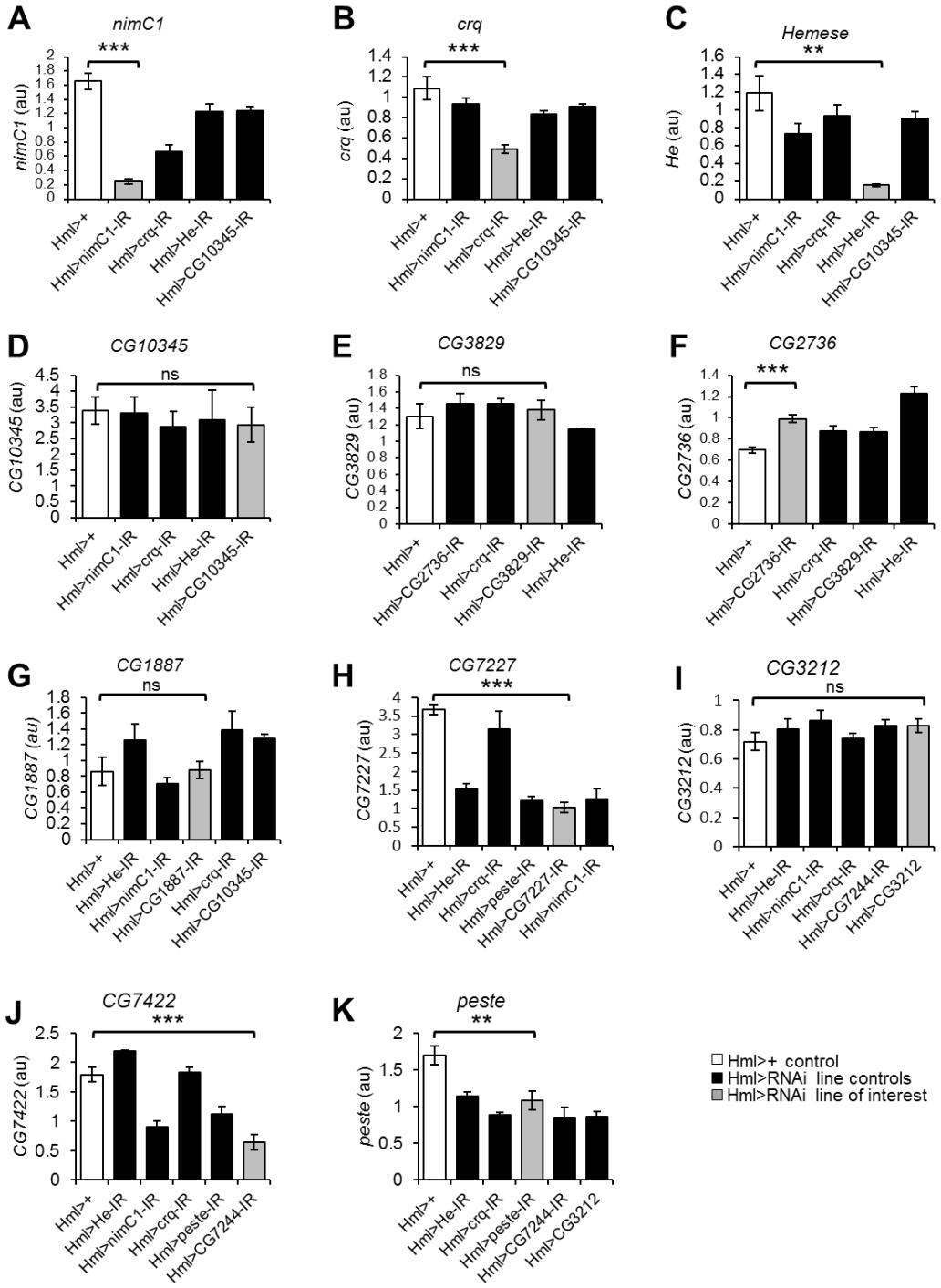


*Figure 5-2 Plasmatocyte specific knock down of candidate genes*

RT qPCR analysis of *Hml* driven scavenger receptor knock down in whole fly cDNA. *Hml*Δ-Gal4,UAS-2xeGFP flies were crossed to the UAS-scavenger-IR flies and whole fly cDNA samples were generated. Various *Hml*Δ-Gal4,UAS-Scavenger-IR lines were run alongside each other as controls for off-target RNAi effects (black bars). Grey bars represent the scavenger receptor knock down line of interest, therefore a reduction of expression should be observed here if the gene is expressed by *Hml*$^{+}$ plasmatocytes. White bars represent control driver only genotype flies. Transcript levels are normalised to the housekeeping gene *Rpl1* and displayed as arbitrary units (au); **A.** *nimC1*, **B.** *crq*, **C.** *He*, **D.** *CG10345*, **E.** *CG3829*, **F.** *CG2736*, **G.** *CG1887*, **H.** *CG7227*, **I.** *CG3212*, **J.** *CG7422* and **K.** *Pes*. Data represents the mean of n=4/5 samples (3 flies per sample), error bars represent the standard error of the mean, statistical analysis of control genotype (*Hml*>+, white bars) against the knock down genotype of interest (*Hml*>RNAi line of interest, grey bars), unpaired t tests, $p<0.05$/*, $p\leq0.01$/** $p\leq0.001$/***.

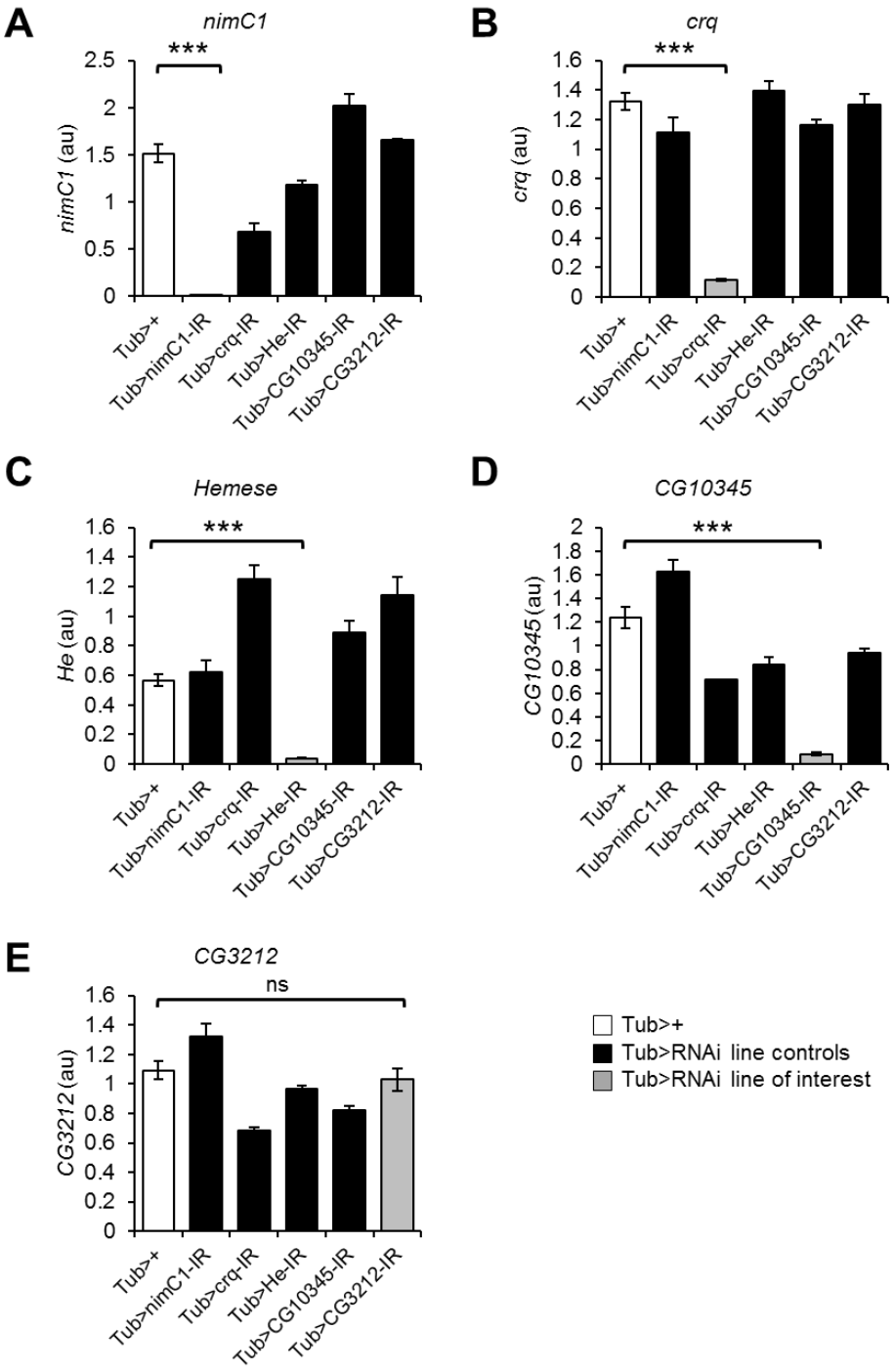


*Figure 5-3 Ubiquitous driven knock down of candidate genes*

RT qPCR analysis of *Tubulin* driven, ubiquitous scavenger receptor knock down in whole fly cDNA. *Tubulin*-Gal4 flies were crossed to the UAS-scavenger-IR flies and whole fly cDNA samples were generated. Various *Tub*-Gal4,UAS-Scavenger-IR lines were run alongside each other as controls for off-target RNAi effects (black bars). Grey bars represent the scavenger receptor knock down line of interest, therefore a reduction of expression should be observed here if the gene is being effectively knocked down. White bars represent control driver only genotype flies. Transcript levels are normalised to the housekeeping gene *Rpl1* and displayed as arbitrary units (au); **A.** *nimC1*, **B.** *crq*, **C.** *He*, **D.** *CG10345*, **E.** *CG3829*, **F.** *CG2736*, **G.** *CG1887*, **H.** *CG7227*, **I.** *CG3212*, **J.** *CG7422* and **K.** *Pes*. Data represents the mean of n=4/5 samples (3 flies per sample), error bars represent the standard error of the mean, statistical analysis of control genotype (*Tub*>+, white bars) against the knock down genotype of interest (*Tub*>RNAi line of interest, grey bars), unpaired t tests, $p<0.05$/*, $p\leq0.01$/** $p\leq0.001$/***.

## 5.3 Characterisation of screened gene expression by plasmatocytes and knock down

### *5.3.1 He, nimC1 and crq: plasmatocyte expressed and knock down clarified genes*

FACS sorting confirmed expression of *He*, *nimC1* and *crq* by plasmatocytes (Figure 5-1 A-C). Plasmatocyte derived *He*, *crq* and *nimC1* has been previously described in larvae and adult *Drosophila* (Kurucz et al., 2007a, Franc et al., 1996, Clark et al., 2011). In addition to this, imaging experiments in this thesis have illustrated that plasmatocytes are fluorescently labelled in *crq*-Gal4, UAS-mRFP reporter flies.

Knock down was also confirmed using whole fly cDNA, in which knock down was driven specifically in plasmatocytes by *Hml*. Using *Hml* as a driver highlighted that *nimC1* and *He* expression appeared to be restricted to plasmatocytes (Figure 5-2 A, C), *crq* expression however, was only partially reduced when using *Hml* as a driver for knock down. This suggests other non-plasmatocyte cell types in the fly may also express *crq* (Figure 5-2 B). Finally, knock down was re-confirmed using the ubiquitous driver *Tub*, in which *He*, *nimC1* and *crq* expression was almost totally knocked down (Figure 5-3 A-C).

Expression of *Hemese* was believed to be low, or non-existent in adult plasmatocytes (Kurucz et al., 2007b), expression is however detected here in FACS sorted adult fly plasmatocytes (Figure 5-1 C). Furthermore, knocking *He* down using the plasmatocyte specific driver *Hml* resulted in a strong reduction of expression, which would suggest adult plasmatocytes do express *He* (Figure 5-2 C).

### *5.3.2 CG3829 and CG2736: expression and knock down confirmed by FACS only*

Plasmatocyte derived expression of *CG3829* and *CG2736* was detected in FACS sorted cells (Figure 5-1 D, E). In both genes some degree of knock down was observed, however, knock down of *CG3829* expression was the least convincing at only 37%. Unfortunately it was not clear in the plasmatocyte *Hml* driven knock down experiment whether these genes were expressed by plasmatocytes (Figure 5-2 E, F), which may suggest they are expressed by many cell types including plasmatocytes. Finally knock

down also could not be clarified using *Tub* as a driver, as ubiquitous knock down of *CG3829* and *CG2736* was lethal in these flies.

### *5.3.3 CG7227, CG7422 and CG1887: potentially plasmatocyte expressed*

Unfortunately expression of *CG7227*, *CG7422* and *CG1887* could not be confirmed in FACS sorted plasmatocytes. Plasmatocyte *Hml* driven knock down did indicate a slight reduction of expression of *CG7227* and *CG7422* (Figure 5-2 H, J) compared to control genotypes. Once more *Tub* driven knock down of *CG7227*, *CG7422* and *CG1887* was lethal, and therefore both plasmatocyte derived expression, and knock down could not be definitively determined.

### *5.3.4 Peste, CG3212 and CG10345*

Expression of *peste*, *CG3212* and *CG10345* could not be confirmed by FACS. Furthermore expression in plasmatocyte *Hml* driven knock down flies suggested that they were not plasmatocyte specific genes, as no reduction of *CG3212* and *CG10345* expression was observed (Figure 5-2 D, I). Expression of *peste* appeared to be abrogated when compared to the control genotype, but when comparing to other scavenger receptor knock down flies this wasn't the case, thus a conclusion could not be made with regard to plasmatocyte specificity of *peste* expression (Figure 5-2 K). Ubiquitous knock down of *CG10345* using *Tub* as a driver was not lethal, and indicated that *CG10345* knock down was efficient (Figure 5-3 E). Flies in which *CG3212* knock down was ubiquitous were viable; however when examining expression levels via RT qPCR no reduction in expression was observed (Figure 5-3 D). This suggests the *CG3212* knock down may not be functioning. Finally ubiquitous knock down of *peste* using *Tub* as a driver was not viable, and therefore knock down could not be confirmed in this line. See Table 5-2 for a summary of the findings with regard to both the candidate scavenger receptors plasmatocyte specific expression and knock down efficiency.

*Table 5-2 Summary of candidate scavenger receptor plasmatocyte specific expression and knock down efficiency*

| Candidate gene | Expression detected in FACS sorted plasmatocytes | Knock down observed with *Hml*Δ-Gal4 (plasmatocyte specific driver) | Knock down observed with *Tub*-Gal4 (ubiquitous driver) |
|---|---|---|---|
| ***nimC1*** | + | + | + |
| ***crq*** | + | + | + |
| ***Hemese*** | + | + | + |
| ***CG10345*** | **No** | **No** | + |
| *CG3829* | + | No | Not viable |
| *CG2736* | + | No | Not viable |
| *CG1887* | No | Inconclusive | Not viable |
| *CG7227* | No | Inconclusive | Not viable |
| *CG3212* | No | No | No |
| *CG7422 (Snmp2)* | No | Inconclusive | Not viable |
| *peste* | No | No | Not viable |

Summary of the findings from RT qPCR experiments detailed in Figures 5.1, 5.2 and 5.3. Table indicates the findings from the screen for plasmatocyte derived expression and effective knock down of candidate genes of interest. + = expression detected/effective knock down detected. No = expression not detected / effective knock down not detected or knock down not functioning. Inconclusive denotes lines in which when knock down was driven with *Hml*, a slight reduction of expression was observed, suggesting that the candidate gene could be expressed by plasmatocytes, as well as other cell types, but this could not be re-confirmed in FACS sorted plasmatocytes and therefore a conclusion as to the plasmatocyte derived expression of these genes could not be confirmed. Not viable = flies did not emerge from crosses to *Tubulin*-Gal4 driver, thus ubiquitous knock down was lethal. Grey cells indicate lines in which knock down could be conclusively confirmed.

### 5.4 Scavenger receptor knock down effect on lipid uptake

As described in Chapter 4, plasmatocytes readily scavenge injected red fluorescent LDL within an hour (see Chapter 4, Figure 4-9). This technique was used as a tool to measure the effect of the loss of a given scavenger receptor upon plasmatocyte lipid scavenging. Changes in lipid uptake induced by scavenger receptor knock down for each of the candidate genes of interest was quantified.

In order to identify the scavenger receptors which might be involved in lipid uptake, plasmatocyte reporter flies (*Hml*Δ-Gal4,UAS-2xeGFP) were crossed to each scavenger receptor, or control gene knock down line. This generated a repertoire of flies with GFP labelled *Hml* positive plasmatocytes, with a given candidate scavenger receptor gene knocked down specifically in plasmatocytes (genotypes are as in the RT qPCR experiment in Figure 5-2). Age matched flies were collected after eclosion, and aged for 7 days before abdominal injection with red fluorescent lipids was carried out (DiI-LDL). After one hour flies were imaged for both plasmatocyte numbers (Figure 5-4 A) and changes in plasmatocyte uptake of DiI-LDL (Figure 5-4 B).

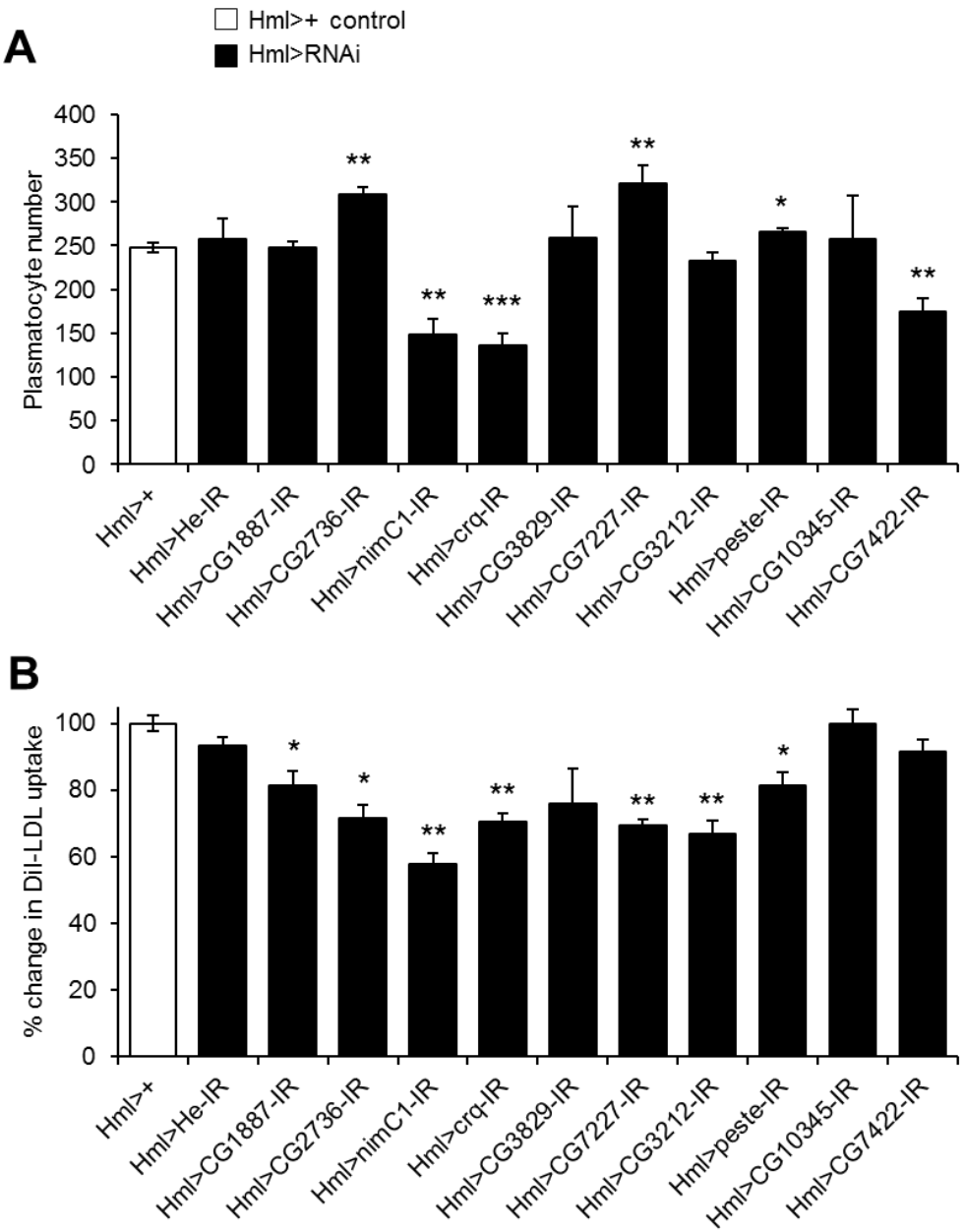


*Figure 5-4 Effect of plasmatocyte specific knock down of candidate genes upon plasmatocyte number and lipid scavenging*

*Hml*Δ-Gal4,UAS-2xeGFP flies were crossed to UAS-knock down genes (black bars). *Hml*Δ-Gal4,UAS-2xeGFP flies crossed to $w^{1118}$ wild type flies were used as driver only control (white bars). Groups of 4, age matched 7 day old flies were injected abdominally with 50nl of DiI-LDL; flies were imaged with a confocal microscope approximately 60 minutes post injection. Flies were anaesthetised with $CO_2$ and imaged laterally on their sides for the most representative image including different body sections. **A.** Total GFP *Hml* positive plasmatocyte count per fly. **B.** Percentage of the total number of plasmatocytes per genotype, which were also positive for DiI-LDL uptake. Percentage uptake was calculated from the control genotype (white bar, HmlΔ-Gal4,UAS-2xeGFP/+). Data represents the mean of n=4 flies per genotype, error bars represent standard error of the mean. Unpaired t tests determined statistical significance between control genotype flies (*Hml*>+, white bar) and each of the knock down genotypes (*Hml*>RNAi, black bars), $p<0.05$/*, $p\leq0.01$/**, $p\leq0.001$/***.

*5.4.1 Knock down consequences on plasmatocyte numbers and lipid uptake*

Encouragingly plasmatocyte specific knock down of the non-scavenger receptor gene *He* did not result in a significant change in either plasmatocyte number, or lipid scavenging. Furthermore, knock down of CG10345, which according to the screen was predicted to be non-plasmatocyte expressed, yet efficiently knocked down, did not have a significant effect on lipid uptake or plasmatocyte numbers.

Of the lines examined, 6 had a significant effect on plasmatocyte number, with *CG7227* and *CG2736* knock down resulting in an increase, and *nimC1*, *crq*, *pes* and *CG7422* resulting in a diminished plasmatocyte population. The changes in plasmatocyte number observed could be due to developmental affects induced by the knock down of the given genes. Expression of *Hml* commences at stage 17, the final stage of embryogenesis. Therefore the knock down would take effect predominantly from 1$^{st}$ instar larvae development onwards.

Plasmatocyte lipid scavenging ability was significantly affected in 7 knock down lines. Interestingly 5 of the 7 were the *CD36* related genes; *CG1887*, *CG2736*, *crq*, *CG7227* and *pes* (Herboso et al., 2011). This is interesting given findings regarding the involvement of *CD36* in lipid scavenging and high fat diet diseases induction in humans and mice (Martin et al., 2011). The remaining two knock down lines which significantly affected DiI-LDL uptake were the phagocytic receptor *nimC1* (Kurucz et al., 2007a) and the class C scavenger receptor *CG3212* (Irving et al., 2004).

*5.4.2 Exclusion of lipid uptake candidates*

Plasmatocyte specific knock down of *He*, *CG3829*, *CG10345*, *CG7422* did not have a significant effect upon plasmatocyte lipid scavenging and so were excluded as possible lipid uptake gene candidates for further experiments for this reason.

Additionally it was not possible to observe expression of *CG1887*, *CG7227* and *pes* in FACS sorted plasmatocytes, yet they did appear to have a mild effect on gene

expression in whole fly RT qPCR experiments, suggesting they may potentially be plasmatocyte expressed. However, as it could not be definitively confirmed that these genes were expressed by plasmatocytes they were not selected for further study with regard to lipid scavenging. In line with this, although expression of *CG2736* was observed by plasmatocytes, it was not possible for us to reconfirm this finding with RT qPCR on whole fly samples, using *Hml* as a driver for knock down. Finally we could not detect *CG3212* expression by plasmatocytes, or any evidence of its effective knock down, even when driving knock down ubiquitously, suggesting a problem with the RNAi functionality.

### *5.4.3 Candidate lipid uptake genes: nimC1 & crq*

While other knock down lines appeared to be interesting in terms of the effects observed upon plasmatocyte lipid scavenging, as described earlier in this chapter, either confirmation of expression by plasmatocytes, or confirmation of knock down was not conclusively determined. For this reason, the two candidate genes which were pursued were *crq* and *nimC1*. Validation of *crq* and *nimC1* expression by plasmatocytes was confirmed by RT qPCR of both FACS sorted plasmatocyte cDNA, as well as using whole fly cDNA, using *Hml* as a driver for knock down. Furthermore, knock down was also confirmed a third way using *Tubulin* to ubiquitously drive knock down.

It was noted that plasmatocyte number in *crq* and *nimC1* knock down flies was diminished, but regardless of the observed reduction in plasmatocytes, the plasmatocytes which were present had a significantly reduced capacity for lipid scavenging (Figure 5-4 A, B). Subsequent experiments were carried out to investigate the role of these plasmatocyte scavenger receptors in response to dietary lipids.

### 5.5 Effect of plasmatocyte *crq* and *nimC1* deficiency upon high fat diet exposure

The confirmed expression of *nimC1* and *crq* by plasmatocytes, in conjunction with the significant reduction of lipid uptake by *crq* and *nimC1* depleted plasmatocytes suggested a potential lipid scavenging role for these receptors.

#### *5.5.1 Survival of plasmatocyte specific nimC1 and crq knock down flies upon high fat diet*

High fat diet exposure in wild type flies causes a dose dependent reduction in lifespan as determined in this thesis, and by others (Driver and Cosopodiotis, 1979). Survival of *Hml* driven, plasmatocyte specific *nimC1* and *crq* knock down flies was examined upon control and lipid enriched diets. Plasmatocyte silencing of *nimC1* expression did not influence the lifespan of flies under a lipid rich diet. Flies fed a high fat diet still had reduced lifespans comparatively to those flies on control diets, regardless of *nimC1* expression (Figure 5-5 A, B). In contrast, plasmatocyte knock down of *crq* resulted in a rescue of fly survival under lipid rich diets, supplemented either with lard or coconut oil (Figure 5-6 A, B). In order to re-confirm this effect, a second *crq* knock down fly, in which the IR was located on a different chromosome, was examined in terms of survival under a lipid rich diet. Survival phenotypes were similar when driving knock down with either of the different *crq*-IR lines (Figure 5-7 A, B).

*NimC1* knock down using the plasmatocyte specific *Hml* driver also suppressed its expression in the whole fly (Figure 5-2 A), suggesting that *nimC1* expression is plasmatocyte restricted, as initially proposed by Kurucz et al. (2007a). However, *Hml* driven *crq* knock down was only sufficient to reduce *crq* expression levels in the whole fly by approximately 50%, when compared to levels of *crq* in the control genotype flies (Figure 5-2 B). This finding suggested that *crq* was expressed in tissues other than *Hml* positive plasmatocytes, although silencing its expression in plasmatocytes was sufficient to rescue lifespan. We therefore investigated the effects of whole fly *crq* deficiency upon survival in flies in which *crq* knock down was driven ubiquitously using *Tubulin* as a

driver. *Tubulin* driven knock down reduced *crq* expression levels by >90% (Figure 5-3 B) however, ubiquitous *crq* knock down flies exhibited an early mortality on all tested diets (Figure 5-8). Therefore expression of *crq* in other cell types appears to be important for a normal lifespan, irrespectively of the lipid content of the diet. These findings would suggest a detrimental role for plasmatocyte expressed *crq*.

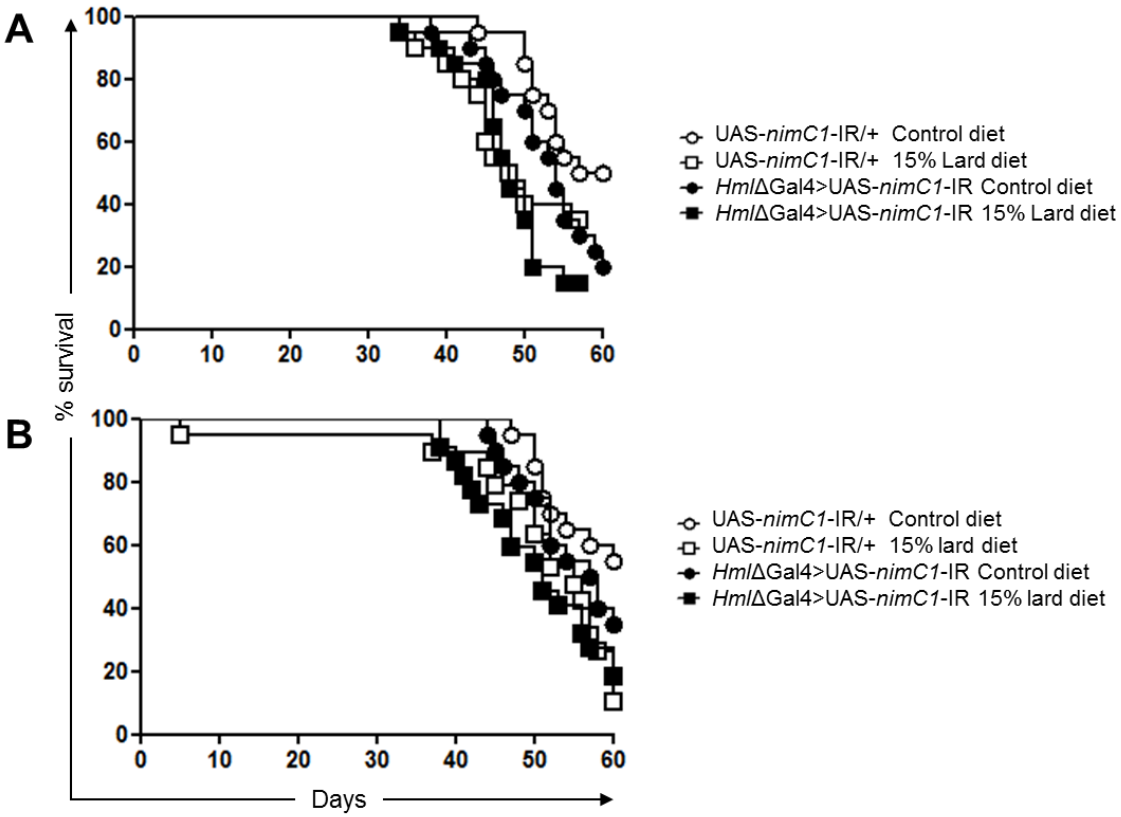


*Figure 5-5 Survival of plasmatocyte specific nimC1 knock down flies*
Age matched *nimC1* knock down flies (w;*HmlΔ*-Gal4/UAS-*nimC1*-IR, black shapes) and *nimC1* competent control flies (w;UAS-*nimC1*-IR, white shapes) were placed on the given diets and vials were checked daily for deaths, (20 flies per genotype per diet). Percentage survival over time was calculated. **A.** Survival of plasmatocyte specific *nimC1* knock down flies (black shapes) compared to *nimC1* competent control flies (white shapes) on control diet (circles, log rank $X^2$=1.831, p=0.1761, Wilcoxon $X^2$=1.947, p=0.1629, 95% CI of ratio 0.1999 to 1.343; ns), and 15% lard diet (squares, log rank $X^2$=0.00001960, p=0.9965, Wilcoxon $X^2$=0.06964, p=0.7919, 95% CI of ratio 0.4446 to 2.257; ns). **B.** Survival of plasmatocyte specific *nimC1* knock down flies (black shapes) compared to *nimC1* competent control flies (white shapes) on control diet (circles, log rank $X^2$=1.453, p=0.2281, Wilcoxon $X^2$=1.321, p=0.2505, 95% CI of ratio 0.2497 to 1.392; ns), and 15% lard diet (squares, log rank $X^2$=0.01014, p=0.9198, Wilcoxon $X^2$=0.2721, p=0.6019, 95% CI of ratio 0.4802 to 1.939; ns). Survival experiments were repeated at least 5 times with reproducible findings, these curves are representative of findings.

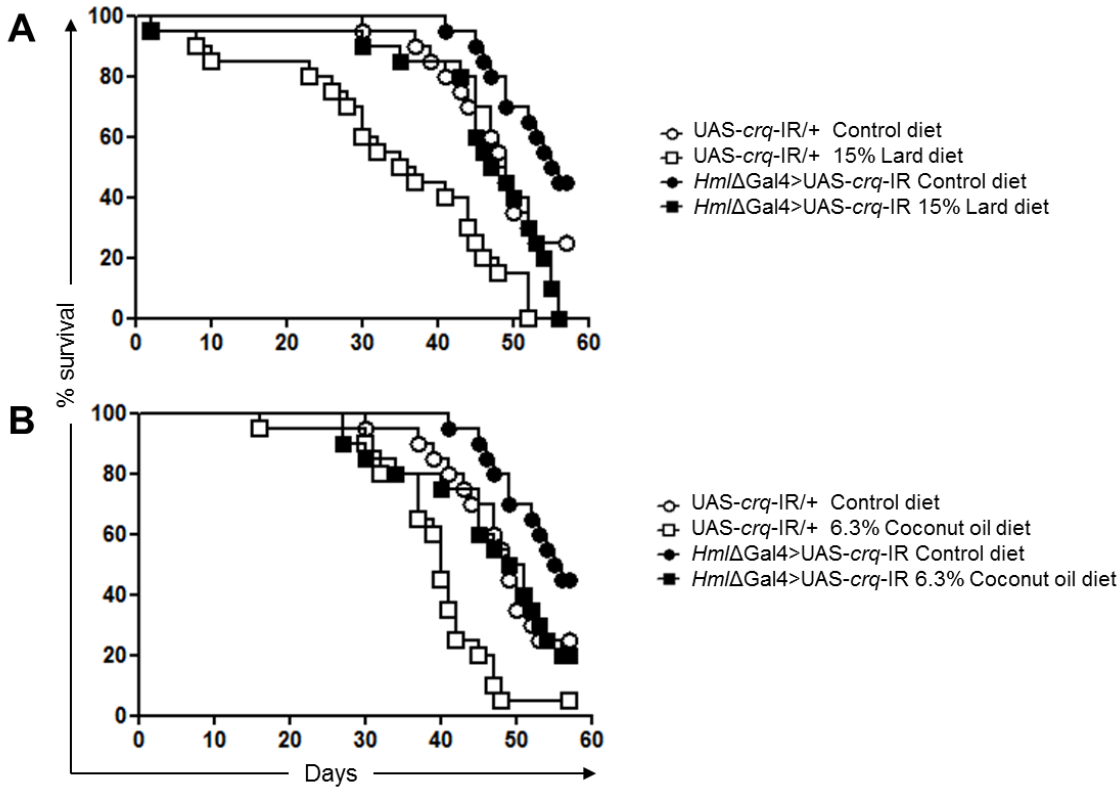


*Figure 5-6 Survival of plasmatocyte specific crq knock down flies (UAS-crq-IR on III)*
Age matched *crq* knock down flies (w;*HmlΔ*-Gal4;UAS-*crq*-IR, on the 3rd chromosome, black shapes) and *crq* competent control flies (w;;UAS-*crq*-IR, white shapes) were placed on the given diets and vials were checked daily for deaths, (20 flies per genotype per diet). Percentage survival over time was calculated. **A.** Survival of plasmatocyte specific *crq* knock down flies (black shapes) compared to *crq* competent control flies (white shapes) on control diet (circles, log rank $X^2$=3.299, p=0.0693, Wilcoxon $X^2$=4.156, p=0.0415, 95% CI of ratio 0.9427 to 4.709) and 15% Lard diet (squares, log rank $X^2$=9.841, p=0.0017, Wilcoxon $X^2$=9.298, p=0.0023, 95% CI of ratio 1.572 to 7.096) **B.** Survival of plasmatocyte specific *crq* knock down flies (black shapes) compared to *crq* competent flies (white shapes) on control diet (circles, log rank $X^2$=3.493, p=0.0616, Wilcoxon $X^2$=2.862, p=0.0907, 95% CI of ratio 0.2091 to 1.038) and 6.3% coconut oil diet (squares, log rank $X^2$=7.937, p=0.0048, Wilcoxon $X^2$=6.448, p=0.0111, 95% CI of ratio 1.396 to 6.423). Survival experiments were repeated at least 5 times with reproducible findings, these curves are representative of findings.

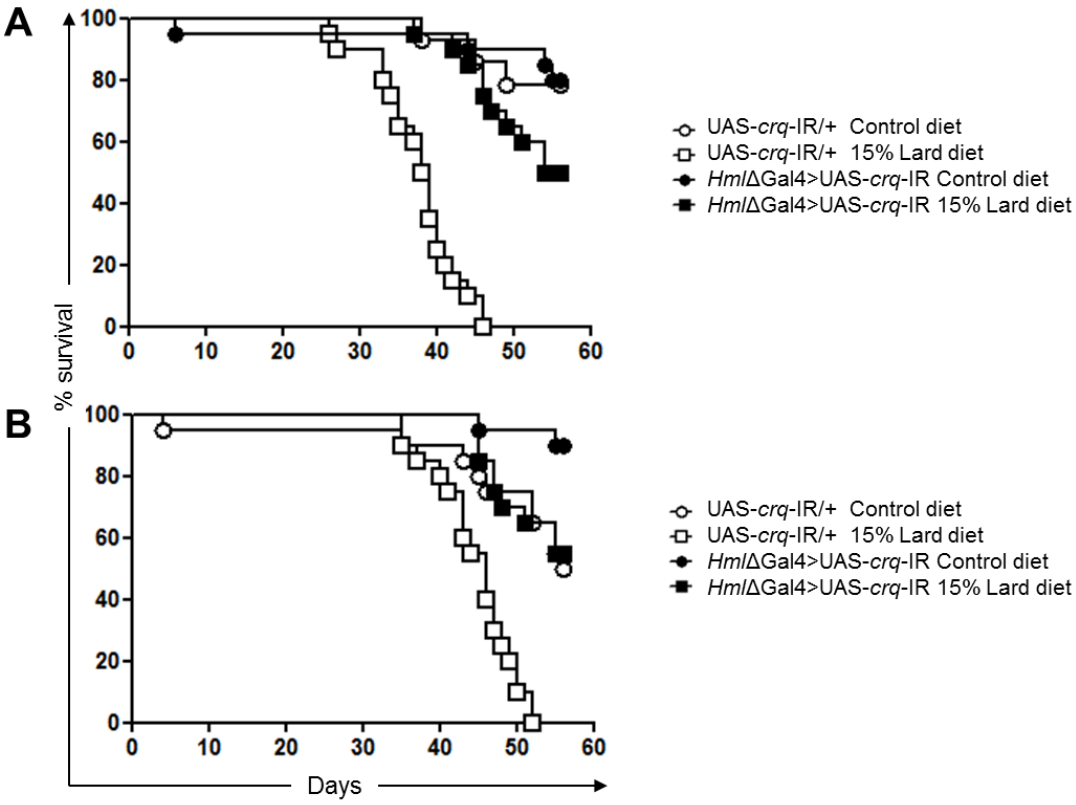


*Figure 5-7 Survival of plasmatocyte specific crq knock down flies (UAS-crq-IR on II)*
Age matched *crq* knock down flies (w;*HmlΔ*-Gal4/UAS-*crq*-IR, on the 2nd chromosome, black shapes) and *crq* competent control flies (w;UAS-*crq*-IR, white shapes) were placed on the given diets and vials were checked daily for deaths, (20 flies per genotype per diet). Percentage survival over time was calculated. **A.** Survival of plasmatocyte specific *crq* knock down flies (black shapes) compared to *crq* competent control flies (white shapes) on control diet (circles, log rank $X^2$=0.01640, p=0.8981, Wilcoxon $X^2$=0.2211, p=0.8818, 95% CI of ratio 0.2438 to 4.995; ns), and 15% lard diets (squares, log rank $X^2$=33.09, p=<0.0001, Wilcoxon $X^2$=28.21, p=<0.0001, 95% CI of ratio 5.836 to 36.14). **B.** Survival of plasmatocyte specific *crq* knock down flies (black shapes) compared to *crq* competent control flies (white shapes) on control diet (circles, log rank $X^2$=7.638, p=0.0057, Wilcoxon $X^2$=7.486, p=0.0062, 95% CI of ratio 1.607 to 16.25), and 15% lard diets (squares, log rank $X^2$=21.26, p=<0.0001, Wilcoxon $X^2$=17.21, p=<0.0001, 95% CI of ratio 3.112 to 16.67). Survival experiments were repeated at least 5 times with reproducible findings, these curves are representative of findings.

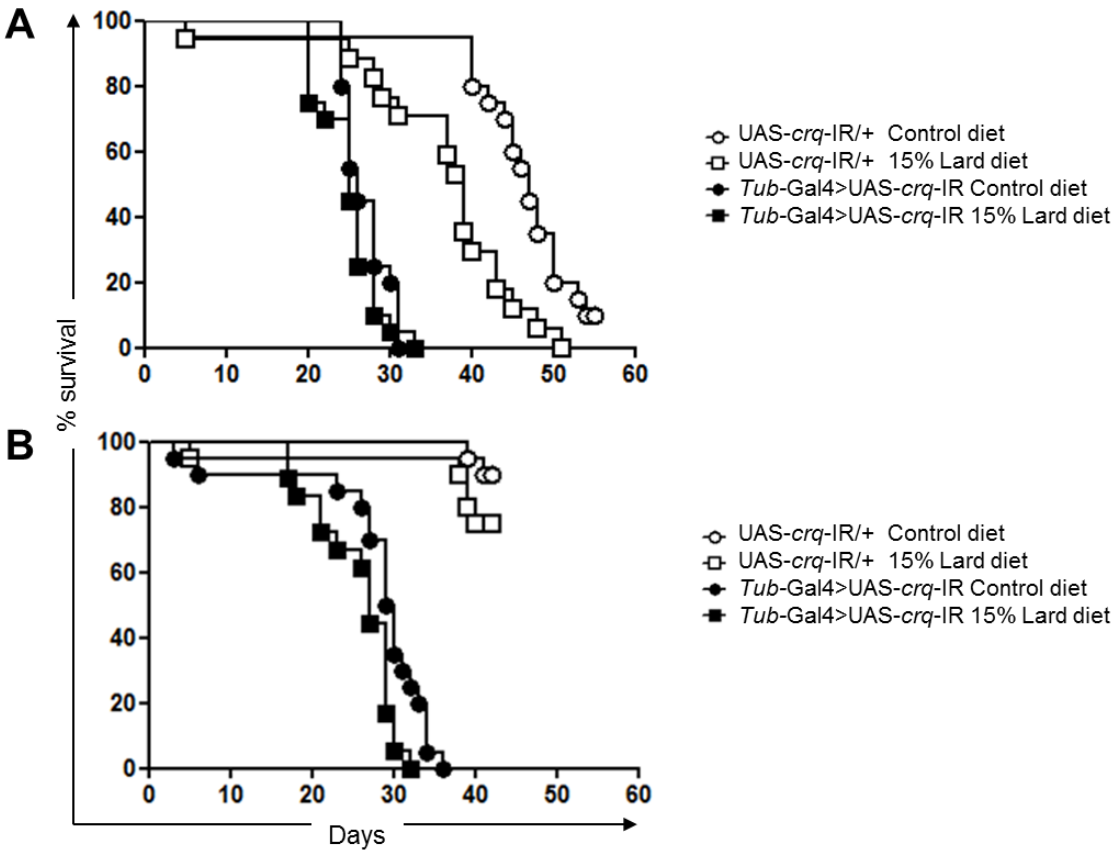


*Figure 5-8 Survival of ubiquitous crq knock down flies*
Age matched *crq* knock down flies (*Tub*-Gal4>*crq*-IR, black shapes) and *crq* competent control flies (UAS-*crq*-IR, white shapes) were placed on the given diets and vials were checked daily for deaths, (20 flies per genotype per diet). Percentage survival over time was calculated. **A.** Survival of whole fly *crq* knock down (*crq*-IR located on the 2nd chromosome) flies (black shapes) compared to *crq* competent control flies (white shapes) on control (circles, log rank $X^2$= 36.10, p=<0.0001, Wilcoxon $X^2$=28.73, p=<0.0001, 95% CI of ratio 0.02002 to 0.1371), and 15% lard diets (squares, log rank $X^2$=23.74, p=<0.0001, Wilcoxon $X^2$=17.82, p=<0.0001, 95% CI of ratio 0.04188 to 0.2586). **B.** Survival of whole fly *crq* knock down (*crq*-IR located on the 3rd chromosome) flies (black shapes) compared to *crq* competent control flies (white shapes) on control (circles, log rank $X^2$=45.01, p=<0.0001, Wilcoxon $X^2$=37.40, p=<0.0001, 95% CI of ratio 0.01265 to 0.09125), and 15% lard diets (squares, log rank $X^2$=35.44, p=<0.0001, Wilcoxon $X^2$=28.29, p=<0.0001, 95% CI of ratio 0.01673 to 0.1269). Survival experiments were repeated at least 5 times with reproducible findings, these curves are representative of findings.

*5.5.2 Metabolic effects of plasmatocyte crq silencing*

Experiments were then carried out to investigate the loss of plasmatocyte derived *crq* expression upon different metabolic readouts. Cohorts of plasmatocyte specific *crq* knock down flies (w;*Hml*Δ-Gal4,UAS-2xeGFP:UAS-crq-IR), and control flies (w;;UAS-crq-IR/+) were age matched and sampled at either days 10, 20 and 30 after 15% lard diet exposure.

*5.5.3 Triglyceride levels in crq and nimC1 deficient flies*

Whole fly triglyceride levels were examined for any changes a plasmatocyte specific *crq* deficiency may induce, and how this might relate to the increased survival observed in these flies. No significant difference was observed in whole fly triglyceride levels between *crq* knock down and control flies, as ascertained by thin layer chromatography (TLC) (Figure 5-9 A). Triglyceride levels in plasmatocyte specific *nimC1* knock down flies was also measured; results indicated that there was also no difference in triglyceride accumulation between *nimC1* knock down flies and controls (Figure 5-9 B). Given the observed rescue in fly survival upon a lipid rich diet which is observed in *crq* knock down flies, but not in *nimC1* flies, these findings would suggest that the enhanced survival phenotypes observed in *crq* knock down flies is not a direct result of differential triglyceride accumulation.

*5.5.4 Glucose regulation in plasmatocyte specific crq deficient high fat diet fed flies*

Unfortunately levels of whole fly glucose could not be ascertained in time for inclusion in this thesis, therefore a conclusion could not be reached with regard to glucose levels in plasmatocyte specific *crq* deficient flies and how this may have contributed to the enhanced survival phenotype observed in these flies. However, it was possible to investigate glucose regulation via RT qPCR for expression levels of *Pepck* and *Dilps* in these flies.

Expression of certain metabolic genes were assessed via RT qPCR in *crq* knock down flies versus control flies upon a 15% lard diet for a designated number of days. Interestingly, levels of the gluconeogenesis rate limiting enzyme, *Pepck,* were decreased in flies lacking plasmatocyte expression of *crq*, which would be suggestive of a reduction of glucose levels in these flies under a high fat diet (Figure 5-10 A). No statistically significant change in expression of *Dilps 2*, *3* and *5* was observed between flies lacking plasmatocyte derived *crq* expression and control *crq* competent flies (Figure 5-10 B). These findings are similar to the lack of change in *Dilp* expression observed between plasmatocyte-less and plasmatocyte competent flies upon a 15% lard diet.

The changes in *Pepck* expression observed in *crq* knock down flies were consistent with findings observed in plasmatocyte-less flies. The reduction of *Pepck* in *crq* deficient flies may suggest a plasmatocyte, *crq* mediated induction of dysregulated glucose metabolism in flies chronically fed a high fat diet, which is detrimental to fly survival. However further experiments to ascertain whole fly glucose levels will need to be carried out in order to further test this hypothesis.

### *5.5.5 Lipid metabolism gene regulation in plasmatocyte specific crq deficient flies*

Expression of the lipid metabolism DGAT *mdy* remained similar at each of the time points examined upon a 15% lard diet, regardless of the lack of plasmatocyte derived *crq* expression (Figure 5-10 C). This finding is consistent with the lack of significant difference in triglyceride accumulation observed between *crq* competent and *crq* knock down flies (Figure 5-9). Expression of *ACC* appeared to be up regulated in *crq* knock down flies after 20 days upon a 15% lard diet, however this up regulation was lost again by day 30 (Figure 5-10 D).

*5.5.6 JAK-STAT pathway gene expression in plasmatocyte specific crq deficient flies*

Due to the rise in expression of JAK-STAT pathway cytokine *upd3* observed in wild type flies under chronic high fat diet exposure and the loss of this expression in plasmatocyte-less flies, expression of JAK-STAT pathway members were assessed in plasmatocyte specific *crq* deficient flies versus control flies. Most interestingly, expression of the cytokine *upd3* and the levels of downstream JAK-STAT pathway target *Socs36E* were both decreased in flies lacking plasmatocyte derived *crq* expression after 20 days upon a 15% lard diet (Figure 5-11 B, C). In addition levels of the *upd2* expression appeared to be reduced in plasmatocyte specific *crq* knock down flies upon high fat diet compared to control, although this decrease was not statistically significant (Figure 5-11 A). The concurrent reduction of *upd3* and *Socs36E* expression would suggest that expression of JAK-STAT pathway family members and target genes are regulated in some way by plasmatocyte expressed *crq*.

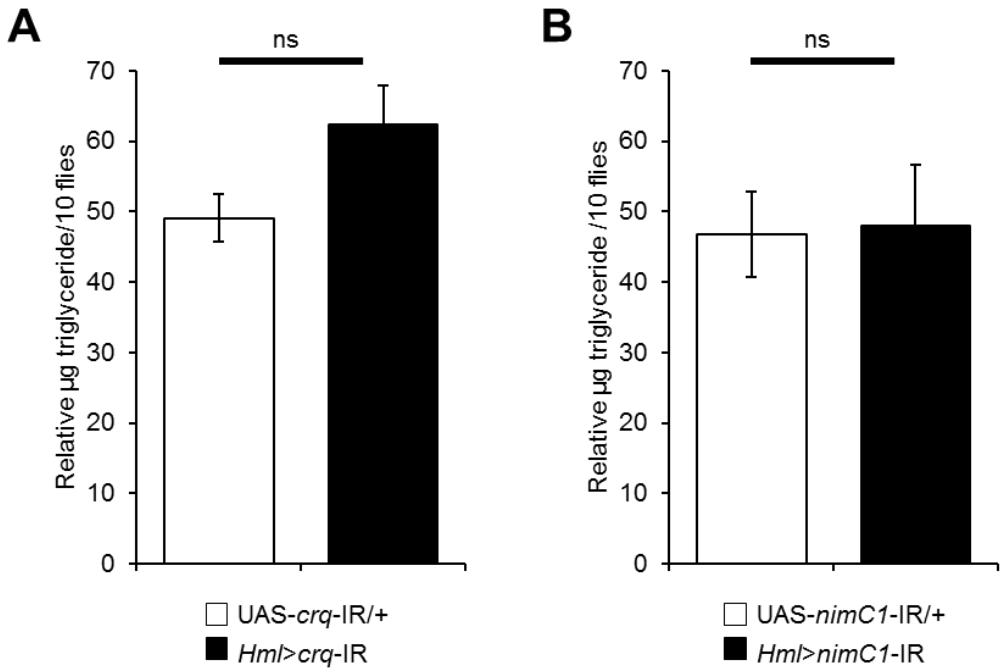


*Figure 5-9 Triglyceride levels in plasmatocyte specific crq and nimC1 deficient flies*
**A.** Age matched *crq* deficient flies (w;HmlΔGal4,UAS-2xeGFP;UAS-*crq*-IR, black bar) and control flies (w;;UAS-*crq*-IR/+, white bar) and **B.** *nimC1* deficient flies (w;*Hml*ΔGal4,UAS-2xeGFP;UAS-*nimC1*-IR, black bar) and control flies (w;;UAS-*nimC1*-IR/+, white bar) were placed on a 15% lard diet for 20 days before being sampled for thin layer chromatography (TLC) analysis of whole fly triglyceride levels. Samples include groups of 10 flies in quadruplicate per genotype, *crq*/*nimC1* deficient (black bars) and control flies (white bars). Data represents the mean of n=4 samples, error bars represent standard error of the mean. (A. unpaired t test p=0.088369, ns, B. unpaired t test p=0.70217, ns).

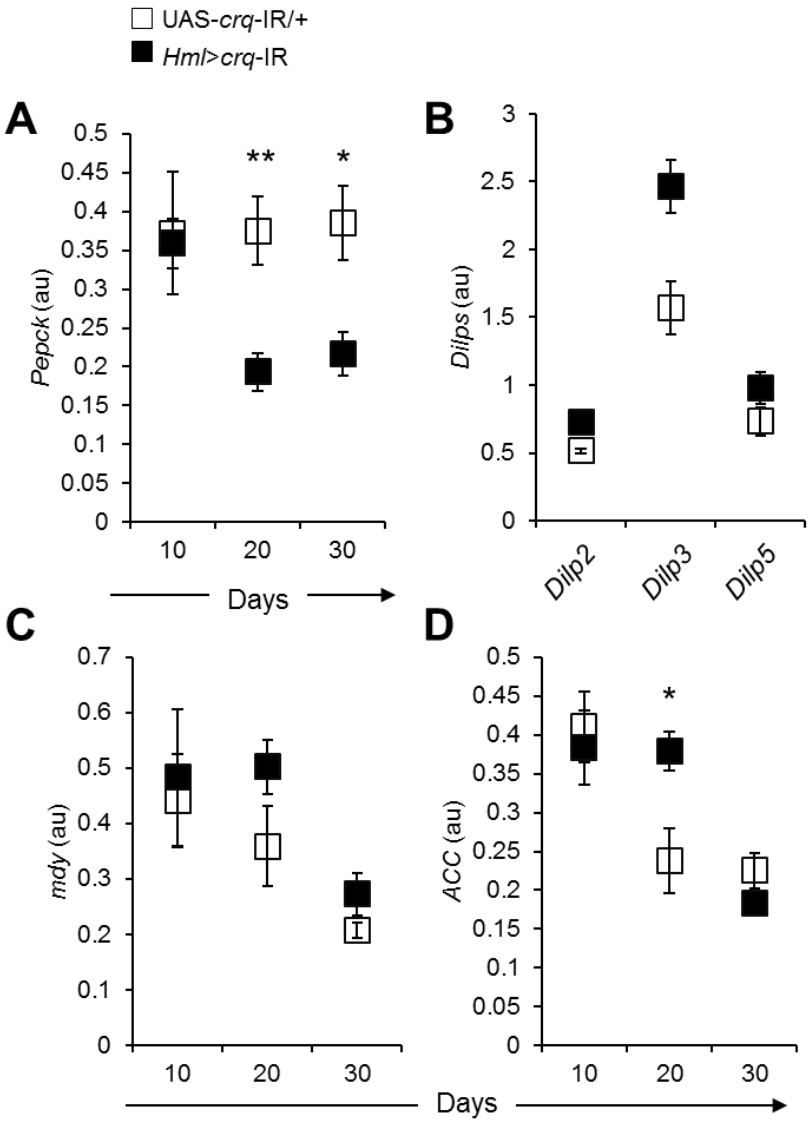


*Figure 5-10 Transcript levels of metabolic genes in crq deficient flies*
RT qPCR with plasmatocyte specific *crq* knock down fly samples (w;*Hml*ΔGal4,UAS-2xeGFP;UAS-*crq*-IR, black squares), and control samples (w;;UAS-*crq*-IR/+, white squares). Age matched flies were placed on a 15% lard diet, and samples were prepared at 10, 20, or 30 days upon high fat diet. All RT qPCR data is normalised to the housekeeping gene *Rpl1*, (au = arbitrary units). **A.** Normalised *Pepck* transcript levels at days 10, 20 and 30 upon a 15% lard diet, unpaired t tests, 20 days (p=0.00689/**), 30 days (p=0.01628/*). **B.** Normalised transcript levels of *Dilp2*, *3* and *5* at 30 days upon 15% lard diet. No significant change in *Dilp* transcript levels was observed (unpaired t test). **C.** Normalised *mdy* transcript levels at days 10, 20 and 30 upon a 15% lard diet **D.** Normalised *ACC* transcript levels at days 10, 20 and 30 upon a 15% lard diet, unpaired t test day 20 p=0.01933/*. Unpaired t tests, * $p<0.05$, ** $p\leq0.01$, lack of stars indicates data was not statistically significant. Error bars represent the standard error of the mean, data is representative of n=5 samples (3 flies per sample) per time point, per genotype.

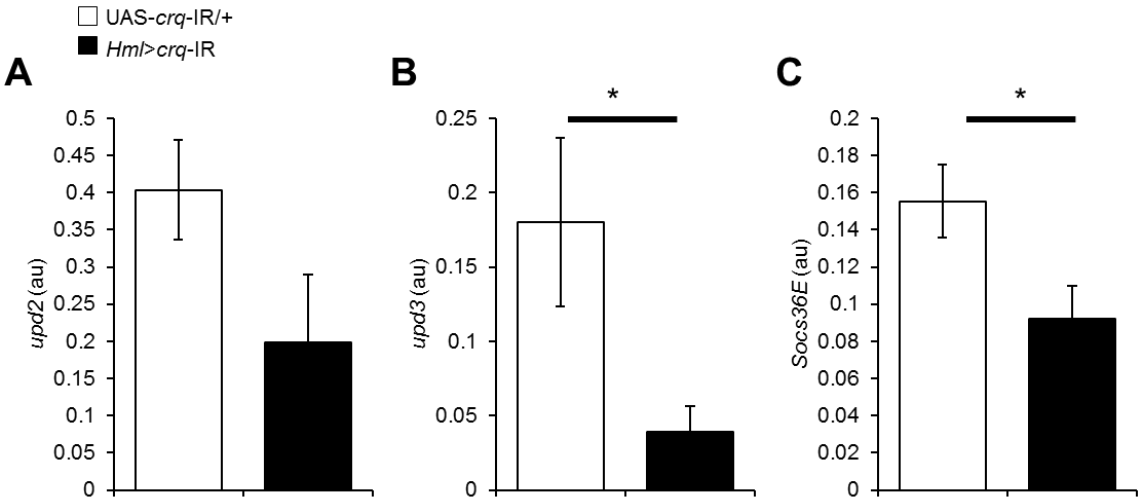


*Figure 5-11 Transcript levels of JAK-STAT pathway genes in plasmatocyte specific crq deficient flies*

RT qPCR with plasmatocyte specific *crq* knock down fly samples (w;*Hml*ΔGal4,UAS-2xeGFP;UAS-*crq*-IR, black bars), and control fly samples (w;;UAS-*crq*-IR/+, white bars). Age matched flies were placed on a 15% lard diet, and cDNA samples were generated at 20 days upon 15% lard diet. All RT qPCR data is normalised to the housekeeping gene *Rpl1*, (au = arbitrary units). Normalised transcript levels of **A.** *upd2*, **B.** *upd3* and **C.** *Socs36E*. (Unpaired t tests; *upd2* p=0.108, ns *upd3* p=0.04473/*, *Socs36E* p=0.04444/*). Unpaired t test, * $p<0.05$, a lack of stars indicates data was not statistically significant. Error bars represent the standard error of the mean, data is representative of n=5 samples (3 flies per sample) per time point, per genotype.

## 5.6 Chapter 5 overview and discussion

The screen for plasmatocyte expressed scavenger receptors identified *nimC1* as plasmatocyte specific (Kurucz et al., 2007b), and *crq* as plasmatocyte expressed (Franc et al., 1996) but not specific. Knock down of these genes using RNA interference was successful, and plasmatocyte lipid uptake ability in flies lacking *nimC1* and *crq* expression by plasmatocytes was significantly impaired.

### *5.6.1 Role of crq in response to lipid rich diet*

Further investigation into the roles of *nimC1* and *crq* in response to dietary lipids illuminated the fact that *crq*, but not *nimC1*, expression by plasmatocytes was detrimental to fly survival. In addition to this, a lack of plasmatocyte derived *crq* expression also resulted in a reduction of both *upd3* and *Pepck* levels, these findings were similar to what was observed in plasmatocyte-less flies after chronic high fat diet exposure. The reduction in *Pepck* levels may be suggestive of a plasmatocyte role in maintaining glucose homeostasis, however further work is required to confirm if this is the case. These data advocate that plasmatocyte derived *crq* expression may promote the onset of a metabolic-like syndrome in chronically high fat diet fed flies. Furthermore, the rescue of these high fat diet induced phenotypes did not appear to be a direct result of a reduction of lipid scavenging, as *nimC1* deficient flies also exhibited the same reduced lipid scavenging capacity, yet their survival under a lipid rich diet was not rescued. In line with this finding, *Hml* driven *crq* knock down flies contained similar levels of whole fly triglycerides as *crq* competent control flies. These data may suggest that the metabolic-like syndrome and early death of the fly could be caused by a remote signal produced by plasmatocytes, downstream of *crq*, in a cell specific manner.

### *5.6.2 CD36 and croquemort*

Mammalian *CD36* is expressed by macrophages and is reported to play a role in lipid scavenging. A number of studies have reported a *CD36* involvement in the development of various high fat diet induced diseases including atherosclerosis, type II diabetes and metabolic syndrome (Martin et al., 2011, Aitman et al., 1999, Kennedy et al., 2011).

Some 14 *CD36* family members have been identified in the fly (Herboso et al., 2011), one of these is membrane glycoprotein CRQ. CRQ has 23% homology at amino acid level with human and murine CD36 and contains a 13 amino acid motif present in all CD36 family members. Initial studies identified *crq* to be a hemocyte receptor, responsible for engulfment of apoptotic cell corpses during development (Franc et al., 1996, Franc et al., 1999). It has also been demonstrated by Stuart et al. (2005) that *crq* is responsible for phagocytosis of the gram positive bacteria *Staphylococcus*. *aureus* (*S. aureus*) but not of gram negative *E. coli* in the hemocyte S2 cell line.

The role that the fly *CD36*-like receptor, *crq*, appears to play in response to chronic dietary lipid exposure is extremely interesting, particularly when considering the strong link which exists between mammalian *CD36* and high fat diet induced diseases. The *crq* role in progression of high fat diet induced disease identified here may represent a conserved function of *CD36* throughout the species.

### *5.6.3 Examination of glucose levels in crq deficient flies*

As described previously, levels of whole fly glucose could not be ascertained in time for inclusion in this thesis. This experiment would need to be carried out in order to further confirm the potential role *crq* may play in glucose homeostasis in the whole fly after chronic high fat diet exposure.

### *5.6.4 Inducible (Gal80$^{ts}$) knock down of crq*

Experiments in this chapter were carried out using flies in which plasmatocyte expression of *crq* and *nimC1* was constitutively knocked down using *Hml*Δ-Gal4 as a driver. Future experiments could examine the inducible loss of *crq* and *nimC1* expression in adult flies using temperature sensitive Gal80 flies. This would allow for the ruling out of potential effects which could be caused by a loss of *crq* or *nimC1* expression during development. Although the loss of *crq* did appear to result in a reduction of plasmatocyte numbers, the same was true for *nimC1* and survival of *nimC1* flies was not rescued upon lipid rich diet, suggesting that the enhanced survival of *crq* knock down flies was not due to the reduction in plasmatocyte number. Nonetheless, this experiment would further clarify both the beneficial effect of *crq* knock down upon survival and metabolism, and the lack of an effect observed upon survival in *nimC1* knock down upon lipid rich diets.

### *5.6.5 FACS sorting and Oil Red O staining of crq knock down plasmatocytes*

FACS sorting of plasmatocytes from high fat diet fed, plasmatocyte specific *crq* knock down flies would be an interesting experiment to confirm the lipid scavenging capacity of *crq* knock down plasmatocytes. This experiment was attempted on several occasions but unfortunately due to low cell numbers it was not possible to fix and stain enough cells for imaging, therefore quantification of Oil Red O fluorescence and intracellular plasmatocyte lipid could not be carried out. This was due to the reduced number of plasmatocytes found in *crq* knock down flies, as well as restrictions during the FACS sorting experiment. It was not possible to sort more than 80-90 flies at once. Furthermore, in order to achieve the cell numbers necessary for Oil Red O staining, the sorting time would be significantly more than 3 hours, making analysis of these cells unreliable. Use of temperature sensitive, inducible *crq* knock down flies may provide a solution to this issue if plasmatocyte numbers are rescued in these flies, which is yet to be determined.

*5.6.6 Investigation into upd2 and upd3 expression in nimC1 knock down flies*

Further investigation as to whether the expression of JAK-STAT pathway family members; *upd2*, *upd3* and *Socs36E* are mediated by a *crq* specific signalling cascade could be performed using *nimC1* knock down flies. Unlike *crq*, plasmatocyte specific knock down of *nimC1* was not sufficient to rescue survival of flies upon a lipid rich diet. However, plasmatocyte specific *crq* and *nimC1* knock down flies exhibited similar reductions in DiI-LDL uptake. Furthermore, both *nimC1* and *crq* knock down flies showed no increase in whole fly triglyceride accumulation when compared with their counterpart control flies upon 15% lard diets. These findings suggest that it was not the effect of the fat itself, but the plasmatocyte and *crq* mediated response to lipids which was detrimental to fly survival. Expression of *upd2*, *upd3* and *Socs36E* in high fat diet fed *nimC1* knock down flies could be investigated to further elucidate the specific role *crq* may play in high fat diet induced pathology.

*5.6.7 Downstream events of CD36 lipid scavenging*

Various downstream signalling pathways have been linked to *CD36*, however due to the broad number of tissues that express *CD36*, coincided with the wide-ranging number of ligands it can bind; determining *CD36* functionality in different tissue types has been difficult in mouse and human models. Most interestingly in humans, macrophage expressed *CD36* has been shown to be responsible for the induction of *IL-6* expression upon lipid scavenging (Janabi et al., 2000). This finding is particularly striking, as data in this thesis illustrates that chronic high fat diet exposure results in a rise in the *IL-6*-like cytokine *upd3* and that a loss of plasmatocytes or loss of expression of the *CD36*-like scavenger receptor, *crq*, specifically in plasmatocytes results in a reduction of *upd3*. These data suggest that *upd3* expression may be regulated in some way by a *crq* lipid binding or sensing and this mechanism could be conserved across the species. The final

results chapter in this thesis examines the specific role of *upd3* expression by plasmatocytes after chronic high fat diet exposure.

# Chapter 6 The JAK-STAT pathway and diet

## 6.1 The production of *upd3* in response to chronic dietary lipid exposure

Findings in previous chapters have illustrated that chronic high fat diet exposure significantly reduced *Drosophila* lifespan, and plasmatocytes adopted a lipid laden, foam cell-like morphology. Interestingly, deletion of plasmatocytes resulted in a rescue of survival upon a lipid rich diet. Furthermore, plasmatocyte specific knock down of *crq*, a *CD36*-like scavenger receptor (Franc et al., 1996), was also sufficient to rescue fly survival upon a lipid rich diet, therefore plasmatocyte derived *crq* expression appeared to be detrimental to fly survival upon a high fat diet. However, whole fly triglyceride levels in *crq* and *nimC1* knock down flies remained similar to their counterpart control genotype flies upon 15% lard diet, suggesting that the enhanced survival of plasmatocyte specific *crq* knock down flies was not due to a difference in whole fly triglyceride accumulation. Furthermore, the *crq* mediated rescue of survival did not appear to be a consequence of a reduced lipid presence within plasmatocytes, as plasmatocyte specific *nimC1* knock down flies displayed a similar reduction in DiI-LDL lipid scavenging capabilities, and yet were not longer lived on a lipid rich diet. Together these data advocate that the metabolic-like syndrome and early death of flies upon a high fat diet may be the result of a plasmatocyte derived signal, downstream of *crq*, rather than due to plasmatocyte lipid storage.

### *6.1.1 Upd cytokines as plasmatocyte derived signals downstream of crq*

The *Drosophila IL-6*-like cytokines *upd2* and *upd3* represent good potential target genes which could be activated or regulated downstream of *crq* lipid uptake, or sensing. This is because expression of *upd2*/*upd3* was induced in wild type flies in response to chronic lipid rich diet exposure. In addition expression of *upd3* was decreased by either plasmatocyte depletion or plasmatocyte specific knock down of *crq.* Plasmatocyte derived expression of *upd3* has been shown to be inducible during infection (Agaisse et al., 2003), and *upd2* has been shown to bind GABAergic neurones and block their inhibitory action though induction of JAK-STAT signalling, ultimately resulting in *Dilp*

production by insulin producing cells (Rajan and Perrimon, 2012). The observed rise in expression of *upd2* and *upd3* in wild type flies chronically fed a high fat diet alongside the previous evidence advocating immune and metabolic roles for the *upds*, poses a possibility for an *upd* related role in the metabolic phenotypes observed in chronically high fat diet fed flies e.g. hyperglycaemia and early death. Therefore, we reasoned that chronic production of *upd3* by plasmatocytes and the consequent regulation of JAK-STAT pathway target genes could play a role in the progression of fly high fat diet induced disease pathophysiology.

### *6.1.2 Hypothesis and aims*

Hypothesis:

Lipid rich diet induced expression of *upd3* by plasmatocytes and the resulting JAK-STAT pathway activation, acts to promote the development of the deleterious phenotypes and subsequent early death observed in high fat diet fed flies.

Aims:

1. To examine the effect of plasmatocyte specific knock down of *upd3* on fly survival.
2. To investigate the consequence of plasmatocyte specific *upd3* knock down on whole fly glucose and triglyceride levels.
3. To examine the effects of plasmatocyte specific knock down of *upd3* on metabolic and inflammatory gene transcript levels in the whole fly.

## 6.2 Survival of plasmatocyte specific *upd3* depleted flies

### *6.2.1 Constitutive plasmatocyte specific knock down of upd3 (Gal4)*

The first question to be addressed was the role of *upd3* and more importantly the role of plasmatocyte produced *upd3* on fly survival under a lipid rich diet. Therefore, plasmatocyte specific *upd3* knock down flies were generated, in which *upd3*-IR was driven by *Hml* and lifespan assays were carried out. Interestingly, similar to survival phenotypes observed in plasmatocyte specific *crq* knock down experiments, flies lacking plasmatocyte derived *upd3* appeared to live significantly longer under a 15% lard diet than control *upd3* competent flies (Figure 6-1 A). This would suggest that plasmatocyte expression of *upd3* may be detrimental to fly survival, and could be involved in promoting pathology in high fat diet fed flies.

### *6.2.2 Inducible plasmatocyte specific knock down of upd3 (Gal80$^{ts}$)*

Survival assays were additionally carried out using temperature sensitive Gal80 flies, allowing for inducible plasmatocyte specific knock down of *upd3* (Figure 6-1 B). This approach allowed for temporally controlled knock down of *upd3* specifically in adult flies. An advantage of this system is that *upd3* can be knocked down once fly embryonic and larval development is over, specifically in adult flies. This allows for exclusion of possible developmental effects which could be induced by a lack of *upd3* in *Drosophila* embryos and larvae.

In these experiments *upd3*-IR expression is controlled by both the temperature sensitive driver, *Tubulin*-Gal80 (*Tub*-Gal80) and the plasmatocyte specific driver *Hml*-Gal4 (*Hml*-Gal4;*Tub*-Gal80$^{ts}$) (McGuire et al., 2004). In w;*Hml*Δ-Gal4/UAS-*upd3*-IR;*Tub*-Gal80$^{ts}$/+ flies the *Tub*-Gal80$^{ts}$ promoter represses Gal4 activity at temperatures lower than 29°C. Upon fly transfer to 29°C, Gal80$^{ts}$ repression is lost, and plasmatocytes express the *upd3* RNAi, therefore survival experiments for these flies were carried out at 29°C to ensure the lack of *upd3* expression was maintained in plasmatocytes. Findings in

the inducible *upd3* knock down survival experiments were reproducible to that of the constitutive, *Hml*-Gal4 driven knock down of *upd3* (Figure 6-1 A), fly lifespan was enhanced in plasmatocyte specific *upd3* knock down flies.

The similarities between survival phenotypes of *crq* and *upd3* plasmatocyte knock down flies could be suggestive of a potential *crq* and *upd3* mediated signalling cascade, elicited upon chronic lipid rich diet exposure. Further experiments in this chapter were carried out in order to further decipher whether this was the case.

### *6.2.3 Effect of loss of upd3 on plasmatocyte number in adult flies*

Plasmatocyte deletion in adult *Drosophila* resulted in an expansion of fly lifespan upon a lipid rich diet (Figure 6-1). It is well known that the JAK-STAT pathway is involved in regulating *Drosophila* haematopoiesis (Jung et al., 2005). It was therefore possible that the increased survival of *upd3* knock down flies may be a result of a lack of plasmatocytes in adult flies, caused by a lack of *upd3*. In order to investigate this, plasmatocyte reporter flies which also lacked *upd3* (w;*Hml*Δ-Gal4,UAS-2xeGFP/UAS-*upd3*-IR) were imaged at day 65 of adult fly life alongside age matched driver only control flies (w;*Hml*Δ-Gal4,UAS-2xeGFP/+). The late time point of day 65 was selected in order to control for an early loss of plasmatocytes in adult flies which could also have been induced by a lack of *upd3*. Quantification of plasmatocyte numbers in *upd3* knock down and control flies indicated no significant difference in plasmatocyte numbers (Figure 6-2). Survival experiments were also carried out using driver only flies (w;*Hml*Δ-Gal4,UAS-2xeGFP/+) comparatively to plasmatocyte specific *upd3* knock down flies (w;*Hml*Δ-Gal4,UAS-2xeGFP/UAS-*upd3*-IR), findings were consistent with survival data shown in Figure 6-1 (survival data not shown).

The similar plasmatocyte number observed in these *upd3* knock down flies would suggest that it is not the lack of plasmatocytes which results in the enhanced survival of

*upd3* knock down flies. This finding therefore supports the possibility that *upd3* production by plasmatocytes could be a signal which may be partially responsible for promotion of high fat diet induced disease pathophysiology.

Experiments were next carried out to examine the effects of plasmatocyte specific loss of *upd3* upon metabolism and upon the expression of other JAK-STAT signalling pathway components.

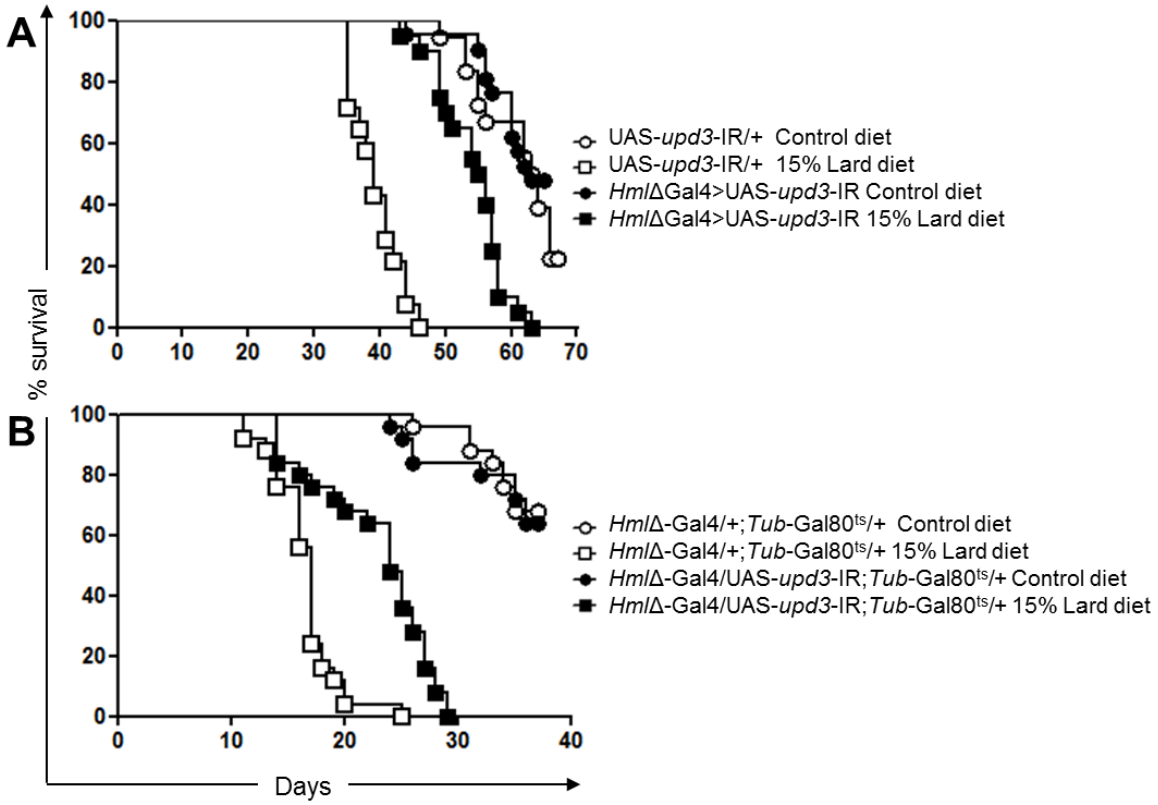


*Figure 6-1 Survival of plasmatocyte specific upd3 knock down flies*
**A.** Age matched plasmatocyte specific *upd3* knock down flies (w;*HmlΔ*-Gal4/UAS-*upd3*-IR, black shapes) and *upd3* competent control flies (w;UAS-upd3-IR/+, white shapes). Flies were placed on the given diets at and vials were checked daily for deaths, (20 flies per genotype per diet, experiment carried out at 25°C). Survival of plasmatocyte specific *upd3* knock down flies (black shapes) compared to *upd3* competent control flies (white shapes) on control diet (circles, log rank $X^2$=3.868, p=0.0592, Wilcoxon $X^2$=2.782, p=0.0953, 95% CI of ratio 0.1326 to 0.9966), and 15% lard diet (squares, log rank $X^2$=28.81, p=<0.0001, Wilcoxon $X^2$=24.03, p=<0.0001, 95% CI of ratio 0.4573 to 26.28). **B.** Age matched, inducible, plasmatocyte specific *upd3* knock down flies (w;*Hml*Δ-Gal4/UAS-*upd3*-IR;*Tubulin*-Gal80$^{ts}$/+, black shapes) and control flies (w;*Hml*Δ-Gal4/+;*Tubulin*-Gal80$^{ts}$/+, white shapes) were developed at 18°C to prevent Gal4 related transgene expression via Gal80$^{ts}$. Adult flies were then placed on the given diets and vials were checked daily for deaths, (20 flies per genotype per diet, experiment carried out at 29°C). Inducible *upd3* knock down flies (black shapes) compared to *upd3* competent control flies (white shapes) on control diet (circles, log rank $X^2$=0.09376, p=0.7930, Wilcoxon $X^2$=0.1110, p=0.7390, 95% CI of ratio 0.3263 to 2.264) and 15% lard diet (squares, log rank $X^2$=21.18, p=<0.0001, Wilcoxon $X^2$=15.11, p=<0.0001, 95% CI of ratio 2.795 to 12.84). Survival experiments were repeated at least 5 times with reproducible findings, these curves are representative of findings.

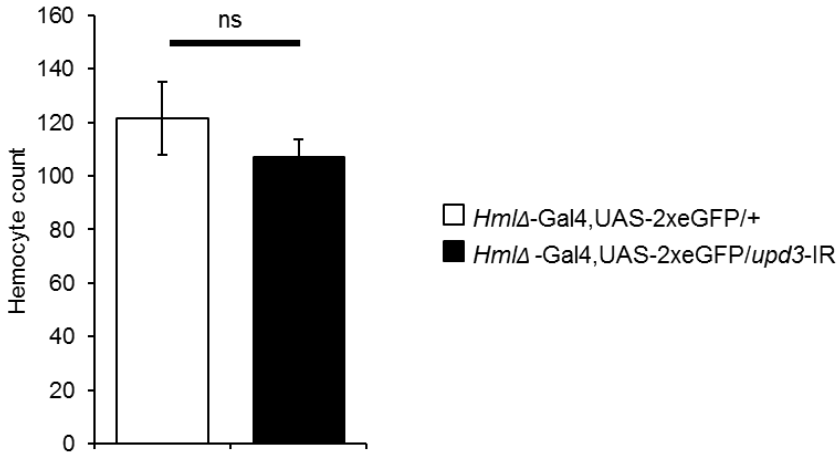


*Figure 6-2 Plasmatocyte numbers in aged Hml driven upd3 knock down flies*
Confocal microscopy imaging was carried out on plasmatocyte specific *upd3* knock down flies (w;*Hml*Δ-Gal4-UAS-2xeGFP/UAS-*upd3*-IR, black bar) and control flies (w;*Hml*Δ-Gal4-UAS-2xeGFP, white bar) at day 65 of adult *Drosophila* life. GFP positive cell numbers were quantified using Imaris spot detection software. Data represents the mean of n=4 flies per genotype, error bars represent standard error of the mean. Unpaired t test p=0.31329, ns.

## 6.3 Metabolic effects of plasmatocyte *upd3* silencing

Experiments were carried out to investigate the effects induced by a loss of *upd3* expression by plasmatocytes, specifically on fly metabolism and JAK-STAT pathway regulation. Cohorts of plasmatocyte specific *upd3* knock down flies (w;*Hml*Δ-Gal4,UAS-2xeGFP/UAS-*upd3*-IR) and controls (w;UAS-*upd3*-IR/+) were age matched and sampled after a differing number of days upon a 15% lard diet. Whole fly glucose and triglyceride levels were measured, along with investigation into the transcript levels of various metabolic and JAK-STAT pathway genes of interest via RT qPCR.

### *6.3.1 Triglyceride and glucose levels in plasmatocyte specific upd3 deficient flies*

Plasmatocyte specific *upd3* knock down flies, alongside control flies were sampled after 20 days upon a 15% lard high fat diet. Lack of plasmatocyte *upd3* expression did not affect the triglyceride accumulation in high fat diet fed flies, as determined by thin layer chromatography (TLC). This result is consistent with the similar levels of triglyceride observed in plasmatocyte-less and *crq* knock down flies compared to their relevant controls (Figure 6-3 A). This finding would indicate it is not a reduction of fat accumulation which results in the expansion of survival observed in plasmatocyte specific *upd3* deficient flies.

Levels of whole fly glucose and trehalose (see Chapter 2 section 2.10.2 for further details of this protocol) were also examined in flies fed a high fat diet for 30 days in plasmatocyte specific *upd3* knock down flies, alongside control flies. Interestingly much like the phenotypes observed in plasmatocyte-less flies, normal glucose homeostasis was restored in high fat diet fed, plasmatocyte specific *upd3* knock down flies, comparatively to control *upd3* competent flies. It appeared that the induction of hyperglycaemia observed in control genotype flies could be prevented specifically by a lack of plasmatocyte derived *upd3* expression (Figure 6-3 B). This finding is suggestive of an *upd3* involvement in the onset of hyperglycaemia in high fat diet fed flies, and could

potentially advocate *upd3* as a signal, involved in the subsequent metabolic dysregulation observed in flies chronically fed a lipid rich diet.

### *6.3.2 Metabolic gene regulation in upd3 deficient high fat diet fed flies*

Expression of metabolic genes including the *Dilps*, and *Pepck*, the rate limiting enzyme of gluconeogenesis, were investigated in a cohort of age matched plasmatocyte specific *upd3* depleted flies and control *upd3* competent flies. Flies were fed a 15% lard diet for 20 days before they were sampled for analysis of gene expression via RT qPCR. Similar to the findings in plasmatocyte less and plasmatocyte specific *crq* depleted flies, plasmatocyte specific knock down of *upd3* resulted in a reduction of *Pepck* (Figure 6-4 A), consistent with the reduction of glucose observed in these flies. This would suggest a better control of glucose homeostasis in plasmatocyte specific *upd3* knock down flies, again potentially highlighting *upd3* itself as a regulator of glucose homeostasis in *Drosophila* after chronic high fat diet exposure.

Expression levels of *Dilp2*, *Dilp3* and *Dilp5* were also examined and a general trend for a rise in *Dilps* was observed in plasmatocyte specific *upd3* knock down flies comparatively to controls, however the increase in expression was only statistically significant for *Dilp5* (Figure 6-4 B). However, regardless of the lack of a clear regulation of *Dilp* levels, the restored glucose homeostasis phenotype and the reduction of *Pepck* transcript levels observed in high fat diet fed plasmatocyte specific *upd3* knock down flies may suggest that these flies are better equipped to maintain glucose homeostasis. In addition, these data would further point towards the lack of plasmatocyte derived *upd3* expression being in some way, metabolically protective in high fat diet fed flies.

The lipid metabolism enzyme genes; *mdy* a DGAT and *ACC* a fatty acid synthase were also examined at 20 days post high fat diet exposure, in plasmatocyte specific *upd3* knock down flies alongside controls. No statistically significantly alteration in *mdy* or *ACC* transcript levels was observed in these flies (Figure 6-4 C, D), which is consistent

with the similar levels of triglyceride observed in *upd3* knock down and control flies (Figure 6-3 A).

### *6.3.3 JAK-STAT pathway regulation in upd3 depleted high fat diet fed flies*

Expression of JAK-STAT pathway activating ligands *upd2* and *upd3* were examined, as well as JAK-STAT pathway target gene *Socs36E*. Interestingly in plasmatocyte specific *upd3* knock down flies, expression of *upd3* was statistically significantly reduced (Figure 6-5 A), suggesting that plasmatocytes are the major cell producing *upd3* after chronic high fat diet exposure. Lack of plasmatocyte derived *upd3* expression also resulted in a decrease in the levels of *upd2* and *Socs36E*, while this reduction was not statistically significant, it may still indicate a decrease of JAK-STAT pathway activation in *upd3* plasmatocyte specific knock down flies (Figure 6-5 B, C). However, expression of further JAK-STAT pathway target genes would need to be examined in order to determine whether this is really the case.

The concurrent increase in levels of *upd2*, *upd3* and *Socs36E* in wild type flies fed a lipid rich diet may suggest that the high fat diet induced rise in *upd3* expression could result in chronic JAK-STAT pathway activation in various different target tissues in the fly. This could result in metabolic dysregulation, for example by affecting glucose homeostasis, which could act to promote high fat diet induced pathophysiology and ultimately fly death.

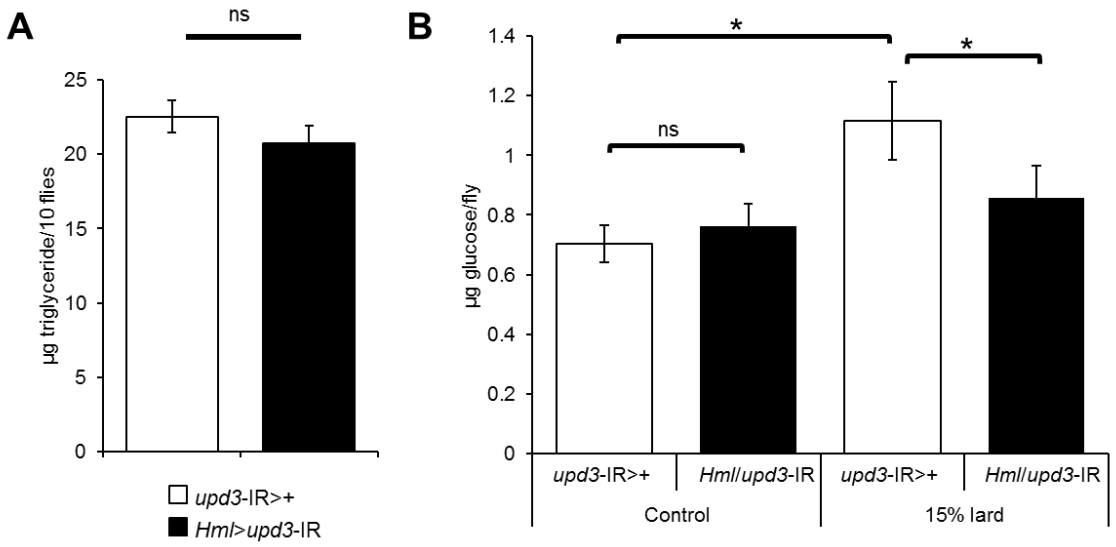


*Figure 6-3 Triglyceride and glucose levels in plasmatocyte upd3 deficient flies*
Age matched plasmatocyte specific *upd3* knock down flies (w;*Hml*ΔGal4,UAS-2xeGFP/UAS-*upd3*-IR, black bars) and control flies (w;UAS-*upd3*-IR/+, white bars) were placed on a 15% lard diet for 20 days before being sampled **A.** Thin layer chromatography (TLC) analysis of whole fly triglyceride. Samples include groups of 10 flies in quadruplicate per genotype, *upd3* deficient (black bars) and control flies (white bars). Data represents mean of n=4 samples per genotype (10 flies per sample). Error bars represent standard error of the mean, (unpaired t test p= 0.3092, ns). **B**. Glucose and trehalose content of plasmatocyte specific *upd3* knock down flies (black bars), and control genotype flies (white bars) on both control and 15% lard diets for 40 days. Trehalose present was converted to glucose with trehalase (see experimental methods), data is representative of the mean of n=5 samples per diet per genotype. Error bars represent standard error of the mean. Glucose and trehalose levels in *upd3* knock down flies compared to control *upd3* competent flies after 30 days upon; control diet, unpaired t test p=0.76163,ns and 15% lard diet, unpaired t test p= 0.04297/ *. Glucose and trehalose levels in *upd3* competent flies upon control diet compared to 15% lard diet, unpaired t test p=0.01702. The data in **A** and **B** is representative of 3 independent experiments.

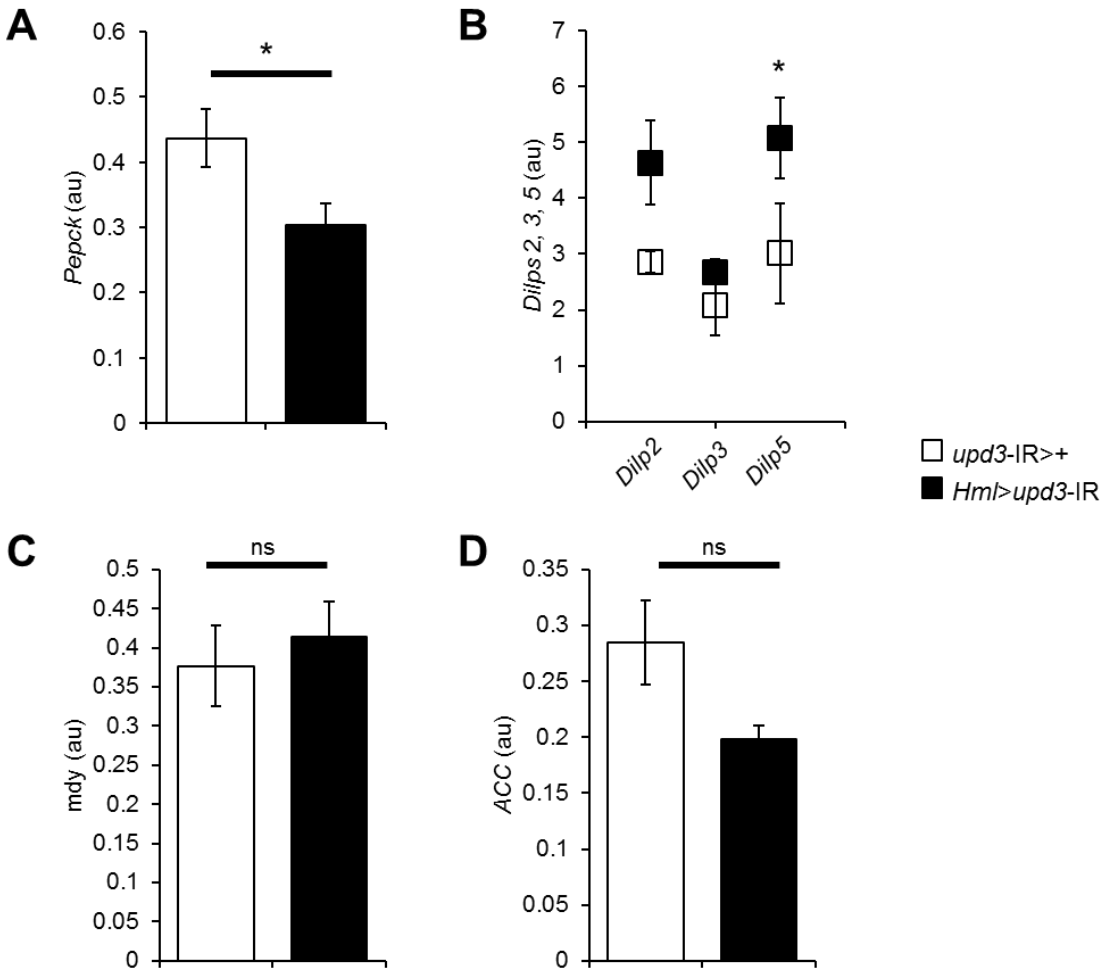


*Figure 6-4 Transcript levels of metabolic genes in plasmatocyte specific upd3 deficient flies*
RT qPCR with plasmatocyte specific *upd3* knock down fly samples (*w;HmlΔGal4,UAS-2xeGFP/UAS-upd3-IR*, black bars/shapes), and control samples (*w;UAS-upd3-IR/+*, white bars/shapes). Age matched flies were placed on a 15% lard diet, and samples were prepared at 20 days upon high fat diet. All RT qPCR data is normalised to the housekeeping gene *Rpl1*, (au = arbitrary units). **A.** Normalised *Pepck* transcript levels at day 20 upon a 15% lard diet, unpaired t tests, 20 days (p=0.04082/*). **B.** Normalised transcript levels of *Dilp2*, *3* and *5* upon 15% lard diet, unpaired t tests (*Dilp2* p=0.05012/ns, *Dilp3*=0.21776/ns, *Dilp5* p=0.02604/*). **C.** Normalised *ACC* transcript levels at day 20 upon a 15% lard diet. **D.** Normalised *mdy* transcript levels at day 20 upon a 15% lard diet. Lack of stars indicates data was not statistically significant (unpaired t tests). Data in this figure represents the mean of n=5 experimental samples per genotype (3 flies per sample), error bars represent standard error of the mean.

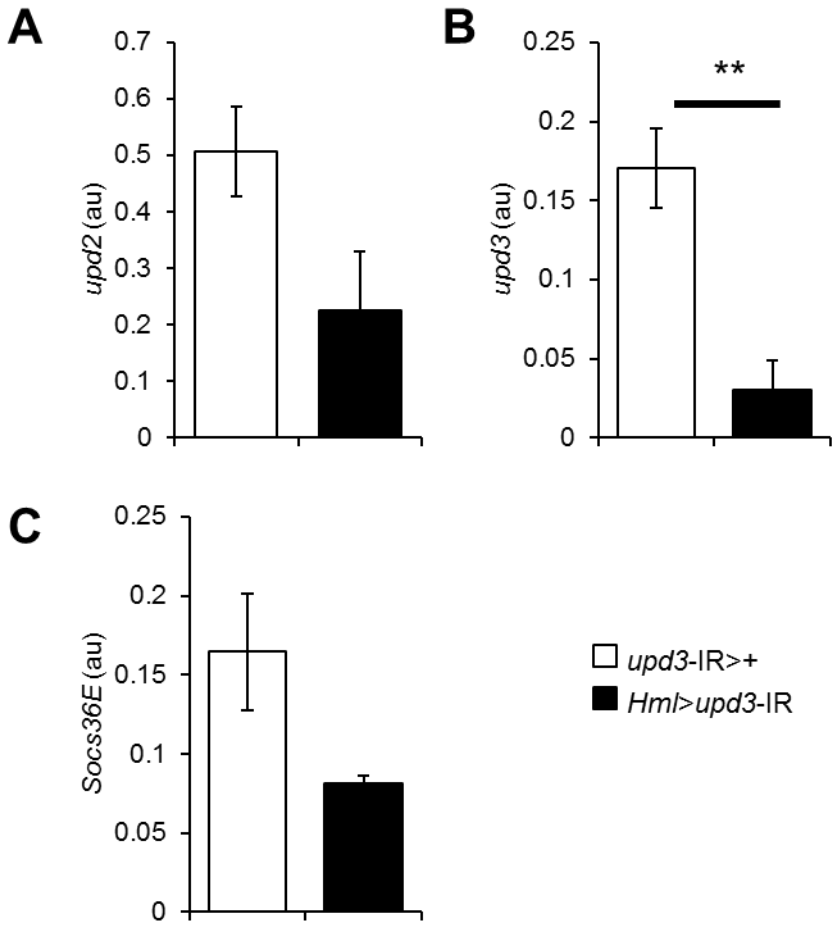


*Figure 6-5 Transcript levels of JAK-STAT pathway genes in plasmatocyte specific upd3 deficient flies*

RT qPCR with plasmatocyte specific *upd3* knock down fly samples (w;*Hml*ΔGal4,UAS-2xeGFP/UAS-*upd3*-IR, black bars), and control samples (w;UAS-*upd3*-IR/+, white bars). Age matched flies were placed on a 15% lard diet, and samples were prepared at 20 days upon high fat diet. All RT qPCR data is normalised to the housekeeping gene *Rpl1*, (au = arbitrary units). Normalised transcript levels of **A.** *upd2*, **B.** *upd3* and **C.** *Socs36E*. (Unpaired t tests; *upd2* p=0.06398/ns, *upd3* p=0.00214/**, *Socs36E* p=0.0548/ns). Lack of stars indicates data was not statistically significant. Data represents the mean of n=5 experimental repeats per genotype (3 flies per sample), error bars represent standard error of the mean.

## 6.4 Chapter 6 overview and discussion

Together these data are suggestive of plasmatocyte mediated control of both survival and glucose homeostasis in high fat died fed *Drosophila*, via the production of the cytokine *upd3*. This conclusion implies that plasmatocyte responses to a chronic excess of dietary lipids, results in an inadequate and clearly detrimental immune and metabolic response.

A recent study has shown that *upd2* mediated activation of the JAK-STAT pathway receptor *dome*, in neurons triggers the secretion of *Dilps* (Rajan and Perrimon, 2012), raising the possibility that chronic activation of the JAK-STAT pathway could contribute to the hyperglycaemia phenotypes observed in wild type high fat diet fed flies. The full spectra of *upd2*/*upd3* target tissues that appear to contribute to the detrimental effects of lipid rich diets remain to be deciphered. Interestingly, previous data in this thesis suggests plasmatocyte expression of *crq* may be involved in the propagation of a signalling cascade which results in plasmatocyte mediated expression of *upd3*, however, the potential existence of this signalling cascade is yet to be confirmed.

The detrimental plasmatocyte specific *crq* and *upd3* mediated response(s) to high fat diet described in this thesis may be conserved in vertebrates. Interestingly, the mammalian counterparts to *Drosophila crq* and *upd3* are *CD36* and *IL-6* respectively. Furthermore both of these molecules have been strongly implicated in the progression of high fat diet induced diseases (Silverstein and Febbraio, 2000, Martin et al., 2011, Vozarova et al., 2003, Yudkin et al., 2000).

### *6.4.1 FACS soring of plasmatocytes to define their expression of upd2 and upd3*

FACS sorting experiments of adult fly plasmatocytes and generation of plasmatocyte derived cDNA would allow for confirmation of expression of *upd2*/*upd3* by plasmatocytes. It has previously been shown that plasmatocytes are capable of producing *upd3* (Agaisse et al., 2003), however no evidence to date exists demonstrating that they are able to express *upd2*. Furthermore, FACS sorting of plasmatocytes from *Hml* GFP

reporter flies chronically exposed to a lipid rich diet compared to flies fed a control diet would allow for reconfirmation of an up regulation of *upd2*/*upd3* specifically in response to lipids.

### *6.4.2 Examination of different JAK-STAT pathway target genes*

Further examination into different JAK-STAT family member targets, via RT qPCR would allow for further confirmation of an enhanced JAK-STAT pathway activation in high fat diet fed flies. A rise in expression of the stress peptide *TotA* and complement-like *Tep2* would be a good indication for increased JAK-STAT pathway activation in high fat diet flies. *Tep2* has been shown to be constitutively expressed in *Hop* gain of function flies (Lagueux et al., 2000) and likewise, *TotA* expression has been shown to be dependent upon expression of the JAK-STAT family receptor *dome* (Agaisse et al., 2003).

### *6.4.3 Diet specificity of upd3 knock down fly survival*

The survival of plasmatocyte-less and plasmatocyte specific *crq* knock down flies appeared, in some instances, to be enhanced upon both control and lipid enriched diets, which was therefore suggestive of a benefit to fly survival regardless of diet. This could be due to a number of possibilities, plasmatocyte derived *crq* expression may be detrimental to fly survival for other reasons than just lipid scavenging. Furthermore, the complete loss of plasmatocytes is likely to affect other aspects of fly physiology, which could ultimately be beneficial to fly survival in non-immune challenged conditions. The common denominating factor which was observed between these two genotypes was the reduction in *upd3* expression, which coincided with the enhanced survival upon a lipid rich diet.

Interestingly, the enhanced survival phenotype observed in plasmatocyte specific *upd3* knock down flies appeared to be more of a high fat diet specific response. The loss

of *upd3* expression was beneficial to flies fed a high fat diet, however, upon a control diet no significant enhancement of survival was observed in *upd3* knock down flies. This finding would suggest that plasmatocyte derived *upd3* expression is a lipid rich diet specific response, which is potentially mediated by plasmatocyte expression of the *CD36*-like scavenger receptor *crq*.

# Chapter 7 Discussion

## 7.1 Summary of findings

### *7.1.1 Characterisation of adult Drosophila plasmatocytes*

This thesis firstly describes the generation of tools which allowed for the in depth study of plasmatocyte characteristics in adult flies. Plasmatocyte numbers slowly fell during fly lifespan and no evidence of a hematopoietic organ or plasmatocyte proliferation was observed in adult flies. Additionally, adult fly plasmatocytes were characterised to express both *Hml* and *crq* during the fly lifespan, with the vast majority of plasmatocytes co-expressing both molecules and approximately 20% of cells expressing either *Hml* alone, or *crq* alone. Expression of *Pxn* was observed in flies in the first days after eclosion, but expression rapidly diminished during the first 7 days of adult fly life. Finally a FACS protocol for plasmatocyte purification was also established, allowing for in depth study of the cells at later points in this thesis.

### *7.1.2 A crq-upd3 mediated response to dietary lipids*

Secondly, this thesis studies in detail the systemic and plasmatocyte specific responses to a lipid rich diet. As described in previous studies (Driver and Cosopodiotis, 1979, Driver et al., 1986), we found that high fat diet resulted in a reduction of fly lifespan in a dose dependent manner. High fat diet exposure additionally induced a metabolic-like syndrome in flies. Flies exhibited a rise in whole fly triglycerides and glucose, as has previously been described by Birse et al. (2010), but more interestingly we observed a marked increase in expression levels of the JAK-STAT pathway *IL-6*-like cytokines *upd2* and *upd3* after chronic high fat diet exposure, which has not been previously shown. Simultaneous to the reduction of lifespan observed in flies upon a lipid rich diet, plasmatocytes adopted a lipid filled foam cell-like morphology, once again this phenotype is regularly observed in mammalian macrophages during high fat diet induced diseases (Rahaman et al., 2006).

Plasmatocyte deletion in adult flies was sufficient to rescue survival under a lipid rich diet, suggestive of a plasmatocyte mediated response to lipids which is detrimental to fly survival. Furthermore, the lack of plasmatocytes also restored normal glucose homeostasis and abrogated the increase of *upd3* expression that was observed in wild type flies. However, the levels of whole fly triglyceride in high fat diet fed flies remained unchanged, regardless of plasmatocyte depletion, therefore it did not appear that plasmatocyte-less flies were longer lived as a consequence of them accumulating less fat.

A screen of candidate scavenger receptors was carried out in order to investigate plasmatocyte mediated effects of lipid scavenging. The screen resulted in the successful identification of two plasmatocyte expressed receptors, which were potentially involved in lipid scavenging, *nimC1* and the *CD36*-like receptor *crq*. Both *nimC1* and *crq* were found to be expressed and efficiently knocked down specifically in plasmatocytes; furthermore they appeared to have similar effects upon plasmatocyte LDL scavenging capacity. Interestingly, a lack of plasmatocyte derived *crq* expression, but not *nimC1* expression, resulted in a rescue of survival under a lipid rich diet. However, upon lipid rich diets, both *nimC1* and *crq* knock down flies contained similar levels of whole fly triglycerides as *crq* and *nimC1* competent flies respectively, once again suggesting that it was not a difference in triglyceride accumulation which caused the increase in fly survival. Therefore we reasoned that it was not the act of plasmatocyte lipid scavenging itself, or an accumulation of fly lipids which was pathological, but the activation of a plasmatocyte and seemingly *crq* mediated signalling response to lipids, which was detrimental to fly survival.

Most interestingly, a lack of plasmatocyte derived *crq* expression additionally resulted in a reduction of *upd3* expression under a high fat diet, much like the response observed in plasmatocyte-less flies. This is suggestive of a plasmatocyte, *crq* mediated signalling pathway for the expression of *upd3*. Plasmatocyte production of *upd3* has previously been reported (Agaisse et al., 2003), therefore, deeper investigation into the

role of *upd3* as a potentially plasmatocyte produced, lipid rich diet induced signal was carried out. Plasmatocyte specific *upd3* knock down flies were generated and effects upon survival, metabolism and the expression of JAK-STAT pathway target genes were examined. Once again, the loss of plasmatocyte derived *upd3* resulted in a rescue of fly survival, and the restoration of fly glucose homeostasis under a lipid rich diet. Furthermore, plasmatocyte specific knock down of *upd3* resulted in a strong loss of *upd3* expression in the whole fly, pinpointing plasmatocytes as a major producer of the *IL-6*-like cytokine.

The next sections of this discussion will describe what is understood with regard to mammalian high fat diet induced diseases, and the roles macrophages are believed to play in disease progression.

### 7.2 High fat diet induced diseases: background

Excessive consumption of lipids has led to a worldwide 'epidemic' of obesity and high fat diet associated diseases in humans. The accumulation of lipids in non-adipose tissue, known as lipotoxicity has been shown to cause pathological consequences in a variety of species (Van Herpen and Schrauwen-Hinderling, 2008, Birse et al., 2010, Birse and Bodmer, 2011). Furthermore, there is a strong evidence suggesting a positive correlation between an increase in serum lipids and the risk of developing heart disease (Kannel et al., 1971). In parallel to the on-going obesity epidemic, the incidence of type II diabetes and metabolic syndrome has drastically risen in recent years, suggesting a strong link between obesity and disease (Kahn et al., 2006). In stark contrast to this, dietary restriction has been found to significantly increase lifespan and slow ageing in a variety of species including rats, *Drosophila,* and *Caenorhabditis elegans* (McCay et al., 1935, Walker et al., 2005, Partridge et al., 2005). To date the mechanisms and specific tissues involved in the progression of high fat diet related diseases in vertebrates remain unclear,

but shifts in energy metabolism are thought to be of central importance (Anderson et al., 2009).

### *7.2.1 A role for macrophages in lipid induced inflammation*

Lipid induced inflammation is proposed to be directly related to the development of many high fat diet related diseases, including atherosclerosis. The immunological signature of high fat diet induced disease is yet to be characterised, but numerous studies have shown a rise in pro-inflammatory cytokine production in response to lipid rich diets (Berliner et al., 1995). Macrophages, the primary phagocytic cells of the innate immune system, have been implicated in high fat diet related disease pathology and progression. Lipid filled macrophages, known as foam cells, are frequently observed in atherosclerotic plaques, and are suggestive of a macrophage involvement in disease pathology and progression (Rahaman et al., 2006).

In mammalian models, macrophages are believed to be responsible for the increase in pro-inflammatory cytokines observed in high fat diet induced diseases. However, study of the macrophage response to lipid rich diet is problematic, due to animal model limitations and the lack of tissue specific tools available. Additionally many experiments examine macrophage responses to lipids in an *in vitro* cell culture environment; often drawing conclusions from these experiments is difficult, given the fact that they exclude the effects of neighbouring endogenous cells and tissues. Furthermore the study of atherosclerosis and lipid induced pathology in mice is limited; this is because studies utilise models which rapidly induce plaque formation, such as in *ApoE* (*Apolipoprotein E*) knockout mice fed a high fat diet (Nakashima et al., 1994). However, these models perhaps do not accurately represent high fat diet disease physiology; for example, it is likely that natural plaque formation in mice would take a number of years. In light of this, interpretation of findings form these ‘accelerated atherosclerosis’ models

is difficult and may possibly result in other important aspects of high fat diet disease induced pathology being missed.

In mammals macrophages are responsible for innate immune responses and have scavenging functionality. Under a lipid rich diet macrophages accumulate intracellular lipids, the presence of these lipids and the main macrophage effector function as pro-inflammatory cytokine producers could provide a link between macrophages and high fat diet disease induced pathology (Linton and Fazio, 2003). The lipid laden, foam cell-like plasmatocytes present within adult flies fed a lipid rich diet and the simultaneous up regulation of the fly *IL-6*-like cytokine *upd3* described in this thesis, is suggestive of conservation across the species of the innate immune response to excess lipids.

### *7.2.2 Macrophage expressed genes associated with high fat diet disease*

Various genes have been implicated in high fat diet disease induction in mammals. Most interestingly these include the scavenger receptor *CD36* and the pro-inflammatory cytokine *IL-6*, both of which are expressed in mammals by macrophages as well as by other tissues (Martin et al., 2011, Mohamed-Ali et al., 1997) and both of which have counterpart genes in the fly, which were identified during the course of this thesis to play a role in *Drosophila* high fat diet disease related pathology. The fly contains some 14 *CD36*-like scavenger receptors (Herboso et al., 2011), one of these is *crq*. Interestingly, the fly counterpart to mammalian *IL-6* is the cytokine *upd3* and expression of *IL-6* has been shown to be induced in macrophages upon *CD36* mediated lipid scavenging in humans (Janabi et al., 2000). This finding is particularly striking with regard to the plasmatocyte responses to lipid rich diet described in this thesis.

The following two sections will compare mammalian *CD36* and *IL-6* to their *Drosophila* counterparts; *crq* and *upd3* respectively, as well as detailing what is currently known in the field with regard to *CD36* and *IL-6* roles in high fat diet related diseases, and in particular how these studies relate to data described in this thesis.

## 7.3 *CD36* and *crq*

### *7.3.1 CD36 in mammals*

CD36 is a glycoprotein receptor which has a single extracellular domain, incorporating two separate binding sites and two cytoplasmic tail domains (Rać et al., 2007). In humans *CD36* is a member of the scavenger receptor class B (SR-B) family and is expressed by a variety of different tissues including platelets, mononuclear phagocytes, adipocytes, hepatocytes, myocytes and some epithelial cells (Silverstein and Febbraio, 2009, Febbraio et al., 2001). The first CD36 extracellular domain recognises thrombospondins, the second is larger and incorporates a hydrophobic compartment, which is able to bind to a variety of ligands (Martin et al., 2011, Jiménez et al., 2000). CD36 has been shown to have downstream signalling functionality, Src protein tyrosine kinases are able to interact with C-terminal tyrosine residues in the cytoplasmic tail, and JNK (c-Jun N-terminal kinase) pathway activation has been shown to be CD36 dependent (Huang et al., 1991, Hirosumi et al., 2002). However, due to the multitude of different tissues which express *CD36* and the variety of roles that it reportedly plays, downstream signalling events are likely to differ significantly in response to differing ligands and in differing expression locations (Figure 7-1 A).

### *7.3.2 The CD36 family in the fly*

The common trend observed in gene families, is that of an increase of genes within human gene families compared to *Drosophila* (Adams et al., 2000). Interestingly 14 SR-B, *CD36* family member related receptors have been identified in the fly (Herboso et al., 2011), while only 3 exist in humans. The observed reduction of *CD36* family members in humans compared to *Drosophila* is unusual and may suggest an evolutionary advantage of fewer *CD36* family members, or the incorporation of multiple functions into fewer receptors, which could also be in some way advantageous.

Expression of the *CD36* family receptors in the fly is tightly regulated, both temporally and spatially during development (Herboso et al., 2011). Many of the *CD36*-like receptors expressed by the fly remain uncharacterised; however a few have been studied in more detail. *Sensory neurone membrane protein* (*SNMP*) is a *CD36*-related pheromone receptor expressed by population of olfactory sensory neurones, involved in both fly courtship and the detection of fatty acids (Benton et al., 2007, Vosshall, 2008). Another *Drosophila CD36*-related receptor is *peste* which has been shown to be required for mycobacterial phagocytosis in hemocyte cell lines (Philips et al., 2005).

Perhaps the most well characterised to date of the fly *CD36* family members is the membrane glycoprotein receptor *croquemort* (*crq*). CRQ shares 23% homology at amino acid level with human and murine CD36, and encompasses a 13 amino acid motif which is conserved amongst all CD36 family members. It also encodes an intracellular putative protein kinase C (PKC) phosphorylation site, indicative of potential downstream signalling events (Franc et al., 1996). *Crq* is expressed by plasmatocytes in adult flies, as well as by other tissues in the fly, see Figure 7-1 B for further structural details of fly *crq*.

Much like mammalian *CD36*, it is clear that *CD36* family members in the fly play a variety of different roles and are expressed by a variety of different tissues. *Crq* in particular emerges as an interesting candidate model for mammalian *CD36* function in response to lipids, given that it is expressed by fly plasmatocytes and has been shown in this thesis to play a role in the fly response to high fat diet.

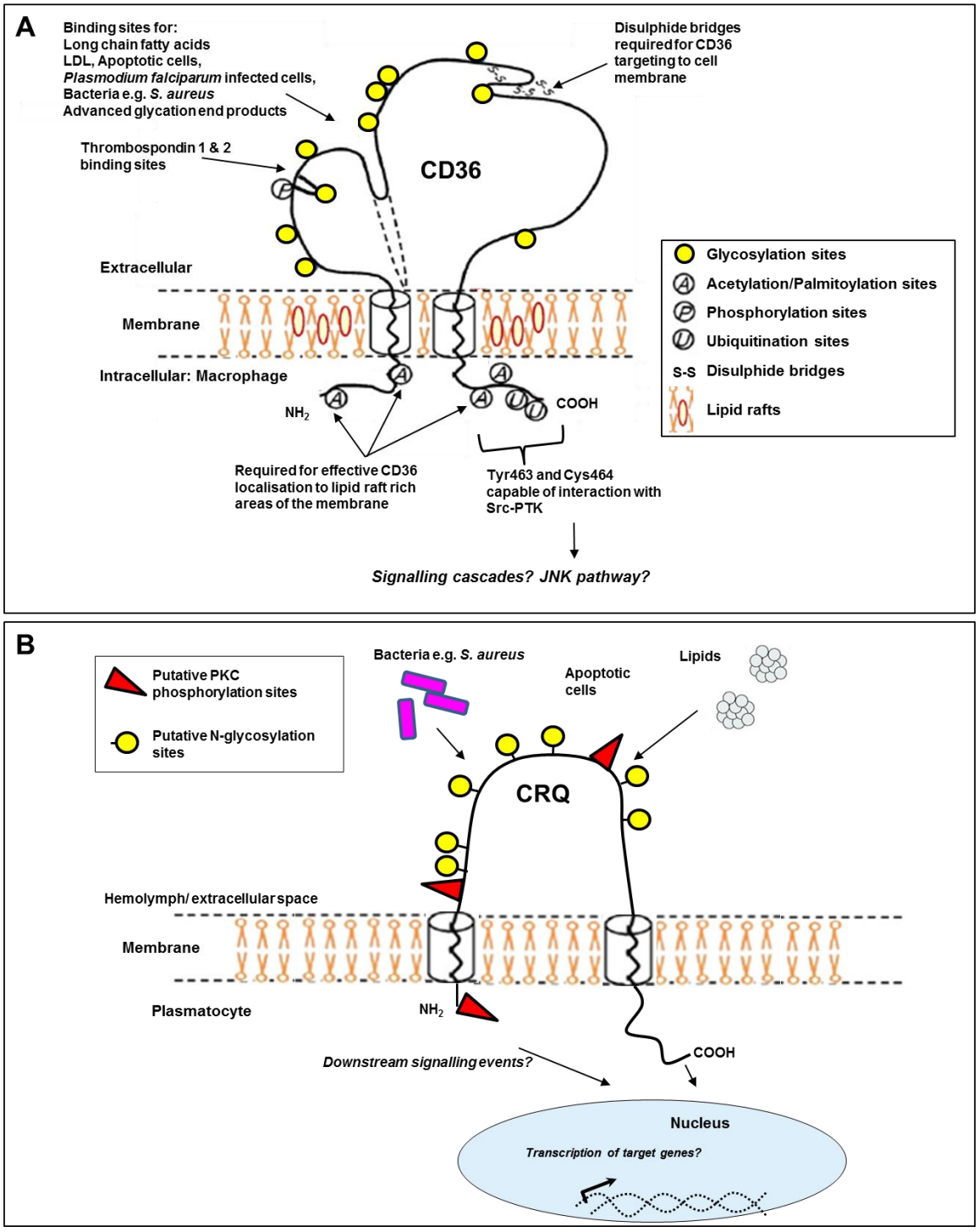


*Figure 7-1 Diagram of the main structural features of mammalian macrophage expressed CD36 and Drosophila plasmatocyte expressed CD36-like receptor croquemort*
Diagrams adapted from Martin et al. (2011) and (Franc et al., 1996), illustrating potential binding partners for and potential sites for induction of downstream signalling events in; **A.** Mammalian CD36, and **B.** *Drosophila* CRQ. PKC (protein kinase C), PTK (protein tyrosine kinase).

### *7.3.3 CD36 in high fat diet disease*

Studies investigating the role of *CD36* in the development of metabolic and cardiovascular diseases frequently offer conflicting findings. For example, a *CD36* deficiency in humans and rats has been shown to promote the development of insulin resistance and cardiovascular diseases (Aitman et al., 1999, Pravenec et al., 2001, Miyaoka et al., 2001, Leprêtre et al., 2004), yet conversely high fat diet induced insulin resistance has been shown to be rescued in *CD36* knockout mice (Kennedy et al., 2011). A further realm of *CD36* expression complexity has been identified in a study highlighting the importance of *CD36* gene dose effects in humans. Love-Gregory et al. (2008) studied a stop codon encoding single nucleotide polymorphism (SNP) in *CD36*, which resulted in a *CD36* deficiency in affected patients. Patients homozygous for the SNP displayed an increased susceptibility to cardiovascular disease, but unexpectedly heterozygote patients were protected from cardiovascular disease comparatively to patients who lacked the SNP completely.

Interestingly, bone marrow specific *CD36* deletion has been shown to significantly reduce macrophage presence within adipose tissue, suggesting *CD36* may influence macrophage migration towards adipose tissue. Macrophage derived *CD36* expression has also been shown to influence metabolism, with a loss of macrophage specific *CD36* expression being sufficient to improve insulin signalling in adipose tissue (Nicholls et al., 2011). These studies highlight the levels of complexity behind *CD36* mediated roles in high fat diet induced pathophysiology, which may well be a result of the broad range of ligand and tissue specific roles the receptor plays.

### *7.3.4 CD36 and lipid induced inflammation*

In mammals *CD36* is strongly implicated in the macrophage mediated inflammatory response to dietary lipids. Macrophage production of the pro-inflammatory cytokine *IL-6* in response to LDL has been shown to be *CD36* dependent in humans (Janabi et al.,

2000). Similar *CD36* dependent, lipid induced, pro-inflammatory phenotypes have been observed in mice. Wild type mice fed a high fat diet up regulate expression of IFN-γ and monocyte chemotactic protein-1 (MCP-1) and display enhanced JNK pathway activation, all of which phenotypes could be rescued in *CD36* knockout mice (Kennedy et al., 2011). Most interestingly, *CD36* mediated JNK pathway activation has been illustrated to be responsible for the development lipid filled 'foam cell' macrophages, the presence of these cells is a distinguishing feature of high fat diet induced cardiovascular diseases. (Rahaman et al., 2006).

Characterisation of *CD36* mediated downstream signalling events has proved difficult, given the broad array of cell types that express the receptor and the multifunctional roles it appears to play dependent on its expression location. There is strong evidence to suggest an important immunological and metabolic regulatory role for *CD36* in mammals, particularly in response to lipids. It is clear that *CD36* is expressed in many different tissues, yet much of the research to date examines a loss of *CD36* in all tissues; consequently the cell specific roles of *CD36* cannot be distinguished in these experiments. Therefore, characterisation of the cell specific functions of *CD36* in mammals is problematic however, the use of *Drosophila* as a model system has allowed for detailed characterisation of the *CD36*-like receptor *crq* specifically in plasmatocytes, in response to dietary lipids in an *in vivo* setting. Data in this thesis indicates that plasmatocyte expression of *crq* is detrimental, resulting in a dysregulation of metabolic and immune homeostasis in flies, ultimately reducing fly lifespan. These findings represent a conserved lipid sensing/scavenging role between fly *crq* and vertebrate *CD36*.

## 7.4 *IL-6* and *upd3*

### *7.4.1 The mammalian IL-6R subunit gp130 and Drosophila dome*

Findings in this thesis have highlighted an up regulation of the *IL-6*-like JAK-STAT pathway activating cytokines; *upd2* and *upd3* in response to chronic lipid rich diet exposure. DOME, the fly JAK-STAT pathway receptor shares structural similarities to the mammalian gp130 subunit of the IL-6 receptor (Figure 7-2) (Brown et al., 2001). Vertebrate interleukin receptors contain a WSXWS (tryptophan, serine, any amino acid, tryptophan and serine) conserved domain within their cytokine binding modules; DOME appears to lack the complete sequence, coding for only WS (tryptophan and serine). These structural similarities are particularly interesting, firstly because various studies have described a link between high fat diet induced disease pathology and the induction of *IL-6* expression, and secondly because data in this thesis illustrates that high fat diet fed flies exhibit an increase in expression of the *IL-6*-like cytokine, *upd3*. This suggests conservation in the response to chronic dietary lipids between mammals and flies.

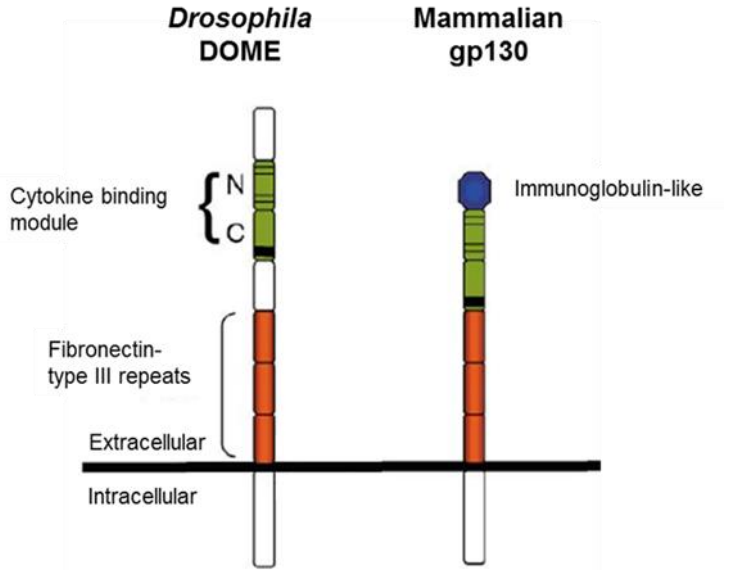


*Figure 7-2 Protein domains of Drosophila DOME and vertebrate gp130*
**Left:** *Drosophila* DOME and **right:** mammalian IL-6R subunit, gp130. The cytokine binding modules of DOME and gp130 (green) contain two domains; firstly the N-terminal domain containing two pairs of cysteine residues (thin black lines), and secondly the C-terminal domain contains the WSXWS motif (thick black lines) in gp130, which is incomplete in DOME, (WS only). The blue hexagon in gp130 depicts an immunoglobulin-like motif, which is absent in DOME. Fibronectin-type III repeats orange, diagram adapted from Brown et al. (2001).

*7.4.2 Induction of IL-6 expression in high fat diet diseases in humans*

Studies have shown that the acute phase response cytokine, *IL-6* is produced by adipose tissue and that *IL-6* concentrations are significantly increased among obese individuals compared to non-obese controls (Mohamed-Ali et al., 1997, Bastard et al., 1999), this is suggestive of a potential pro-inflammatory *IL-6*-related role in high fat diet disease induction and progression. Furthermore, *IL-6* production in response to LDL has been shown to be dependent upon the scavenger receptor *CD36* (Janabi et al., 2000). This is extremely interesting in the context of the findings in this thesis. Expression of the *IL-6*-like cytokines *upd2* and *upd3* was induced in response to chronic high fat diet exposure in the fly. In addition, a lack of expression of the *CD36*-like receptor *crq*, specifically in plasmatocytes was sufficient to result in a reduction of *upd3* expression. This may suggest conservation throughout the species of a macrophage mediated *CD36*/*crq* induction of *IL-6*/*upd3* expression in response to a lipid rich diet.

*7.4.3 IL-6 and insulin resistance in mammals*

*IL-6* in mammals appears to play a metabolic role, particularly in high fat diet induced disease. Both an increase in *IL-6* plasma concentrations and an *IL-6* promoter region polymorphism which results in a rise of plasma *IL-6* levels have been demonstrated to be a predicting factor for the onset of type II diabetes and insulin resistance in humans (Vozarova et al., 2001, Vozarova et al., 2003) (Figure 7-3). Furthermore, peripheral infusion of *IL-6* has been shown to result in a generalised enhancement of whole body energy metabolism and in particular an increase in fatty acid metabolism in humans (Petersen et al., 2005). Conversely, *IL-6* knockout mice rapidly become obese, insulin resistant and exhibit perturbed carbohydrate and lipid metabolism (Wallenius et al., 2002).

These data suggest that *IL-6* expression levels are important in maintaining metabolic homeostasis, yet a complete loss or an increase of *IL-6* both prove to be

detrimental in terms of metabolic disease induction. Societal eating habit changes mean people are consuming higher quantities of lipid than ever before. In obese individuals metabolism may become overloaded due to chronic lipid exposure. This could mean inflammatory and metabolic responses elicited as protection mechanisms could ultimately become detrimental. Tissue specific *IL-6* expression and action appear to be of central importance to the progression of metabolic and high fat diet induced disease pathology.

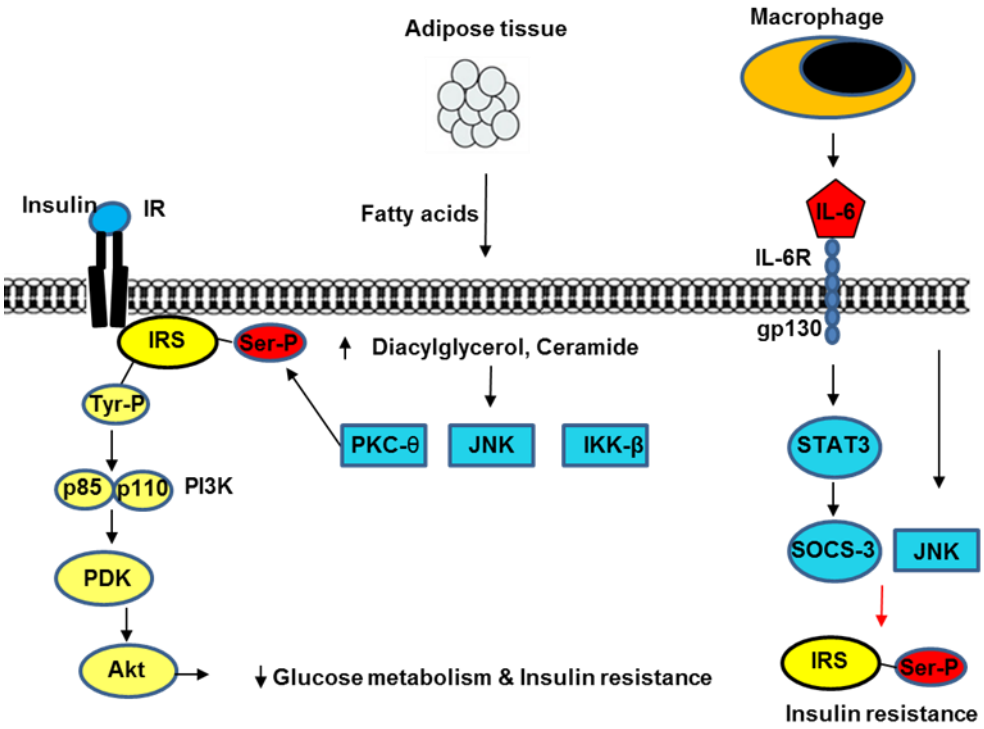


*Figure 7-3 IL-6 mediated insulin resistance in humans*
**Left:** during obesity, insulin resistant adipose tissue releases excess fatty acids, resulting in a concurrent increase in lipid uptake and in the presence of lipid metabolites (e.g. diacylglycerol and ceramide). Lipid metabolites can activate serine kinases (e.g. PKC-$\theta$, IKK-$\beta$, JNK and S6K) which cause serine phosphorylation (Ser-P) of the insulin receptor substrate (IRS). This results in a reduction of insulin mediated tyrosine phosphorylation (Tyr-P) of the IRS, PI3K phosphoinositide-dependent kinase (PDK) and Akt, which ultimately reduces glucose metabolism. Adipose tissue inflammation also adds to systemic insulin resistance. **Right:** macrophages and adipocytes secrete the pro-inflammatory cytokine IL-6, which binds the IL-6 receptor (IL-6R), activating STAT3, which increases SOCS-3 expression. SOCS-3 targets the IRS for degradation. IL-6 can also activate JNK, promoting phosphorylation of IRS proteins, which promotes insulin resistance. Figure is adapted from Gray and Kim (2011).

*7.4.4 The role of upd3 in gut homeostasis*

An increase in expression of both *dome* and *upd3* is induced after *Drosophila* gut infection with *Erwinia carotovora* (Buchon et al., 2009b, Buchon et al., 2009a). However, it was shown that *upd3* up regulation was not induced by the bacteria itself, but by the stress and damage the infection initiated. In addition, JAK-STAT pathway activation was shown to be required for intestinal stem cell renewal after enterocyte infection or apoptosis (Jiang et al., 2009).

These data pose an interesting question with regard to the role ingested lipids may play in the gut. It could be hypothesised that chronic lipid exposure could induce intestinal damage, resulting in JAK-STAT activation in the gut. This mechanism could be synergistic to the plasmatocyte mediated responses observed in this thesis, ultimately promoting whole fly high fat diet induced pathology, and early fly death. Equally it would be interesting to investigate the existence of gut associated plasmatocytes and the roles they might play in chronic high fat diet exposure.

Study of the mammalian *IL-6* counterpart gene *upd3* in *Drosophila* and particularly the plasmatocyte mediated roles of this cytokine has allowed for a deeper understanding of the innate immune reaction to chronic dietary lipid exposure. Furthermore, the conservation between the both up regulation of mammalian *IL-6* and fly *upd3* and the metabolic phenotypes observed during chronic lipid exposure is striking, once again promoting the fly as an attractive *in vivo* model to further study high fat diet induced diseases.

The following section will give a general conclusion of findings as well as a discussion of questions and potential future experiments which could be carried out on the basis of the findings described in this thesis. In addition to this, models for potential *crq* and *upd3* signalling pathways are proposed.

## 7.5 Discussion points and future work

### *7.5.1 Downstream signalling of crq*

Data included in this thesis are suggestive of a *crq* and therefore scavenger receptor mediated signalling cascade activated in plasmatocytes, in response to the scavenging of dietary lipids. A model for lipid induced *crq* mediated *upd3* production is illustrated in Figure 7-4. This *crq* interaction with lipid coincides with the increased transcription of the JAK-STAT pathway cytokines *upd2* and *upd3*. Potential *crq* initiated signalling cascades have not been characterised in the fly, however study of the vertebrate *CD36* response to lipids has identified JNK pathway activation as a downstream signalling event of *CD36* lipid scavenging (Rahaman et al., 2006), this could also be conserved in *Drosophila*.

The JNK pathway has been demonstrated to be required for wound healing in *Drosophila* (Rämet et al., 2002, Galko and Krasnow, 2004). Activation of both the JNK and *NFκB* pathways in the fly is dependent upon *Tak1* (*transforming growth factor β-activated kinase 1*), the homolog of mammalian MAPK kinase kinase (mitogen-activated protein kinase). Interestingly JNK pathway activation does not lead to AMP transcription in the fly, but transcription of other immune genes is initiated, including *Punch*, *sulfated*, and *malvolio* (Silverman et al., 2003).

Studies have highlighted that *CD36* lipid binding induces JNK pathway activation in mice (Kennedy et al., 2011) and blocking JNK pathway activation has also been shown to be sufficient to prevent foam cell formation in mice (Rahaman et al., 2006). Therefore, experiments involving the knock down of JNK pathway components in the fly such as the JNK kinases *hemipterous* (*hep*), or *basket* (*bsk*) specifically in plasmatocytes may allow for further investigation into a possible *crq* mediated, JNK pathway activation upon high fat diet (Riesgo-Escovar et al., 1996). In addition, experiments could also be conducted to assess whether the loss of JNK pathway activation in plasmatocytes is sufficient to block plasmatocyte foam cell formation upon a lipid rich diet. Furthermore, expression of *upd3* in high fat diet fed flies lacking plasmatocyte derived JNK pathway activation could be

investigated, to determine if JNK signalling is involved or required for the induction of *upd3* expression in plasmatocytes.

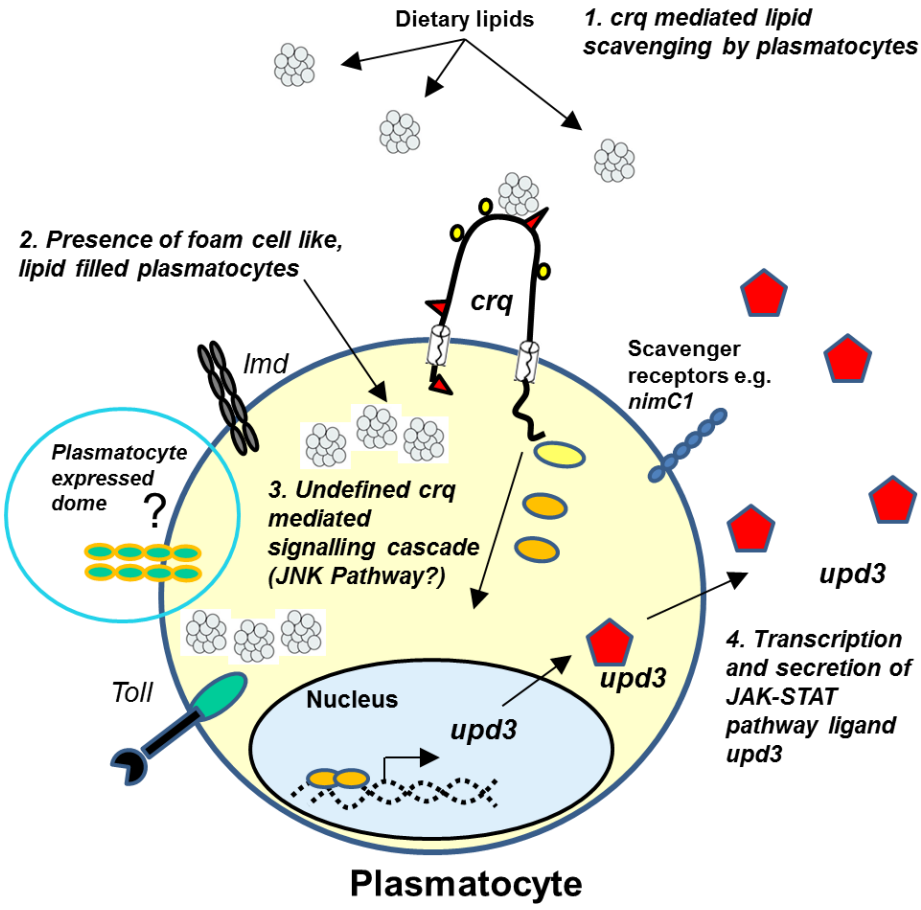


*Figure 7-4 A model for a lipid induced crq mediated signalling cascade*
**1.** Chronic high fat diet exposure in *Drosophila* results in *crq* mediated scavenging/sensing of lipids. **2.** and the subsequent formation of foam cell-like plasmatocytes. **3, 4.** Through an as yet uncharacterised signalling cascade (possibly JNK pathway activation) transcription and secretion of the JAK-STAT activating cytokine *upd3* is initiated by plasmatocytes. It is not known if plasmatocytes themselves express *dome*, if they do there is potential that *crq* mediated expression of *upd3* by plasmatocytes could result in autocrine activation of the JAK-STAT pathway in plasmatocytes themselves.

*7.5.2 Crq lipid scavenging specificity*

It is unknown whether *crq* displays any specificity for certain lipid types. Similar phenotypes with regard to the rescue of survival in plasmatocyte specific knock down flies were observed in both coconut oil and lard supplemented lipid rich diets. This finding would be suggestive of *crq* being relatively unspecific in terms of dietary lipid uptake, as coconut oil and lard are vegetable and animal fats respectively. In addition to this, each of the dietary fats tested also possessed quite different levels of fat saturation. However it would be interesting to test different types of dietary lipids to determine whether similar survival phenotypes are observed in plasmatocyte specific *crq* knock down flies.

Mass spectrometry for fly lipid profiles, and plasmatocyte lipid profiles may shed further light on the plasmatocyte and fly responses to chronic lipid rich diets. The lipid droplet subproteome in *Drosophila* fat body cells has been investigated; findings were suggestive of differential types of lipid droplets, which played different roles dependent upon the metabolic state of the fly (Beller et al., 2006). In this thesis plasmatocytes were shown to contain lipid vacuoles, with the quantity of intracellular lipid being significantly higher in high fat diet compared to control diet fed flies. It could be hypothesised that the roles of the plasmatocyte derived lipid droplets are distinctly different dependent upon diet.

*7.5.3 What are the peripheral target tissues of upd2 /upd3?*

This thesis demonstrates that chronic high fat diet exposure in wild type flies resulted in an up regulation of the JAK-STAT pathway cytokines *upd2* and *upd3,* this up regulation coincided with a dysregulation of glucose metabolism in flies. Identification of the particular target tissues for *upd2* and *upd3* action could provide insight into which tissues are responsible for promoting dysregulated glucose homeostasis, and ultimately allow a better understanding of high fat diet induced disease mechanisms.

A recent study has shown that *upd2* plays a role in the regulation of *Dilp* production. The binding of *upd2* to its cognate receptor *dome* in neurones triggers neuronal release of *Dilps* (Rajan and Perrimon, 2012). This raises the possibility that chronic activation of the JAK-STAT pathway may contribute to the disruption of glucose homeostasis observed upon a lipid rich diet, through an effect on neurones. Experiments to investigate this could be carried out by either knocking down or over-expressing a dominant negative form of the JAK-STAT receptor, *dome*, in various potential target tissues. Loss of *dome* expression would result in an inability of *upd2* and *upd3* to act upon that given tissue. Survival assays could be carried out using these flies on control and lipid rich diets to determine whether loss of *dome* expression by the tissue of interest plays a role in fly survival upon high fat diet. Furthermore, analysis of whole fly glucose levels in flies may enable identification of the target tissues involved in regulating glucose metabolism during chronic high fat diet exposure.

The role of the fat body in *upd2*/*upd3* mediated lipid induced pathophysiology may be of particular interest, given the role of the fat body as the major metabolic organ in the fly. Furthermore, loss of *dome* expression in neurones could provide an interesting candidate for high fat diet disease induced glucose dysregulation, particularly due to the role neurones have already been shown to play in production of *Dilps* in an *upd2* mediated manner (Rajan and Perrimon, 2012). Finally experiments could be conducted in order to examine plasmatocyte specific loss of *dome* expression. During haematopoiesis prohemocytes express *dome*, but it appears to be down regulated in the mature larval hemocyte subsets (plasmatocytes, larval cells and crystal cells), however it is not yet determined if plasmatocytes in adult flies express *dome*, or in fact if chronic lipid exposure could induce *dome* expression in plasmatocytes. Experiments could be carried out to investigate a potential positive feedback loop of JAK-STAT activation via plasmatocyte expressed *dome*. For example, if plasmatocytes expressed *dome*, their *crq*, lipid scavenging induced expression of *upd3* would result in autocrine induction of JAK-

STAT target genes, such as complement like factor *Tep2* (Lagueux et al., 2000) or stress peptide *TotA* (Agaisse et al., 2003) in plasmatocytes themselves, and could ultimately result in a promotion of lipid induced pathology.

Confocal microscopy of *Stat92E*-GFP reporter flies could also allow for identification of potential *upd2*/*upd3* target tissues, by giving an indication of which tissues may display a high fat diet dependent enhancement of JAK-STAT pathway activation. A model for the potential peripheral targets of *upd2* and *upd3* is illustrated in (Figure 7-5).

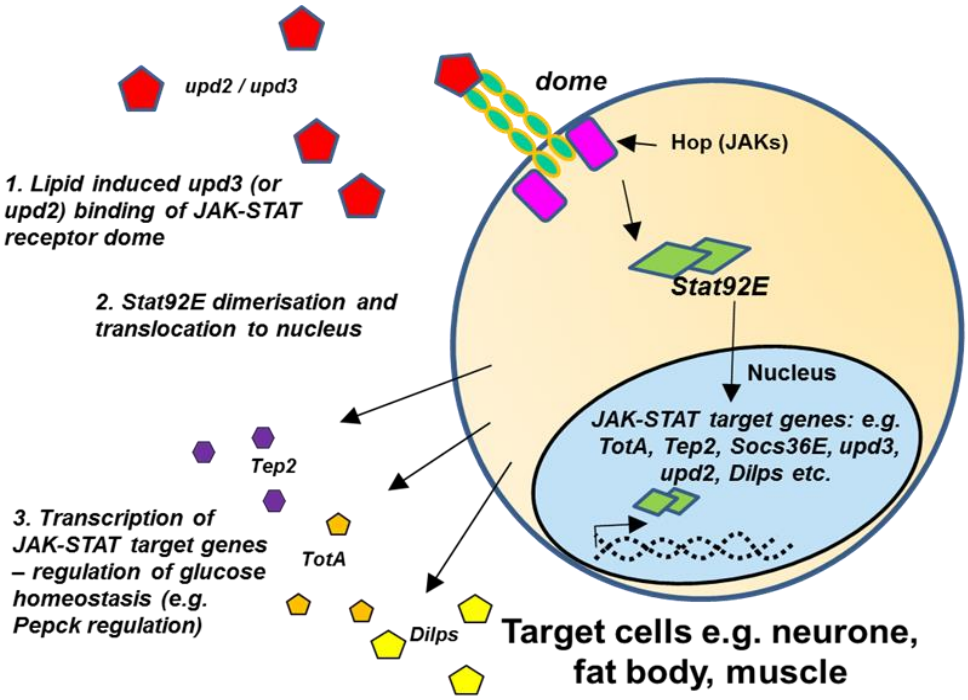


*Figure 7-5 A model for upd2 and upd3 peripheral target tissues*
Chronically high fat diet fed flies exhibit an increase in JAK-STAT pathway activating cytokines; *upd2* and *upd3*. **1.** *upd2* and *upd3* act upon JAK-STAT receptor *dome* expressing cells (e.g. neurones, fat body, muscle, and plasmatocytes) **2.** This results in *Stat92E* dimerization and translocation to the nucleus. **3.** Transcription of JAK-STAT target genes is initiated (e.g. *TotA*, *Tep2*, *Socs36E, Dilps? upd2 and upd3?*). The chronic presence of lipid results in chronic JAK-STAT pathway activation, which coincides with hyperglycaemia and an early death in high fat diet fed flies. The mechanism for hyperglycaemia induction is not yet determined.

*7.5.4 Knock down of JAK-STAT family members*

To further confirm the JAK-STAT related role in response to chronic high fat diet, experiments could be carried out in which different components of the JAK-STAT pathway are knocked down in various tissues. For example knock down of the fly JAK, *hopscotch*, or the fly STAT, *Stat92E* could be studied in flies with regard to potential survival, metabolic and immune phenotypes induced by a high fat diet. Theoretically a loss of *hop* or *Stat92E* in target tissues should phenocopy the loss of *upd2* or *upd3* expression and therefore prevent JAK-STAT pathway activation in these tissues, resulting in an expansion of fly lifespan upon a lipid rich diet.

*7.5.5 Over expression of upd3*

Transcript levels of whole fly *upd3* rise significantly after chronic high fat diet exposure, this coincides with hyperglycaemia and early death in the fly. Given this finding, it poses the question as to how the fly would fare, in terms of both survival and glucose level phenotypes if plasmatocytes over-expressed *upd3*. The high fat diet induced rise in expression of *upd3* is observed only after a period of approximately 20-30 days upon a lipid rich diet. It would be interesting to determine if overexpression of *upd3* is sufficient to phenocopy the survival and glucose phenotypes observed in high fat diet fed flies, but at earlier time points. In addition to this, it would be particularly intriguing if the phenotypes observed in high fat diet exposure could be mimicked upon a control diet, purely by over expression of *upd3*.

*7.5.6 Investigation of plasmatocyte specific upd2 knock down*

In order to investigate the plasmatocyte responses to chronic high fat diet exposure, plasmatocyte specific knock down of *crq* and *upd3*, but not *upd2* was studied. Expression of *upd2* by plasmatocytes has not been previously reported. Therefore, examination of plasmatocyte specific *upd2* knock down may firstly allow us to determine whether *upd2*

is produced by plasmatocytes. Secondly, comparing the effects of plasmatocyte specific *upd2* knock down to the phenotypes observed in *crq* and *upd3* plasmatocyte specific knock down flies may allow for further characterisation of the differential roles *upd2* and *upd3* may play in metabolism and immunity.

### *7.5.7 Study of upd2 and upd3 mutant flies*

A total loss of *crq* expression in the whole fly was achieved using the ubiquitous driver *Tubulin* to drive knock down. Survival of these flies upon a high fat diet was actually worse than that of *crq* competent flies, suggesting that expression of *crq* in non-plasmatocytes is actually beneficial to fly survival. This finding, alongside the rescue of survival observed in plasmatocyte driven *crq* knock down flies highlighted the plasmatocyte specific role of *crq* expression being particularly detrimental to fly survival.

It would be interesting to investigate the survival, metabolic and immune phenotypes of *upd2* and *upd3* ubiquitous knock down, or mutant flies. This would allow for deeper characterisation of the degree to which plasmatocytes are specifically responsible for regulating high fat diet disease pathology. In addition it would provide an indication of differential phenotypes induced by the loss of *upd2* and the loss of *upd3*, and therefore allowing for clarification of the similar, or different roles the cytokines may play, specifically with regard to high fat diet induced phenotypes.

### *7.5.8 In depth study of the insulin pathway response to a lipid rich diet*

Deeper characterisation of insulin pathway regulation in high fat diet fed flies, and particularly in flies lacking plasmatocyte derived expression of *crq* or *upd3,* could provide further insight into the dysregulation of glucose metabolism induced by excess dietary lipids. This thesis includes RT qPCR expression level data of *Dilp2, Dilp3* and *Dilp5* in high fat diet fed flies, however, it was not possible to definitively clarify the role of the insulin pathway, or its regulation in response to chronic high fat diet exposure as

*Dilp* expression levels remained relatively static, regardless of diet. Conversely, findings with regard to whole fly glucose levels were very suggestive of a dysregulation of glucose homeostasis. Interestingly, both the early death and hyperglycaemia phenotypes observed in wild type flies after chronic high fat diet exposure, were rescued in plasmatocyte-less flies and flies lacking plasmatocyte derived expression of *upd3*. These data would strongly suggest an involvement of the insulin pathway. Western blot experiments examining levels of Akt phosphorylation could be carried out with plasmatocyte-less flies and flies lacking plasmatocyte derived *crq* and *upd3* on both control and lipid rich diets, to further clarify the insulin pathway response and how plasmatocytes and plasmatocyte derived *crq* and *upd3* expression may regulate insulin signalling.

In addition to this, microscopy experiments using *Dilps* to drive expression of fluorophores could allow for better characterisation of the fly insulin pathway response to chronic high fat diet exposure.

### *7.5.9 Is chronic dietary lipid eventually viewed as a threat?*

Intriguingly, it did not seem to be the lipid itself that was detrimental to fly survival, but the plasmatocyte response to it, as plasmatocyte depleted flies survived for longer on a lipid rich diet than control plasmatocyte competent flies. Perhaps chronic dietary lipid exposure in the fly could be compared to a dampened chronic inflammatory response, which ultimately becomes pathological due to a lack of clearance.

Studies have already identified a role for *crq* in phagocytosis of *S. aureus* by hemocyte cell lines, similarly, in mouse macrophages *CD36* mediated phagocytosis was required for an up regulation of various pro-inflammatory cytokines, including *IL-6* (Stuart et al., 2005). Furthermore, expression of *upd3* by adult *Drosophila* plasmatocytes in response to infection has already been described (Agaisse et al., 2003). It would be interesting if the response observed after chronic high fat diet exposure was reminiscent of the response to infection. Experiments could be carried out with plasmatocyte specific

*crq* and *upd3* knock down flies in order to study similarities between the two responses. The expression levels of the AMP genes *Drs* and *Dpt* were monitored over time in flies fed a high fat diet, however changes in expression characteristics observed to date were not consistent enough to be included in this thesis. Future experiments could further study the AMP gene regulation in response to chronic lipid rich diet exposure comparatively to that of infection.

Examination of different JAK-STAT pathway target genes, such as complement-like *Tep2* protein, or the stress peptide *TotA* in response to a lipid rich diet could be carried out to further elucidate the mechanisms behind high fat diet disease physiology. This could also provide a further link as to whether a lipid rich diet induces a state of chronic low inflammation as these peptides are expressed by the fat body after immune challenge (Agaisse et al., 2003, Lagueux et al., 2000).

### 7.6 Conclusion and a model for *crq-upd3* mediated lipid induced pathology

To conclude; the loss of plasmatocytes or the loss of expression of the scavenger receptor *crq* or fly cytokine *upd3* by plasmatocytes is sufficient to rescue fly survival upon a lipid rich diet. The rescue of survival coincided with a reduction of *upd3* expression alongside a rescue of the hyperglycaemia-like phenotype induced in flies under a lipid rich diet. These data suggest a possible plasmatocyte *crq* and *upd3* mediated signalling cascade, which is activated after chronic dietary lipid exposure, resulting in dysregulation of metabolism, and premature fly death. Figure 7-6 represents a model for the potential *crq-upd3* mediated response to excess dietary lipids, including potential *dome* expressing target tissues.

On the basis of the findings described in this thesis, potential high fat diet disease preventive therapies would aim at reducing macrophage derived *CD36* activity or JAK-STAT pathway activation. Tissue specific gene inactivation or silencing of *CD36* and *IL-*

*6* in murine macrophages may help to further characterise the high fat diet induced disease mechanism in a mammalian model.

This thesis highlights a plasmatocyte specific and therefore macrophage specific role in the progression of high fat diet induced diseases. Further research is required to fully decipher the signalling pathways and mechanisms involved, however the identification of a macrophage specific role could prove significant in enabling a better understanding of high fat diet disease aetiology.

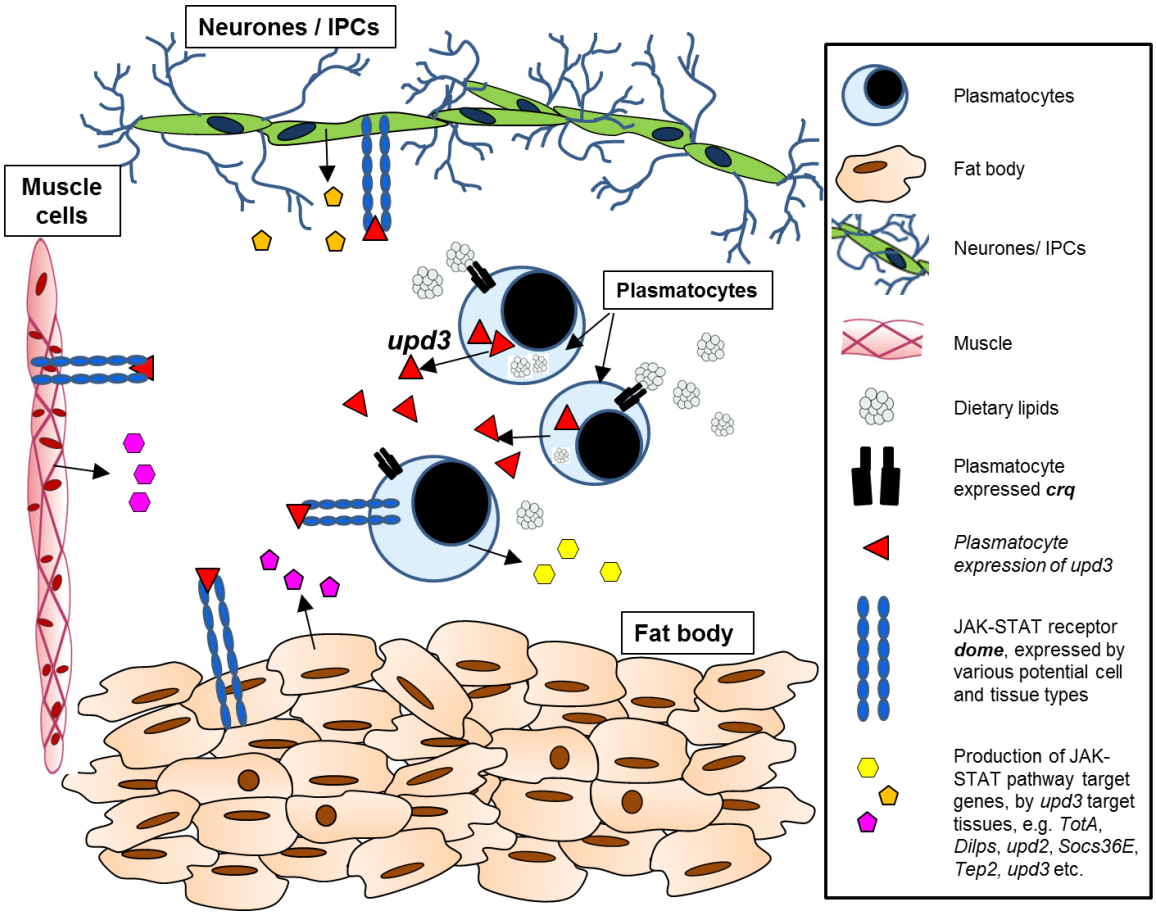


*Figure 7-6 A model for plasmatocyte crq-upd3 mediated high fat diet induced pathology*
Lipid sensing/scavenging by *crq* induces plasmatocyte derived expression and secretion of *upd3*. *Upd3* goes on to bind to its cognate receptor, *dome*, on target tissues, which are yet to be defined, such as neurones, IPCs, muscle cells the fat body or potentially plasmatocytes themselves. This consequently activates JAK-STAT pathway signalling in these target tissues, resulting in transcription of undefined downstream JAK-STAT pathway target genes, such as *upd2*, *TotA*, *Tep2*, *Socs36E*, *Dilps*, *upd3* itself and potentially other as yet undefined molecules, which results in the progression of high fat diet induced metabolic dysregulation and ultimately early death.

# References


Abrams, J. M., Lux, A., Steller, H. & Krieger, M. 1992. Macrophages in Drosophila embryos and L2 cells exhibit scavenger receptor-mediated endocytosis. *Proceedings of the National Academy of Sciences,* 89**,** 10375-10379.

Adams, M. D., Celniker, S. E., Holt, R. A., Evans, C. A., Gocayne, J. D., Amanatides, P. G., Scherer, S. E., Li, P. W., Hoskins, R. A. & Galle, R. F. 2000. The genome sequence of Drosophila melanogaster. *Science,* 287**,** 2185-2195.

Agaisse, H., Petersen, U. M., Boutros, M., Mathey-Prevot, B. & Perrimon, N. 2003. Signaling Role of Hemocytes in Drosophila JAK/STAT-Dependent Response to Septic Injury. *Developmental Cell,* 5**,** 441-450.

Aguila, J. R., Suszko, J., Gibbs, A. G. & Hoshizaki, D. K. 2007. The role of larval fat cells in adult Drosophila melanogaster. *Journal of Experimental Biology,* 210**,** 956-963.

Aitman, T. J., Glazier, A. M., Wallace, C. A., Cooper, L. D., Norsworthy, P. J., Wahid, F. N., Al-Majali, K. M., Trembling, P. M., Mann, C. J. & Shoulders, C. C. 1999. Identification of Cd36 (Fat) as an insulin-resistance gene causing defective fatty acid and glucose metabolism in hypertensive rats. *Nature Genetics,* 21**,** 76-83.

Al-Anzi, B. & Zinn, K. 2010. Colorimetric measurement of triglycerides cannot provide an accurate measure of stored fat content in Drosophila. *PLoS ONE,* 5**,** e12353.

Anderson, R. M., Shanmuganayagam, D. & Weindruch, R. 2009. Caloric restriction and aging: studies in mice and monkeys. *Toxicologic Pathology,* 37**,** 47-51.

Arrese, E. L. & Soulages, J. L. 2010. Insect fat body: energy, metabolism, and regulation. *Annual Review of Entomology,* 55**,** 207.

Ascherio, A., Rimm, E. B., Giovannucci, E. L., Spiegelman, D., Meir, S. & Willett, W. C. 1996. Dietary fat and risk of coronary heart disease in men: cohort follow up study in the United States. *Bmj,* 313**,** 84-90.

Ashburner, M. 1989. *Drosophila A laboratory manual,* Cold Spring Harbour Press, New York.

Babcock, D. T., Brock, A. R., Fish, G. S., Wang, Y., Perrin, L., Krasnow, M. A. & Galko, M. J. 2008. Circulating blood cells function as a surveillance system for damaged tissue in Drosophila larvae. *Proceedings of the National Academy of Sciences,* 105**,** 10017-10022.

Badimon, L., Storey, R. F. & Vilahur, G. 2011. Update on lipids, inflammation and atherothrombosis. *Thrombosis and haemostasis,* 105**,** 34.

Baird, G. S., Zacharias, D. A. & Tsien, R. Y. 2000. Biochemistry, mutagenesis, and oligomerization of DsRed, a red fluorescent protein from coral. *Proceedings of the National Academy of Sciences,* 97**,** 11984-11989.

Baker, K. D. & Thummel, C. S. 2007. Diabetic Larvae and Obese Flies - Emerging Studies of Metabolism in Drosophila. *Cell Metab,* 6**,** 257-266.

Barolo, S., Castro, B., Posakony J. W. 2004. New Drosophila transgenic reporters: insulated P-element vectors expressing fast-maturing RFP. *BioTechniques,* 36**,** 436-442.

Bastard, J. P., Jardel, C., Delattre, J., Hainque, B., Bruckert, E. & Oberlin, F. 1999. Evidence for a link between adipose tissue interleukin-6 content and serum C-reactive protein concentrations in obese subjects. *Circulation,* 99**,** 2219c-2222.

Beckingham, K. M., Armstrong, J. D., Texada, M. J., Munjaal, R. & Baker, D. A. 2007. Drosophila melanogaster-the model organism of choice for the complex biology of multi-cellular organisms. *Gravitational and Space Biology,* 18.

Beller, M., Riedel, D., Jänsch, L., Dieterich, G., Wehland, J., Jäckle, H. & Kühnlein, R. P. 2006. Characterization of the Drosophila lipid droplet subproteome. *Molecular & Cellular Proteomics,* 5**,** 1082-1094.

Benton, R., Vannice, K. S. & Vosshall, L. B. 2007. An essential role for a CD36-related receptor in pheromone detection in Drosophila. *Nature,* 450**,** 289-293.

Berliner, J. A., Navab, M., Fogelman, A. M., Frank, J. S., Demer, L. L., Edwards, P. A., Watson, A. D. & Lusis, A. J. 1995. Atherosclerosis: basic mechanisms: oxidation, inflammation, and genetics. *Circulation,* 91**,** 2488-2496.

Bernardoni, R., Vivancos, V. & Giangrande, A. 1997. glide/gcm is expressed and required in the scavenger cell lineage. *Developmental Biology,* 191**,** 118.

Binari, R. & Perrimon, N. 1994. Stripe-specific regulation of pair-rule genes by hopscotch, a putative Jak family tyrosine kinase in Drosophila. *Genes & Development,* 8**,** 300-312.

Birse, R. T. & Bodmer, R. 2011. Lipotoxicity and cardiac dysfunction in mammals and Drosophila.

Birse, R. T., Choi, J., Reardon, K., Rodriguez, J., Graham, S., Diop, S., Ocorr, K., Bodmer, R. & Oldham, S. 2010. High-fat-diet-induced obesity and heart dysfunction are regulated by the TOR pathway in Drosophila. *Cell Metab,* 12**,** 533-44.

Biswas, S. K. & Mantovani, A. 2012. Orchestration of Metabolism by Macrophages. *Cell Metab,* 15**,** 432-437.

Brand, A. H. & Perrimon, N. 1993. Targeted gene expression as a means of altering cell fates and generating dominant phenotypes. *Development,* 118**,** 401-415.

Broughton, S. J., Piper, M. D. W., Ikeya, T., Bass, T. M., Jacobson, J., Driege, Y., Martinez, P., Hafen, E., Withers, D. J. & Leevers, S. J. 2005. Longer lifespan, altered metabolism, and stress resistance in Drosophila from ablation of cells making insulin-like ligands. *Proc Natl Acad Sci U S A,* 102**,** 3105-3110.

Brown, S., Hu, N. & Hombría, J. 2001. Identification of the first invertebrate interleukin JAK/STAT receptor, the Drosophila gene domeless. *Current biology: CB,* 11**,** 1700.

Buchon, N., Broderick, N. A., Chakrabarti, S. & Lemaitre, B. 2009a. Invasive and indigenous microbiota impact intestinal stem cell activity through multiple pathways in Drosophila. *Genes & Development,* 23**,** 2333-2344.

Buchon, N., Broderick, N. A., Poidevin, M., Pradervand, S. & Lemaitre, B. 2009b. Drosophila intestinal response to bacterial infection: activation of host defense and stem cell proliferation.

Buszczak, M., Lu, X., Segraves, W. A., Chang, T. Y. & Cooley, L. 2002. Mutations in the midway gene disrupt a Drosophila acyl coenzyme A: diacylglycerol acyltransferase. *Genetics,* 160**,** 1511-1518.

Buttitta, L. A., Katzaroff, A. J., Perez, C. L., De La Cruz, A. & Edgar, B. A. 2007. A Double-Assurance Mechanism Controls Cell Cycle Exit upon Terminal Differentiation in Drosophila. *Developmental Cell,* 12**,** 631-643.

Canavoso, L. E., Jouni, Z. E., Karnas, K. J., Pennington, J. E. & Wells, M. A. 2001. Fat metabolism in insects. *Annual Review of Nutrition,* 21**,** 23-46.

Cavaillon, J. 1994. Cytokines and macrophages. *Biomedicine & pharmacotherapy,* 48**,** 445-453.

Charroux, B. & Royet, J. 2009. Elimination of plasmatocytes by targeted apoptosis reveals their role in multiple aspects of the Drosophila immune response. *Proceedings of the National Academy of Sciences,* 106**,** 9797-9802.

Clark, R. I., Woodcock, K. J., Geissmann, F., Trouillet, C. & Dionne, M. S. 2011. Multiple TGF-β Superfamily Signals Modulate the Adult Drosophila Immune Response. *Current Biology*.

Clementi, A. H., Gaudy, A. M., Van Rooijen, N., Pierce, R. H. & Mooney, R. A. 2009. Loss of Kupffer cells in diet-induced obesity is associated with increased hepatic steatosis, STAT3 signaling, and further decreases in insulin signaling. *Biochimica et biophysica acta,* 1792**,** 1062.

Colombani, J., Bianchini, L., Layalle, S., Pondeville, E., Dauphin-Villemant, C., Antoniewski, C., Carré, C., Noselli, S. & Léopold, P. 2005. Antagonistic actions of ecdysone and insulins determine final size in Drosophila. *Science Signalling,* 310**,** 667.

Cowley, D. E. & Atchley, W. R. 1988. Quantitative genetics of Drosophila melanogaster. II. Heritabilities and genetic correlations between sexes for head and thorax traits. *Genetics,* 119**,** 421-433.

Crozatier, M. & Meister, M. 2007. Drosophila haematopoiesis. *Cell Microbiol,* 9**,** 1117-26.

Dearolf, C. 1999. JAKs and STATs in invertebrate model organisms. *Cellular and Molecular Life Sciences,* 55**,** 1578-1584.

Dostert, C., Jouanguy, E., Irving, P., Troxler, L., Galiana-Arnoux, D., Hetru, C., Hoffmann, J. A. & Imler, J. L. 2005. The Jak-STAT signaling pathway is required but not sufficient for the antiviral response of drosophila. *Nature Immunology,* 6**,** 946-953.

Driver, C., Wallis, R., Cosopodiotis, G. & Ettershank, G. 1986. Is a fat metabolite the major diet dependent accelarator of aging? *Experimental gerontology,* 21**,** 497-507.

Driver, C. J. I. & Cosopodiotis, G. 1979. The effect of dietary fat on longevity of Drosophila melanogaster. *Experimental gerontology,* 14**,** 95-100.

Dushay, M. S., Asling, B. & Hultmark, D. 1996. Origins of immunity: Relish, a compound Rel-like gene in the antibacterial defense of Drosophila. *Proceedings of the National Academy of Sciences,* 93**,** 10343-10347.

Duvic, B., Hoffmann, J. A., Meister, M. & Royet, J. 2002. Notch Signaling Controls Lineage Specification during Drosophila Larval Hematopoiesis. *Current Biology,* 12**,** 1923-1927.

Eckel, R. H., Grundy, S. M. & Zimmet, P. Z. 2005. The metabolic syndrome. *The Lancet,* 365**,** 1415-1428.

Ekengren, S. & Hultmark, D. 2001. A family of Turandot-related genes in the humoral stress response of Drosophila. *Biochemical and Biophysical Research Communications,* 284**,** 998-1003.

Elrod-Erickson, M., Mishra, S. & Schneider, D. 2000. Interactions between the cellular and humoral immune responses in Drosophila. *Current biology: CB,* 10**,** 781.

Evans, C. J., Hartenstein, V. & Banerjee, U. 2003. Thicker Than Blood: Conserved Mechanisms in Drosophila and Vertebrate Hematopoiesis. *Developmental Cell,* 5**,** 673-690.

Evans, C. J., Sinenko, S. A., Mandal, L., Martinez-Agosto, J. A., Hartenstein, V. & Banerjee, U. 2007. Genetic Dissection of Hematopoiesis Using Drosophila as a Model System. *Advances in Developmental Biology,* 18**,** 259-299.

Falagas, M. E. & Kompoti, M. 2006. Obesity and infection. *The Lancet infectious diseases,* 6**,** 438-446.

Febbraio, M., Hajjar, D. P. & Silverstein, R. L. 2001. CD36: a class B scavenger receptor involved in angiogenesis, atherosclerosis, inflammation, and lipid metabolism. *Journal of Clinical Investigation,* 108**,** 785-792.

Feng, B., Jiao, P., Nie, Y., Kim, T., Jun, D., Van Rooijen, N., Yang, Z. & Xu, H. 2011. Clodronate liposomes improve metabolic profile and reduce visceral adipose macrophage content in diet-induced obese mice. *PLoS ONE,* 6**,** e24358.

Fessler, L., Nelson, R. & Fessler, J. 1994. Drosophila extracellular matrix. *Methods in Enzymology,* 245**,** 271.

Festa, A., D'agostino, R., Tracy, R. P. & Haffner, S. M. 2002. Elevated Levels of Acute-Phase Proteins and Plasminogen Activator Inhibitor-1 Predict the Development of Type 2 Diabetes The Insulin Resistance Atherosclerosis Study. *Diabetes,* 51**,** 1131-1137.

Feuerer, M., Herrero, L., Cipolletta, D., Naaz, A., Wong, J., Nayer, A., Lee, J., Goldfine, A. B., Benoist, C. & Shoelson, S. 2009. Lean, but not obese, fat is enriched for a unique population of regulatory T cells that affect metabolic parameters. *Nature Medicine,* 15**,** 930-939.

Ford, E. S., Giles, W. H. & Mokdad, A. H. 2004. Increasing prevalence of the metabolic syndrome among US adults. *Diabetes care,* 27**,** 2444-2449.

Franc, N. C., Dimarcq, J. L., Lagueux, M., Hoffmann, J. & Ezekowitz, R. a. B. 1996. Croquemort, a novel Drosophila hemocyte/macrophage receptor that recognizes apoptotic cells. *Immunity,* 4**,** 431-443.

Franc, N. C., Heitzler, P. & White, K. 1999. Requirement for croquemort in phagocytosis of apoptotic cells in Drosophila. *Science,* 284**,** 1991-1994.

Galko, M. J. & Krasnow, M. A. 2004. Cellular and genetic analysis of wound healing in Drosophila larvae. *PLoS Biology,* 2**,** e239.

Gay, N. J. & Keith, F. J. 1991. Drosophila Toll and IL-1 receptor. *Nature,* 351**,** 355.

Glass, C. K. 2002. The macrophage foam cell as a target for therapeutic intervention. *Nat. Med,* 8**,** 1235-1242.

Gorski, S. M., Chittaranjan, S., Pleasance, E. D., Freeman, J., Anderson, C. L., Varhol, R. J., Coughlin, S. M., Zuyderduyn, S. D., Jones, S. J. M. & Marra, M. A. 2003. A SAGE approach to discovery of genes involved in autophagic cell death. *Current Biology,* 13**,** 358-363.

Goto, A., Kadowaki, T. & Kitagawa, Y. 2003. Drosophila hemolectin gene is expressed in embryonic and larval hemocytes and its knock down causes bleeding defects1. *Developmental Biology,* 264**,** 582-591.

Goto, A., Kumagai, T., Kumagai, C., Hirose, J., Narita, H., Mori, H., Kadowaki, T., Beck, K. & Kitagawa, Y. 2001. A Drosophila haemocyte-specific protein, hemolectin, similar to human von Willebrand factor. *Biochemical Journal,* 359**,** 99.

Gray, S. & Kim, J. K. 2011. New insights into insulin resistance in the diabetic heart. *Trends in Endocrinology & Metabolism,* 22**,** 394-403.

Greenspan, R. J. 2004. Fly Pushing: The Theory and Practice of *Drosophila* Genetics. Cold Spring Harbor, New York: Cold Spring Harbor Laboratory Press.

Grönke, S., Beller, M., Fellert, S., Ramakrishnan, H., Jäckle, H. & Kühnlein, R. 2003. Control of fat storage by a Drosophila PAT domain protein. *Current biology: CB,* 13**,** 603.

Grönke, S., Mildner, A., Fellert, S., Tennagels, N., Petry, S., Müller, G., Jäckle, H. & Kühnlein, R. 2005. Brummer lipase is an evolutionary conserved fat storage regulator in Drosophila. *Cell Metab,* 1**,** 323.

Gutierrez, E., Wiggins, D., Fielding, B. & Gould, A. P. 2006. Specialized hepatocyte-like cells regulate Drosophila lipid metabolism. *Nature,* 445**,** 275-280.

Hardie, D. & Pan, D. 2002. Regulation of fatty acid synthesis and oxidation by the AMP-activated protein kinase. *Biochemical Society Transactions,* 30**,** 1064-1070.

Harrison, D. A., Mccoon, P. E., Binari, R., Gilman, M. & Perrimon, N. 1998. Drosophila unpaired encodes a secreted protein that activates the JAK signaling pathway. *Genes & Development,* 12**,** 3252-3263.

Heinrichsen, E. T. & Haddad, G. G. 2012. Role of High-Fat Diet in Stress Response of Drosophila. *PLoS ONE,* 7**,** e42587.

Helmchen, F. & Denk, W. 2005. Deep tissue two-photon microscopy. *Nature Methods,* 2**,** 932-940.

Herboso, L., Talamillo, A., Pérez, C. & Barrio, R. 2011. Expression of the Scavenger Receptor Class B type I (SR-BI) family in Drosophila melanogaster. *Int. J. Dev. Biol,* 55**,** 603-611.

Hirosumi, J., Tuncman, G., Chang, L., Gorgun, C., Uysal, K. T., Maeda, K., Karin, K. & Hotamisligil, G. S. 2002. A central role for JNK in obesity and insulin resistance. *Nature,* 420**,** 333-336.

Holz, A., Bossinger, B., Strasser, T., Janning, W. & Klapper, R. 2003. The two origins of hemocytes in Drosophila. *Development,* 130**,** 4955-4962.

Hombría, J., Brown, S., Häder, S. & Zeidler, M. 2005. Characterisation of Upd2, a Drosophila JAK/STAT pathway ligand. *Developmental Biology,* 288**,** 420.

Hombría, J. C. G. & Brown, S. 2002. The fertile field of Drosophila Jak/STAT signalling. *Current Biology,* 12**,** 569-575.

Hoshizaki, D. K., Lunz, R., Johnson, W. & Ghosh, M. 1995. Identification of fat-cell enhancer activity in Drosophila melanogaster using P-element enhancer traps. *Genome,* 38**,** 497-506.

Hou, X., Melnick, M. & Perrimon, N. 1996. Marelle acts downstream of the Drosophila HOP/JAK kinase and encodes a protein similar to the mammalian STATs. *Cell,* 84**,** 411.

Hu, F. B., Manson, J. a. E. & Willett, W. C. 2001. Types of dietary fat and risk of coronary heart disease: a critical review. *Journal of the American College of Nutrition,* 20**,** 5-19.

Huang, M. M., Bolen, J. B., Barnwell, J. W., Shattil, S. J. & Brugge, J. S. 1991. Membrane glycoprotein IV (CD36) is physically associated with the Fyn, Lyn, and Yes protein-tyrosine kinases in human platelets. *Proceedings of the National Academy of Sciences,* 88**,** 7844-7848.

Ip, Y., Reach, M., Engstrom, Y., Kadalayil, L., Cai, H., González-Crespo, S., Tatei, K. & Levine, M. 1993. Dif, a dorsal-related gene that mediates an immune response in Drosophila. *Cell,* 75**,** 753.

Irving, P., Ubeda, J. M., Doucet, D., Troxler, L., Lagueux, M., Zachary, D., Hoffmann, J. A., Hetru, C. & Meister, M. 2004. New insights into Drosophila larval haemocyte functions through genome-wide analysis. *Cellular Microbiology,* 7**,** 335-350.

Jacques, C., Soustelle, L., Nagy, I., Diebold, C. & Giangrande, A. 2009. A novel role of the glial fate determinant glial cells missing in hematopoiesis. *Int J Dev Biol,* 53**,** 1013-22.

Janabi, M., Yamashita, S., Hirano, K., Sakai, N., Hiraoka, H., Matsumoto, K., Zhang, Z., Nozaki, S. & Matsuzawa, Y. 2000. Oxidized LDL–Induced NF-κB Activation and Subsequent Expression of Proinflammatory Genes Are Defective in Monocyte-Derived Macrophages From CD36-Deficient Patients. *Arteriosclerosis, Thrombosis, and Vascular Biology,* 20**,** 1953-1960.

Jenkins, S. J., Ruckerl, D., Cook, P. C., Jones, L. H., Finkelman, F. D., Van Rooijen, N., Macdonald, A. S. & Allen, J. E. 2011. Local macrophage proliferation, rather than recruitment from the blood, is a signature of TH2 inflammation. *Science,* 332**,** 1284-1288.

Jiang, H., Patel, P. H., Kohlmaier, A., Grenley, M. O., Mcewen, D. G. & Edgar, B. A. 2009. Cytokine/Jak/Stat signaling mediates regeneration and homeostasis in the Drosophila midgut. *Cell,* 137**,** 1343.

Jiménez, B., Volpert, O. V., Crawford, S. E., Febbraio, M., Silverstein, R. L. & Bouck, N. 2000. Signals leading to apoptosis-dependent inhibition of neovascularization by thrombospondin-1. *Nature Medicine,* 6**,** 41-48.

Jung, S. H., Evans, C. J., Uemura, C. & Banerjee, U. 2005. The Drosophila lymph gland as a developmental model of hematopoiesis. *Development,* 132**,** 2521-2533.

Kahn, S. E., Hull, R. L. & Utzschneider, K. M. 2006. Mechanisms linking obesity to insulin resistance and type 2 diabetes. *Nature,* 444**,** 840-846.

Kamei, N., Tobe, K., Suzuki, R., Ohsugi, M., Watanabe, T., Kubota, N., Ohtsuka-Kowatari, N., Kumagai, K., Sakamoto, K. & Kobayashi, M. 2006. Overexpression of monocyte chemoattractant protein-1 in adipose tissues causes macrophage recruitment and insulin resistance. *Journal of Biological Chemistry,* 281**,** 26602-26614.

Kanda, H., Tateya, S., Tamori, Y., Kotani, K., Hiasa, K., Kitazawa, R., Kitazawa, S., Miyachi, H., Maeda, S. & Egashira, K. 2006. MCP-1 contributes to macrophage infiltration into adipose tissue, insulin resistance, and hepatic steatosis in obesity. *Journal of Clinical Investigation,* 116**,** 1494.

Kaneko, T., Goldman, W. E., Mellroth, P., Steiner, H., Fukase, K., Kusumoto, S., Harley, W., Fox, A., Golenbock, D. & Silverman, N. 2004. Monomeric and Polymeric Gram-Negative Peptidoglycan but Not Purified LPS Stimulate the Drosophila IMD Pathway. *Immunity,* 20**,** 637-649.

Kaneko, T. & Silverman, N. 2005. Bacterial recognition and signalling by the Drosophila IMD pathway. *Cellular Microbiology,* 7**,** 461-469.

Kannel, W. B., Castelli, W. P., Gordon, T. & Mcnamara, P. M. 1971. Serum cholesterol, lipoproteins, and the risk of coronary heart disease. The Framingham study. *Annals of Internal Medicine,* 74**,** 1.

Karsten, P., Häder, S. & Zeidler, M. P. 2002. Cloning and expression of Drosophila SOCS36E and its potential regulation by the JAK/STAT pathway. *Mechanisms of development,* 117**,** 343.

Kennedy, D. J., Kuchibhotla, S., Westfall, K. M., Silverstein, R. L., Morton, R. E. & Febbraio, M. 2011. A CD36-dependent pathway enhances macrophage and adipose tissue inflammation and impairs insulin signalling. *Cardiovascular research,* 89**,** 604-613.

Kocks, C., Cho, J. H., Nehme, N., Ulvila, J., Pearson, A. M., Meister, M., Strom, C., Conto, S. L., Hetru, C. & Stuart, L. M. 2005. Eater, a Transmembrane Protein Mediating Phagocytosis of Bacterial Pathogens in Drosophila. *Cell,* 123**,** 335-346.

Konopka, R. J. & Benzer, S. 1971. Clock mutants of Drosophila melanogaster. *Proceedings of the National Academy of Sciences,* 68**,** 2112-2116.

Koopman, R., Schaart, G. & Hesselink, M. K. 2001. Optimisation of oil red O staining permits combination with immunofluorescence and automated quantification of lipids. *Histochemistry and cell biology,* 116**,** 63-68.

Krupp, J. J. & Levine, J. D. 2010. Dissection of Oenocytes from Adult Drosophila melanogaster. *Journal of Visualized Experiments: JoVE*.

Krzemien, J., Crozatier, M. & Vincent, A. 2010. Ontogeny of the Drosophila larval hematopoietic organ, hemocyte homeostasis and the dedicated cellular immune response to parasitism. *International Journal of Developmental Biology,* 54**,** 1117.

Kurucz, E., Márkus, R., Zsámboki, J., Folkl-Medzihradszky, K., Darula, Z., Vilmos, P., Udvardy, A., Krausz, I., Lukacsovich, T. & Gateff, E. 2007a. Nimrod, a putative phagocytosis receptor with EGF repeats in Drosophila plasmatocytes. *Current biology: CB,* 17**,** 649.

Kurucz, É., Vaczi, B., Markus, R., Laurinyecz, B., Vilmos, P., Zsamboki, J., Csorba, K., Gateff, E., Hultmark, D. & Ando, I. 2007b. Definition of Drosophila hemocyte subsets by cell-type specific antigens. *Acta Biologica Hungarica,* 58**,** 95-111.

Kurucz, E., Zettervall, C. J., Sinka, R., Vilmos, P., Pivarcsi, A., Ekengren, S., Hegedüs, Z., Ando, I. & Hultmark, D. 2003. Hemese, a hemocyte-specific transmembrane protein, affects the cellular immune response in Drosophila. *Proceedings of the National Academy of Sciences,* 100**,** 2622-2627.

Lagueux, M., Perrodou, E., Levashina, E. A., Capovilla, M. & Hoffmann, J. A. 2000. Constitutive expression of a complement-like protein in toll and JAK gain-of-function mutants of Drosophila. *Proceedings of the National Academy of Sciences,* 97**,** 11427-11432.

Lanot, R., Zachary, D., Holder, F. & Meister, M. 2001. Postembryonic Hematopoiesis in Drosophila. *Developmental Biology,* 230**,** 243-257.

Lanthier, N., Molendi-Coste, O., Horsmans, Y., Van Rooijen, N., Cani, P. D. & Leclercq, I. A. 2010. Kupffer cell activation is a causal factor for hepatic insulin resistance.

*American Journal of Physiology-Gastrointestinal and Liver Physiology,* 298**,** G107-G116.

Lazzaro, B. P. 2005. Elevated polymorphism and divergence in the class C scavenger receptors of Drosophila melanogaster and D. simulans. *Genetics,* 169**,** 2023-2034.

Lebestky, T., Chang, T., Hartenstein, V. & Banerjee, U. 2000. Specification of Drosophila hematopoietic lineage by conserved transcription factors. *Science,* 288**,** 146-149.

Lee, C. Y., Cooksey, B. a. K. & Baehrecke, E. H. 2002. Steroid Regulation of Midgut Cell Death during Drosophila Development. *Developmental Biology,* 250**,** 101-111.

Lemaitre, B. & Hoffmann, J. 2007. The host defense of Drosophila melanogaster. *Annual Review of Immunology,* 25**,** 697-743.

Lemaitre, B., Kromer-Metzger, E., Michaut, L., Nicolas, E., Meister, M., Georgel, P., Reichhart, J. M. & Hoffmann, J. A. 1995. A recessive mutation, immune deficiency (imd), defines two distinct control pathways in the Drosophila host defense. *Proceedings of the National Academy of Sciences,* 92**,** 9465-9469.

Lemaitre, B., Nicolas, E., Michaut, L., Reichhart, J. M. & Hoffmann, J. A. 1996. The Dorsoventral Regulatory Gene Cassette spa tzle/Toll/cactus Controls the Potent Antifungal Response in Drosophila Adults. *Cell,* 86**,** 973-983.

Lemaitre, B., Reichhart, J. M. & Hoffmann, J. A. 1997. Drosophila host defense: differential induction of antimicrobial peptide genes after infection by various classes of microorganisms. *Proceedings of the National Academy of Sciences,* 94**,** 14614-14619.

Leopold, P. & Perrimon, N. 2007. Drosophila and the genetics of the internal milieu. *Nature,* 450**,** 186-8.

Leprêtre, F., Vasseur, F., Vaxillaire, M., Scherer, P. E., Ali, S., Linton, K., Aitman, T. & Froguel, P. 2004. A CD36 nonsense mutation associated with insulin resistance and familial type 2 diabetes. *Human Mutation,* 24**,** 104-104.

Lesch, C., Goto, A., Lindgren, M., Bidla, G., Dushay, M. S. & Theopold, U. 2007. A role for Hemolectin in coagulation and immunity in Drosophila melanogaster. *Developmental & Comparative Immunology,* 31**,** 1255-1263.

Li, A. C. & Glass, C. K. 2002. The macrophage foam cell as a target for therapeutic intervention. *Nature Medicine,* 8**,** 1235-1242.

Linton, M. R. F. & Fazio, S. 2003. Macrophages, inflammation, and atherosclerosis. *International Journal of Obesity,* 27**,** S35-S40.

Love-Gregory, L., Sherva, R., Sun, L., Wasson, J., Schappe, T., Doria, A., Rao, D. C., Hunt, S. C., Klein, S. & Neuman, R. J. 2008. Variants in the CD36 gene associate with the metabolic syndrome and high-density lipoprotein cholesterol. *Human Molecular Genetics,* 17**,** 1695-1704.

Lumeng, C. N., Deyoung, S. M., Bodzin, J. L. & Saltiel, A. R. 2007. Increased inflammatory properties of adipose tissue macrophages recruited during diet-induced obesity. *Diabetes,* 56**,** 16-23.

Luo, H., Rose, P., Barber, D., Hanratty, W. P., Lee, S., Roberts, T. M., D'andrea, A. D. & Dearolf, C. R. 1997. Mutation in the Jak kinase JH2 domain hyperactivates Drosophila and mammalian Jak-Stat pathways. *Molecular and Cellular Biology,* 17**,** 1562-1571.

Manfruelli, P., Reichhart, J. M., Steward, R., Hoffmann, J. A. & Lemaitre, B. 1999. A mosaic analysis in Drosophila fat body cells of the control of antimicrobial peptide genes by the Rel proteins Dorsal and DIF. *The EMBO journal,* 18**,** 3380-3391.

Martin, C., Chevrot, M., Poirier, H., Passilly-Degrace, P., Niot, I. & Besnard, P. 2011. CD36 as a lipid sensor. *Physiology & Behavior,* 105**,** 36-42.

Martinez-Agosto, J. A., Mikkola, H. K. A., Hartenstein, V. & Banerjee, U. 2007. The hematopoietic stem cell and its niche: a comparative view. *Genes & Development,* 21**,** 3044-3060.

Mccay, C. M., Crowell, M. F. & Maynard, L. 1935. The effect of retarded growth upon the length of life span and upon the ultimate body size. *J Nutr,* 10**,** 63-79.

Mcgraw, L., Gibson, G., Clark, A. & Wolfner, M. 2004. Genes regulated by mating, sperm, or seminal proteins in mated female Drosophila melanogaster. *Current biology: CB,* 14**,** 1509.

Mcguire, S. E., Mao, Z. & Davis, R. L. 2004. Spatiotemporal gene expression targeting with the TARGET and gene-switch systems in Drosophila. *Science Signalling,* 2004**,** pl6.

Meister, M. & Lagueux, M. 2003. Drosophila blood cells. *Cellular Microbiology,* 5**,** 573-580.

Miyaoka, K., Kuwasako, T., Hirano, K., Nozaki, S., Yamashita, S. & Matsuzawa, Y. 2001. CD36 deficiency associated with insulin resistance. *The Lancet,* 357**,** 686-687.

Mohamed-Ali, V., Goodrick, S., Rawesh, A., Katz, D., Miles, J., Yudkin, J., Klein, S. & Coppack, S. 1997. Subcutaneous adipose tissue releases interleukin-6, but not tumor necrosis factor-α, in vivo. *Journal of Clinical Endocrinology & Metabolism,* 82**,** 4196-4200.

Nakashima, Y., Plump, A. S., Raines, E. W., Breslow, J. L. & Ross, R. 1994. ApoE-deficient mice develop lesions of all phases of atherosclerosis throughout the arterial tree. *Arteriosclerosis, Thrombosis, and Vascular Biology,* 14**,** 133-140.

Nelson, R., Fessler, L., Takagi, Y., Blumberg, B., Keene, D., Olson, P., Parker, C. & Fessler, J. 1994. Peroxidasin: a novel enzyme-matrix protein of Drosophila development. *The EMBO journal,* 13**,** 3438.

Nicholls, H. T., Kowalski, G., Kennedy, D. J., Risis, S., Zaffino, L. A., Watson, N., Kanellakis, P., Watt, M. J., Bobik, A. & Bonen, A. 2011. Hematopoietic Cell–Restricted Deletion of CD36 Reduces High-Fat Diet–Induced Macrophage Infiltration and Improves Insulin Signaling in Adipose Tissue. *Diabetes,* 60**,** 1100-1110.

Nichols, Z. & Vogt, R. G. 2007. The SNMP/CD36 gene family in Diptera, Hymenoptera and Coleoptera: Drosophila melanogaster, D. pseudoobscura, Anopheles gambiae, Aedes aegypti, Apis mellifera, and Tribolium castaneum. *Insect Biochemistry and Molecular Biology,* 38**,** 398-415.

Odegaard, J. I., Ricardo-Gonzalez, R. R., Goforth, M. H., Morel, C. R., Subramanian, V., Mukundan, L., Eagle, A. R., Vats, D., Brombacher, F. & Ferrante, A. W. 2007. Macrophage-specific PPAR&ggr; controls alternative activation and improves insulin resistance. *Nature,* 447**,** 1116-1120.

Oldham, S. 2011. Obesity and nutrient sensing TOR pathway in flies and vertebrates: Functional conservation of genetic mechanisms. *Trends in Endocrinology & Metabolism,* 22**,** 45-52.

Olofsson, B. & Page, D. T. 2005. Condensation of the central nervous system in embryonic Drosophila is inhibited by blocking hemocyte migration or neural activity. *Developmental Biology,* 279**,** 233-243.

Partridge, L., Piper, M. & Mair, W. 2005. Dietary restriction in Drosophila. *Mechanisms of ageing and development,* 126**,** 938.

Patsouris, D., Li, P. P., Thapar, D., Chapman, J., Olefsky, J. M. & Neels, J. G. 2008. Ablation of CD11c-positive cells normalizes insulin sensitivity in obese insulin resistant animals. *Cell Metab,* 8**,** 301-309.

Petersen, E., Carey, A., Sacchetti, M., Steinberg, G., Macaulay, S., Febbraio, M. & Pedersen, B. 2005. Acute IL-6 treatment increases fatty acid turnover in elderly

humans in vivo and in tissue culture in vitro. *American Journal of Physiology-Endocrinology And Metabolism,* 288**,** E155-E162.

Philips, J. A., Rubin, E. J. & Perrimon, N. 2005. Drosophila RNAi screen reveals CD36 family member required for mycobacterial infection. *Science,* 309**,** 1251-1253.

Pravenec, M., Landa, V., Zidek, V., Musilova, A., Kren, V., Kazdova, L., Aitman, T. J., Glazier, A. M., Ibrahimi, A. & Abumrad, N. A. 2001. Transgenic rescue of defective Cd36 ameliorates insulin resistance in spontaneously hypertensive rats. *Nature Genetics,* 27**,** 156.

Rać, M. E., Safranow, K. & Poncyljusz, W. 2007. Molecular basis of human CD36 gene mutations. *Molecular Medicine,* 13**,** 288.

Rahaman, S. O., Lennon, D. J., Febbraio, M., Podrez, E. A., Hazen, S. L. & Silverstein, R. L. 2006. A CD36-dependent signaling cascade is necessary for macrophage foam cell formation. *Cell Metab,* 4**,** 211-221.

Rajan, A. & Perrimon, N. 2012. Drosophila Cytokine Unpaired 2 Regulates Physiological Homeostasis by Remotely Controlling Insulin Secretion. *Cell,* 151**,** 123-137.

Rämet, M., Lanot, R., Zachary, D. & Manfruelli, P. 2002. JNK Signaling Pathway Is Required for Efficient Wound Healing in Drosophila. *Developmental Biology,* 241**,** 145-156.

Reichhart, J., Georgel, P., Meister, M., Lemaitre, B., Kappler, C. & Hoffmann, J. 1993. Expression and nuclear translocation of the rel/NF-kappa B-related morphogen dorsal during the immune response of Drosophila. *Comptes rendus de l'Académie des sciences. Série III, Sciences de la vie,* 316**,** 1218.

Riesgo-Escovar, J. R., Jenni, M., Fritz, A. & Hafen, E. 1996. The Drosophila Jun-N-terminal kinase is required for cell morphogenesis but not for DJun-dependent cell fate specification in the eye. *Genes & Development,* 10**,** 2759-2768.

Rizki, M. & Rizki, R. M. 1959. Functional significance of the crystal cells in the larva of Drosophila melanogaster. *The Journal of Biophysical and Biochemical Cytology,* 5**,** 235-240.

Rizki, T. & Rizki, R. M. 1992. Lamellocyte differentiation in Drosophila larvae parasitized by Leptopilina.

Rosetto, M., Engstrom, Y., Baldari, C. T., Telford, J. L. & Hultmark, D. 1995. Signals from the IL-1 receptor homolog, Toll, can activate an immune response in a Drosophila hemocyte cell line. *Biochemical and Biophysical Research Communications,* 209**,** 111-116.

Sakaue-Sawano, A., Kurokawa, H., Morimura, T., Hanyu, A., Hama, H., Osawa, H., Kashiwagi, S., Fukami, K., Miyata, T. & Miyoshi, H. 2008. Visualizing spatiotemporal dynamics of multicellular cell-cycle progression. *Cell,* 132**,** 487-498.

Samakovlis, C., Asling, B., Boman, H., Gateff, E. & Hultmark, D. 1992. In vitro induction of cecropin genes--an immune response in a Drosophila blood cell line. *Biochemical and Biophysical Research Communications,* 188**,** 1169.

Scheller, J. & Rose-John, S. 2012. The interleukin 6 pathway and atherosclerosis. *Lancet,* 380**,** 338.

Schlegel, A. & Stainier, D. Y. R. 2007. Lessons from "lower" organisms: what worms, flies, and zebrafish can teach us about human energy metabolism. *PLoS Genetics,* 3**,** e199.

Sears, H. C., Kennedy, C. J. & Garrity, P. A. 2003. Macrophage-mediated corpse engulfment is required for normal Drosophila CNS morphogenesis. *Development,* 130**,** 3557-3565.

Silverman, N., Zhou, R., Erlich, R. L., Hunter, M., Bernstein, E., Schneider, D. & Maniatis, T. 2003. Immune activation of NF-κB and JNK requires Drosophila TAK1. *Journal of Biological Chemistry,* 278**,** 48928-48934.

Silverstein, R. L. & Febbraio, M. 2000. CD36 and atherosclerosis. *Current opinion in lipidology,* 11**,** 483-491.

Silverstein, R. L. & Febbraio, M. 2009. CD36, a scavenger receptor involved in immunity, metabolism, angiogenesis, and behavior. *Science Signalling,* 2**,** re3.

Sinenko, S. A. & Mathey-Prevot, B. 2004. Increased expression of Drosophila tetraspanin, Tsp68C, suppresses the abnormal proliferation of ytr-deficient and Ras/Raf-activated hemocytes. *Oncogene,* 23**,** 9120-9128.

Spann, N. J., Garmire, L. X., Mcdonald, J. G., Myers, D. S., Milne, S. B., Shibata, N., Reichart, D., Fox, J. N., Shaked, I. & Heudobler, D. 2012. Regulated accumulation of desmosterol integrates macrophage lipid metabolism and inflammatory responses. *Cell,* 151**,** 138-152.

Stenbak, C. R., Ryu, J. H., Leulier, F., Pili-Floury, S., Parquet, C., Hervé, M., Chaput, C., Boneca, I. G., Lee, W. J. & Lemaitre, B. 2004. Peptidoglycan molecular requirements allowing detection by the Drosophila immune deficiency pathway. *The Journal of Immunology,* 173**,** 7339-7348.

Stramer, B., Wood, W., Galko, M. J., Redd, M. J., Jacinto, A., Parkhurst, S. M. & Martin, P. 2005. Live imaging of wound inflammation in Drosophila embryos reveals key roles for small GTPases during in vivo cell migration. *The Journal of cell biology,* 168**,** 567-573.

Stuart, L. M., Deng, J., Silver, J. M., Takahashi, K., Tseng, A. A., Hennessy, E. J., Ezekowitz, R. a. B. & Moore, K. J. 2005. Response to Staphylococcus aureus requires CD36-mediated phagocytosis triggered by the COOH-terminal cytoplasmic domain. *The Journal of cell biology,* 170**,** 477-485.

Suzuki, H., Kurihara, Y., Takeya, M., Kamada, N., Kataoka, M., Jishage, K., Ueda, O., Sakaguchi, H., Higashi, T. & Suzuki, T. 1997. A role for macrophage scavenger receptors in atherosclerosis and susceptibility to infection.

Szendroedi, J. & Roden, M. 2009. Ectopic lipids and organ function. *Current opinion in lipidology,* 20**,** 50-56.

Takemoto, S., Mulloy, J. C., Cereseto, A., Migone, T. S., Patel, B. K. R., Matsuoka, M., Yamaguchi, K., Takatsuki, K., Kamihira, S. & White, J. D. 1997. Proliferation of adult T cell leukemia/lymphoma cells is associated with the constitutive activation of JAK/STAT proteins. *Proceedings of the National Academy of Sciences,* 94**,** 13897-13902.

Tanji, T. & Ip, Y. T. 2005. Regulators of the Toll and Imd pathways in the Drosophila innate immune response. *Trends in Immunology,* 26**,** 193.

Taubes, G. 2001. The soft science of dietary fat. *Science,* 291**,** 2536-2545.

Teleman, A. A., Chen, Y. W. & Cohen, S. M. 2005. 4E-BP functions as a metabolic brake used under stress conditions but not during normal growth. *Genes & Development,* 19**,** 1844-1848.

Tepass, U., Fessler, L. I., Aziz, A. & Hartenstein, V. 1994. Embryonic origin of hemocytes and their relationship to cell death in Drosophila. *Development,* 120**,** 1829-1837.

Thannickal, V. J. & Fanburg, B. L. 2000. Reactive oxygen species in cell signaling. *American Journal of Physiology-Lung Cellular and Molecular Physiology,* 279**,** L1005-L1028.

Tirouvanziam, R., Davidson, C. J., Lipsick, J. S. & Herzenberg, L. A. 2004. Fluorescence-activated cell sorting (FACS) of Drosophila hemocytes reveals important functional similarities to mammalian leukocytes. *Proc Natl Acad Sci U S A,* 101**,** 2912-7.

Van Herpen, N. & Schrauwen-Hinderling, V. 2008. Lipid accumulation in non-adipose tissue and lipotoxicity. *Physiology & Behavior,* 94**,** 231-241.

VDRC 2013. Transgenic RNAi in Drosophila. CSF Campus Science Support Facilities GmbH.

Vosshall, L. B. 2008. Scent of a fly. *Neuron,* 59**,** 685-689.
Vozarova, B., Fernández-Real, J. M., Knowler, W. C., Gallart, L., Hanson, R. L., Gruber, J. D., Ricart, W., Vendrell, J., Richart, C. & Tataranni, P. A. 2003. The interleukin-6 (-174) G/C promoter polymorphism is associated with type-2 diabetes mellitus in Native Americans and Caucasians. *Human Genetics,* 112**,** 409-413.
Vozarova, B., Weyer, C., Hanson, K., Tataranni, P., Bogardus, C. & Pratley, R. 2001. Circulating interleukin-6 in relation to adiposity, insulin action, and insulin secretion. *Obes Res,* 9**,** 414-7.
Walker, G., Houthoofd, K., Vanfleteren, J. & Gems, D. 2005. Dietary restriction in C. elegans: From rate-of-living effects to nutrient sensing pathways. *Mech Ageing Dev,* 126**,** 929-937.
Wallenius, V., Wallenius, K., Ahrén, B., Rudling, M., Carlsten, H., Dickson, S. L., Ohlsson, C. & Jansson, J. O. 2002. Interleukin-6-deficient mice develop mature-onset obesity. *Nature Medicine,* 8**,** 75-79.
Waltzer, L., Ferjoux, G., Bataille, L., Haenlin, M., Zhao, J., Cao, Y., Zhao, C., Postlethwait, J., Meng, A. & Hernández-Sánchez, C. 2003. Cooperation between the GATA and RUNX factors Serpent and Lozenge during Drosophila hematopoiesis FREE. *The EMBO journal,* 22**,** 6516-6525.
Weisberg, S. P., Mccann, D., Desai, M., Rosenbaum, M., Leibel, R. L. & Ferrante Jr, A. W. 2003. Obesity is associated with macrophage accumulation in adipose tissue. *Journal of Clinical Investigation,* 112**,** 1796-1808.
Wellen, K. E. & Hotamisligil, G. S. 2005. Inflammation, stress, and diabetes. *J Clin Invest,* 115**,** 1111-1119.
Welte, M. A., Cermelli, S., Griner, J., Viera, A., Guo, Y., Kim, D. H., Gindhart, J. G. & Gross, S. P. 2005. Regulation of lipid-droplet transport by the perilipin homolog LSD2. *Current Biology,* 15**,** 1266-1275.
White, K., Grether, M. E., Abrams, J. M., Young, L., Farrell, K. & Steller, H. 1994. Genetic control of programmed cell death in Drosophila. *Science (New York, NY),* 264**,** 677.
Wood, W. & Jacinto, A. 2007. Drosophila melanogaster embryonic haemocytes: masters of multitasking. *Nature Reviews Molecular Cell Biology,* 8**,** 542-551.
Wullschleger, S., Loewith, R. & Hall, M. N. 2006. TOR signaling in growth and metabolism. *Cell,* 124**,** 471-484.
Xu, H., Barnes, G. T., Yang, Q., Tan, G., Yang, D., Chou, C. J., Sole, J., Nichols, A., Ross, J. S. & Tartaglia, L. A. 2003. Chronic inflammation in fat plays a crucial role in the development of obesity-related insulin resistance. *Journal of Clinical Investigation,* 112**,** 1821-1830.
Yan, R., Small, S., Desplan, C., Dearolf, C. & Darnell Jr, J. 1996. Identification of a Stat gene that functions in Drosophila development. *Cell,* 84**,** 421.
Yang, J., Kalhan, S. C. & Hanson, R. W. 2009. What is the metabolic role of phosphoenolpyruvate carboxykinase? *Journal of Biological Chemistry,* 284**,** 27025-27029.
Yudkin, J. S., Kumari, M., Humphries, S. E. & Mohamed-Ali, V. 2000. Inflammation, obesity, stress and coronary heart disease: is interleukin-6 the link? *Atherosclerosis,* 148**,** 209-214.
Ziegler, U. & Groscurth, P. 2004. Morphological features of cell death. *Physiology,* 19**,** 124-128.

# Appendix 1

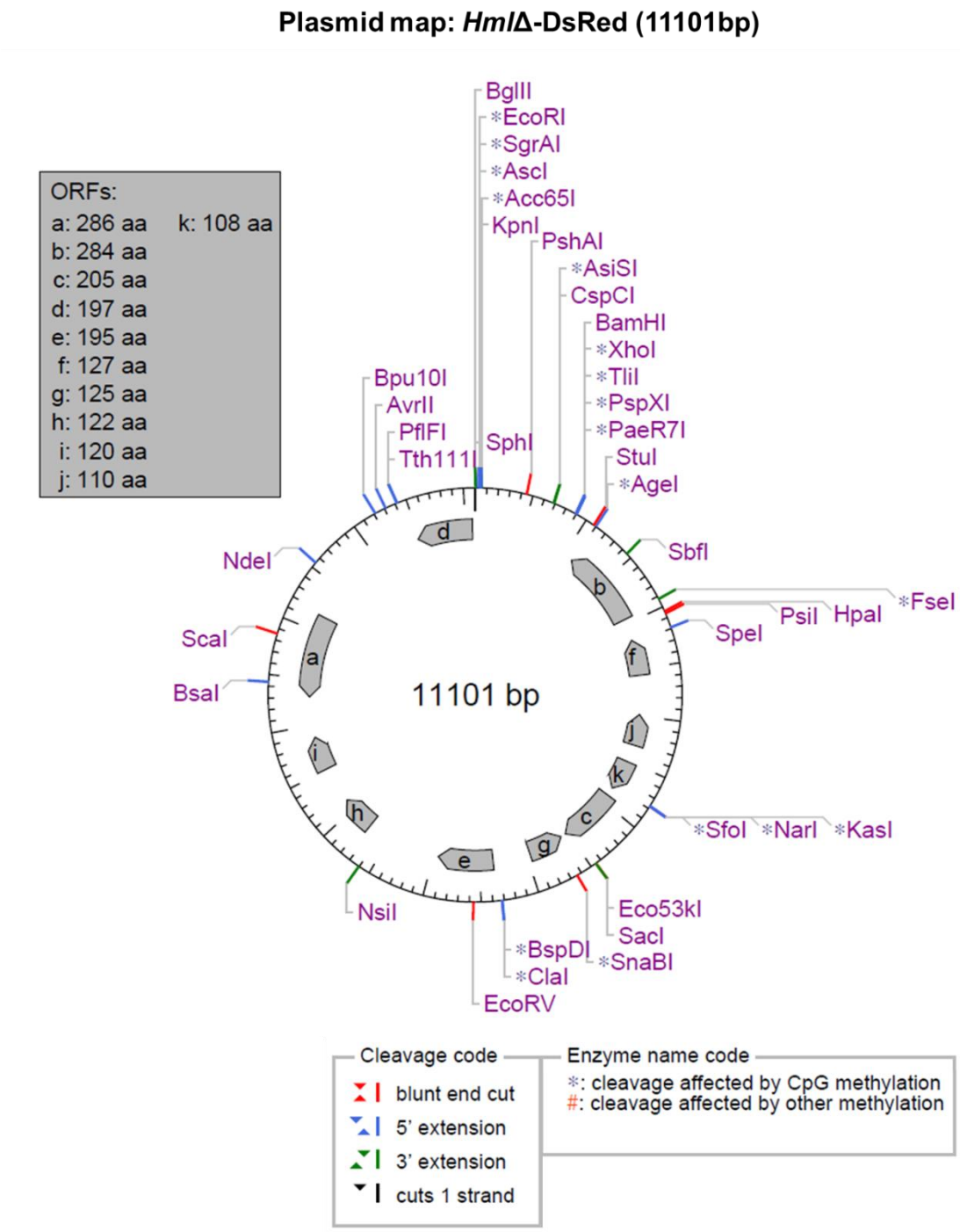


Plasmid map generated using NEB (New England Biolabs) cutter V2.0.

# Appendix 2

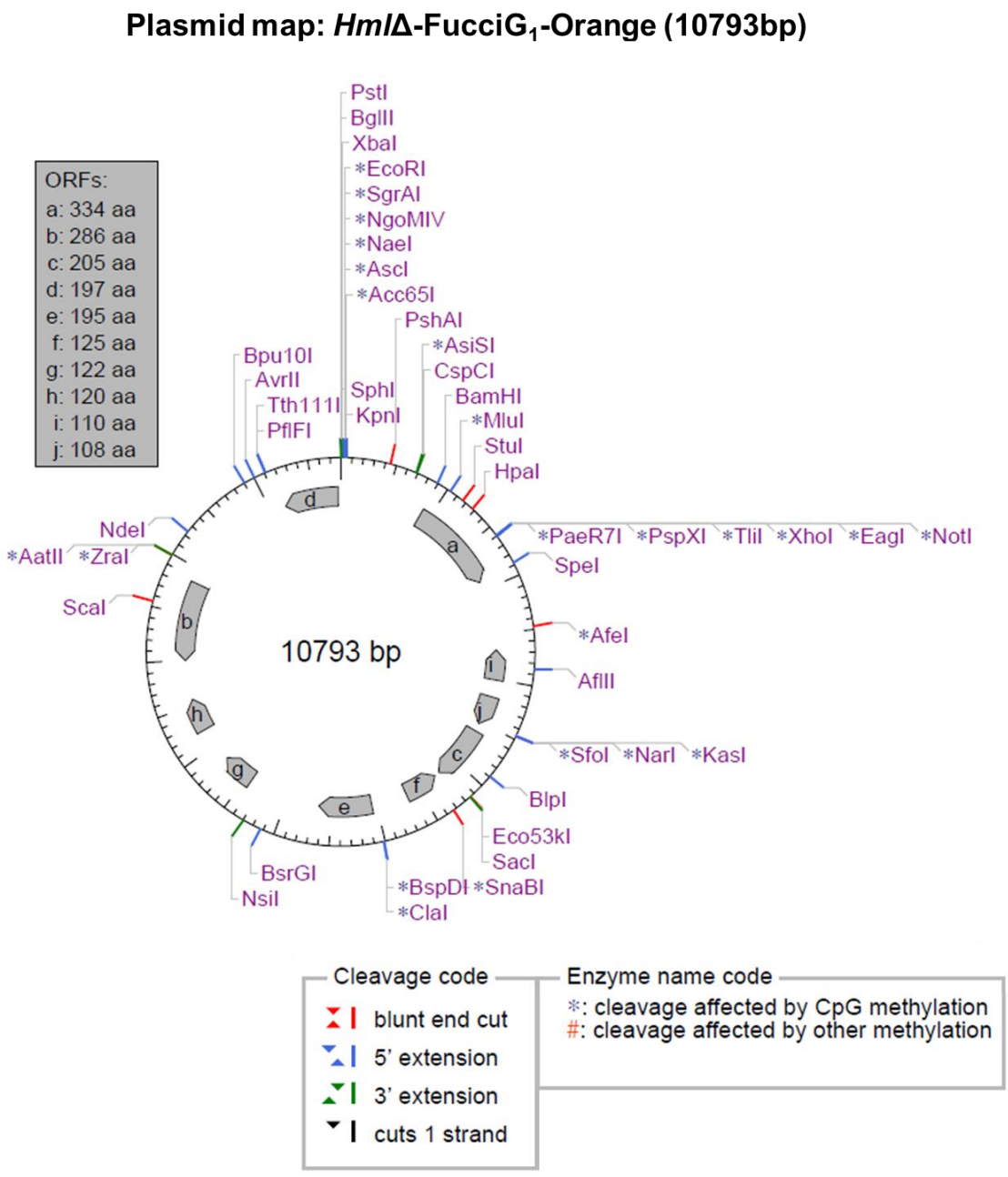


Plasmid map generated using NEB cutter V2.0.

# Appendix 3

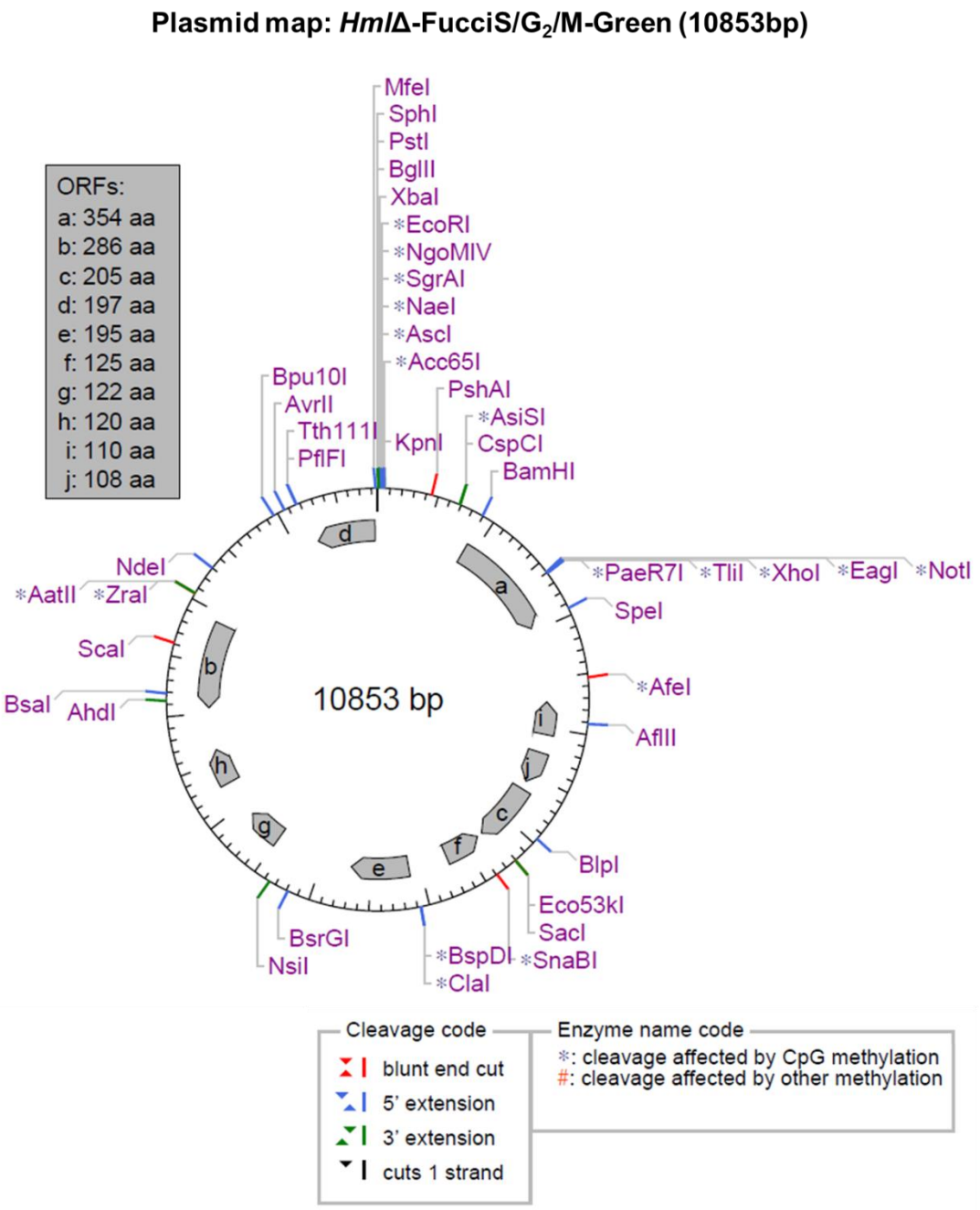


Plasmid map generated using NEB cutter V2.0.